21 JANUARY 2022

Report of the Inquiry Committee for the accident at Stars Engrg Pte Ltd on 24 February 2021

(PART II – ANNEXES)

TABLE OF CONTENTS

Part II – Annexes

ANNEX I – EXPERT REPORTS

MATCOR TECHNOLOGY & SERVICES PTE LTD
3 Seletar Aerospace Link Singapore 797550 Tel: (65) 6778 8285 Fax: (65) 6773 0625
Email: matcor@matcor.asia Website: www.matcor.com.sg Co Reg No.: 199201190R

MATCOR a cetim company

TECHNICAL REPORT

Report No: M21091	Subject Group.: 11219	Date: 10th September 2021
Title of Report: Failure Analysis of a Failed Mixer Machine Retrieved from Unit 32E of Platinum @ Pioneer Building involved in a Fire Explosion Incident		Date of Last Revision/Revision No: Work Verified By: Robert Shandro
Client/Sponsor of Project: Ministry of Manpower (OSHD)		Client/Sponsor Ref: Ms Jaime Lim, Mr Mohamed Haniffa Ibrahim
Work Carried Out By: Ashley Ng, Lim Kie Yong, Naing Aung and Muhammad Hafiz bin Amzah		Reporters Sign:

Summary

Failure analysis was conducted on a failed Mixer Machine involved in an explosion that had occurred on 24th February 2021 at Unit 32E of Platinum @ Pioneer Building.

The scope of work included review of documents, visual/macroscopic examination, fractographic examination, chemical and energy dispersive X-ray analysis, metallographic examination, micro-hardness and shore hardness tests.

The oil jacket of the Mixer Machine had sustained overload rupture along the left, right and bottom edge of the rear side weld. This was evidenced by the equiaxed and elongated dimples present across the fracture surface of the oil jacket walls (welded areas).

The lack of heat transfer fluid inside the oil jacket made the heaters overheat in order to compensate for the poor heat transfer efficiency.

The rupture was essentially due to high pressure inside the oil jacket, resulting in cracks along the welds. The high pressure inside the oil jacket was caused by the boiling and evaporation of the heat transfer fluid, which arose from overheating, and the closure of all openings/ports.

Over time, the high internal pressure caused cracks to initiate at the weld roots. Improper weld repairs at those cracks may have stopped the leakages temporarily but with poor weld quality and unresolved high internal pressure, a failure at the oil jacket was bound to occur.

The details of the findings are discussed in the report.

Indexing Terms
Oil jacket
Heater
Overpressure
Repair weld

Distribution Statement:

- [X] No distribution without permission from the responsible company concerned
- [ ] Limited distribution
- [ ] Free distribution

Number of Pages: 186

Table of Contents

1.0 INTRODUCTION

Failure analysis was conducted on a failed kneader/Mixer Machine ("**Mixer Machine**") involved in an explosion that had occurred on 24th February 2021 at Stars Engrg Pte Ltd's factory unit located on the first level of 32E Tuas Avenue 11 (the "**Factory**"). The Mixer Machine was located on a purpose-built platform constructed at the Factory (the "**Platform**").

The Mixer Machine and other relevant exhibits were retrieved from the Factory on 24th March 2021. The specification of the Mixer Machine is presented in the User Guide. [1]

The objective was to establish the possible cause of the failure of the Mixer Machine.

1.1 Scope of Work

The analysis was based on the information provided by, samples received from and requests/discussion with the Ministry of Manpower ("**MOM**"). This report covers the following scope of work.

- (i) Pick up of exhibits samples from the incident site
- (ii) Review of documents
- (iii) Visual and macroscopic examination
- (iv) Fractographic examination
- (v) Chemical and Energy Dispersive X-ray (EDX) analysis
- (vi) Metallographic examination
- (vii) Micro-hardness and shore hardness tests
- (viii) Evaluation and reporting

Yong Chun Hao, a licensed electrical worker ("**LEW**") with Yogo Engineering, and Vincent Char Poh Fang, a Switchboard Manufacturer of One Electric Pte Ltd, were engaged to assist in the analysis with regard to the wiring inside the Mixer Machine, and their 'Electrical Report on Local Electric Panel' dated 25th July 2021 ("**LEW Report**") is attached as *Annex 3*.

2.0 OBSERVATIONS FROM SITE VISIT

A site assessment was conducted by Matcor on 2nd and 8th March 2021. The physical condition of the damaged industrial unit and the machineries within the unit was examined, documented (by Matcor) and presented in Figure 1 to 22, in Appendix A. The key findings are discussed as follows.

[1] See NH Sigma Kneader User's Guide furnished by MOM in *Annex 1.*

2.1 Damaged Industrial Unit

- The front of the unit had a shutter door and was facing the common driveway. Several rolls of fire rated products, either in white packaging or aluminium foils, were found stacked on the open space area immediately outside the unit (Figure 1).
- The internal walls of the unit revealed varying extent of charring, with the upper half of the wall appearing more severe (Figure 2 to Figure 4).
- The explosion at the time of incident had cracked and punctured through the side wall in the vicinity of the Platform floor as well as top half of the rear walls (Figure 3 to Figure 7).
- Cracks were also observed on the side walls next to the lift near to the Platform floor (Figure 4).
- The lighting fixtures in the vicinity of the Platform floor were observed to be more thermally deformed as compared to the ones towards the front of the unit (Figure 3 and Figure 4).
- Based on the fire damage features observed in the unit, it appeared that the fire explosion likely initiated from the Mixer Machine on the Platform floor.

2.2 Mixer Machine and Electrical Panel

The physical condition of the Mixer Machine and its associated components is shown in Figure 8 to Figure 17. The identification tag of the Mixer Machine is shown in Figure 8.

- The Mixer Machine comprised a W-shaped mixing chamber which was enclosed with an oil jacket. Nine heaters were located at the bottom of the oil jacket to heat the oil to a desired temperature.
- Remnant whitish insulation wool was observed to remain attached to the front and rear sides of the oil jacket (Figure 8 and Figure 9). A resistance temperature detector/sensor (RTD) was observed in the mixing tank, but not in the oil jacket.
- Close examination of the oil jacket revealed tearing damage along the bottom-rear corner weld joints, adjacent to the heaters (Figure 9 and Figure 10). The fractured bottom-rear corner weld joint configuration appeared different from the original weld joints further away, suggesting that the fractured joints were weld repair areas.
- Further examination of the weld joints on the front side of the oil jacket revealed that the bottom-front corner weld joints were weld repaired prior to the fire explosion incident (Figure 11).

- Examinations of the heaters revealed faulty connections on the second coil set (Figure 12). A new heater, that was placed next to the Mixer Machine, appeared relatively unaffected by the fire explosion (Figure 15).
- The interior of the mixing tank was partially filled with water and dough-form product mixture, apart from the sigma blades (Figure 13). Some remnant insulation wools at the bottom of the Mixer Machine on the Platform floor were charred at the time of inspection (Figure 13).
- The access and vent ports of the oil jacket were in closed mode at the time of inspection (Figure 14). The drain port at the bottom of the oil jacket was also in a closed state.
- The electrical switches and buttons as well as the display screens on the electrical panel were damaged by the fire explosion (Figure 15 and Figure 16).
- The electrical circuit system within the panel box appeared relatively intact (Figure 16).
- Three oil tubs, which were contaminated by water, were found on the Platform floor next to the hopper (Figure 17).
- The oil funnel, which was used to top up oil in oil jacket, was found on the ground floor at the time of inspection (Figure 17).

3.0 LABORATORY RESULTS

The laboratory results of the exhibits are presented in Appendix B to E, based on the examination conducted. Appendix F shows the results obtained from the 3D model made based on the measurements made on the Mixer Machine.

3.1 As-Received Exhibits

The following exhibits were retrieved from the incident site on 24th March 2021 (Figure 19 to Figure 34).

- Mixer Machine (Figure 19 to Figure 32)
- Oil funnel (Figure 33)
- Resistance Temperature Detector/Sensor (RTD) A (Figure 33)
- RTD B (Figure 33)
- Heater found beside the Mixer Machine after the incident (Figure 33)
- Two new heaters from the storeroom at level 2 (Figure 33)
- Electrical panel, also known as local control panel of the Mixer Machine (Figure 34)

In addition to the above, two heaters were received from MOM on 28th May 2021 and 1st June 2021 respectively (Figure 35 to Figure 36).

For ease of reference, the parts of the Mixer Machine were labelled and presented using a 3D sketch shown in Figure 18 (reproduced below).

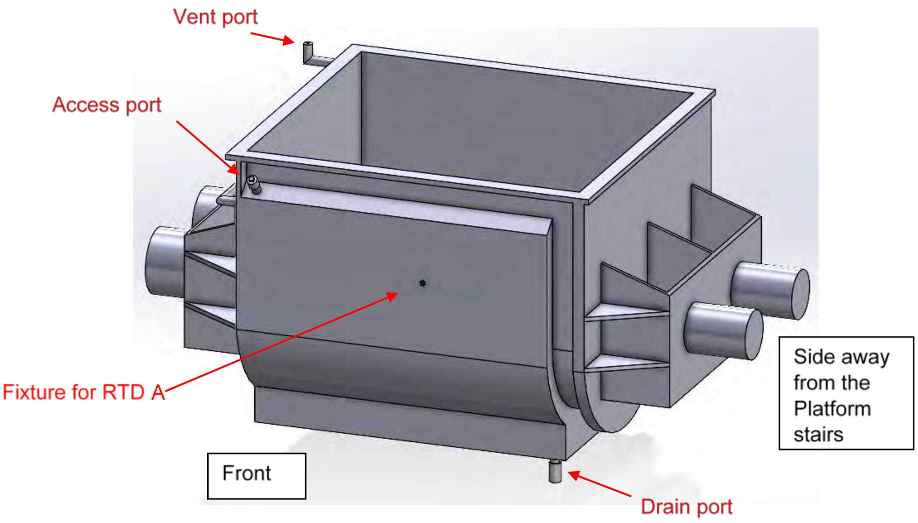

Figure 18 (see Appendix B)

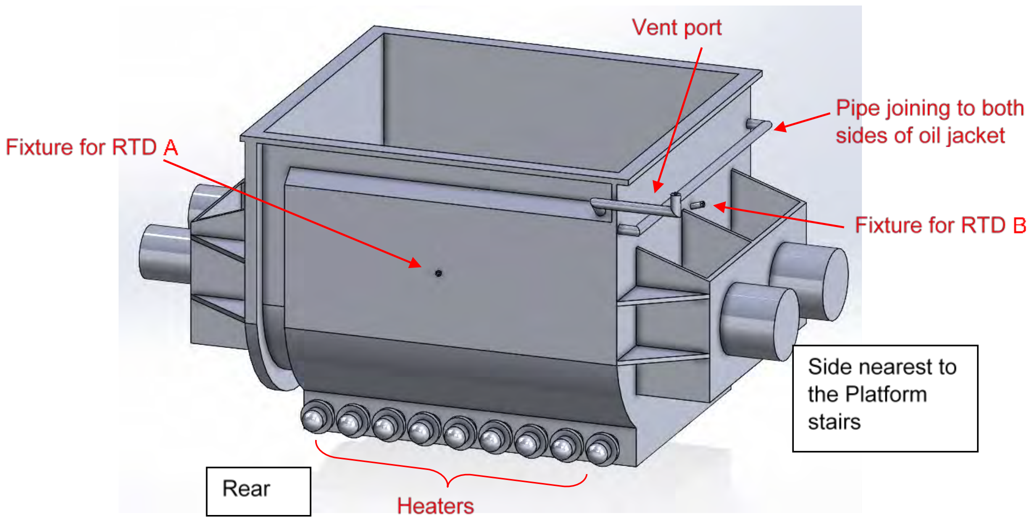

Figure 18 (Appendix B)

The front of the Mixer Machine was determined based on how the lid opened up for access to the mixing chamber. The User's Guide[2] also stated, "*An oil vapour vent is provided at the highest point behind the machine…*". The opening at the pipe elbow located behind the machine was the highest point and hence, referred to as the vent port.

[2] See User Guide at p4 in *Annex 1*.

3.2 Visual and Macroscopic Examination

In this examination, a digital camera with general purpose and macro lenses was used to document the findings and critical features of the exhibits.

3.2.1 Oil jacket (Figure 37 to Figure 98)

The Mixer Machine has an oil jacket around the main mixing chamber. For ease of reference, the following sketch is presented to identify the orientation and edges of the oil jacket.

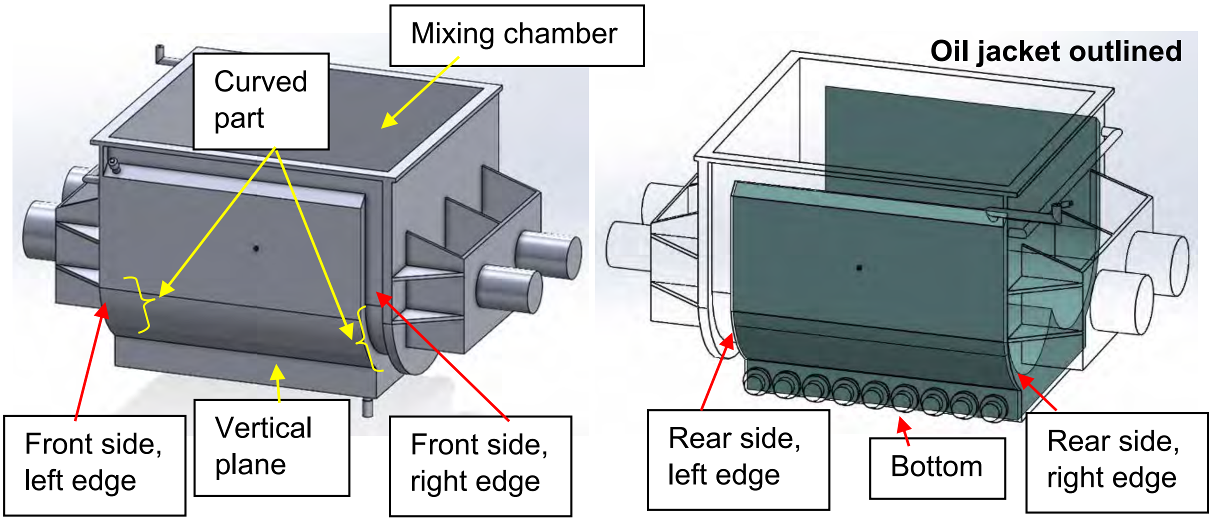

Identification of the oil jacket parts. Oil jacket space coloured in blue (right image).

By design, the various sides/faces of the oil jacket were welded together along their edges. On examination, some repair welds were found in addition to the original welding done during the manufacture of the machine. The original welds had weld caps with consistent appearance and intact paint coating of the Machine. In contrast, the repair welds had weld caps that are uneven in appearance and without the paint coating. The welding edges are discussed further below.

3.2.1.1 Front side (Figure 37 to Figure 56)

- The internal surfaces of the oil jacket were generally masked by a layer of black soot/deposits. The internal surface of the bottom face was masked by a relatively thicker layer of black soot/deposits with hard debris of various sizes (Figure 40).
- Oil stain and drip marks were visible on the internal surface of the oil jacket.
- Both left and right edges had repair welds while the bottom corners had reinforcement plates (about 165 mm by 132 mm plates, one on each corner) welded onto the oil jacket (Figure 41 and Figure 50). A metal base plate was also added by welding ("base plate").

A. Front side, left edge weld

- At the front side, left edge weld, the face width[3] of the repair weld increased towards the bottom, measuring up to about 30 mm (Figure 42 and Figure 43).
- The weld root of the original weld had an irregular shape (Figure 46).
- The root of the repair weld had a root surface width of about 4 mm and increased up to 9 mm towards the bottom. Some areas of the weld root had gaps and lack of penetration[4] (Figure 46 and Figure 47).
- A sector near the bottom end of the curved part (just above the vertical plane) an insert plate with length of 120 mm was observed at the weld root (Figure 47). See also Section 3.4 for chemical analysis and Figure 153 for cross sectional examination.

B. Front side, right edge weld

- At the front side, right edge weld, the face width of the repair weld face was up to about 20 mm. The weld root was smaller and had signs of lack of root penetration at some areas (Figure 51 and Figure 52).
- The bottom reinforcement plate was found to be folded over the original weld and welded to the side wall (side away from Platform stairs) (Figure 54).
- Cross sections made across the corner reinforcement plate revealed voids in the weld metal of reinforcement plate (Figure 56).

3.2.1.2 Rear side (Figure 57 to Figure 68)

- The internal surface of the oil jacket wall at the rear side was generally covered by black soot (Figure 59).
- Oil stains and drip marks were visible on the internal surface of the oil jacket (Figure 60).

A. Rear side, left edge weld

- A fracture opening was observed at the rear side, left edge weld (repair weld). The fracture path was predominantly centred along the weld face at the curved part of the oil jacket. The path changed and propagated along the weld toe at the vertical plane of the oil jacket (Figure 62).
- On the fracture surface of the rear side, left edge weld, voids were visible especially along the curved part (Figure 63). At the vertical plane, the fracture surface was flatter (Figure 64).

B. Rear side, right edge weld

- The fracture at the rear side, right edge weld had a similar fracture path at the repair weld. The fracture path was slightly off-centred along the weld face at the curved part of the oil jacket and along the weld toe at the vertical plane of the oil jacket (Figure 66 and Figure 67).

---

[3] Weld terminology presented in *Annex 2*.

[4] Incomplete root penetration is a joint root condition in which weld metal does not extend through the joint thickness.

- Similarly, on the fracture surface of the rear, right edge weld, voids were visible along the curved part while at the vertical plane the fracture surface was flatter (Figure 68).

3.2.1.3 Bottom (Figure 69 to Figure 74)

- The bottom of the Mixer Machine had bulged outwards, with the bulge nearer to the rear side of the Mixer Machine (Figure 69).
- The internal surface of the bottom face was generally covered in black soot (Figure 70).
- A fracture was observed along the rear side, bottom edge weld (repair weld), nearer the right side of the Mixer Machine. Closer examination of the fractured weld revealed that the fracture path was generally along the weld toe (Figure 71 and Figure 72).
- Upon removing the bottom face of the Mixer Machine to examine the interior of the Mixer Machine, the W-shaped profile of the mixing chamber can be seen from the bottom up. The W-shaped profile of the mixing chamber was generally covered with soot and oil remnants (Figure 73 and Figure 74).

3.2.1.4 Heaters (Figure 75 to Figure 92)

There are nine heaters installed on the Mixer Machine. These heaters were connected together by wires in groups of three (heaters #1 to #3, #4 to #6 and #7 to #9).

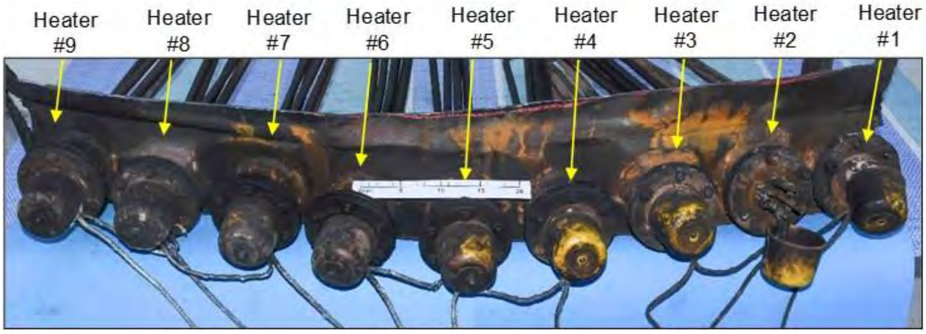

Extracted from Figure 75.

The wire connections in a group of heaters are shown in Figure 76 (extracted in the following page). For ease of reference, the terminals were numbered clockwise in increasing order, starting from the topmost terminal as terminal #1. Each heater is connected in two ways. First, each heater is connected to the electrical panel by a wire between the electrical panel and one of its terminals. Second, within each group of three heaters, two wires connect the middle heater to each of the heaters on its left and right side by one of their terminals (Figure 76 and Figure 77).The position of the connected terminals and terminal bridges vary depending on the flange orientation during bolting.

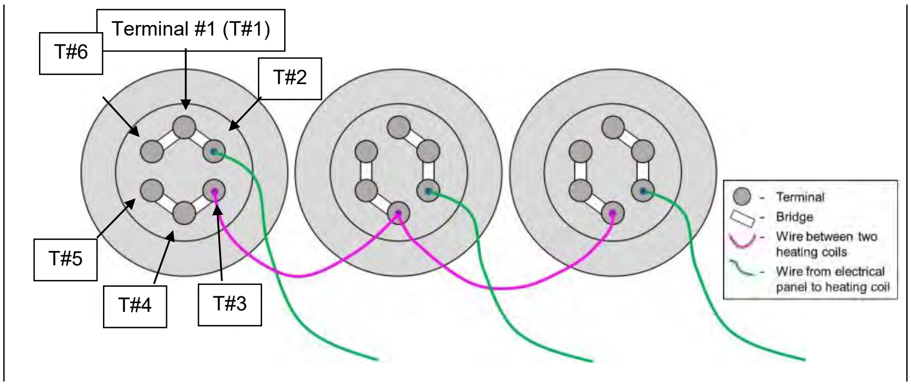

Extracted from Figure 76.

The heaters were sheathed-type heating elements (also known as Calrod™ heaters). For ease of reference, the various parts of the heater are identified in the following figure.

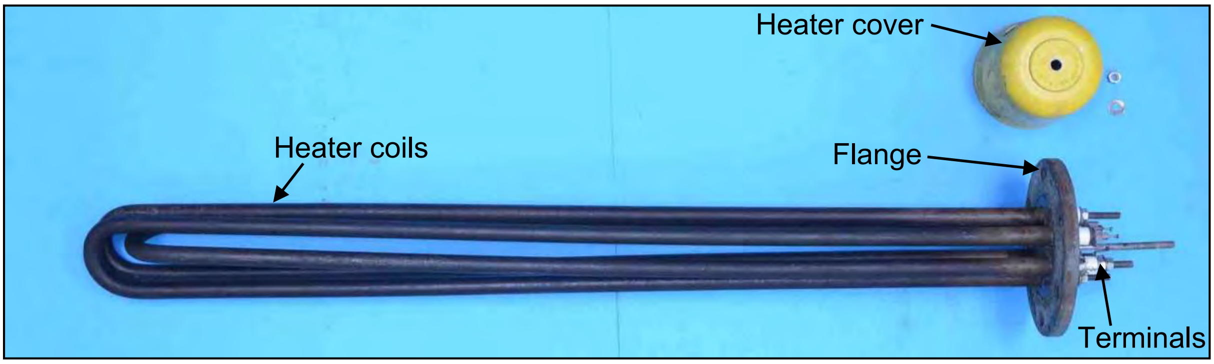

Extracted from Figure 36

The heater (inside the coil) consisted of resistive heating elements surrounded by ceramic insulator inside a metal tube (or sheath). The resistance wire was connected to the terminal near the end of the metal tube and sealed by seal and terminal insulator. The metal tube was bent in the middle, like a "U" shape, such that its two ends connect the two terminals across from each other. The internal construction is depicted in the following sketch.

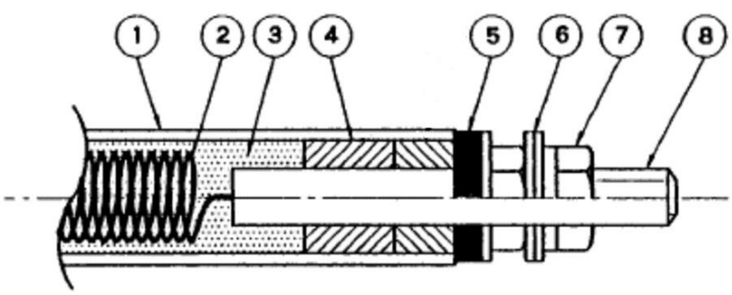

1 – Metal tube (sheath)
2 – Resistance wire
3 – Insulating powder
4 – Seal insulator
5 – Terminal insulator
6 – Washer
7 – Nut
8 – Terminal

Sketch showing the cross sectional view inside a metal tube of the heater.

The key observations are summarised below:

- The flanges generally had a blackish appearance (Figure 77, Figure 81 and Figure 83). Some of the terminal covers (rounded yellow caps) were blackish on the internal surface as well (Figure 77, Figure 81 and Figure 83).
- The terminals of heater #2 also had a blacker appearance compared to the terminals of the rest of the heaters (Figure 77).
- Green tapes were observed wrapped around the wires of both terminal #3 and terminal #4 of heater #2. The tapes on each of the aforementioned wire, had likely melted and adhered together. The position of both wire lugs were close together. Beneath the green tape wrapped around the wires at terminal #4 was a yellow clip tab that bound the end of the wire from heater #1 to the wire to heater #3 (Figure 79 and Figure 80).
- Taking heater #5 as reference for how the wires were connected to the lugs, the end of the wires from/to heater #4 and heater #6 were clamped together by a single lug (Figure 82).
- Signs of corrosion and peeling of coating were observed at various parts of the metal tubes (Figure 86).
- All the gaskets had degraded and were generally brittle to the point where they broke with slight pressure (Figure 87 and Figure 90).
- The LEW reported that heater #2 had an unusually high resistance among the coils.[5] Examination revealed that the metal tube between terminals #3 and #6 had a bulging area of about 15.5 mm diameter (the normal diameter of the metal tube is 11.9 mm) (Figure 93 and Figure 94).
- The resistance wire inside the metal tube between terminals #3 and #6 had separated by melting and the surrounding insulation powder was very loose (Figure 96). There was a small melted bulb adhering to the inner wall of the metal tube at this location (Figure 95). This suggested that the unusually high resistance in heater #2 was caused by damaged resistance wire.

3.2.1.5 Access and Vent ports (Figure 97 to Figure 99)

- Both access and vent ports were plugged by square head plugs. Along with the closed drain port, all three of the oil jacket openings were closed (Figure 97 and Figure 98).
- The oil funnel was not in use and was found at the ground floor of the Factory during the retrieval of the Mixer Machine onsite (Figure 99).

[5] See LEW Report at p5 in *Annex 3*.

3.2.2 Resistance Temperature Detector/Sensors - RTDs (Figure 100 to Figure 106)

Resistance Temperature Detectors/Sensors, also known as RTDs are temperature-sensing devices that change resistance at a predetermined rate in response to changes in temperature. They are circuit elements whose resistance increases with increasing temperature in a predictable manner. The increase in resistance is converted to temperature and displayed by the thermostat it is connected to.

Both RTD A and B were retrieved onsite.

- For RTD A, the sensor end was found inside the mixing chamber while the wire was still connected to the electrical panel (Figure 100 and Figure 101). RTD A was still intact, with the sensor in working condition.[6] The wire connectors (red and green) were still intact, which was originally connected to the "Jacket temp" thermostat (see Figure 107 and Figure 108).
- For RTD B, only the holder was found onsite (Figure 102 and Figure 103). There was no sensor inside the holder - the sensor had separated from the wire. Although this RTD was not attached to the electrical panel during the onsite inspection, the wires were originally connected to the "Material temp" thermostat as the connectors were still in place inside the panel (see Figure 107 and Figure 108).
- RTD A was used to test the fitting of the fixtures on the Mixer Machine and oil jacket. The RTD was able to fit all three RTD fixtures (Figure 104 to Figure 106).
- The fixtures at the front and rear walls were on the external surface of the wall while the fixture on the left wall slightly protruded into the wall thickness, like a small depressed well.

3.2.3 Electrical Panel (Figure 107 to Figure 110)

- The electrical panel's (or local control panel) external surface was covered with black soot and sustained fire damage, especially to the buttons and the thermostats display screens (Figure 107).
- The thermostats and buttons had melted, and the label on the electrical panel had burnt off. The text on the labels were ascertained by a photo of the electrical panel taken prior to the accident on 24th February 2021, furnished by MOM in *Annex 4*.
- The wires inside the electrical panel were generally intact before the removal of the Mixer Machine to Matcor's laboratory (Figure 110).

3.2.4 Additional heaters (Figure 111 to Figure 116)

- The heater found on the Platform beside the Mixer Machine had no significant damage or sign of usage observed, therefore the heater was most likely a new heater (Figure 111).

[6] See LEW Report at p4.

- Two new heaters retrieved from storeroom on the second level of 32E Tuas Avenue 11 were used as reference. These two new heaters had labels on their terminal covers, indicating that the heaters were designed with specifications of 220V and 5kW (Figure 112).
- The measured length of the heater coils was about 630 mm, the outer perimeter (circular) of the coils was about 51.2 mm and the flange’s outer diameter was about 115 mm (Figure 112).
- The used/failed heater received for analysis on 28th May 2021 was reportedly replaced in August 2020 after failing (Figure 113). One of the coils had broken off. The metal tube had deformed and melted off around the breakage location as evidenced by the bulbous and droplet-like shape of the metal (Figure 114). This was an indication of high temperature experienced by the metal tube, leading to localised melting of tube.
- The other heater was received for analysis on 1st June 2021 (Figure 115 and Figure 116). The metal tubes had black appearance similar to the heaters inside the Mixer Machine. Several blisters of up to about 5 mm were also observed on the metal tubes. These observations suggested that this heater had been used before (see also Chapter 4.5.3 for metallographic examination findings). There was no information provided on when and why this heater was replaced.

3.3 Fractographic Examination using Digital Microscope and SEM

In this examination, examined samples (representative area of the fracture surface and lugs from heater #2) were cleaned in an ultrasonic bath of Alconox solution for detailed examination under a Keyence Digital Microscope, followed by JEOL IT-300LV Scanning Electron Microscope (SEM) using a higher magnification (Figure 117 to Figure 140).

3.3.1 Rear side, left edge weld (Figure 119 to Figure 124)

- Macroscopic view of fracture surface revealed weld porosities throughout the fracture surface (which was the weld metal), predominantly at about the mid-depth from the external surface (Figure 120).
- Voids were confirmed under the SEM (Figure 121 and Figure 122).
- Relatively equiaxed dimples were generally observed throughout the fracture surface at regions adjacent to the internal side (Figure 123).
- Elongated dimples were observed at regions adjacent to the external side (Figure 124).

- The presence of dimples was evidence of overloading fracture. The locations of equiaxed and elongated dimples suggested that at regions adjacent to internal side (with equiaxed dimples) had cracked open with direction perpendicular to the fracture surface while the region adjacent to the external side (with elongated dimples) had torn apart in an outward direction at final instance of the rupture.

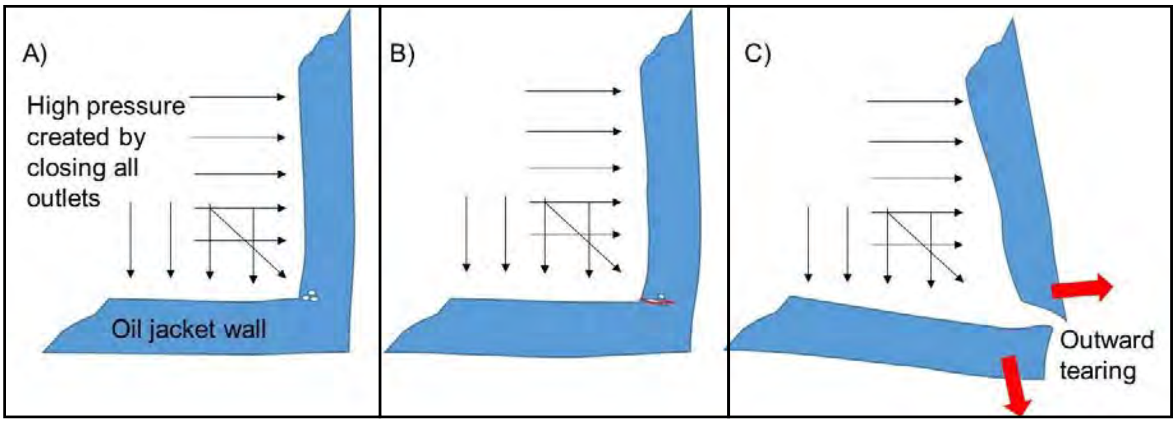

Micro-mechanism of ductile fracture due to overload: A) High pressure from inside the oil jacket leads to deformation of wall, void nucleation and crack. Evidenced by equiaxed dimples. B) Wall deformed more with void growth and coalescence to deeper cracks. C) Oil jacket wall fractured/torn apart and severely deformed outward. Evidenced by elongated dimples.

3.3.2 Rear side, bottom-right and bottom-middle welds (Figure 125 to Figure 130)

- Similarly, dimples were observed throughout the fracture surface of both examined samples. Equiaxed dimples were observed on the fracture surface at the regions adjacent to the internal side while elongated dimples were observed at the regions adjacent to the external side (Figure 129 and Figure 130).

3.3.3 Lugs from heater #2 (Figure 131 to Figure 140)

- Resolidification waves and great extent of porosity, characteristics of arcing damage, were observed at the bottom edge of the lug from terminal 3 (Figure 133 and Figure 134). SEM examination confirmed the arcing characteristic with large percentage of voids and concentric rings observed to be emanating from the centre of the arcing[7] damage (Figure 135 and Figure 136).
- Similarly, for the lug from terminal 4, resolidification waves were observed at the lug and washer that had fused them together (Figure 137 and Figure 138). SEM examination confirmed the arcing characteristic with concentric rings observed to be emanating from the centre of the arcing damage (Figure 139 and Figure 140).

[7] Arcing is a phenomenon where a flashover of electric current leaves its intended path and travels through the air from one conductor to another, or to ground.

3.4 Chemical and EDX Analysis

Chemical analysis was conducted on the base metal of the specimens sampled from the oil jacket walls using ARL 3460 OES Metal Analyzer/Hitachi Foundry-Master Smart in accordance with ASTM E415-17. The chemical composition results are presented in Figure 141.

- All the tested oil jacket walls revealed similar elements and weight percentages that are typical of low carbon steel (Figure 141).

EDX analysis was conducted on the fracture surface of the weld (rear side, left edge), soot and debris from inside the oil jacket, and heater materials using an Oxford instrument Xmax20 EDS detector coupled to a JEOL IT-300LV SEM (Figure 142 to Figure 144).

- The major elements detected on the fracture surface were generally associated with the weld metal and constituents of the thermic oil especially the high carbon peak (Figure 142).
- The major elements detected on the fine black soot were mainly associated with the burnt thermic oil with major carbon peak. The hard debris had high peaks of silicon and magnesium apart from elements associated with the service medium (Figure 143).
- Based on the major elements detected during testing of the heaters’ wires, the resistance wire was most likely constructed using Kanthal or Fe–Cr–Al material. The insulation powder was mainly magnesium oxide. The metal tube was constructed using carbon steel. All the materials were typical of heating element construction (Figure 144).

3.5 Metallographic and Microscopic Examination

In this examination, the metallographic sections were mounted, ground, polished and etched in accordance with ASTM E3-11 and ASTM E407-07e1. The prepared samples were examined under an optical microscope and/or digital microscope.

3.5.1 Weld (Figure 145 to Figure 176)

Sectional metallographic examination was conducted across various locations of the weld as shown in Figure 145 and Figure 146. The sampled locations were selected to represent the various point of interest detailed in previous chapters, as discussed with MOM and communicated to other parties' representatives.

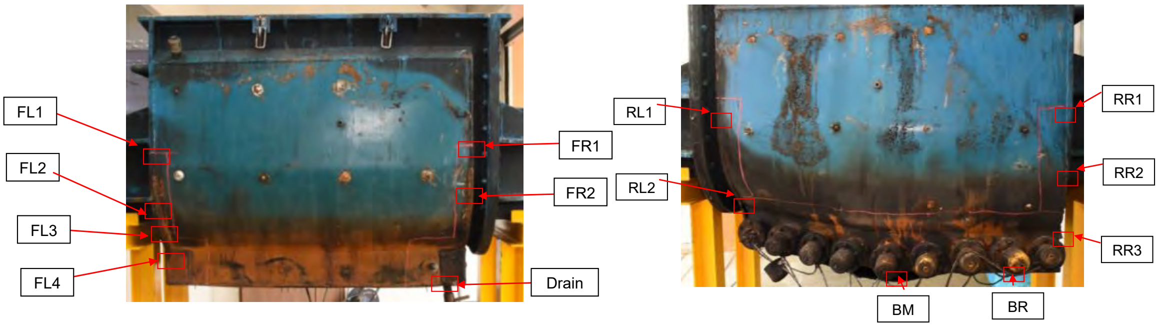

Extracted from Figure 145 and Figure 146.

At each weld edge, the top half portion of the weld was still in its as manufactured state (original weld) while the bottom half had been altered and repaired (repair weld) as detailed in Section 3.2.1. The sectional metallographic examination results are presented as follows.

A. Original weld:

- Apart from location FL1, the weld joint examined at FR1 (Figure 157), RL1 (Figure 163) and RR1 (Figure 167) were generally similar with no discontinuity found.
- The weld at location FL1 had excessive root penetration with a void of about 2 mm wide (Figure 147).
- Incipient cracks were observed at location FL1 (Figure 148), RL1 (Figure 164) and RR1 (Figure 168).

B. Repair weld:

- All nine examined locations either had through-thickness cracks (RL2 [Figure 165], RR2 [Figure 169], RR3 [Figure 171], BM [Figure 173] and BR [Figure 175]) or incipient cracks (FL2 [Figure 149], FL3 [Figure 151], FL4 [Figure 155], FR2 [Figure 159]) that initiated from the weld root and propagated towards the external surface of the weld. Most of the incipient cracks were observed to be oxide filled.

- Seven out of nine examined locations had voids scattered within the weld metal (FL3 [Figure 151], FL4 [Figure 155], FR2 [Figure 159], RL2 [Figure 165], RR2 [Figure 169], BM [Figure 173] and BR [Figure 175]). The voids were up to 2.5 mm wide in size.
- For locations RL2 [Figure 166], RR2 [Figure 170], BM [Figure 174] and BR [Figure 176], the through-cracks had propagated through some voids.
- Four out of nine locations had lack of root penetration with root openings of up to about 5.5 mm wide (FL2 [Figure 149], FL4 [Figure 155], FR2 [Figure 159] and RR3 [Figure 171]).
- At location FL3 (Figure 153 and Figure 154), the insert plate between the weld joint was confirmed to be a separate (and different) metal piece that was welded in between the front left side and front walls. Although their microstructures consisted of ferrite with pearlite, their microstructures differ such that the front left wall has flow lines from rolling process (manufacturing), the insert plate does not have flow lines and the front wall has finer grains.
- The width and thickness of the insert plate were approximately 8.0 mm and 16.0 mm respectively (the length was measured earlier at about 120.0 mm, see also Figure 47). At the time of reporting, the source of the insert plate and when it was welded into the oil jacket were unknown.
- All the locations had non-uniform distribution of weld structure with several passes and layers of weld and heat affected zone (HAZ).
- The weld at the repair weld locations had an obtuse joint angle (i.e. Figure 169) or large root opening (i.e. Figure 149) compared to the original weld locations that had relatively right angle joint. This suggested that severe deformation and opening of the weld seams had occurred before repairs were conducted.

C. Drain port:

- The weld had undercut at the weld toe (Figure 161). Voids of up to about 1.0 mm wide were observed scattered in the weld metal. The weld metal had a non-uniform distribution of weld structure (Figure 162).

3.5.2 Heater terminals (Figure 177 to Figure 180)

Sectional metallographic examination was conducted across the terminals #3 and #4 (connected with lugs) of heater #2 and across two terminals from the new heater as reference.

- Close up view of the arcing location on the lug (see also Figure 122) revealed emanating pattern of metal melting and porosities which confirmed the occurrence of arcing (Figure 180).

3.5.3 Heater metal tube (Figure 181 to Figure 210)

Heaters #2, #5 and #8 were sectioned 100 mm from the end of the heaters, across the metal tubes for metallographic examination. A new heater was also sectioned the same way and examined for comparison.

The grain sizes were measured based on ASTM E 112-13. Grain size is categorised using the “ASTM grain size number”, where larger ASTM numbers correspond to finer grain sizes (i.e. ASTM number 9 is finer than ASTM number 2).

- The new heater had an average grains size of about 9 µm or ASTM number range of 9 – 10 throughout all the metal tubes (Figure 203 and Figure 204).
- All the resistance wires within the metal tubes of heaters #2 (Figure 184), #5 (Figure 190) and #8 (Figure 196) were generally similar in microstructure and had experienced grain growth to similar degree when compared to the resistance wire in the new and unused heaters (Figure 202).
- Similarly, all the metal tubes of heaters #2 (Figure 185 to Figure 188), #5 (Figure 191 to Figure 194) and #8 (Figure 197 to Figure 200) were generally similar in microstructure and had experienced grain growth when compared to the metal tube of the new heater (Figure 203 to Figure 204).
- Heater #2 had an average grain size of about 222 µm or ASTM number range of 0 – 3 at metal tube corresponding to position of terminal #2 (upper half of metal tubes located above the centreline of the bore of the heater flange, Figure 185 and Figure 186) and about 124 µm or ASTM number range of 3 – 4 at metal tube corresponding to orientation of terminal 4 (lower half of metal tubes located below centreline of the bore the heater flange, Figure 187 and Figure 188). The centreline of the bore of the heater flange was indicated in Figure 212.
- Heater #5 had a mixture of grain sizes where the upper half of the metal tubes had higher density of large grains compared to lower half of metal tubes. The tubes had an average grains size of about 63 µm at metal tube corresponding to position of terminal 1 (upper half of tubes, Figure 191 and Figure 192) and about 58 µm at metal tube corresponding to orientation of terminal 4 (lower half of tubes, Figure 193 and Figure 194). Both metal tubes’ had grains with a mix of sizes ranging between ASTM number 3 – 4 and 8 – 9.
- Heater #8 had an average grain size of about 188 µm or ASTM number range of 0 – 3 at metal tube corresponding to position of terminal 6 (upper half of tubes, Figure 197 and Figure 198) and about 110 µm or ASTM number range of 3 – 5 at metal tube corresponding to orientation of terminal 3 (lower half of tubes, Figure 199 and Figure 200).
- The finding that the metal tubes (for heater #2 and #8) located higher up within a heater generally had a larger grain size compared to the metal tubes located lower down in the heater (nearer the bottom face of the oil jacket) means that the metal tubes located higher up in the heater likely sustained higher heating temperatures than the metal tubes located lower down.

Additionally, the heater with blisters was sectioned across one of its blistered metal tubes for examination (Figure 205 to Figure 210).

- The metal tubes had an average grain size of about 106 µm or ASTM number range of 3 – 4, indicating that it had been used and experienced grain growth (Figure 209 and Figure 210).

3.6 Micro-Hardness and Shore Hardness Test

Micro-hardness test was conducted on the metallographic sections FL1, RL1, RL2, RR2, and BR (refer to Figure 145 and Figure 146 for their respective locations) in accordance with ASTM E384-16. The test was performed using a LTF Isoscan HV1 AC Plus micro-hardness tester at 400x with penetration load of 500gf.

High HV number corresponds to high hardness at the test location. The hardness results of the metallographic sections are tabulated in Table 1 and Table 2 and presented in the following pages, showing five test readings and the average hardness values.

3.6.1 FL1 and RL1 – Original weld

- The average hardness measured at the base metals of the front, rear and side walls were 157 HV, 148 HV and 141 to 151 HV, and were generally consistent at their respective locations without significant hard spots.
- The average hardness at the weld metal of FL1 was 178 HV with consistent single readings. For weld metal at RL1, the average hardness was 197 HV with single readings ranging from 193 to 210 HV.

3.6.2 RL2, RR2 and BR – Repair Weld/Reinforcement plate weld

- Comparing RL2 with RL1, RL2 had significantly higher average hardness at all the tested regions except the weld metal. The average hardness at base metal and HAZ (at rear wall) were 170 HV and 174 HV respectively while the base metal and HAZ (at side wall) were 159 HV and 219 HV respectively. The base metal hardness is typical of carbon steel material.
- The hardness across RR2 weld were generally similar with RL1 except for the HAZ and base metal (at side wall) where the average hardness were 176 HV and 180HV respectively.
- For the BR weld sample, the base metals of the rear wall, bottom plate and reinforcement plate had consistent hardness distribution.

2

AREA	MICRO HARDNESS VALUE (HV)						STANDARD DEVIATION (%)
	#1	#2	#3	#4	#5	AVG	
Front Left 1 (FL1) – Original weld							
Base metal (Front wall)	158	166	155	153	152	**157**	3.59
HAZ (Front wall)	154	152	165	162	152	**157**	3.87
Weld metal	184	183	178	173	172	**178**	3.10
HAZ (Side wall)	163	160	161	166	160	**162**	1.57
Base metal (Side wall)	144	141	149	151	141	**145**	3.17
Rear Left 1 (RL1) – Original weld							
Base metal (Rear wall)	144	147	151	150	150	**148**	1.94
HAZ (Rear wall)	160	154	155	150	157	**155**	2.38
Weld metal	194	202	210	193	188	**197**	4.38
HAZ (Side wall)	152	152	153	148	151	**151**	1.27
Base metal (Side wall)	148	150	148	141	155	**148**	3.39
Rear Left 2 (RL2) – Repair weld							
Base metal (Rear wall)	163	163	166	174	182	**170**	4.87
HAZ (Rear wall)	185	177	169	167	171	**174**	4.20
Weld metal	196	194	196	200	192	**196**	1.52
HAZ (Side wall)	219	212	220	216	226	**219**	2.37
Base metal (Side wall)	153	162	159	157	164	**159**	2.71
Rear Right 2 (RR2) – Repair weld							
Base metal (Rear wall)	149	150	153	148	145	**149**	1.96
HAZ (Rear wall)	154	163	156	157	154	**157**	2.36
Weld metal	210	209	197	199	200	**203**	2.98
HAZ (Side wall)	177	183	185	183	154	**176**	7.30
Base metal (Side wall)	172	178	179	185	187	**180**	3.32

4 **Table 1:** Summary of micro-hardness results.

AREA	MICRO HARDNESS VALUE (HV)						STANDARD DEVIATION (%)
	#1	#2	#3	#4	#5	AVG	
Bottom right Section (BR) – Reinforce plate added							
Base metal (Rear wall)	164	161	156	158	159	**160**	1.91
HAZ (Rear wall)	174	173	168	157	167	**168**	4.03
Weld metal	223	208	212	203	226	**214**	4.58
HAZ (Bottom plate)	197	185	178	173	180	**183**	5.00
Base metal (Bottom plate)	176	170	169	167	178	**172**	2.76
HAZ (Reinforcement plate)	201	183	191	193	198	**193**	3.59
Base metal (Reinforcement plate)	184	174	173	171	178	**176**	2.92

Table 2: Summary of micro-hardness results.

Shore hardness test, adapted from ASTM D2240-15(2021), was conducted on the gaskets for heaters #2 and #9. The test was performed using a Teclock GS-615 with type D Durometer and penetration load of 5kg. The hardness results of the gaskets are tabulated in the following table.

AREA	SHORE HARDNESS VALUE (Shore D)						STANDARD DEVIATION (%)
	#1	#2	#3	#4	#5	AVG	
Gasket for heater #2	73	76	76	77	77	76	2.17
Gasket for heater #9	73	79	76	72	79	76	4.32

Table 3: Summary of shore hardness results.

As there was no new gasket available for testing and compared to as reference, the gasket from heater #9 was selected for comparison to the gasket from heater #2. Both gaskets had the same average hardness which suggested that they had most likely degraded to a similar degree, over their time in service with similar exposure to high temperature.

3.7 3D Model and Volume Calculation

The oil jacket's dimensions were measured and the results were used to create a 3D model using SOLIDWORKS 2021 software (see *Annex 5* for drawing with dimension).

MOM's instructions were that the maximum amount of thermic oil used by Stars Engrg in the Mixer Machine's oil jacket at any time would have been from 40L (corresponding to two 20L buckets of thermic oil) to 160L (corresponding to eight 20L buckets of thermic oil). Therefore, models containing 40L, 60L, 80L, 100L, 120L, 140L and 160L were made to simulate the oil levels corresponding to the different number of buckets that could have been used.

Based on the Mixer Machine's User Guide,[8] it was stated that the oil should be filled up to "half the height of the cylinder". The Mixer Machine comprised of 2 different cylinder-shaped parts — the mixing chamber (red dotted line), and the oil jacket (green dotted line). Assuming that the cylinder referred to in the User Guide was the oil jacket cylinder (which has a shorter height than the mixing chamber), half the height of the oil jacket corresponded to a fill level of about 245L of oil[9].

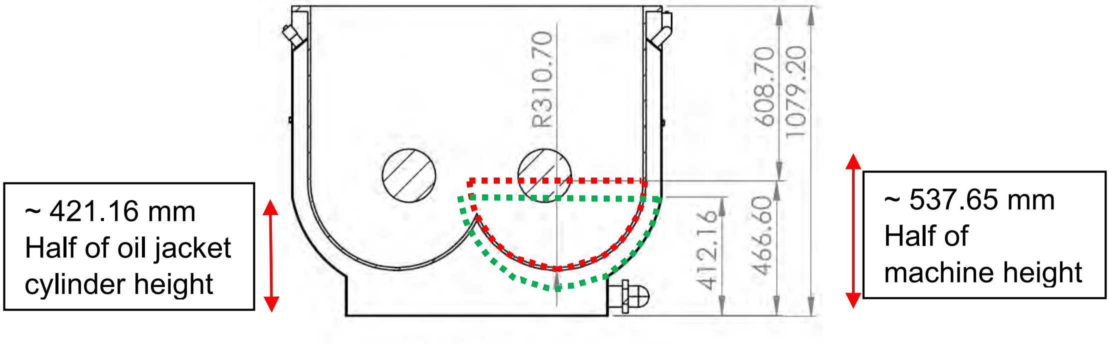

SECTION A-A

Oil volumes of 279L and 308L corresponded to oil levels up to both the RTD sensor ports and the full capacity of the oil jacket respectively.

The oil level needed to touch the metal tube at the lowest possible location was 39.1 mm while the oil level needed to fully cover the metal tube at the highest possible location was 90.3 mm. The following table summarises the oil volumes and the corresponding estimated fill level inside the oil jacket (Figure 211 to Figure 228).

Volume of Oil	Fill level (Estimated)
40L (2 buckets of oil)	37.8 mm from base surface (likely not touching any metal tubes of the heaters)
60L (3 buckets of oil)	56.5 mm from base surface
80L (4 buckets of oil)	75.5 mm from base surface
100L (5 buckets of oil)	94.3 mm from base surface (likely fully covering the heaters)
120L (6 buckets of oil)	113.2 mm from base face, fully covering the heaters
140L (7 buckets of oil)	132.0 mm from base face, fully covering the heaters
160L (8 buckets of oil)	151.0 mm from base face, fully covering the heaters
245L (half height of oil jacket cylinder)	421.16 mm from base face, fully covering the heaters
279L	700.0 mm from base face, fully covering the heaters and above the RTD fixture locations
308L	Oil jacket completely filled

Table 4: Volume of oil and estimated fill level.

[8] *Annex 1*.
[9] The oil volumes are estimated using the modelled jacket without the heaters. Therefore, the volume may have a slight variation (up to 5L) due to the displacement of the oil within the jacket caused by the volume of heaters.

4.0 DISCUSSION

The observations and findings detailed in the previous chapters are evaluated and discussed in this chapter.

4.1 Insufficient oil

Based on the background information provided, the oil jacket did not have sufficient oil inside during its operating life. The User Guide states that heat conduction oil is to be added up to half the height of the cylinder (as stated in Section 3.7). The 3D model shows that the amount of oil needed to fill to the stated level is approximately 245L (Figure 225), much higher than the initial 40L or subsequent 80L.

The heaters are immersion type heaters which are meant to be completely immersed in the service medium, such as heat transfer fluid (oil), during operation. At 40L, the oil level was too low and cannot submerge/cover any of the heaters' metal tubes. At 80L of oil, this could only cover the heaters' metal tubes up to about 10 mm above the centre of the bore of the heater flange, leaving almost half the metal tubes above the oil. Even if all eight tubs of oil were used in a filling, giving a total of 160L, the oil fill level would still have been inadequate.

4.2 Overheating of heaters

Since the oil level in the oil jacket was insufficient during operation, the overall heat transfer efficiency from the heaters to the material being mixed inside the mixing chamber was very low.

The transfer medium was essentially the air and oil vapour between the heaters and the wall of the mixing chamber (the semi-cylindrical wall) and not the heating oil as per design. This caused the heaters to compensate for the poor heat transfer efficiency by heating more and up to higher temperatures in order to bring the mixing material up to the target temperature. With the absence of RTD to measure the temperature in the oil jacket, the operators of the Mixer Machine were blind to the temperature in the oil jacket.

As per the LEW Report (*Annex 3*), the heaters were interlocked only to the "Jacket Temp" thermostat where they would be turned off when the set temperature was attained. The RTD connected to the "Jacket Temp" thermostat was found inside the mixing chamber instead of being affixed on screw-on fixture on the oil jacket (Figure 8).

Such temperature increase of the heaters caused the heaters to overheat and inclined to fault (failure). This was evidenced by the failed heater reported in August 2020 where the metal tubes had localised melted area as a result of faulting.

The grain growth (also known as grain coarsening) observed in the microstructures of the resistance wires and metal tubes were also evidence of high metal temperature experienced by the heating elements. For the metal tubes, increment in grain size in the range of ASTM number 0 to 4 indicates that they had been exposed to temperature 830˚C to 1095˚C based on API 579-1 Fitness-For-Service standards, Curve B[10] (see graph below).

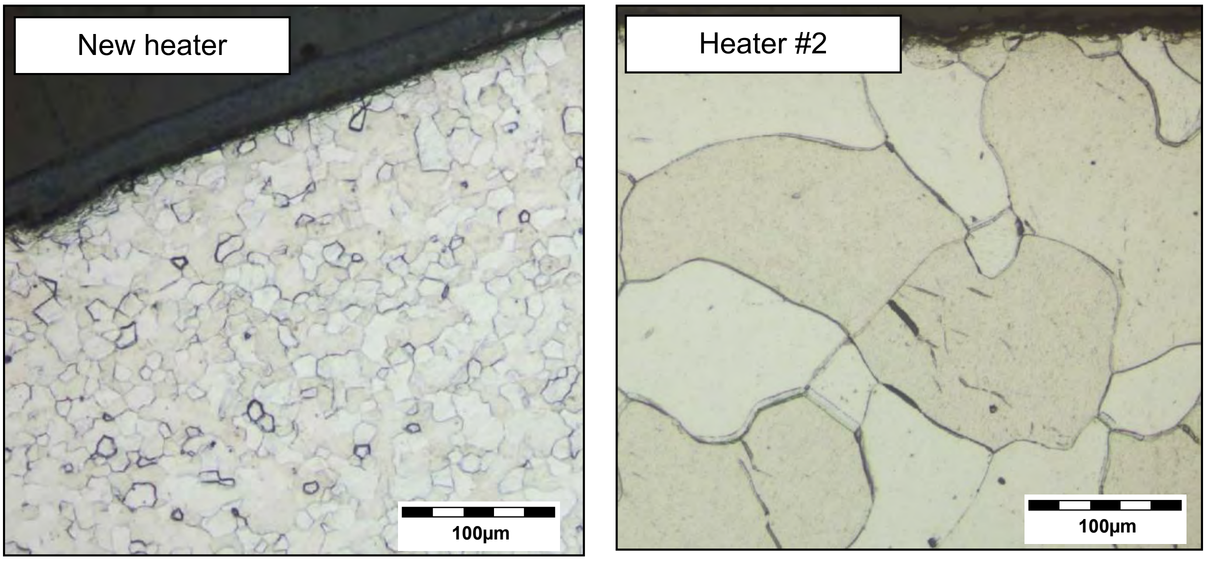

Micrographs of metal tubes at 200X magnification, extracted from Figure 204 (left) and Figure 186 (right)

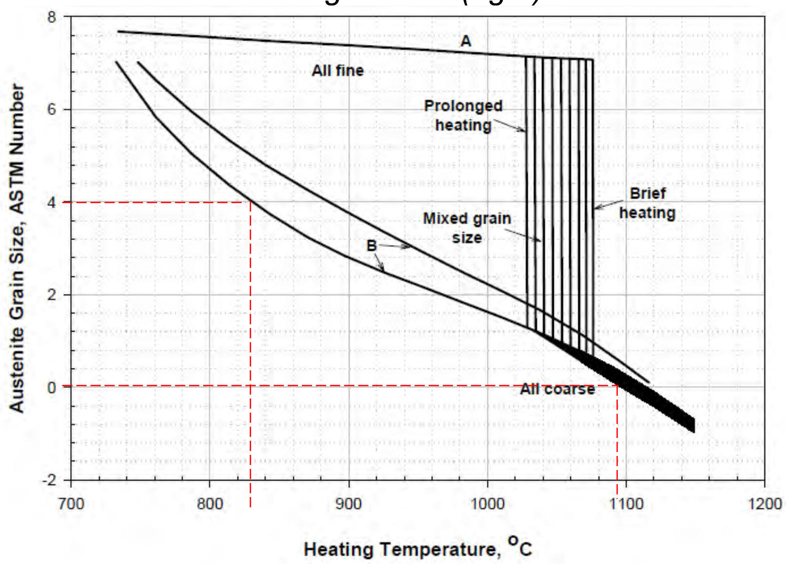

Notes:
1. Curve A – killed steel with a fine austenitic grain size (e.g. ASTM A 516).
2. Curve B – killed steel with a coarse austenitic grain size (e.g. ASTM A 515).

Coarsening Behavior of Carbon Steels as a Function of Temperature. Extracted from API 579-1/ASME FFS-1 2016 Fitness-For-Service (page 11-48 of document)

---

[10] *"General purpose carbon steels such as ASTM A53 show a gradual coarsening of the grains as the temperature is increased above the austenitizing temperature. Exposure above about 930°C (1700°F) produces very large grains. The effect of temperature on grain growth of carbon steel is shown in Figure 11.8. Fine-grained carbon steels of high toughness are used for low-temperature service; typical specifications included ASME SA 333 for pipe and SA 350 for flanges. The fine grain size is produced by deoxidizing practice (usually aluminum additions), normalizing, and cooling at a controlled rate. Steels made to fine-grained practice (ASTM 333, 516, etc.) show little grain coarsening between the austenitizing temperature and 1030°C (1900°F). Between 1030°C to 1095°C (1900°F to 2000°F), the grain size increases dramatically."* Extracted from API 579-1, pg11-27.

4.3 Degradation of oil and increase of internal pressure

Due to the inadequate amount of oil used in the oil jacket resulting in high temperatures of the heaters (see Section 4.2), any oil in contact with the metal tubes of the heaters will burn. The high heat inside the oil jacket would also have caused the oil to boil, evaporate and thermal crack[11] whenever the heaters were in operation. The repeated heating cycles would also degrade and reduce the oil quality, as evidenced by the high carbon percentage debris and soot inside the oil jacket.

The boiling and evaporation of oil increased the (oil vapour) pressure inside the oil jacket. With all the oil jacket's openings/ports blocked, the oil jacket was highly pressured from inside and the applied load on the weld joint increased.

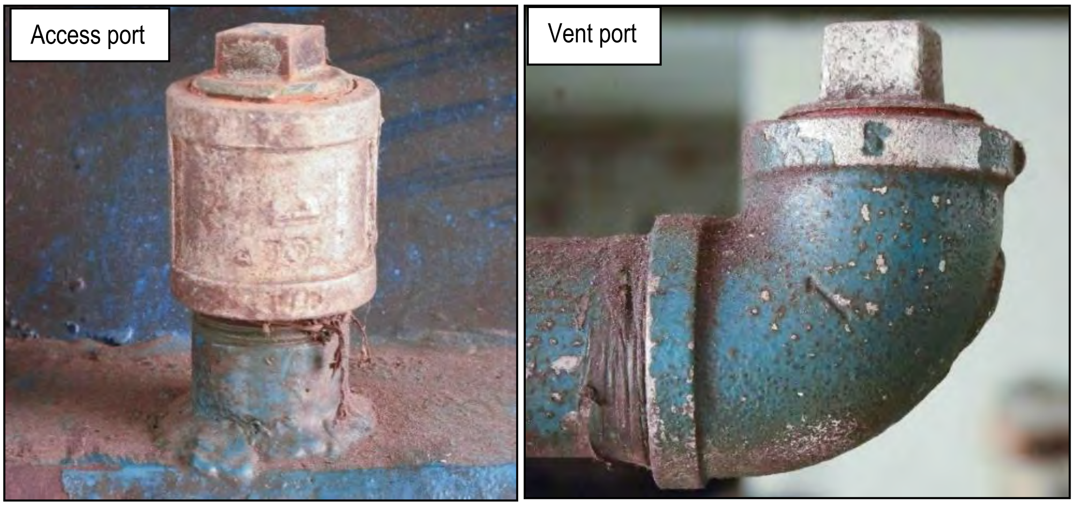

Extracted from Figure 97 and Figure 98

4.4 Earlier rupture and repair welding

The lack of root penetration with wide root opening (up to about 5.5 mm wide) at the repair welds of the oil jacket edges strongly suggested that the original welds at had ruptured open before repair weld and reinforcement plates were added (Figure 149, Figure 155, Figure 159, Figure 171). Such large root gaps are evidence of severe deformation in the oil jacket walls, typical of overpressure failure. The deformation of the walls prevented a close fit for repair welding, leading to lack of root penetration. When the rupture was repaired, the macro and micro features of earlier cracks were removed/destroyed.

[11] Thermal cracking happens when heat transfer fluid (oil) is heated past its boiling point by exceeding its maximum recommended film temperature. When hot oils boil, they go from the liquid stage to the vapour stage and then back after being cooled down. This process creates large oil molecules that decompose into solid coke (90 to 95 percent carbon) and light-end molecules that act like water in a system. The larger molecules polymerize or join with other larger molecules and develop a sludge-type material. This sludge-type material coats the internal components and changes the efficiency and performance of the system.

Based on the metallographic examination, weld repairs were made and the quality of the welds were poor and had porosities. This reduced the integrity and strength of the oil jacket. The presence of weld porosities and poor weld root shapes act as stress raisers and promote cracking.

Cracks that were not removed completely before adding a repair layer is detrimental to the overall weld integrity, also acting as stress raisers.

4.5 Oil jacket final rupture

The combination of repair welds with porosities and high internal pressure promoted cracks and leakages to occur at the welds. When the weakened welds could not withstand the high pressure inside the oil jacket, it ruptured with large opening. This was evidenced by the dimples observed at the fracture surfaces.

4.6 Post failure damages

The rupture of the oil jacket due to overpressure had caused post-failure damages in the Mixer Machine and the Factory's surrounding.

5.0 CONCLUSION

The oil jacket of the Mixer Machine had sustained overload rupture along the left, right and bottom edge of the rear side weld. This was evidenced by the equiaxed and elongated dimples present across the fracture surface of the oil jacket walls (welded areas).

The lack of heat transfer fluid inside the oil jacket made the heaters overheat in order to compensate for the poor heat transfer efficiency.

The rupture was essentially due to high pressure inside the oil jacket, resulting in cracks along the welds. The high pressure inside the oil jacket was caused by the boiling and evaporation of the heat transfer fluid, which arose from overheating, and the closure of all openings/ports.

Over time, the high internal pressure caused cracks to initiate at the weld roots. Improper weld repairs at those cracks may have stopped the leakages temporarily but with poor weld quality and unresolved high internal pressure, a failure at the oil jacket was bound to occur.

Appendix A:
Onsite Inspection

The site assessment was conducted by Matcor on 2nd and 8th March 2021.
The photographs were taken by Matcor and presented in this Appendix.

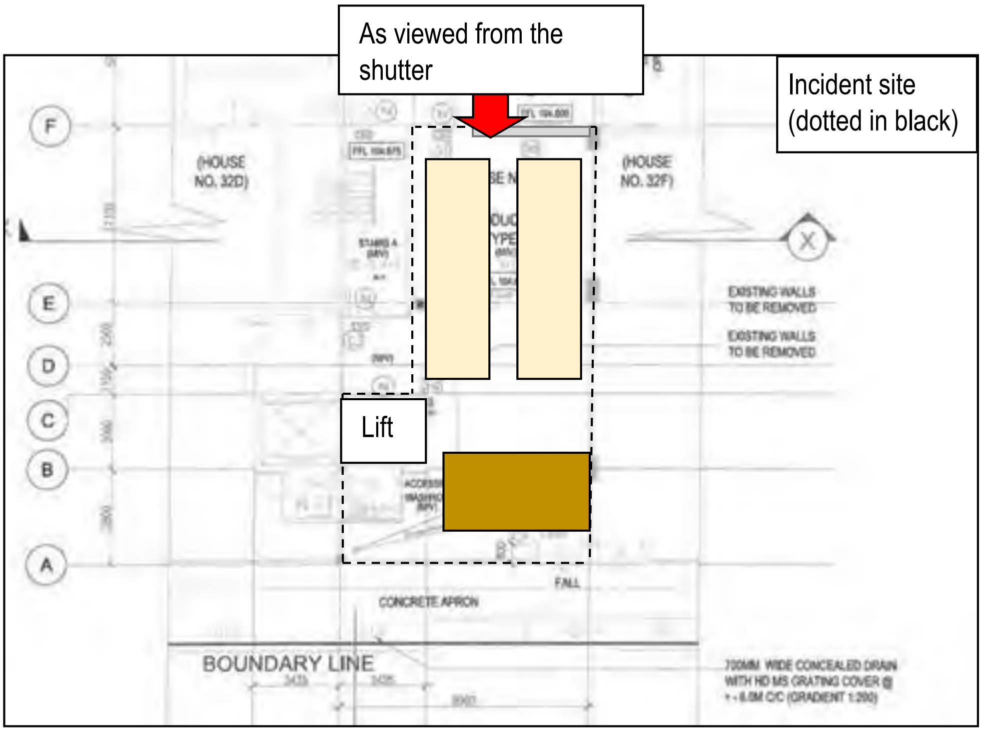

For ease of reference, the floor plan provided by MOM is used and annotated to indicate the examined area and findings. Figure above shows the point of view for the figure below.

Front end of the incident unit

Figure 1: __Front End of Unit__. The front of the unit had a shutter door and was facing the common driveway. Several rolls of fire rated products, either in white packaging or aluminium foils, were found stacked on the open space area immediately outside the unit.

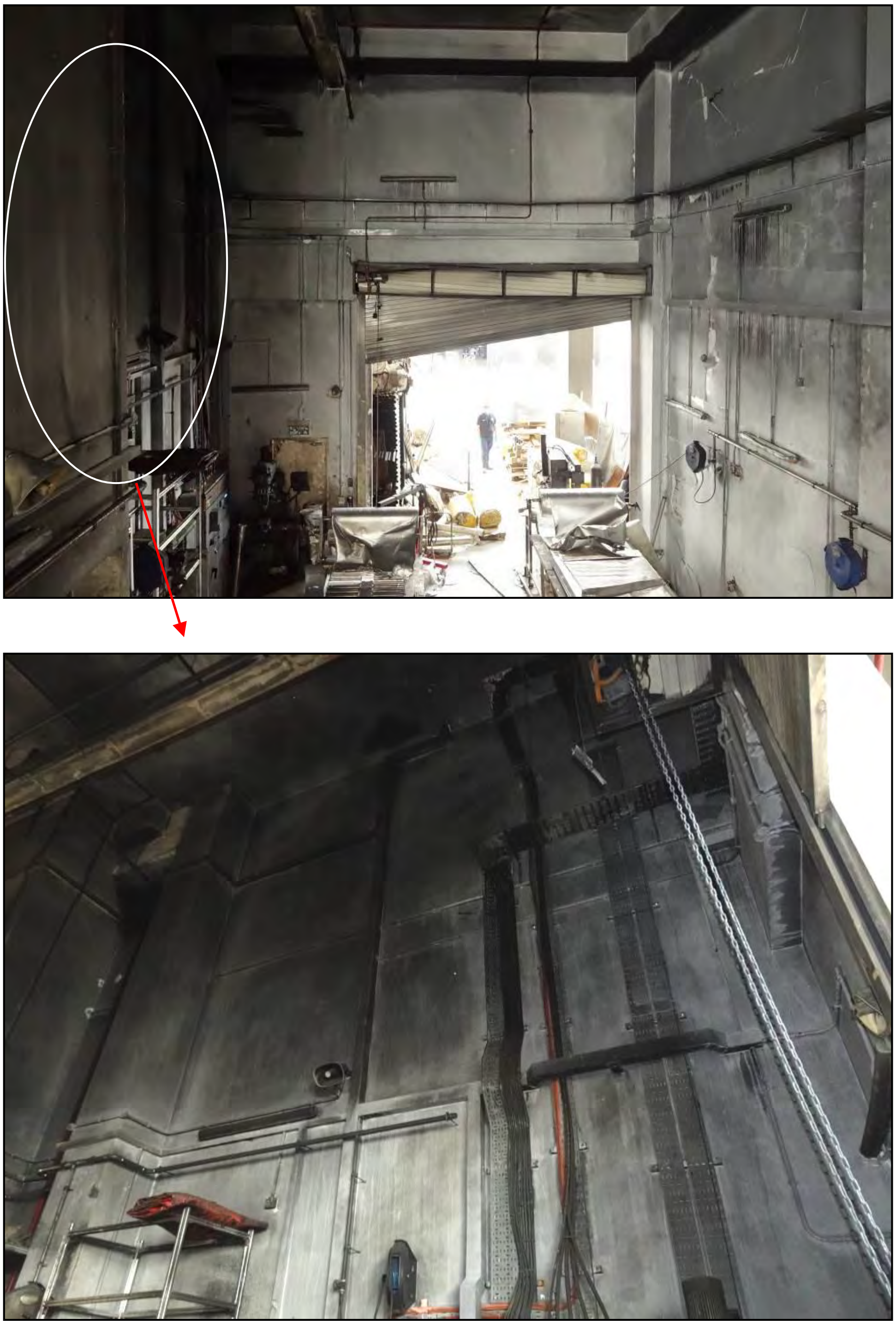

Charred walls towards the front of the unit

Figure 2: **<u>Interior of the Unit</u>**. The internal walls of the unit revealed varying extent of charring, with the upper half of the wall appearing more severe.

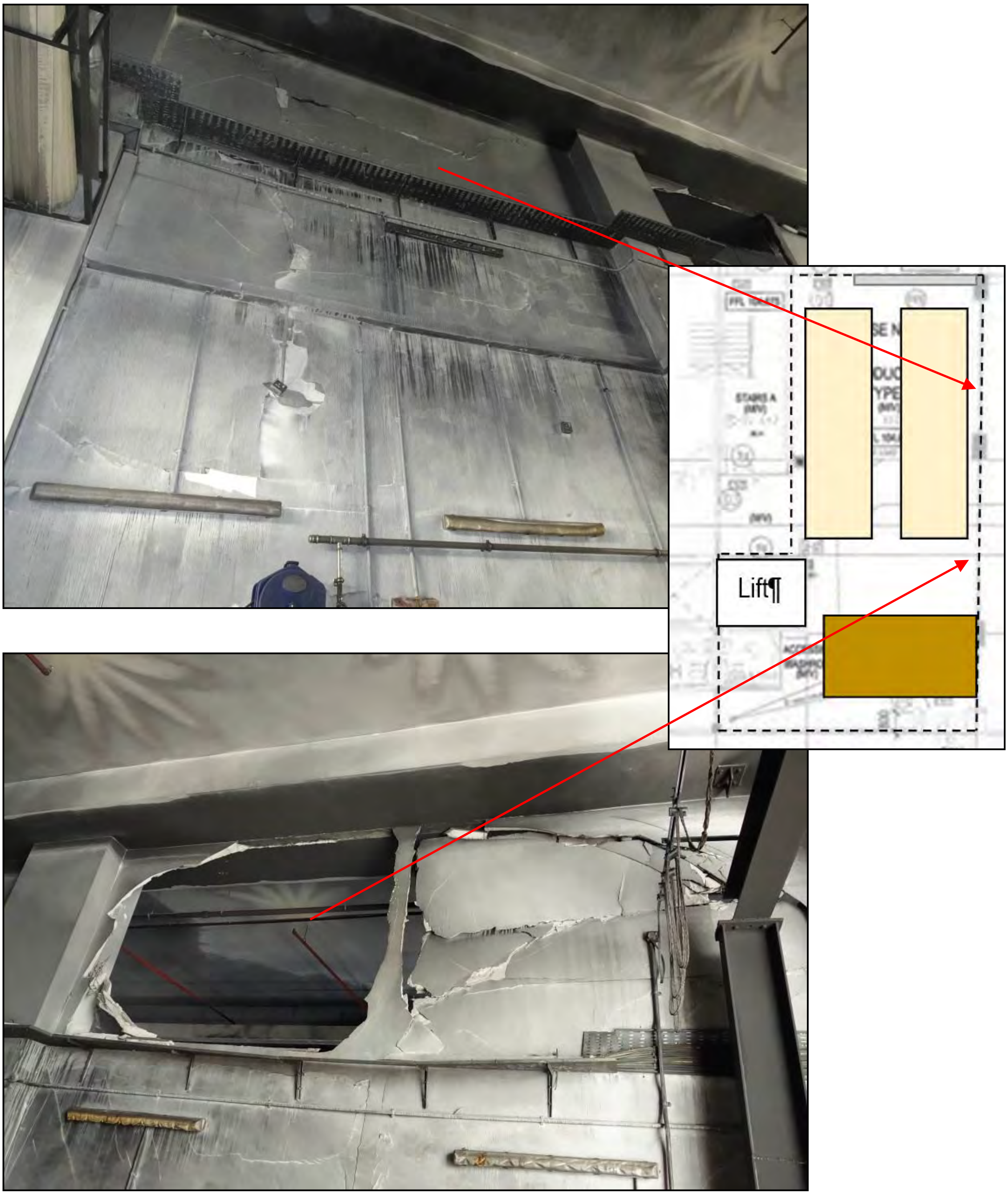

Punctured and cracked wall at localized areas on the top of the unit

Figure 3: **<u>Interior of the Unit</u>**. The internal walls of the unit revealed varying extent of charring, with the upper half of the wall appearing more severe. The explosion at the time of incident had cracked and punctured through the side walls in the vicinity of Platform floor. The lighting fixtures in the vicinity of the Platform floor were more thermally deformed as compared to the ones further away.

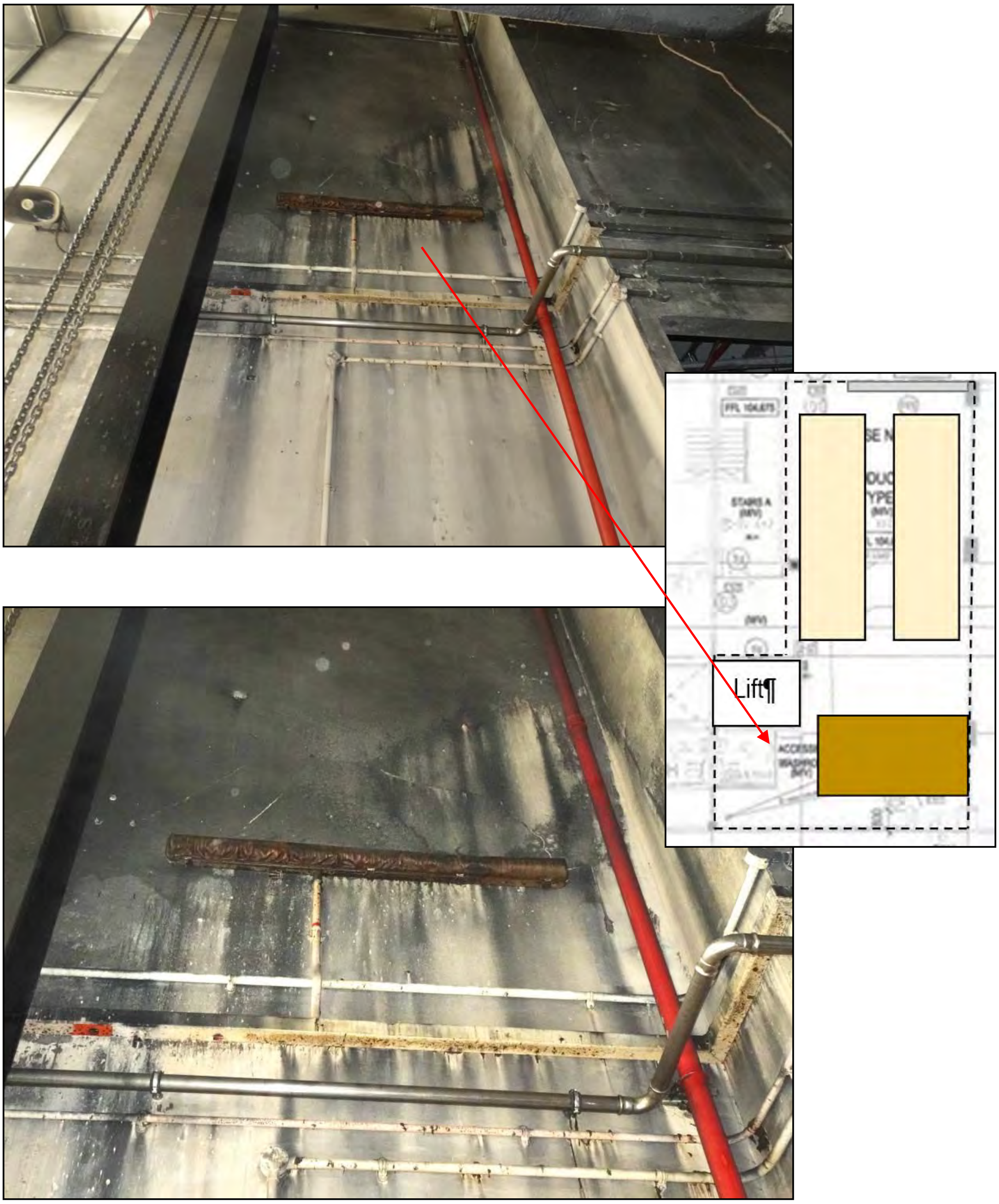

Cracked wall at localized area in the vicinity of the Platform floor

Figure 4: **Interior of the Unit**. The internal walls of the unit revealed varying extent of charring, with the upper half of the wall appeared to be more severe. Cracks were observed on the side walls next to the lifts near to the Platform floor. The lighting fixtures in the vicinity of the Platform floor were more thermally deformed as compared to the ones further away.

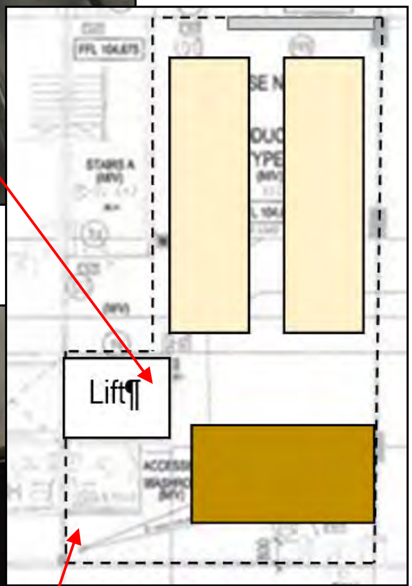

Top of the area near the lift

Rear end of the unit

Figure 5: <u>**Rear End of Unit**</u>. The top partition wall of the lift area was also damaged in the fire explosion incident. The rear walls were cracked and punctured through, especially for the top half sections.

Punctured wall at the rear end of the unit

Figure 6: **<u>Rear End of Unit</u>**. The rear walls were cracked and punctured through, especially for the top half sections.

Cracked wall at the rear end of the unit

External of the unit

Figure 7: **Rear End of Unit**. The rear walls were cracked and punctured through, especially for the top half sections.

Front side of Mixer Machine

Figure 8: **<u>Mixer Machine</u>**. Remnant whitish insulation wool was observed to remain secured to the front and rear sides of the Mixer Machine. A RTD sensor was observed in the mixing tank, but not in the oil jacket.

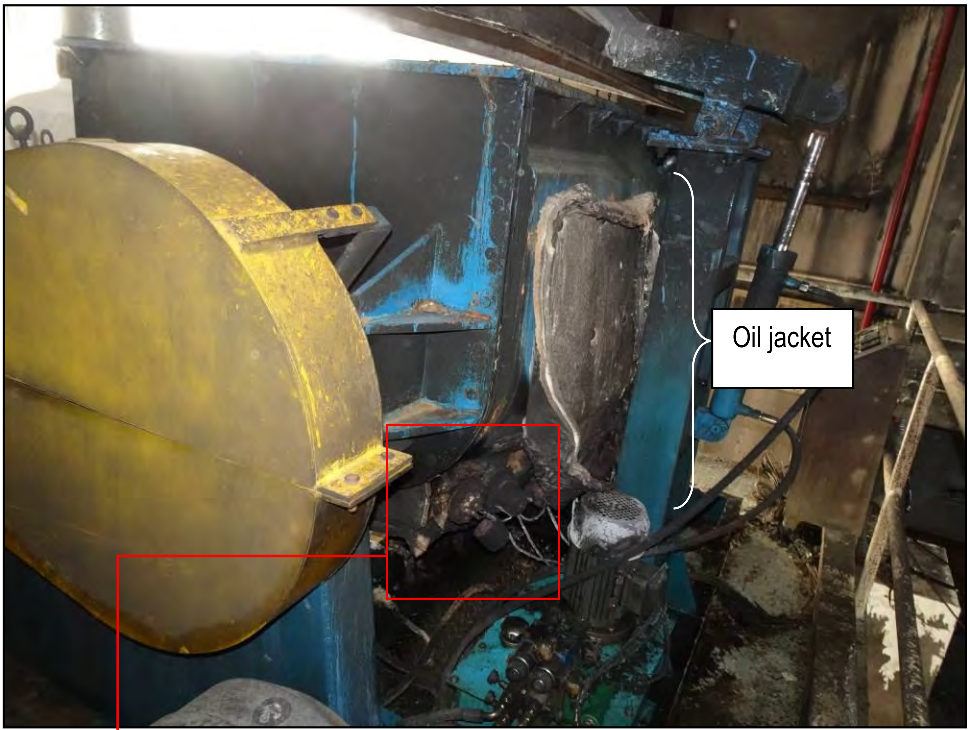

Rear side of the Mixer Machine

Tearing along the weld joint of the oil jacket around the heater

Figure 9: **<u>Mixer Machine, Oil Jacket Around Heater</u>**. Close examination of the oil jacket revealed tearing damage along the bottom-rear corner weld joints, adjacent to the heaters. The fractured bottom-rear weld joint configuration appeared different from the original weld joints further away.

Tearing of oil jacket along the weld joint around the heater on the other end of the Mixer Machine

Figure 10: **<u>Mixer Machine, Oil Jacket Around Heater</u>**. Close examination of the oil jacket revealed tearing damage along the bottom-rear corner weld joints, adjacent to the heaters. The fractured bottom-rear weld joint configuration appeared different from the original weld joints further away.

Weld repair area on the oil jacket at the front of the Mixer Machine

Figure 11: **Mixer Machine, Oil Jacket at the Front Side**. Examination of the weld joints on the front side of the oil jacket revealed that the bottom-front corner weld joints were weld repaired prior to the fire explosion incident.

Faulty heater

Figure 12: **Mixer Machine, Faulty Heater**. Examination of the heaters revealed faulty connections on the second heater.

Internal condition of mixing tank

Charred insulation wools on the Platform floor under the oil jacket

Figure 13: **<u>Mixer Machine, Internal Condition and Bottom Area</u>**. The interior of the mixing tank was partially filled with water and dough-form product mixture, apart from the sigma blades. Some remnant insulation wools at the bottom of the Mixer Machine on the Platform floor were charred.

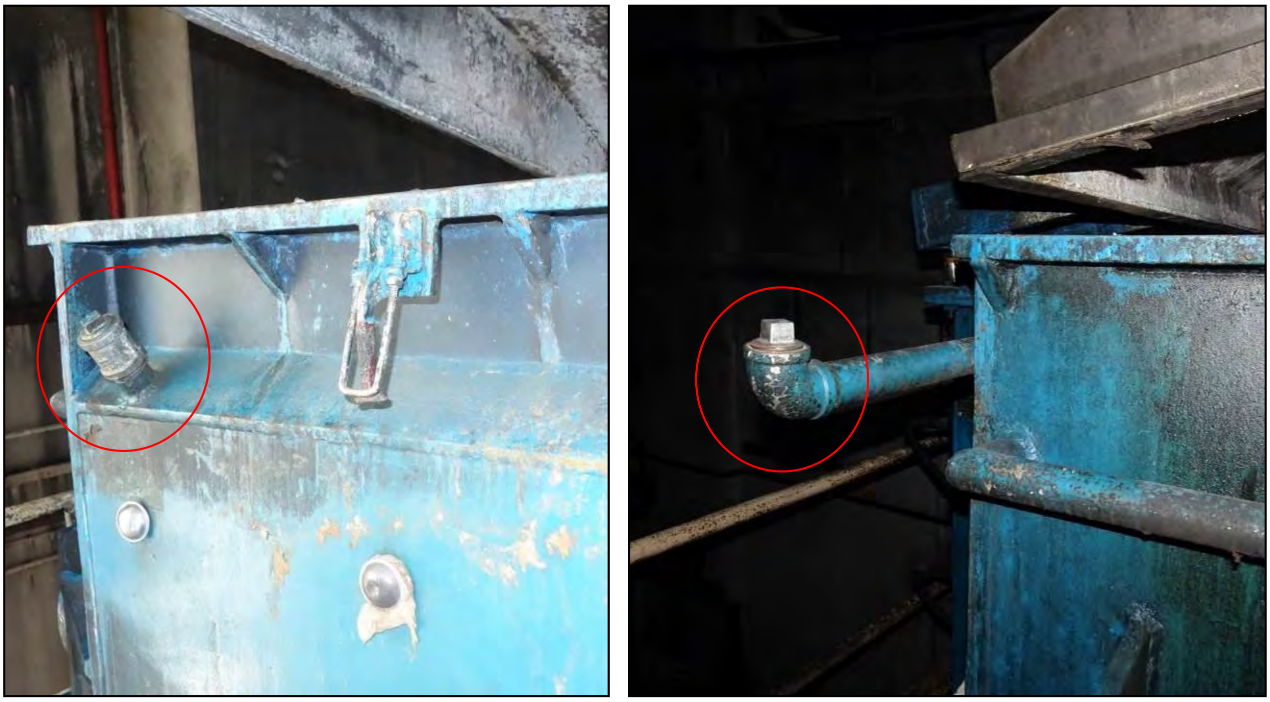

Access port to top up oil (circled, left) and vent port of oil jacket at the rear side (circled, right)

Drain port for oil jacket (circled)

Figure 14: **Mixer Machine, Access, Vent and Drain Ports for Oil Jacket**. The access and vent ports of the oil jacket were in closed mode at the time of inspection. The drain port at the bottom of the oil jacket was also in closed state.

Electrical panel box (top, left) and new heater (circled)

Figure 15: **Electrical Panel Box and New Heater**. A new heater, that was placed next to the Mixer Machine, appeared relatively unaffected by the fire explosion. The electrical switches and buttons as well as the display screens on the electrical panel box were damaged by the fire explosion.

Partially melted electrical switches and buttons

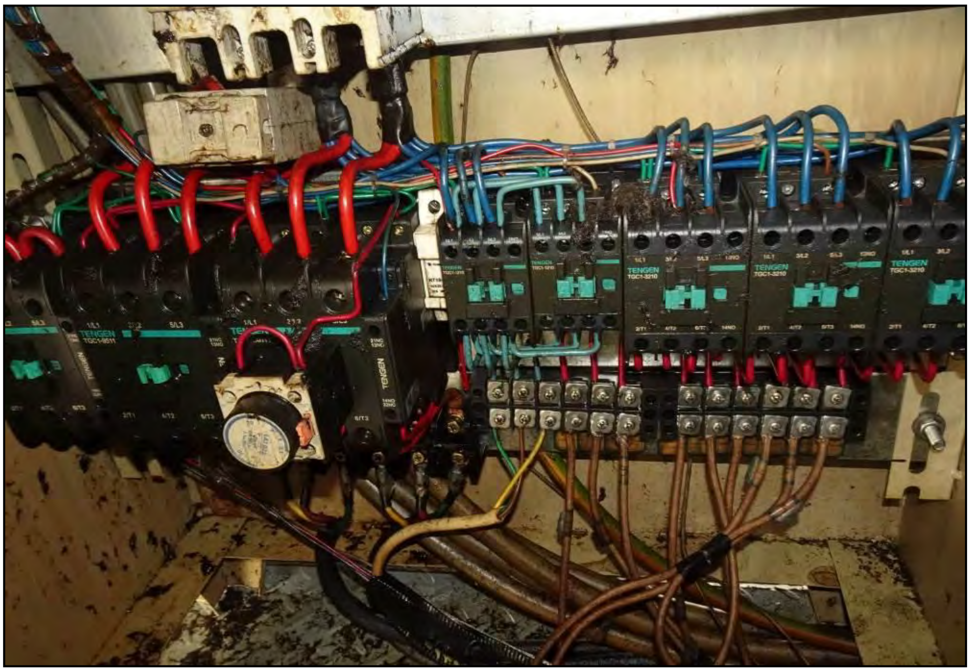

Intact electrical wiring within the panel box

Figure 16: **Electrical Panel**. The electrical switches and buttons as well as the display screens on the electrical panel were damaged by the fire explosion. The electrical circuit system within the panel box appeared relatively intact.

Oil pails on Platform floor

Oil funnel

Figure 17: **Oil Pails and Funnel**. Three oil tubs, which were contaminated by water, were found on the Platform floor next to the hopper. The oil funnel was found on the ground floor at the time of inspection.

Appendix B:
As-Received Exhibits

3D Sketch for Illustration Purpose with General Terminology

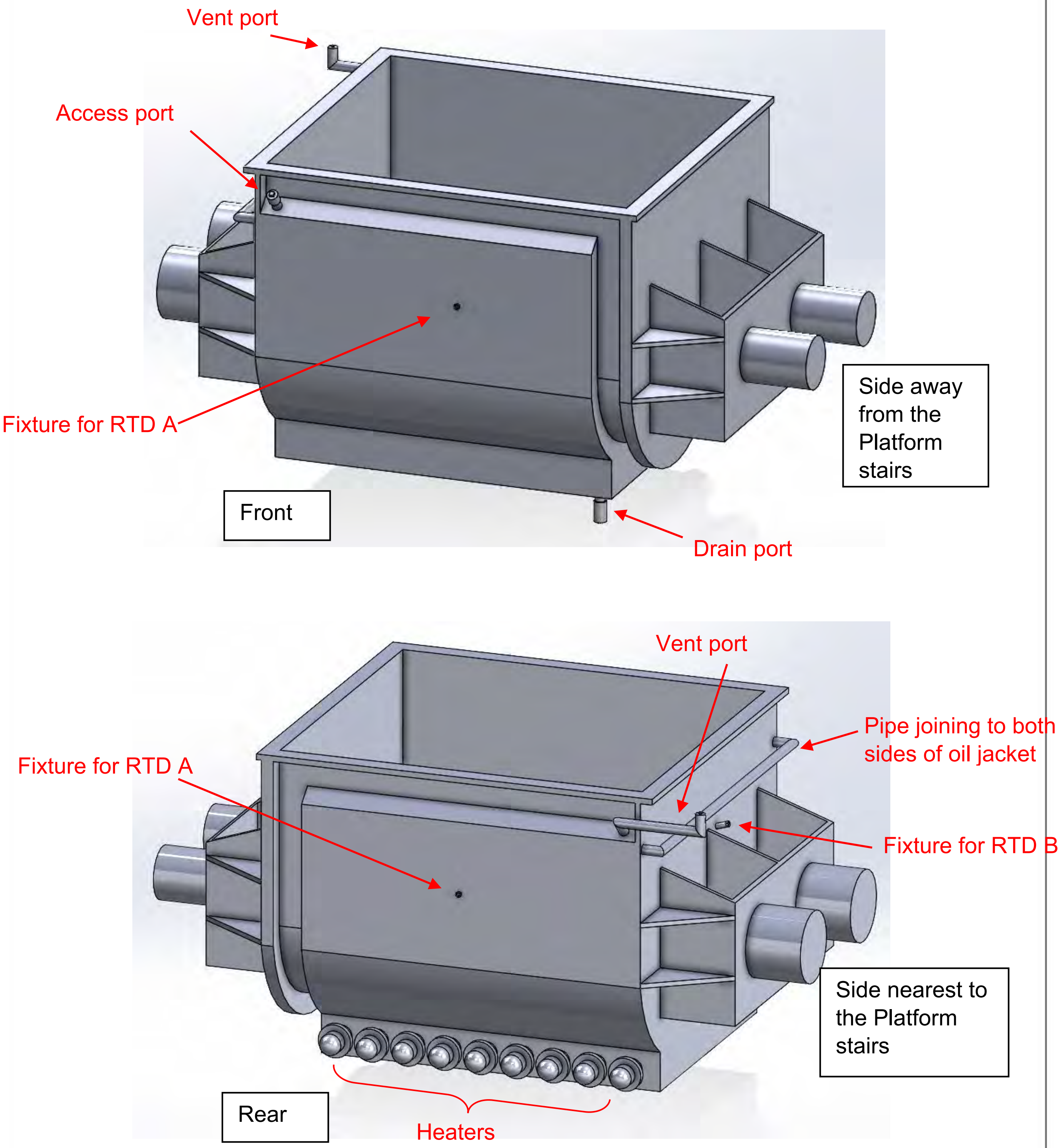

Figure 18: Mixer Machine and some used terminologies.

As-Received Mixer Machine

Side away from the Platform stairs

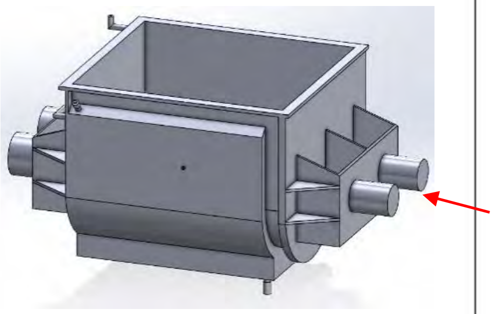

Figure 19: As-received condition of the Mixer Machine as viewed from the side away from the Platform stairs.

Side nearest to the Platform stairs

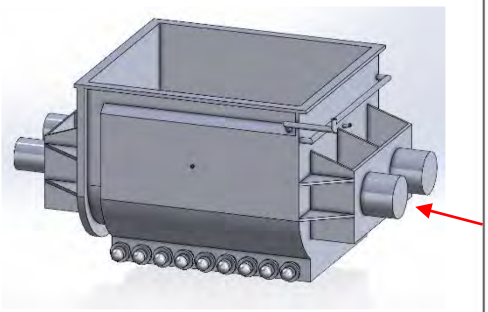

Figure 20: As-received condition of the Mixer Machine as viewed from the side nearest to the Platform stairs.

As-Received Mixer Machine

View from the front

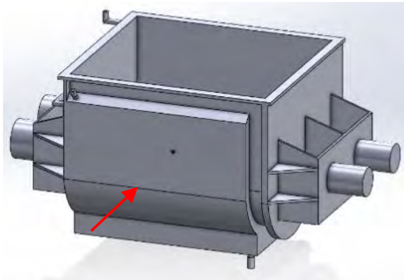

Figure 21: As-received condition of the Mixer Machine from the front.

View from the rear

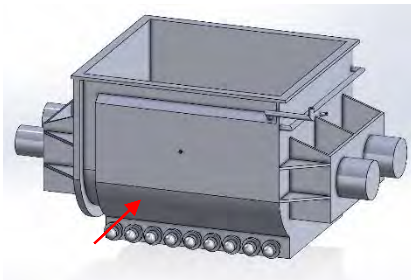

Figure 22: As-received condition of the Mixer Machine from the rear.

After Removal of Insulation

View from the front


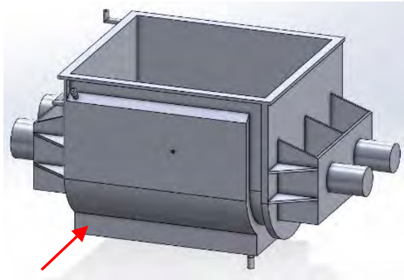

Figure 23: As-received condition of the Mixer Machine as seen from the front.


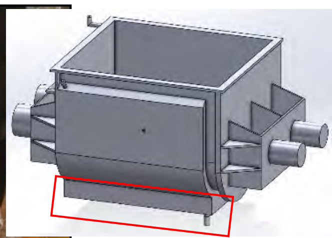

Figure 24: As-received condition of the Mixer Machine as seen from the front bottom.

After Removal of Insulation

View from the front

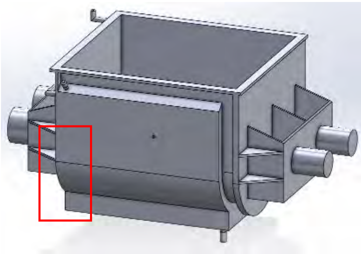

Figure 25: As-received condition of the Mixer Machine as seen from the front left bottom corner.

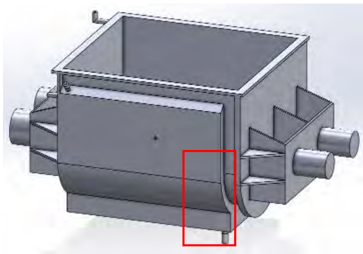

Figure 26: As-received condition of the Mixer Machine as seen from the front right bottom corner.

After Removal of Insulation

View from the rear

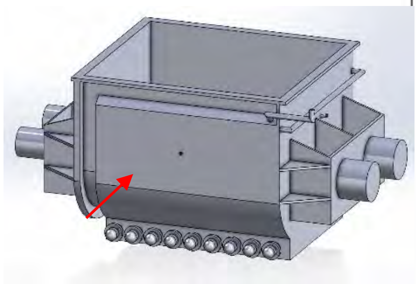

Figure 27: As-received condition of the Mixer Machine as seen from the rear.

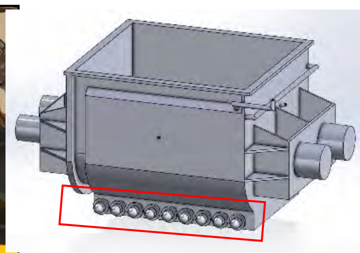

Figure 28: As-received condition of the Mixer Machine as seen from the rear bottom.

After Removal of Insulation

View from the rear

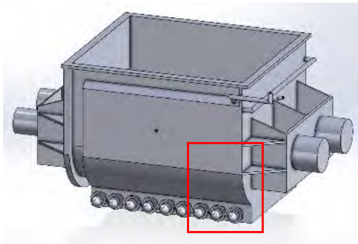

Figure 29: As-received condition of the Mixer Machine as seen from the rear right bottom corner.

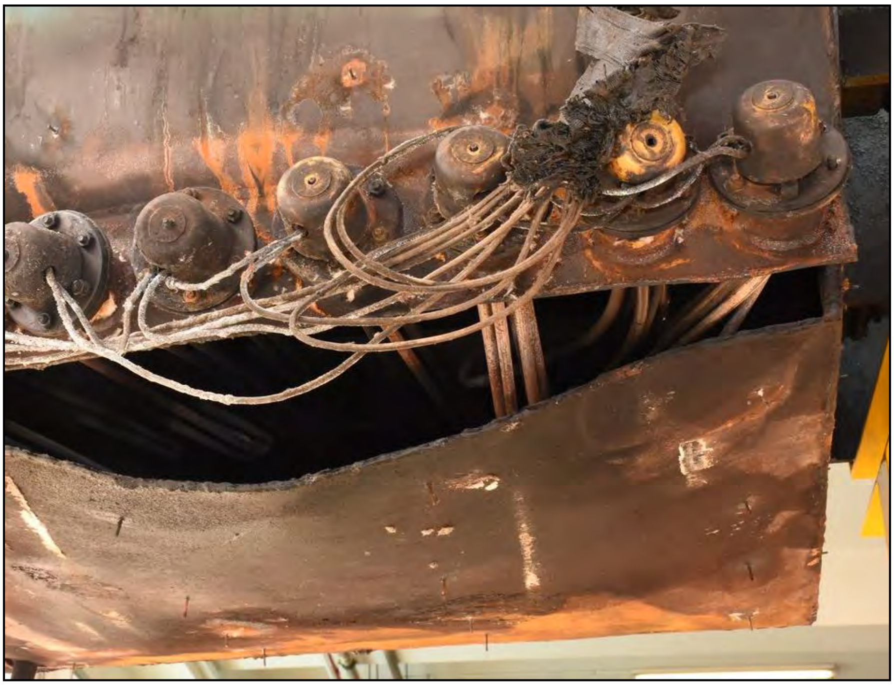

Figure 30: As-received condition of the Mixer Machine as seen from the rear bottom.

After Removal of Insulation

View from the rear

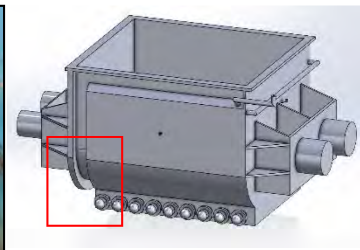

Figure 31: As-received condition of the Mixer Machine as seen from the rear left bottom corner.

Figure 32: Close-up view of the rear left bottom corner.

Other Received Exhibits

Other Samples

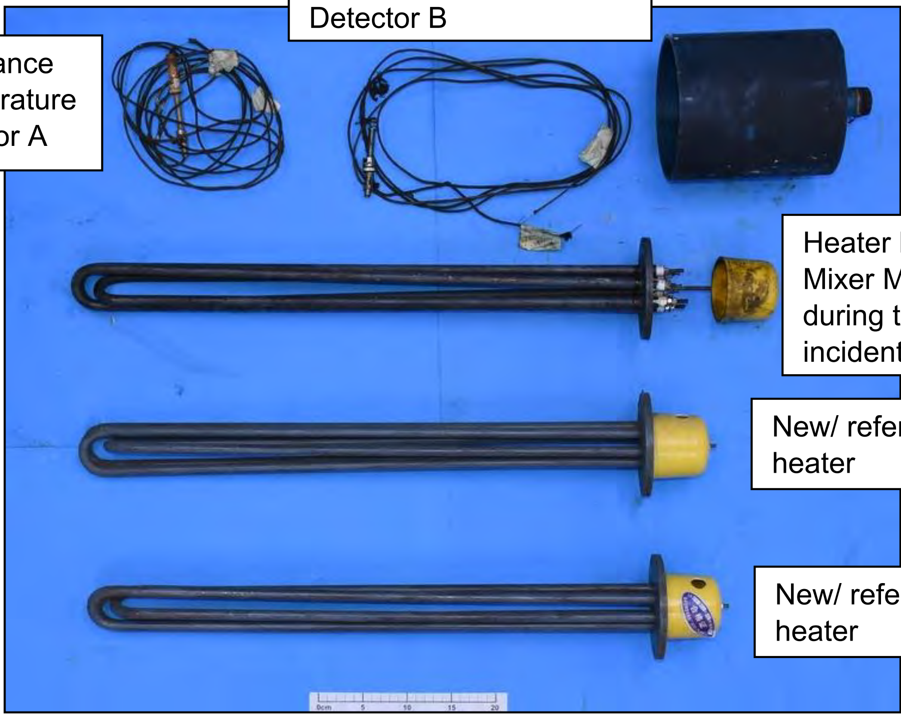

Figure 33: As-received condition of the additional samples.

Electrical Panel

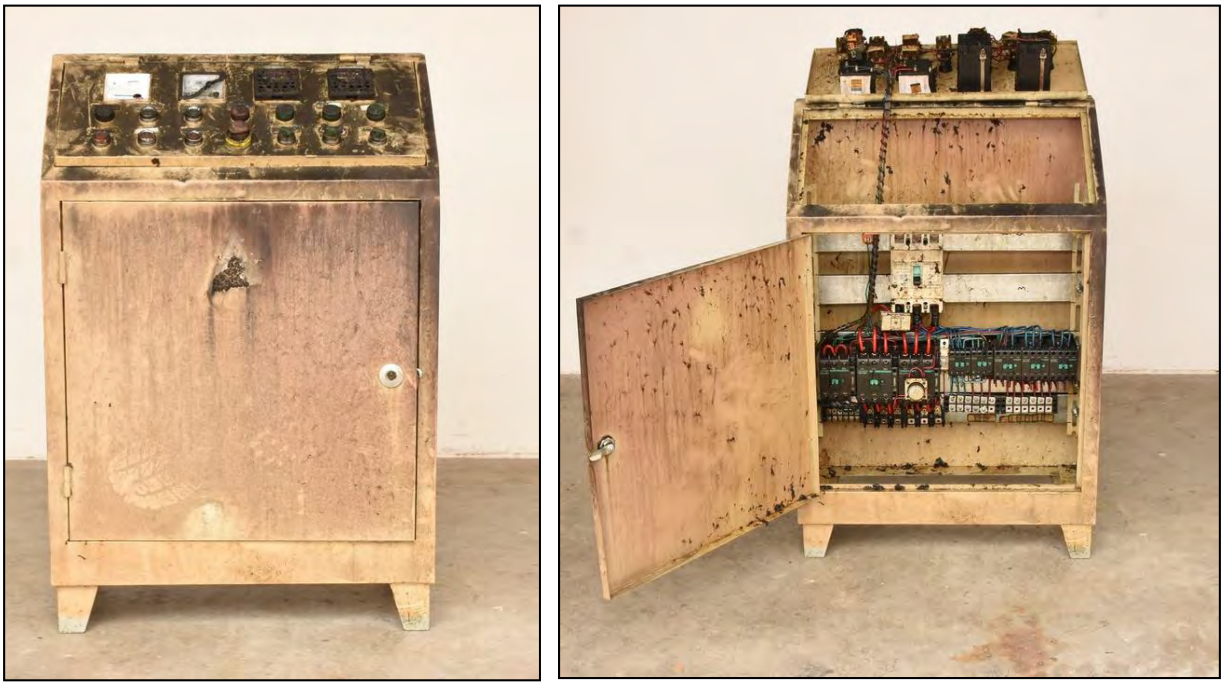

Figure 34: As-received condition of the electrical panel.

Other Received Exhibits

Used/Failed Heaters

Figure 35: Used heater received on 28th May 2021.

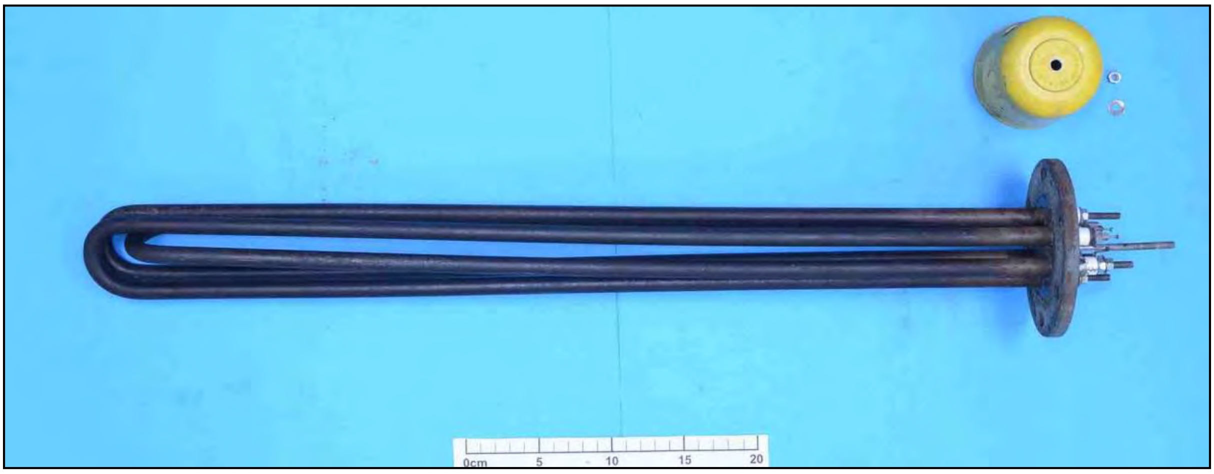

Figure 36: Used heater received on 1st June 2021.

Appendix C:
Visual and Macroscopic Examination

Visual and Macroscopic Examination

Front

Figure 37: Marked out locations on the front for detailed examination.

Figure 38: Marked out locations on the front corners for detailed examination.

Visual and Macroscopic Examination

Front

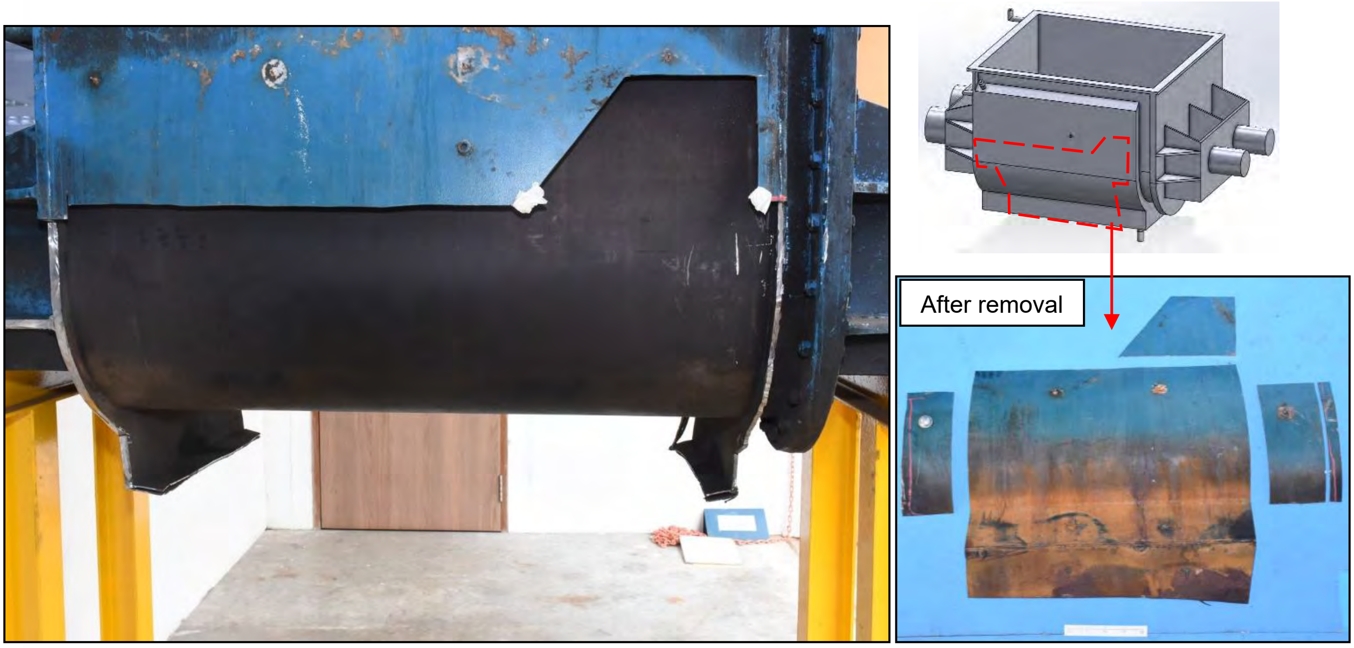

Figure 39: Internal condition of the oil jacket from the front side. The internal surface was generally covered by black soot.

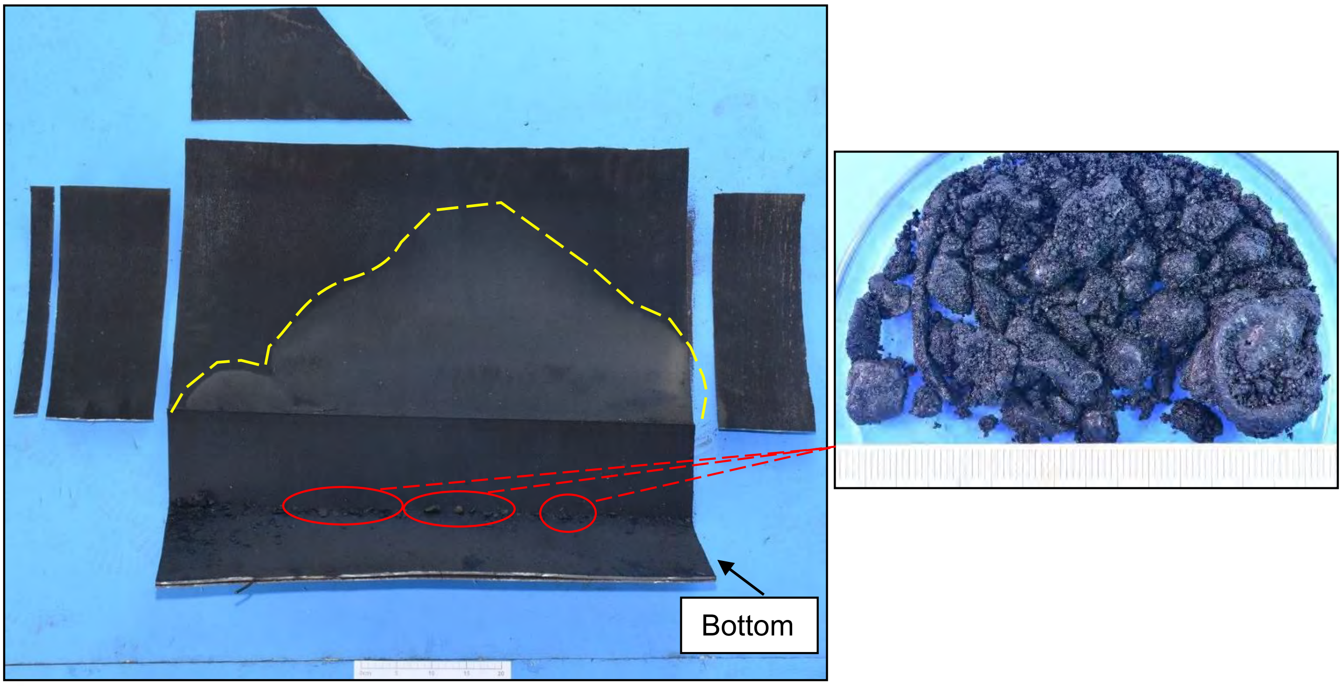

Figure 40: Cut out sections of oil jacket wall and bottom. Hard debris of various sizes (up to about 20 mm) were found at the bottom face (see red). There was also a layer of black soot/deposits masking the internal surface and the bottom face of the oil jacket (see also Figure 143). Oil stains and drips pattern were visible (see yellow line).

Visual and Macroscopic Examination

Front side, left edge weld

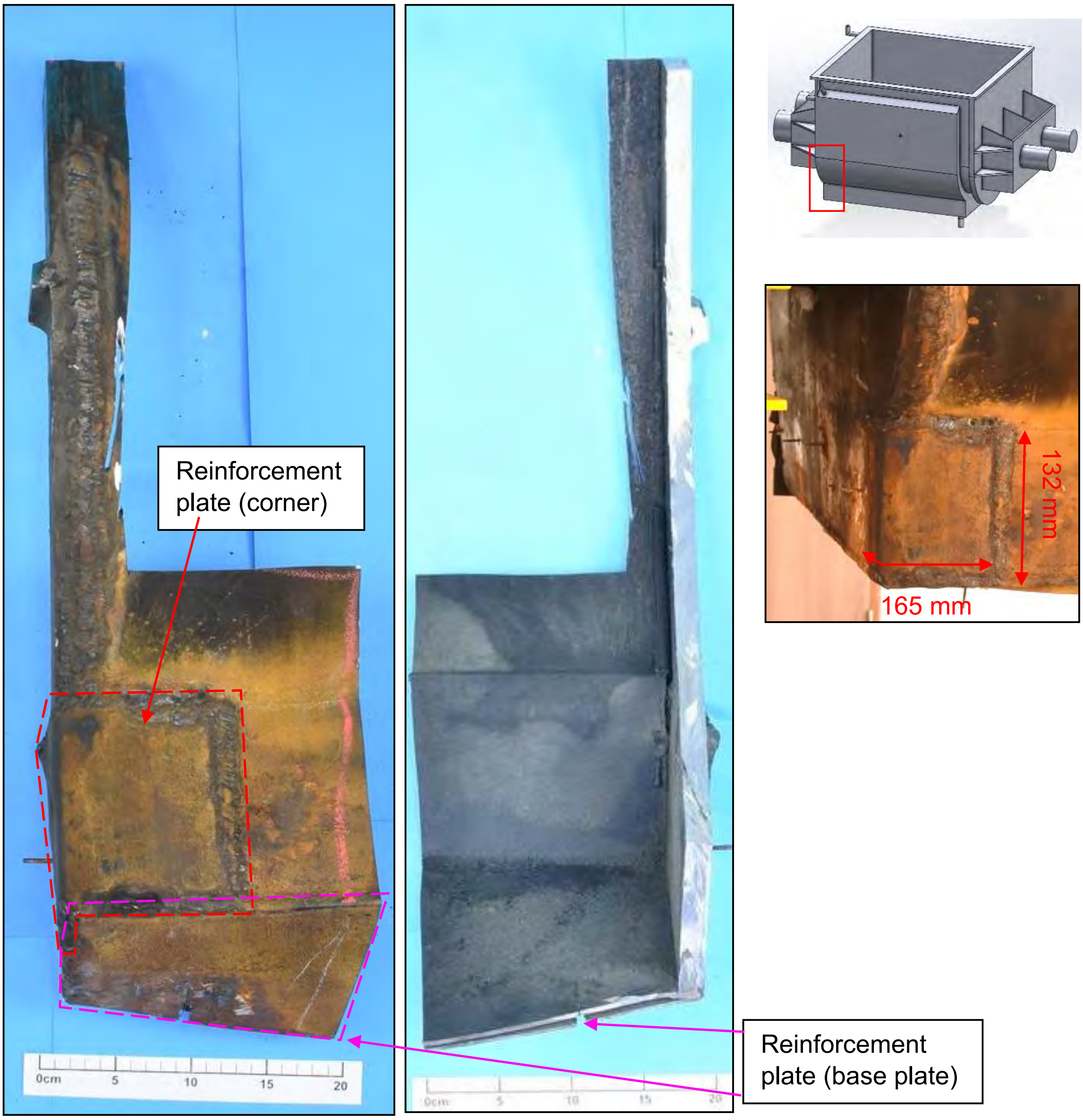

Figure 41: Cut out section of the front side, left edge weld. The left figure shows the external condition and the right figure shows the internal condition of this section. This cut out section included the original and repair welds. Parts of the reinforcement plates (corner and base plate identified with red and pink dotted lines) were visible here. The corner reinforcement plate had dimension of about 165 mm by 132 mm.

Visual and Macroscopic Examination

Front side, left edge weld (External Side)

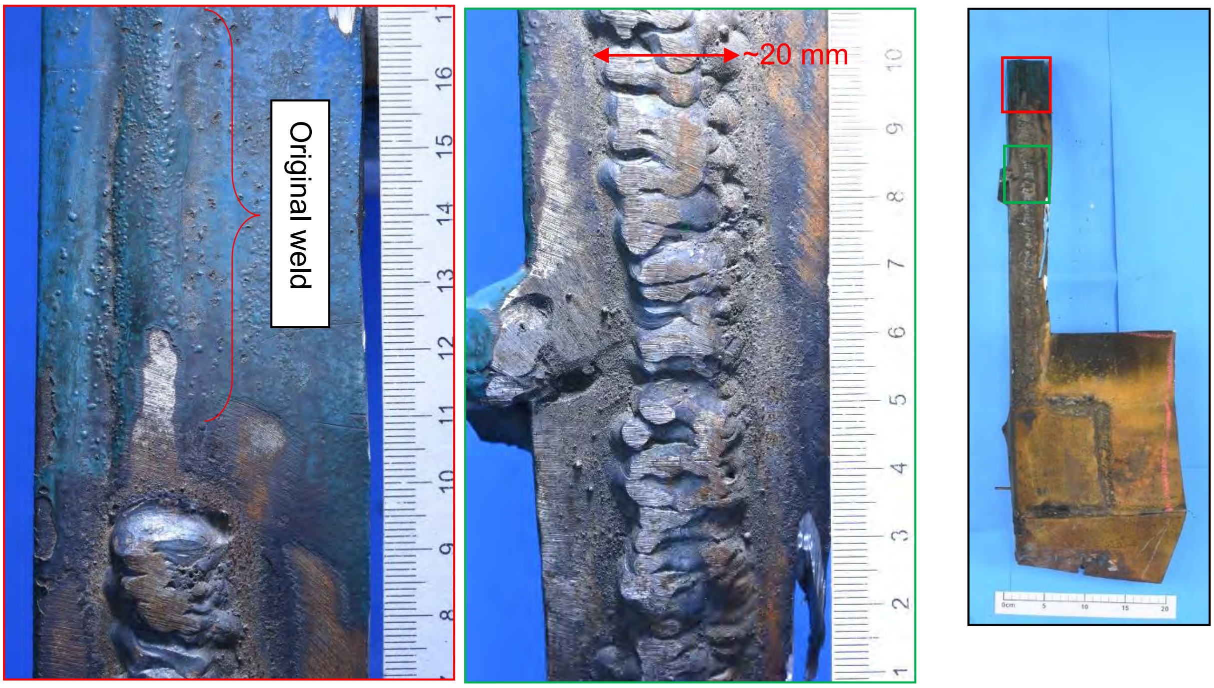

Figure 42: Close up view of side weld. Part of the original weld is indicated (in red) in the left figure. The rest of the weld towards the bottom was repaired and had a face width of about 20 mm.

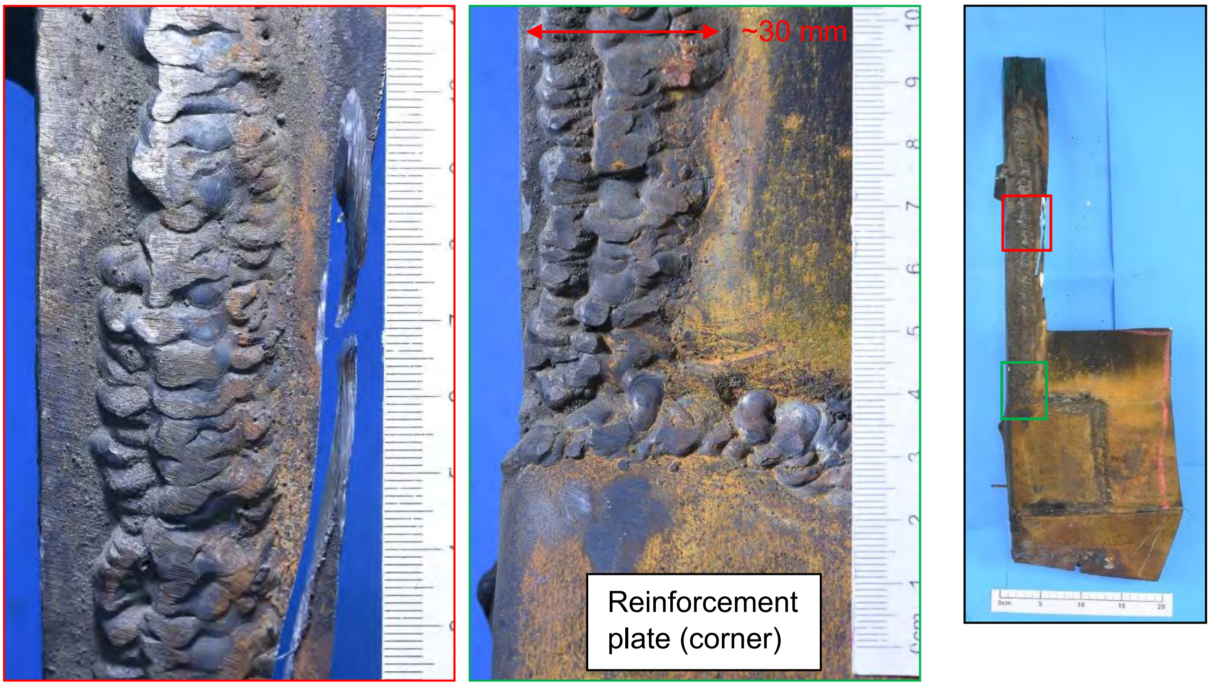

Figure 43: Close up view of side weld. The face width of the weld increases towards the bottom and reinforcement corner plate. The face width was up to about 30 mm.

Visual and Macroscopic Examination

Front side, left edge weld (External Side)

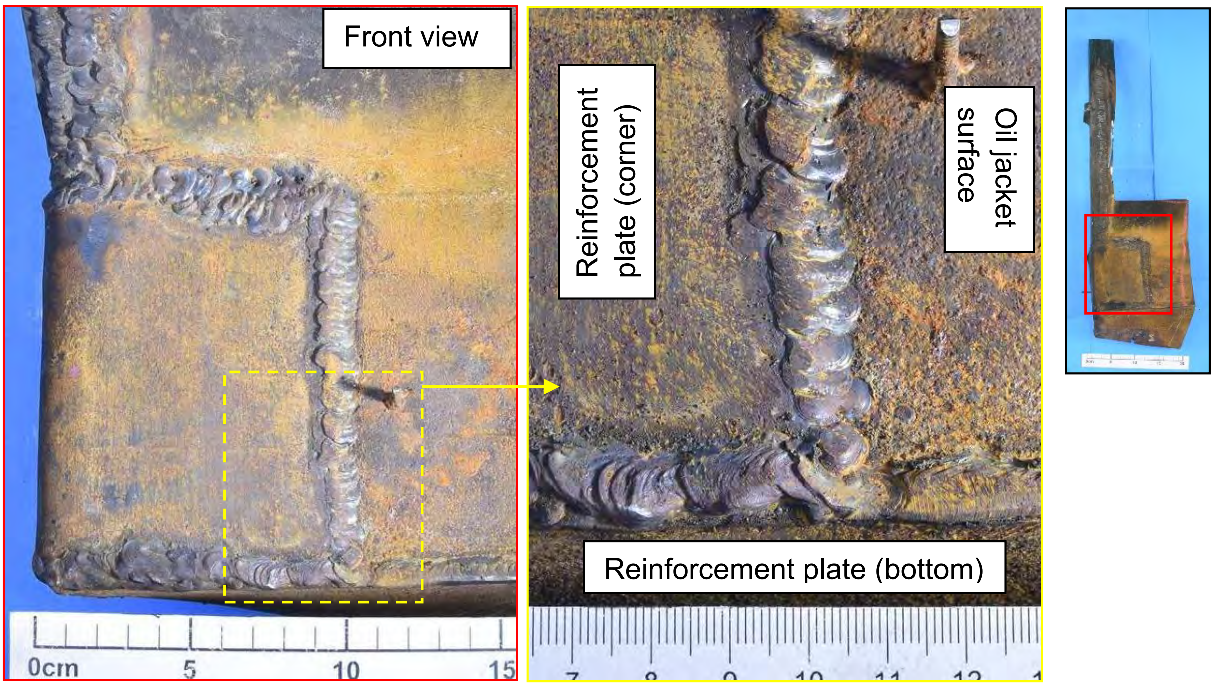

Figure 44: Close up view of bottom corner. The reinforcement plate was added at the corner by welding.

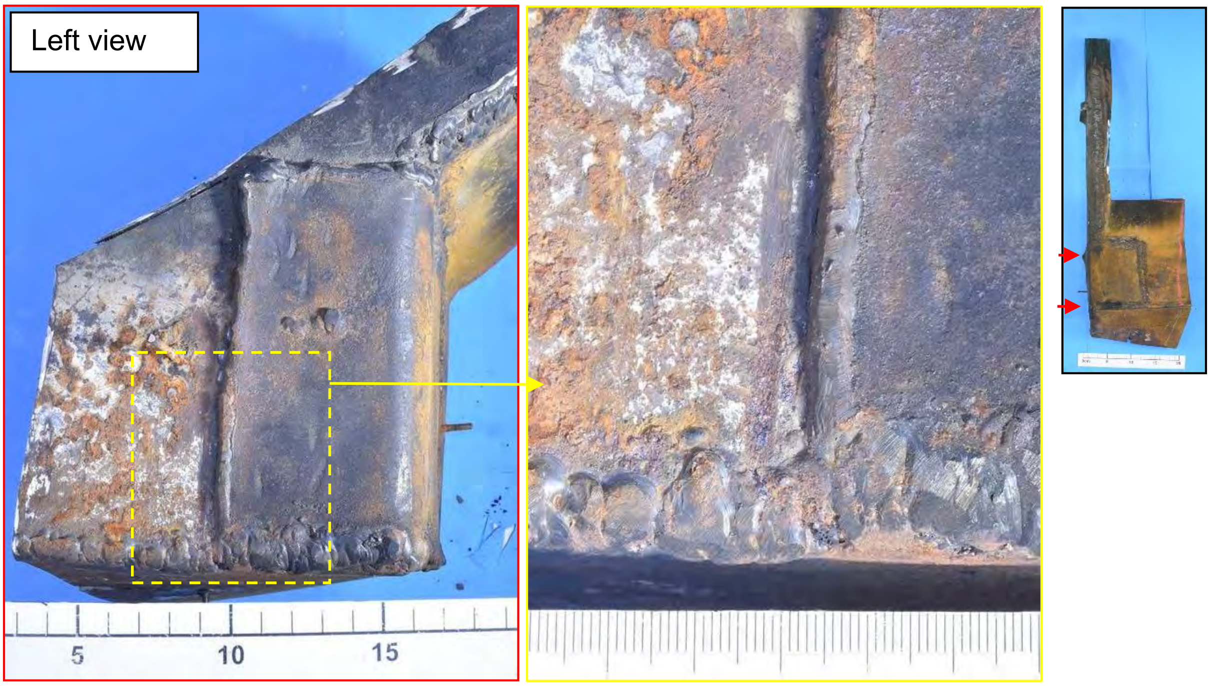

Figure 45: Close up view of bottom corner from another angle. Similar welding done to the oil jacket wall to add the reinforcement plate.

Visual and Macroscopic Examination

Front side, left edge weld (Internal Side)

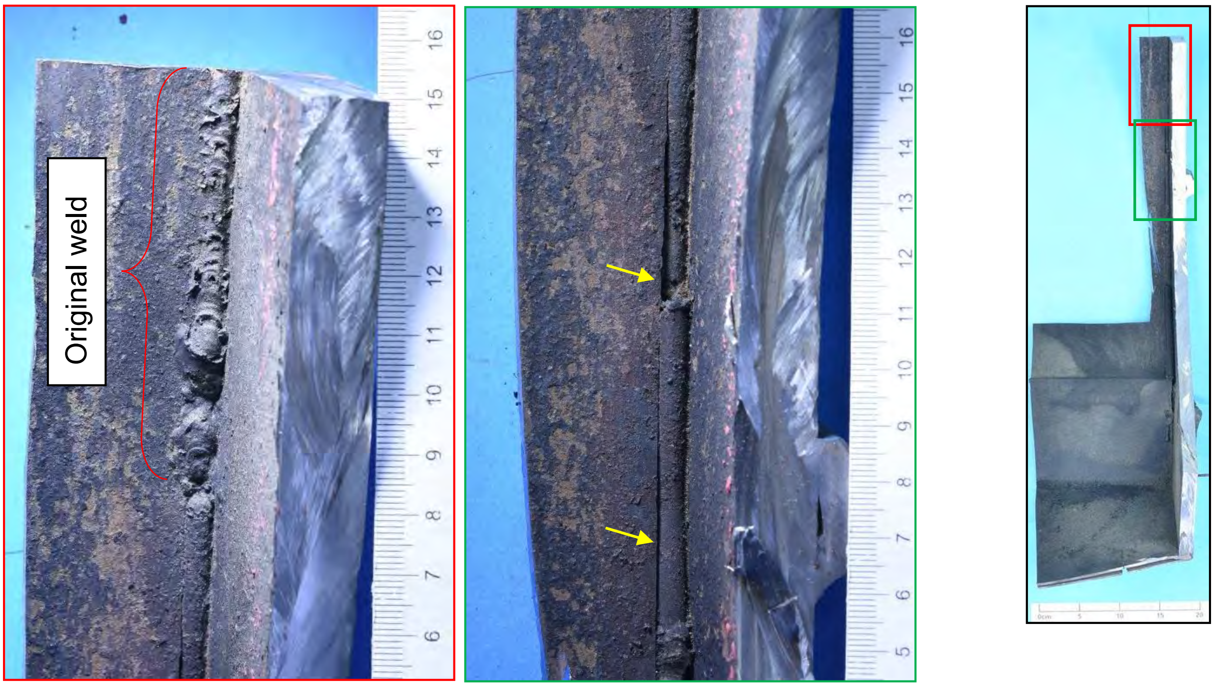

Figure 46: Condition of weld from inside the oil jacket. Part of the original weld is indicated (in red) in the left figure. The original weld root had an irregular shape. The rest of the weld was repaired, had a root surface width of about 4 mm and lack of penetration at some areas (indicated with yellow arrows).

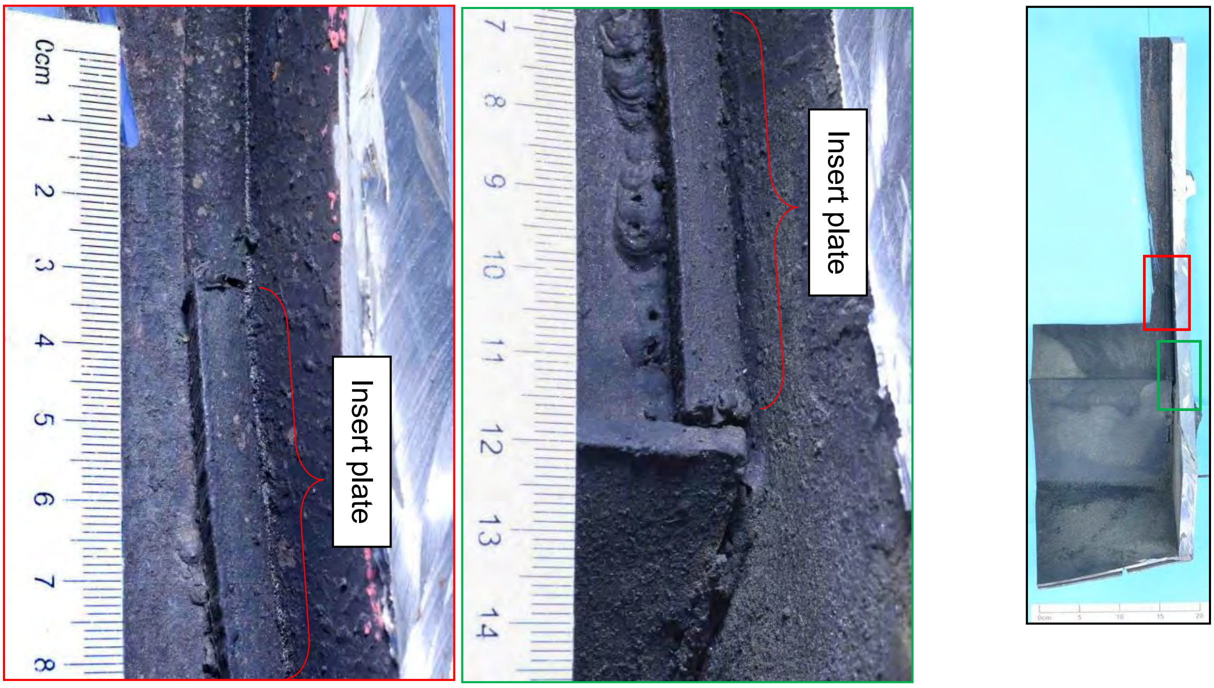

Figure 47: Condition of weld from inside the oil jacket. The width of the root surface increases towards the bottom (up to 9 mm). An insert plate with length of 120 mm was observed at a sector of the bottom end of the curved edge. (see also Section 3.4 and Figure 151)

Visual and Macroscopic Examination

Front side, left edge weld (Internal Side)

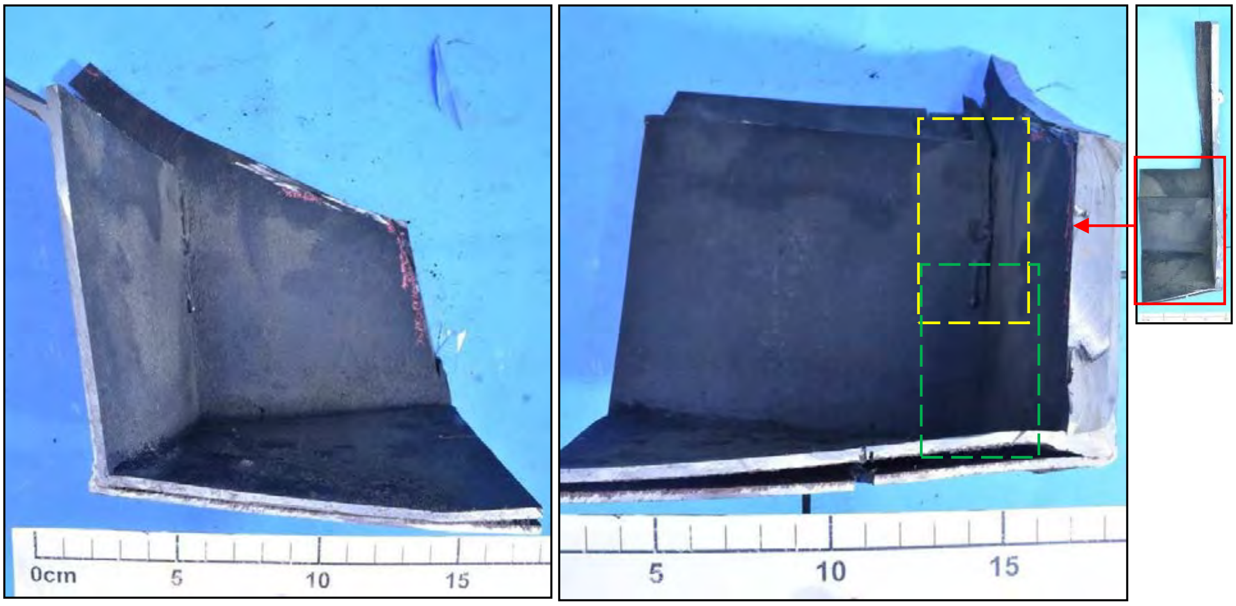

Figure 48: Condition of the internal surface of oil jacket corner. Close up views presented below with their respective colour borders.

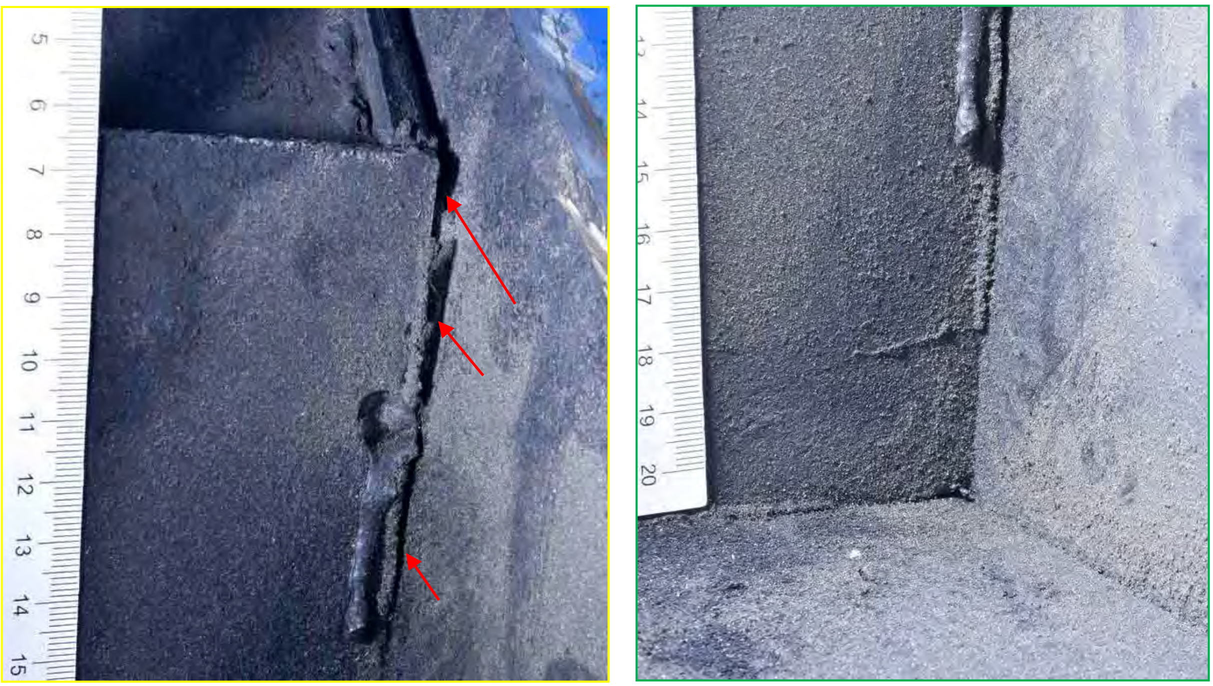

Figure 49: Close up view of the corner from inside the oil jacket. Gaps were observed between the walls (indicated with red arrows). The gap narrowed and stopped towards the bottom corner.

Visual and Macroscopic Examination

Front side, right edge weld

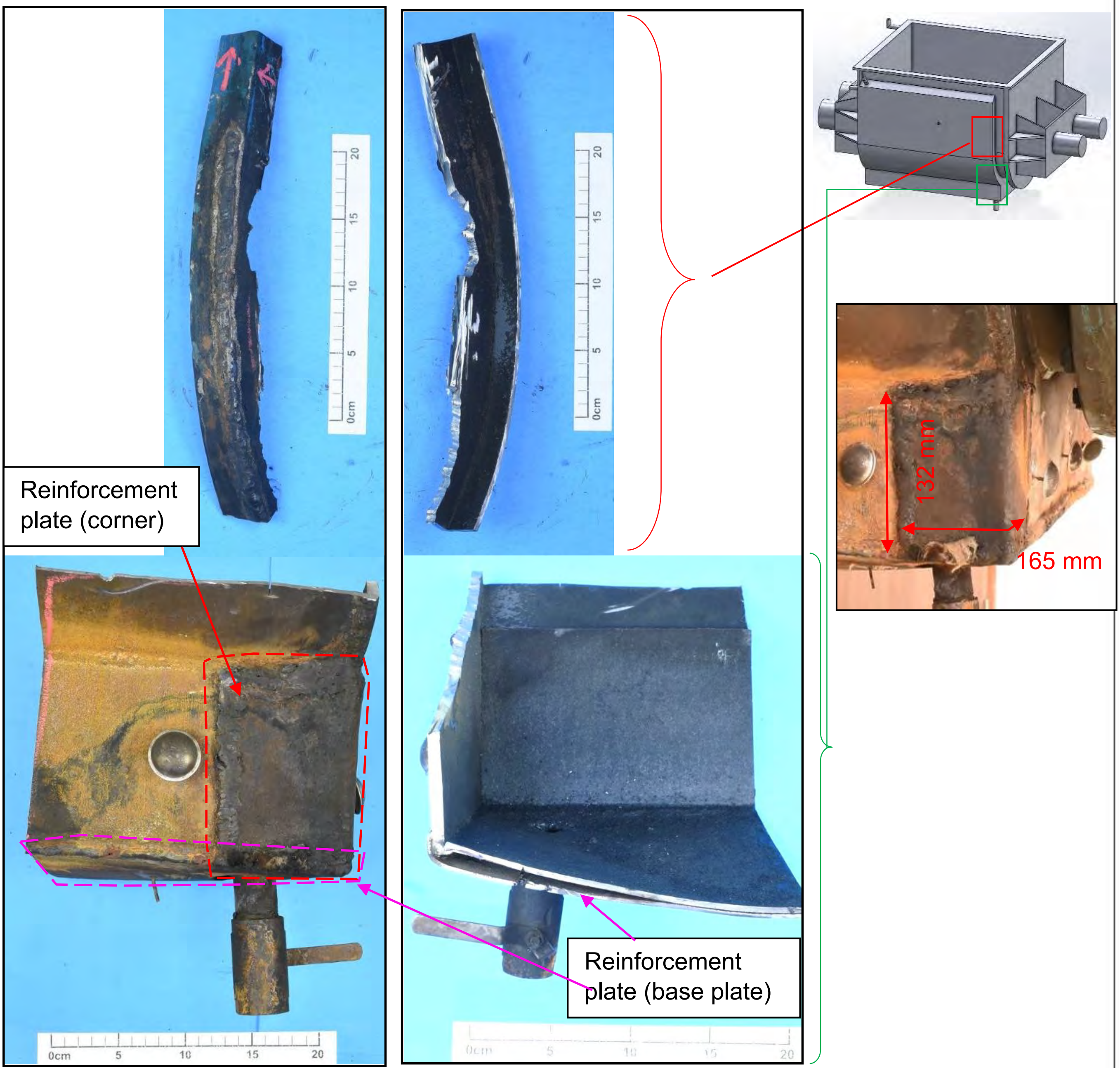

Figure 50: Cut out section of the front side, right edge weld. The left figure shows the external condition and the right figure shows the internal condition of this section. This cut out section included the original and repair welds. Parts of the reinforcement plates (corner and base plate identified with red and pink dotted lines) were visible here. The corner reinforcement plate had dimension of about 165 mm by 132 mm.

Visual and Macroscopic Examination

Front side, right edge weld (Side Edge)

Figure 51: Close up view of side weld. Part of the original weld is indicated (in red) in the left figure. The rest of the weld was repaired and had a face width of about 20 mm.

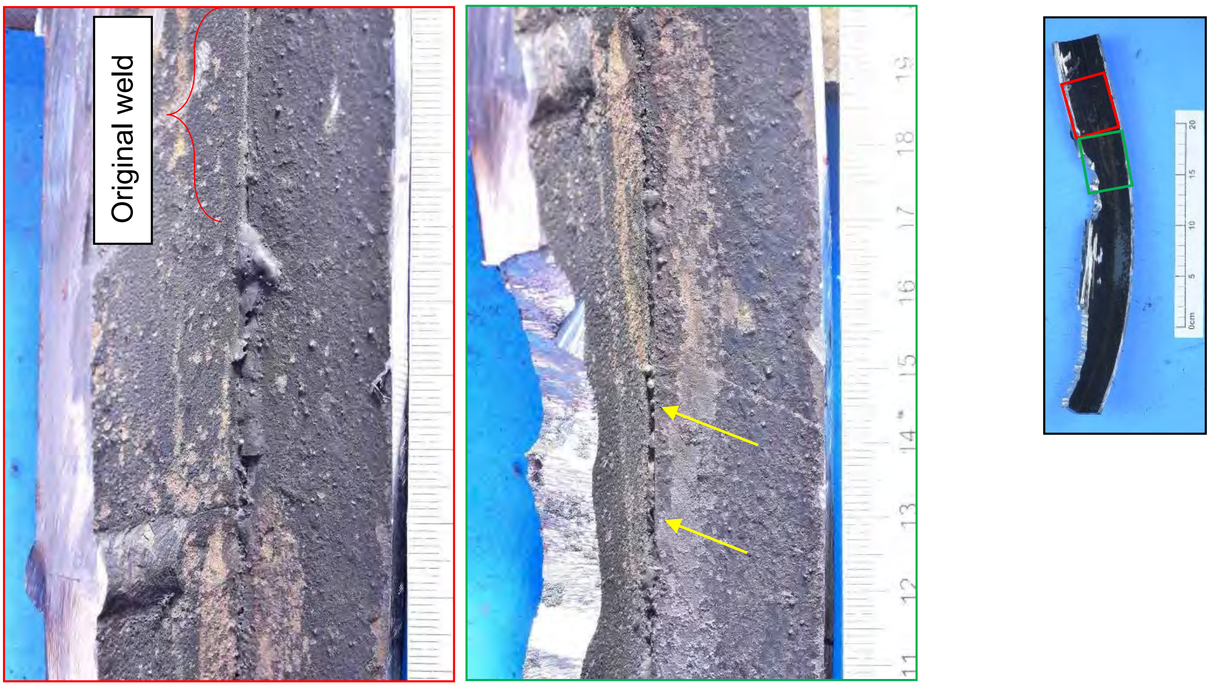

Figure 52: Condition of weld from inside the oil jacket. Part of the original weld is indicated (in red) in the left figure. The original weld root was small. The rest of the weld was repaired and had signs of lack of root penetration at some areas (indicated with yellow arrows).

Visual and Macroscopic Examination

Front side, right edge weld (Bottom Corner)

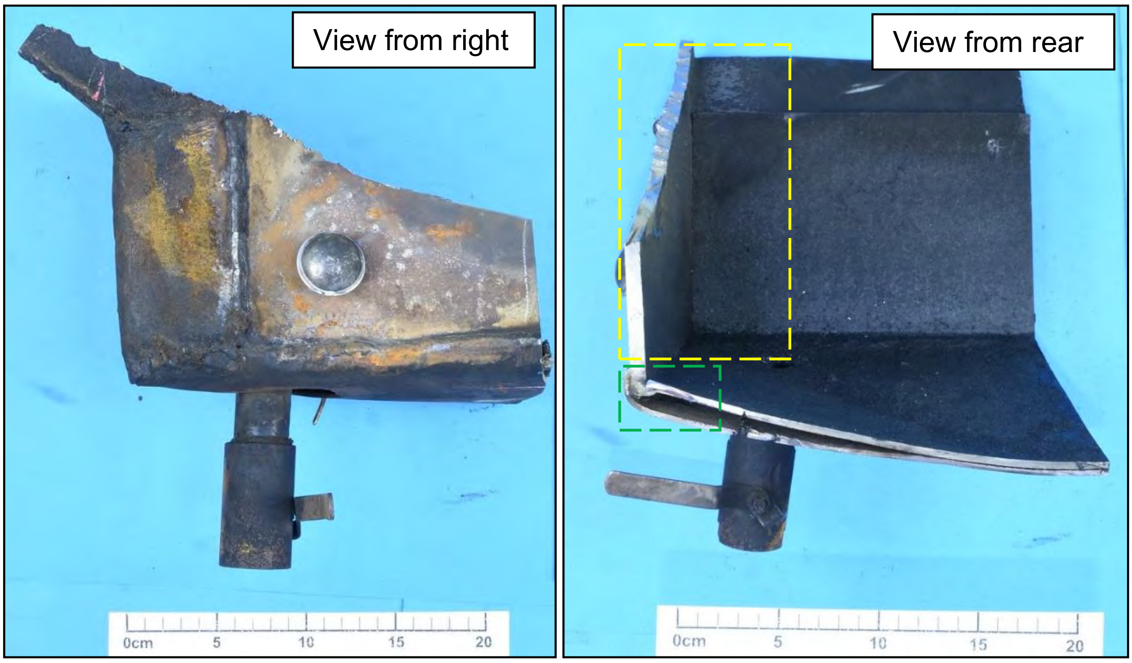

Figure 53: Condition of the internal surface of oil jacket corner. Close up views presented below with their respective colour borders.

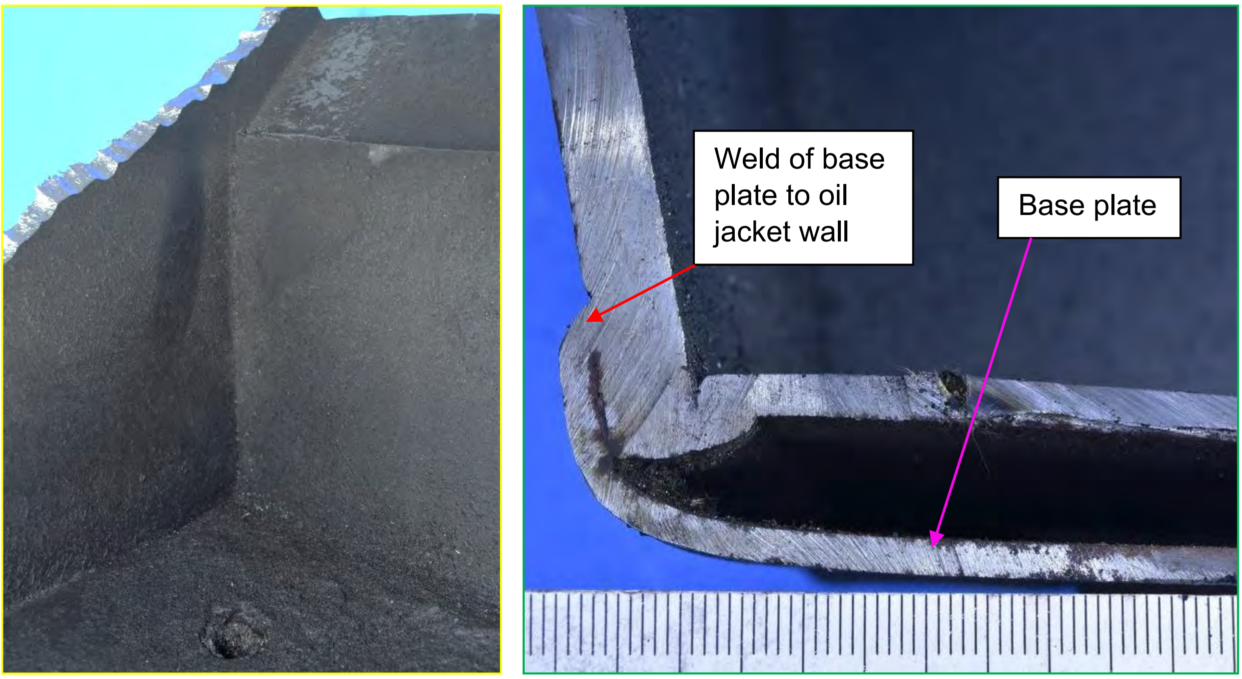

Figure 54: Close up view of the corner from inside the oil jacket (left figure). No gaps were visible at the corner joint. The base plate was folded over the original weld and welded onto the oil jacket wall (right figure).

Visual and Macroscopic Examination

Front side, right edge weld

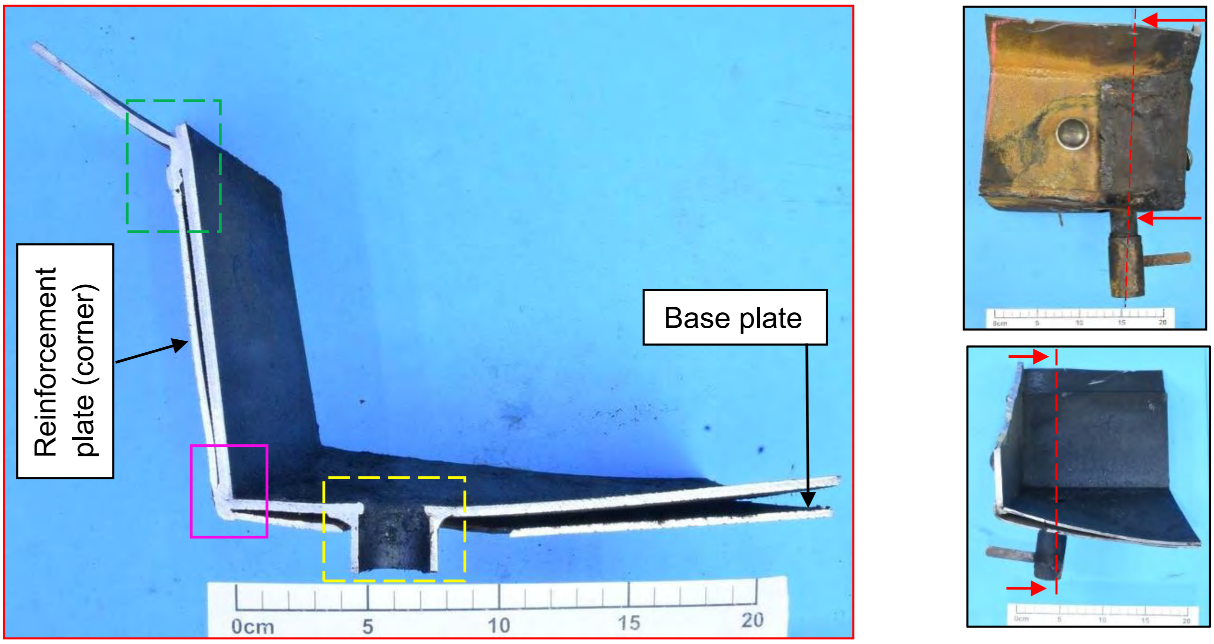

Figure 55: A cross section was made vertically across the drain port, revealing the weld configuration of the corner plate, base plate and the drain port weld. Close up views presented below with their respective colour borders.

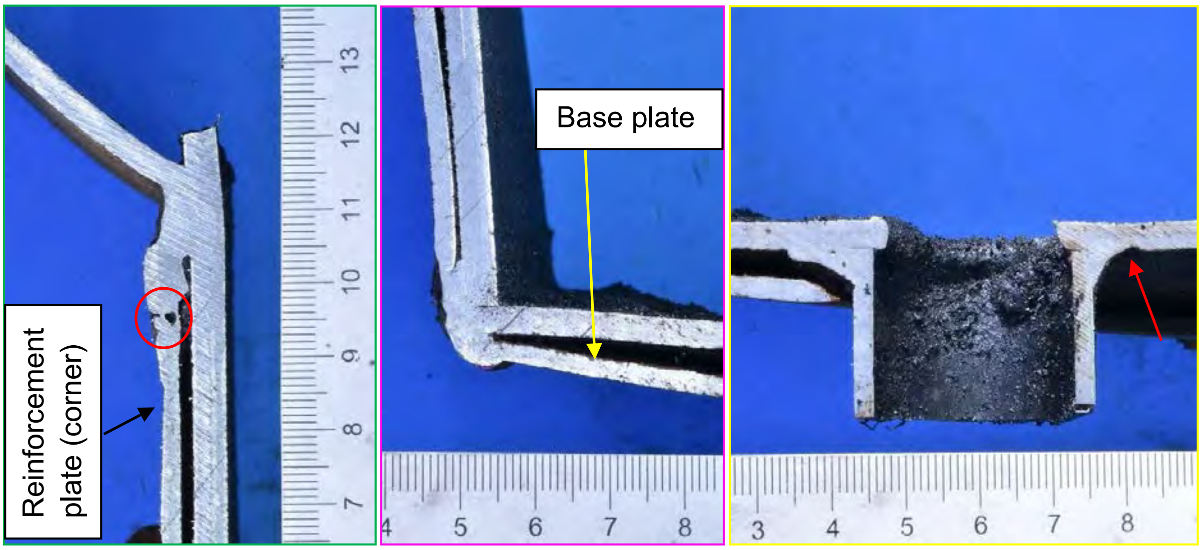

Figure 56: Cross section revealed the corner and base plates were welded together at the bottom edge of the oil jacket (middle figure). Void was visible at the corner reinforcement plate weld (left figure). The drain port weld had an undercut at the weld toe (right figure).

Visual and Macroscopic Examination

Rear

Figure 57: Marked out locations on the front for detailed examination.

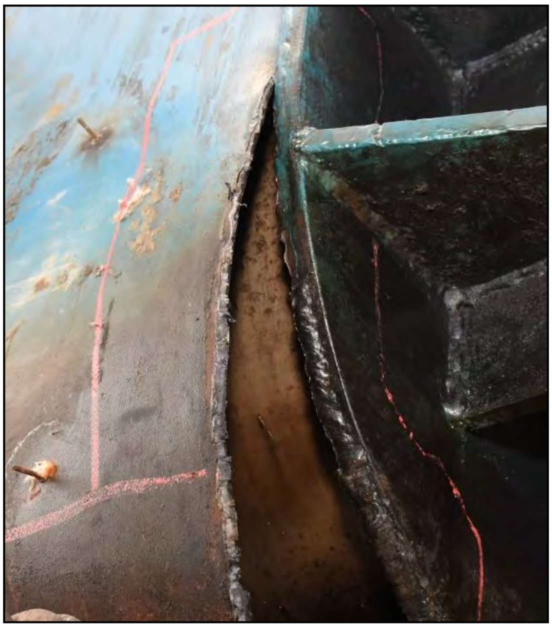

Figure 58: Marked out locations on the rear edges and corners for detailed examination.

Visual and Macroscopic Examination

Rear

Figure 59: Internal condition of the oil jacket from the rear side. The internal surface was generally covered by black soot.

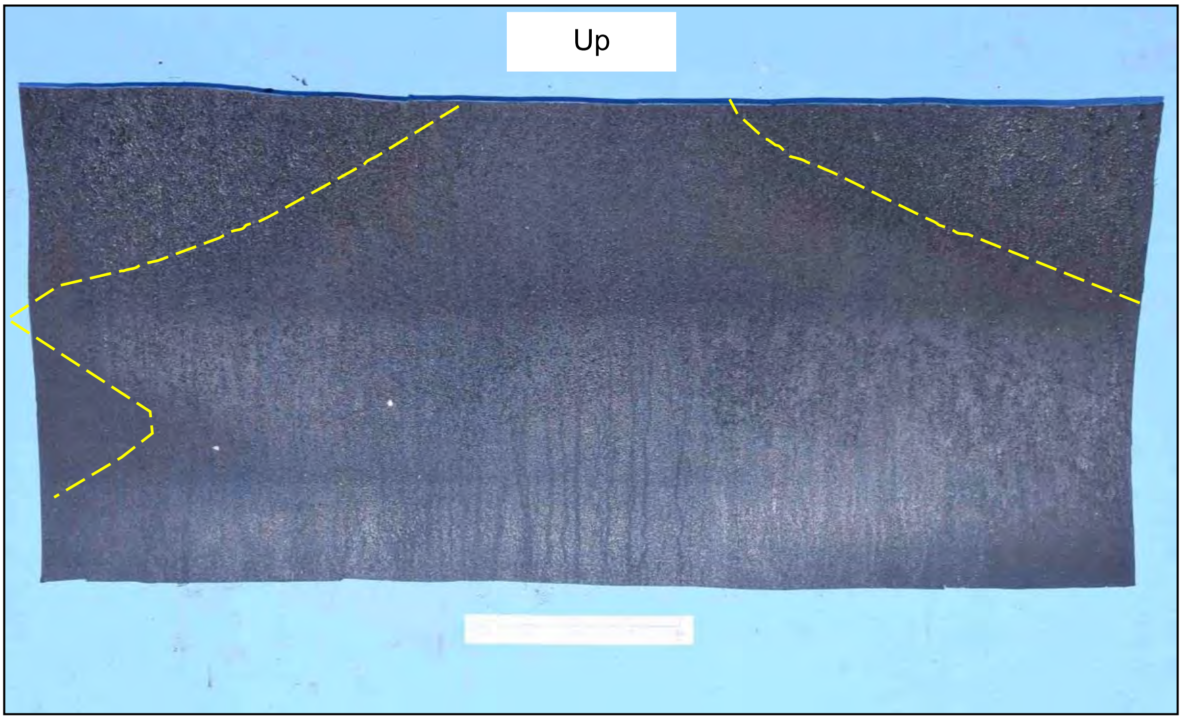

Figure 60: Cut out section of oil jacket wall, internal condition. The surface was generally covered with black soot. Oil stains and drip pattern were visible (see yellow line).

Visual and Macroscopic Examination

Heaters and adjacent welds

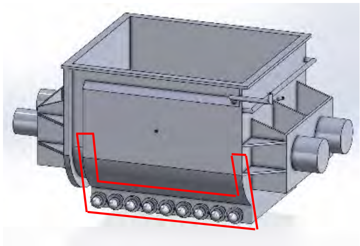

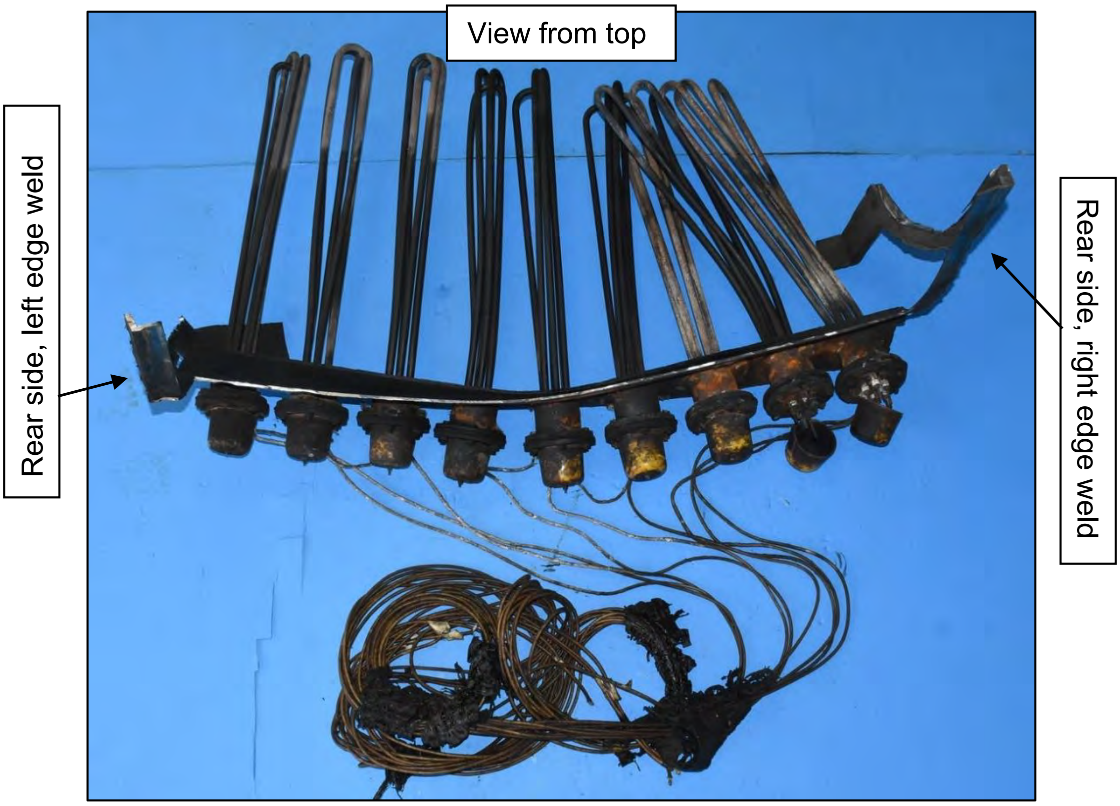

Figure 61: Cut out section consisting of the side welds and heaters. The side welds are referenced as rear side, left edge and rear side, right edge welds.

Visual and Macroscopic Examination

Rear side, left edge weld

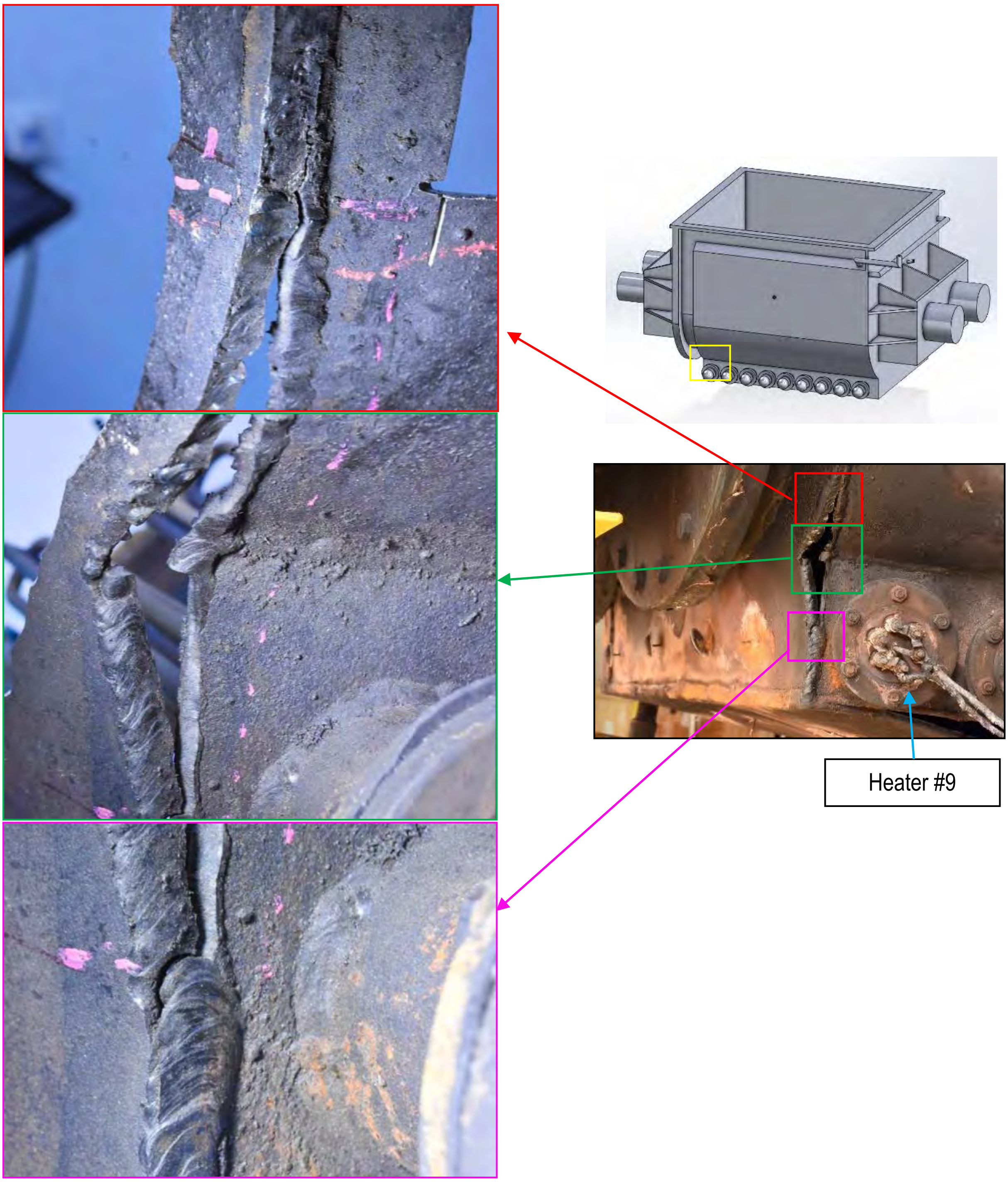

Figure 62: Close up view of rear-left side weld. The fracture path was predominantly centred along the weld face at the curved part of the oil jacket (see red and green bordered figures). The fracture path changes and propagated along the weld toe at the vertical plane of the oil jacket (see green and pink bordered figures).

Visual and Macroscopic Examination

Rear side, left edge weld

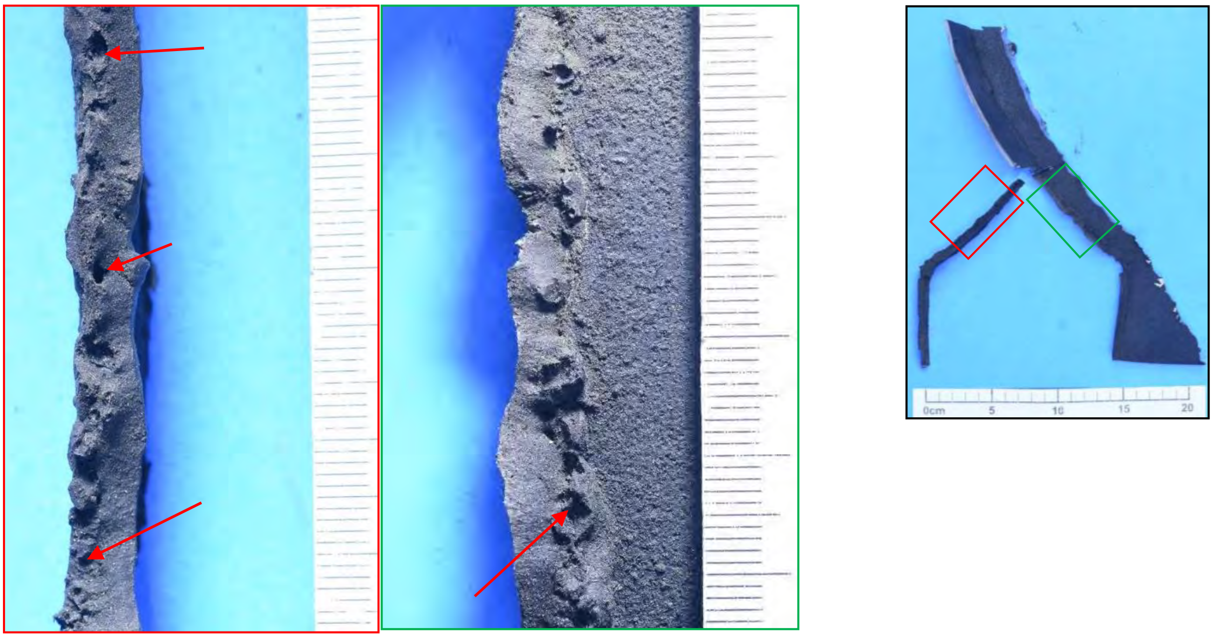

Figure 63: Close up view of side weld fracture surface at the curved part. Voids were visible along the fracture surface. (see also Figure 119)

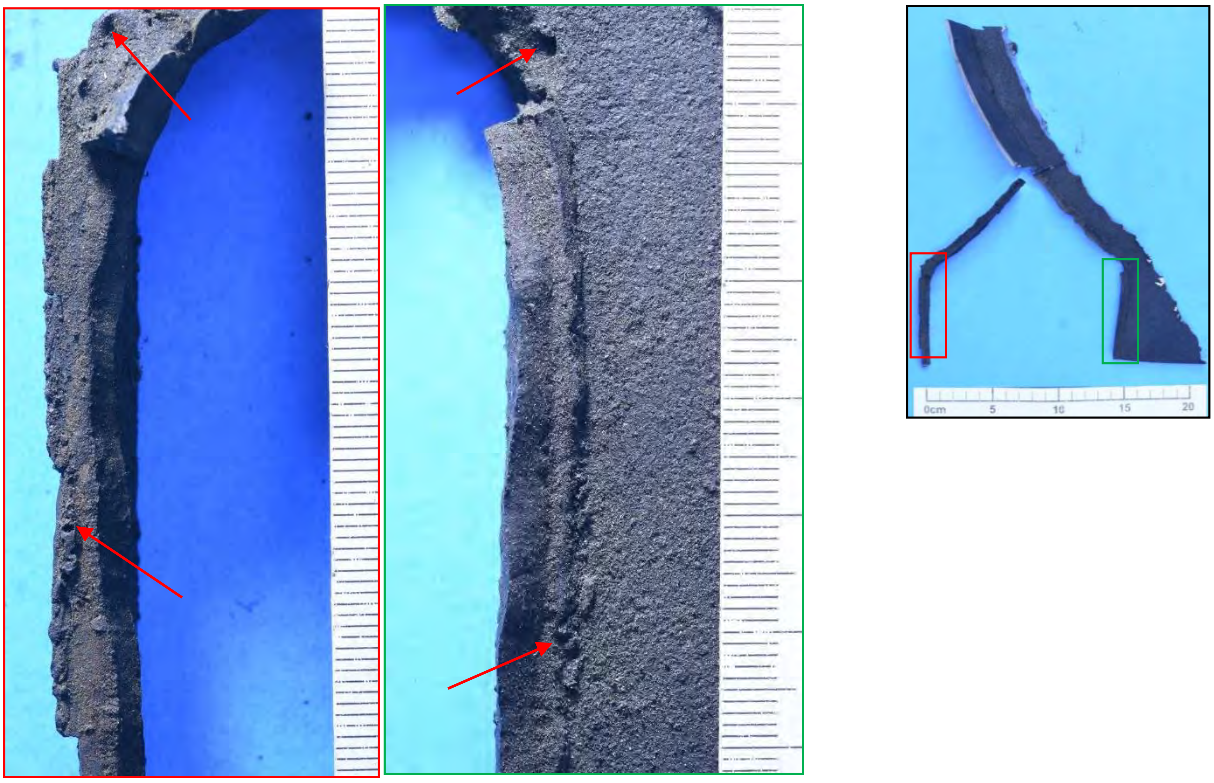

Figure 64: Close up view of side weld fracture surface at the straight and vertical plane. Some voids were observed.

Visual and Macroscopic Examination

Rear side, right edge weld

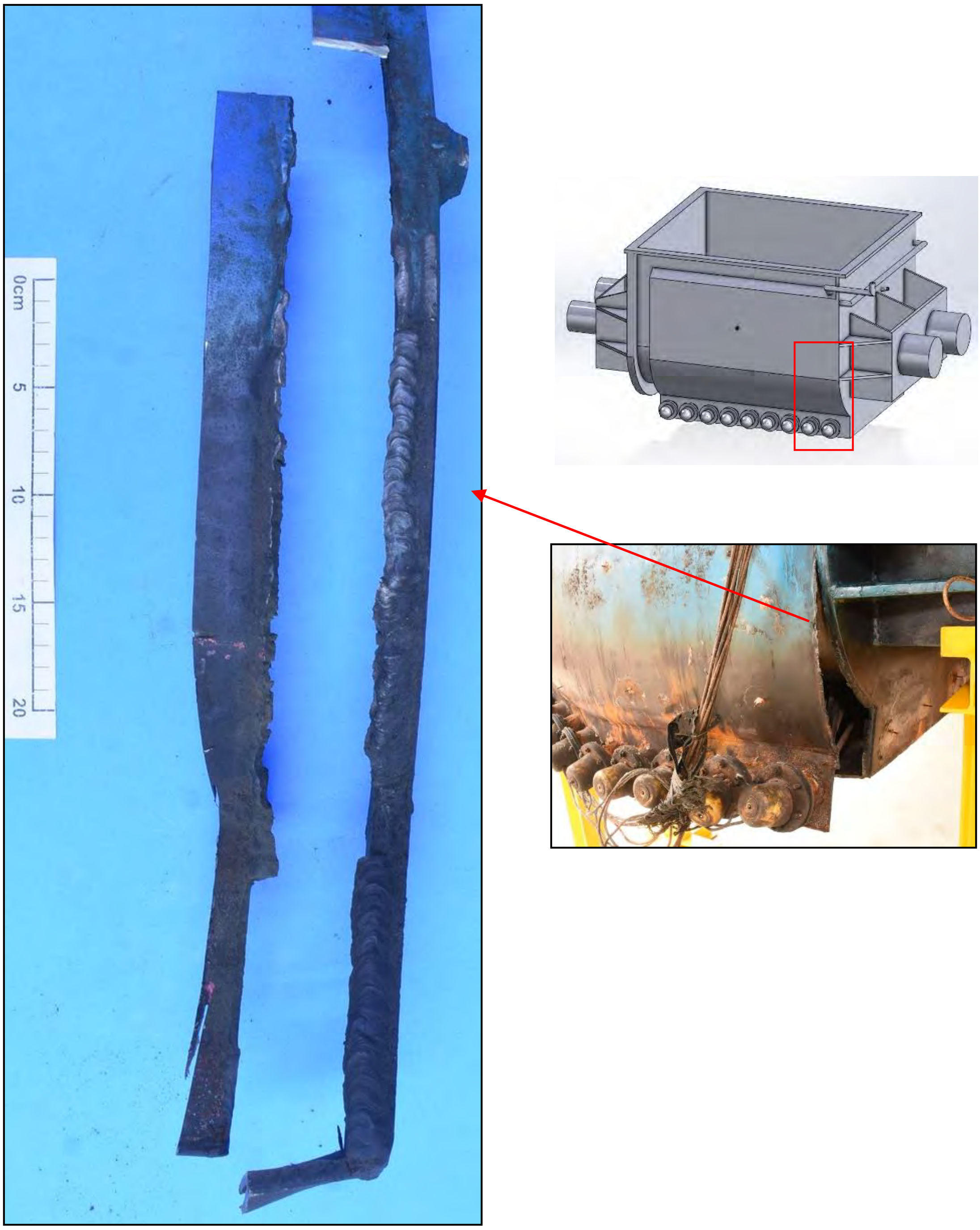

Figure 65: Cut out section of the rear side, right edge weld. The observations made in the following figures were generally similar to the rear side, left edge weld. (see also Figure 62)

Visual and Macroscopic Examination

Rear side, right edge weld

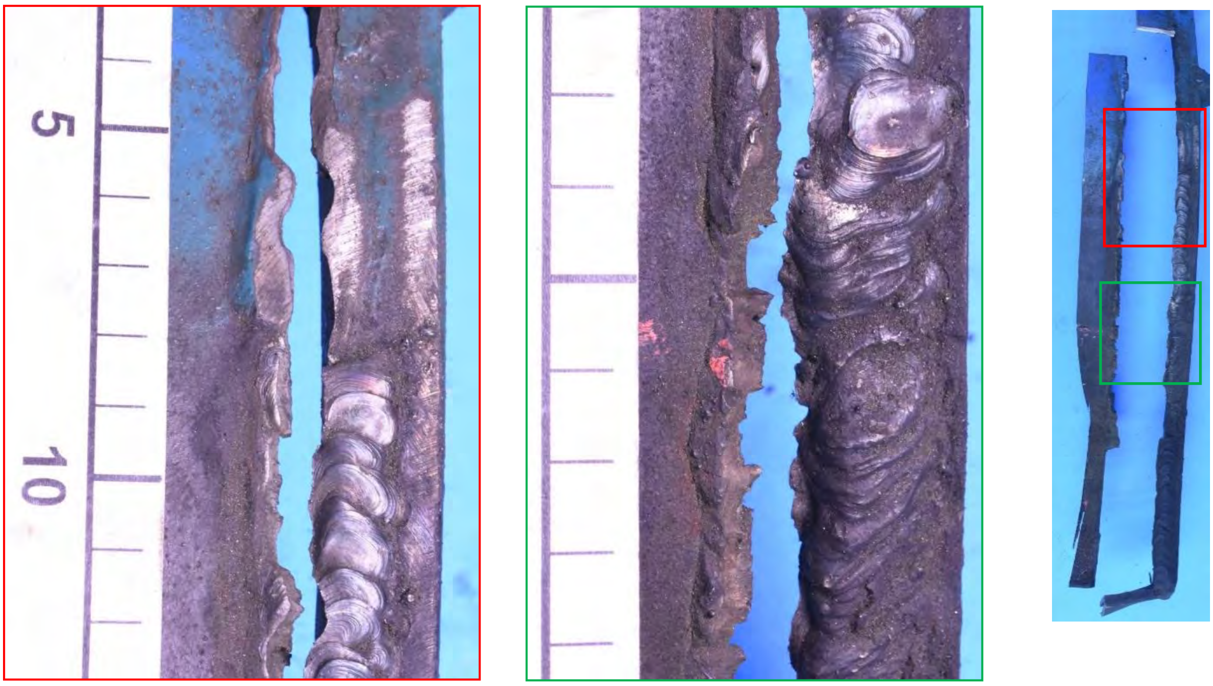

Figure 66: Close up view of side weld fracture surface at the curved part. The fracture path was slightly off-centred along the weld face at the curved part of the oil jacket.

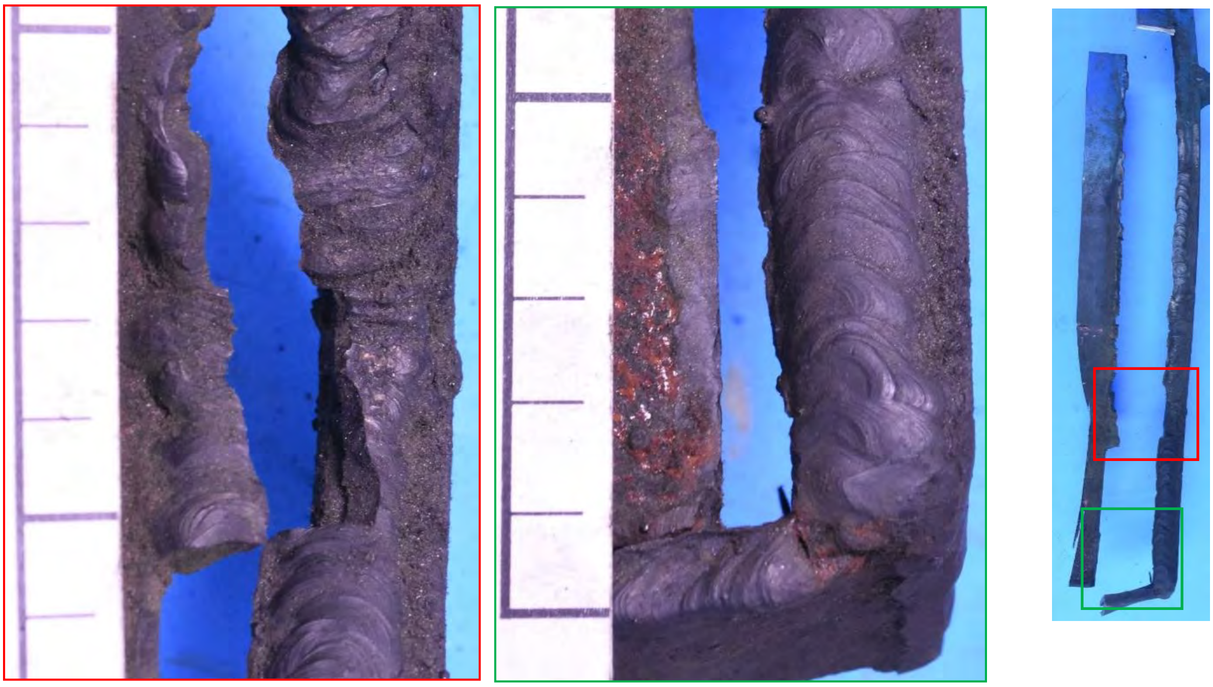

Figure 67: Close up view of side weld fracture surface at the straight and vertical part. The fracture path changes and propagated along the weld toe at the vertical plane of the oil jacket.

Visual and Macroscopic Examination

Rear side, right edge weld

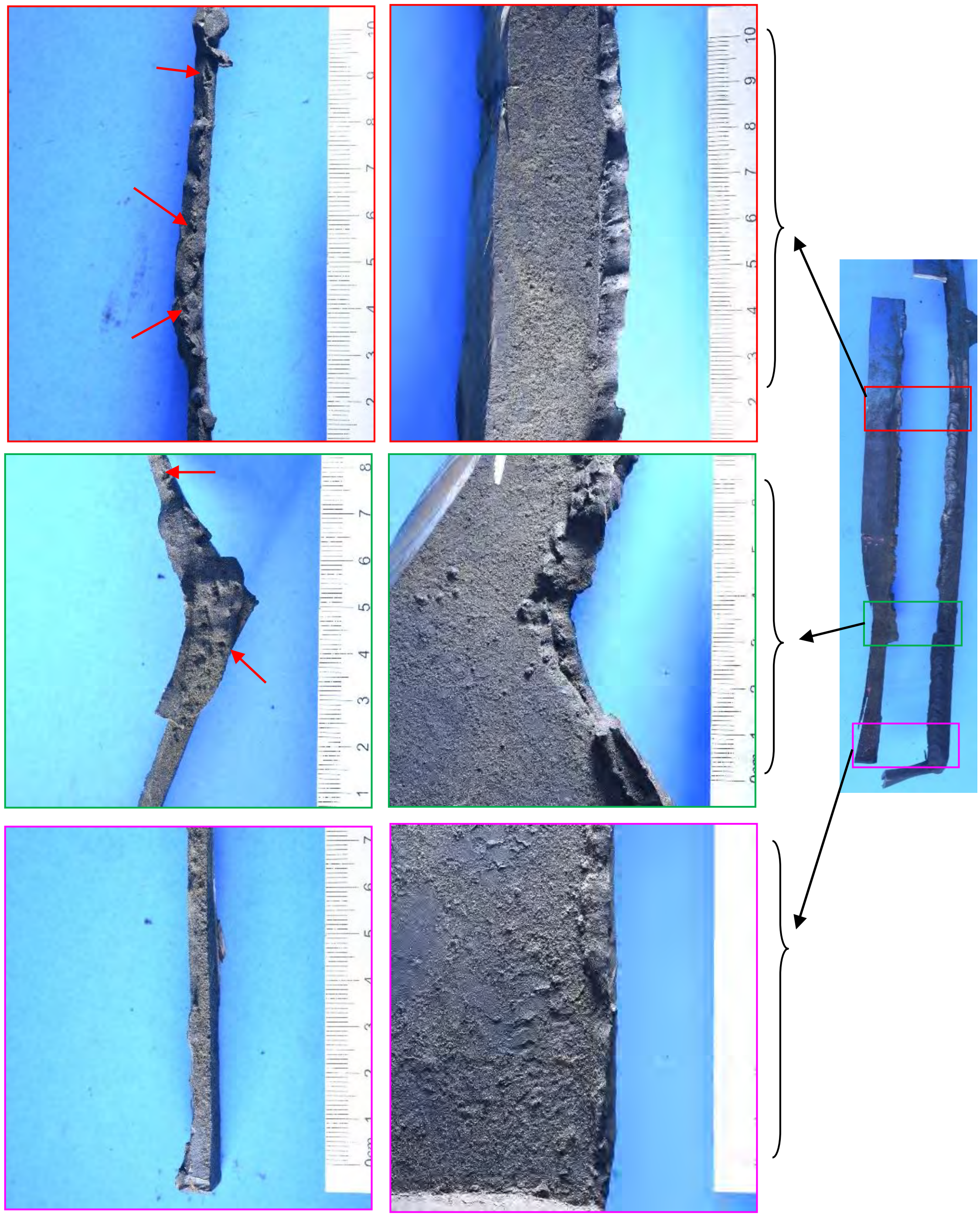

Figure 68: Close up view of the side weld fracture surface. Voids were observed along the fracture surface of the curved part where the fracture was slightly off-centred on the weld face (see red and green bordered figures). At the vertical plane of the wall, the fracture surface was relatively flat (see pink bordered figures).

Visual and Macroscopic Examination

Bottom

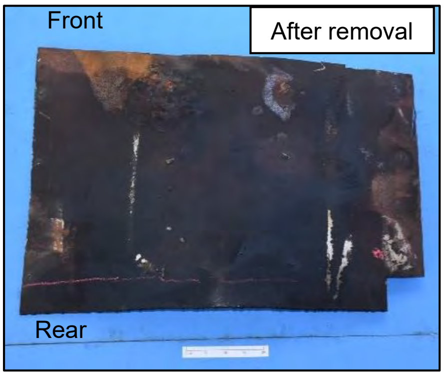

Figure 69: Bottom view of the Mixer Machine. The rear side bottom had bulged outwards.

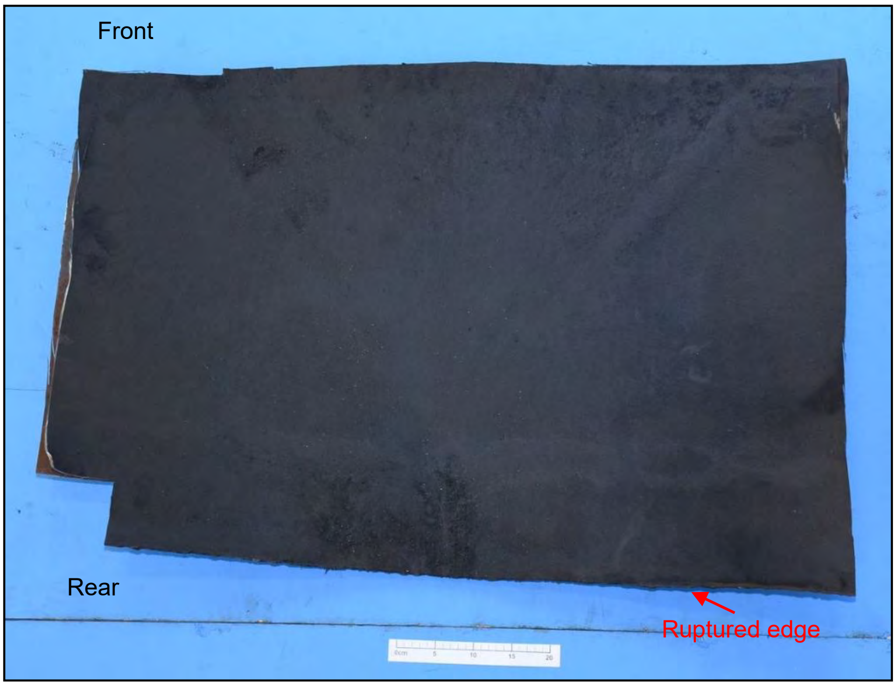

Figure 70: Internal condition of the bottom face. The internal surface was generally covered in black soot.

Visual and Macroscopic Examination

Bottom

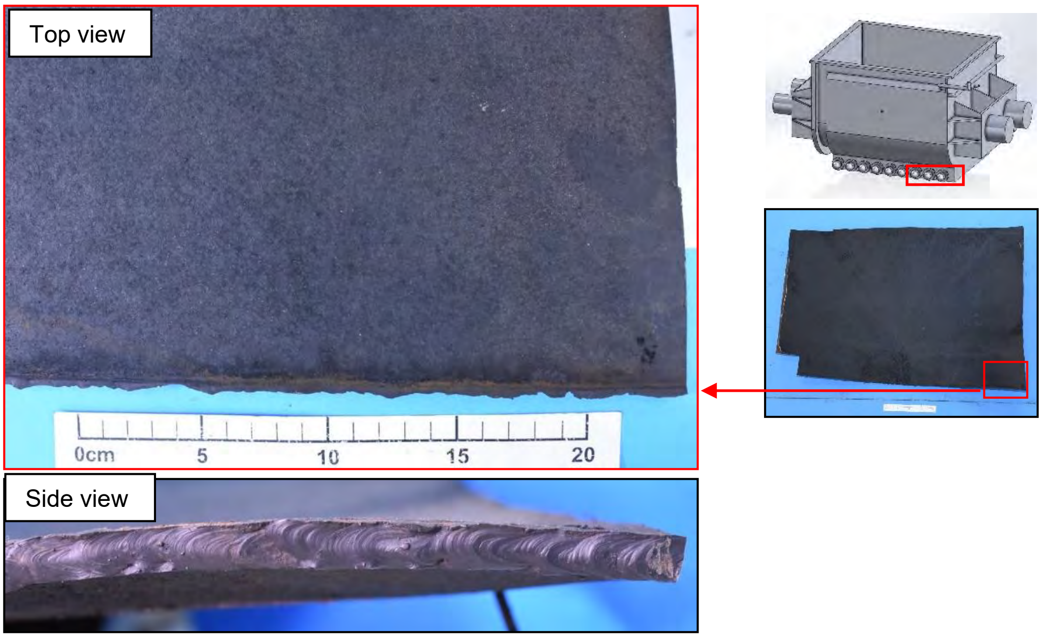

Figure 71: Close up on weld condition of the bottom plate. The fracture was generally along the weld toe.

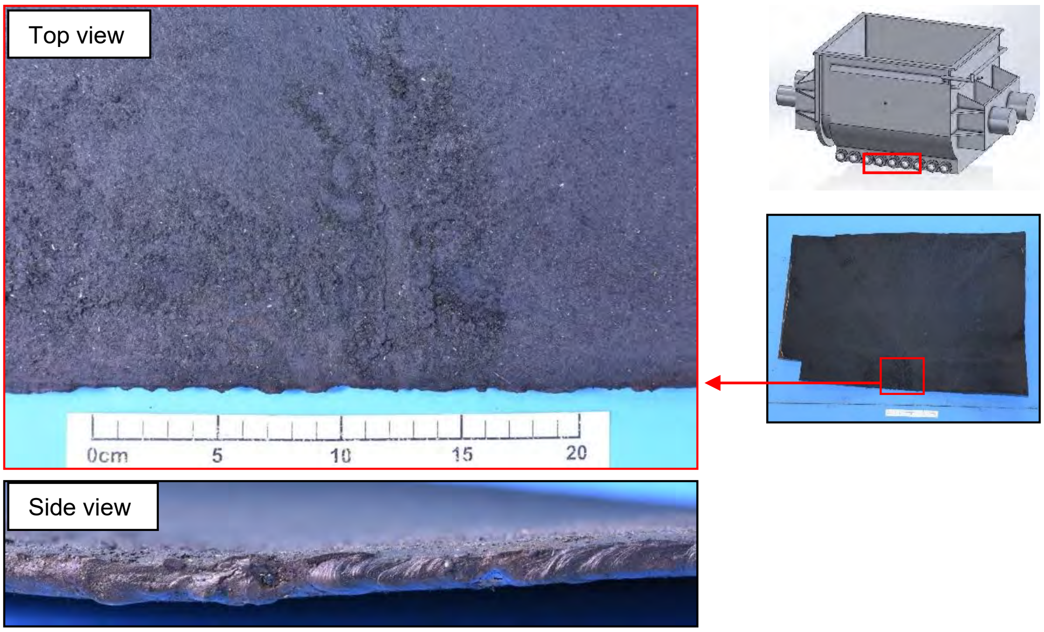

Figure 72: Close up on weld condition of the bottom plate. The fracture was generally along the weld toe.

Visual and Macroscopic Examination

Bottom

Figure 73: Internal condition of the oil jacket surface, view from the bottom showing the "W" shape of the mixing chamber formed by joining two half cylinders. Surface was generally covered with soot and oil remnant.

Figure 74: Internal condition of the oil jacket surface, view from the bottom. Surface was generally covered with soot and oil remnant.

Visual and Macroscopic Examination

Heaters configurations

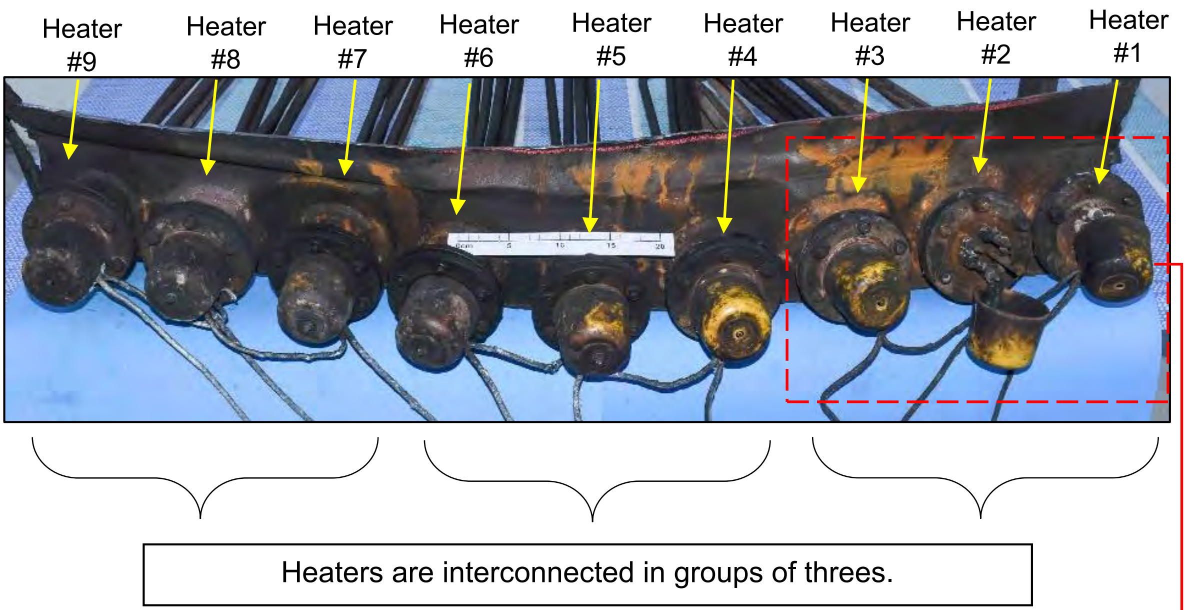

Figure 75: From right, heaters are referred to as heater #1 to #9.

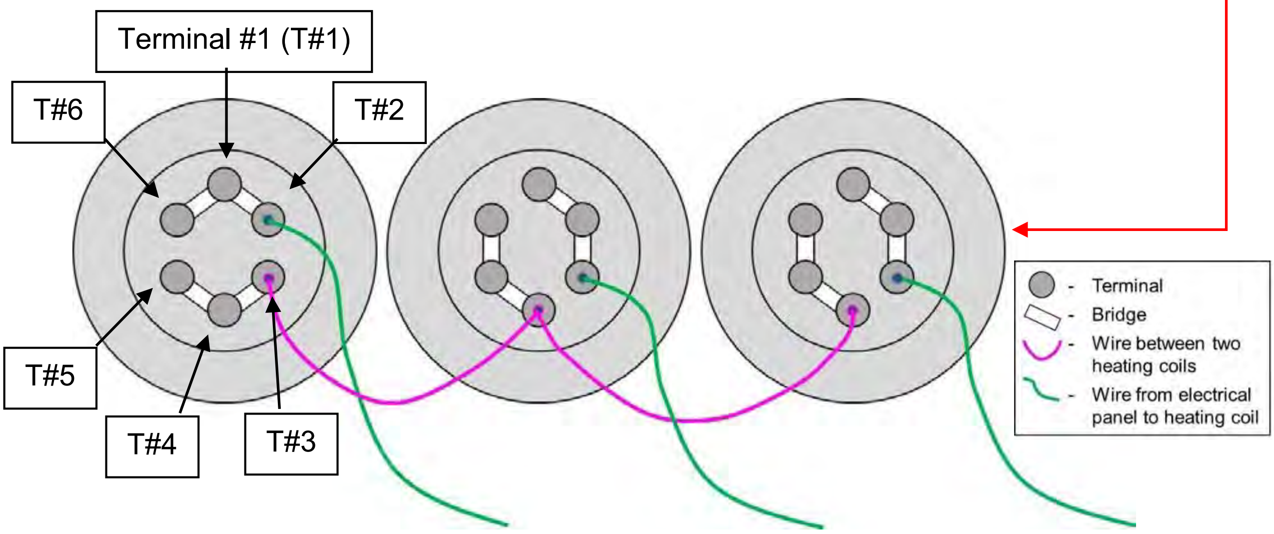

Figure 76: For ease of reference, the terminals are numbered clockwise in increasing order, starting from the topmost terminal as terminal #1. Each heater is connected in two ways. First, each heater is connected to the electrical panel by a wire between the electrical panel and one of its terminals. Second, within each group of three heaters, two wires connect the middle heater to each of the heaters on its left and right side by one of their terminals. The position of the connected terminals and terminal bridges vary depending on the flange orientation during bolting.

Visual and Macroscopic Examination

Heaters #1 to #3

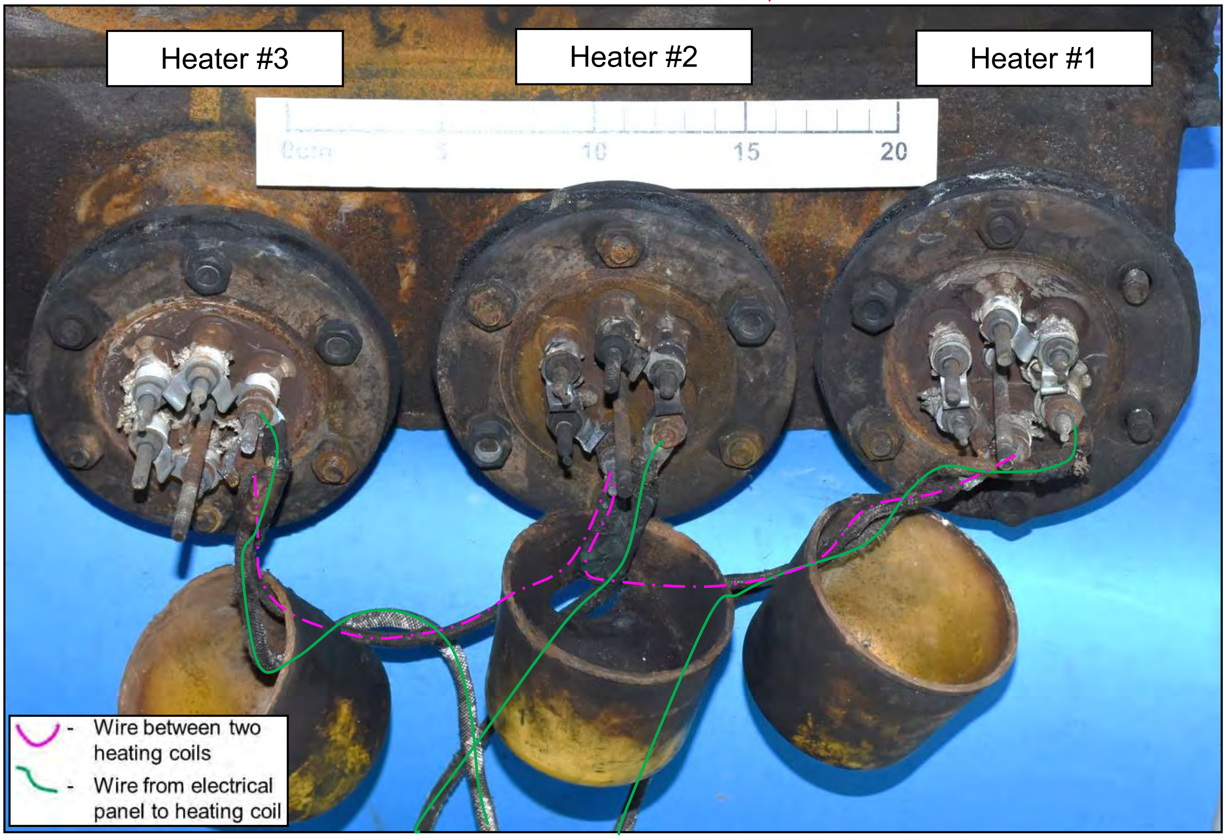

Figure 77: The as-received condition of the heaters (from right, heaters #1, #2 and #3). The flanges generally had blackish appearance. Some of the terminal covers (rounded yellow caps) were blackish on the internal surface as well. The terminals of heater #2 also had a blacker appearance compared to the terminals of the rest of the heaters

Visual and Macroscopic Examination

Heaters #1 to #3

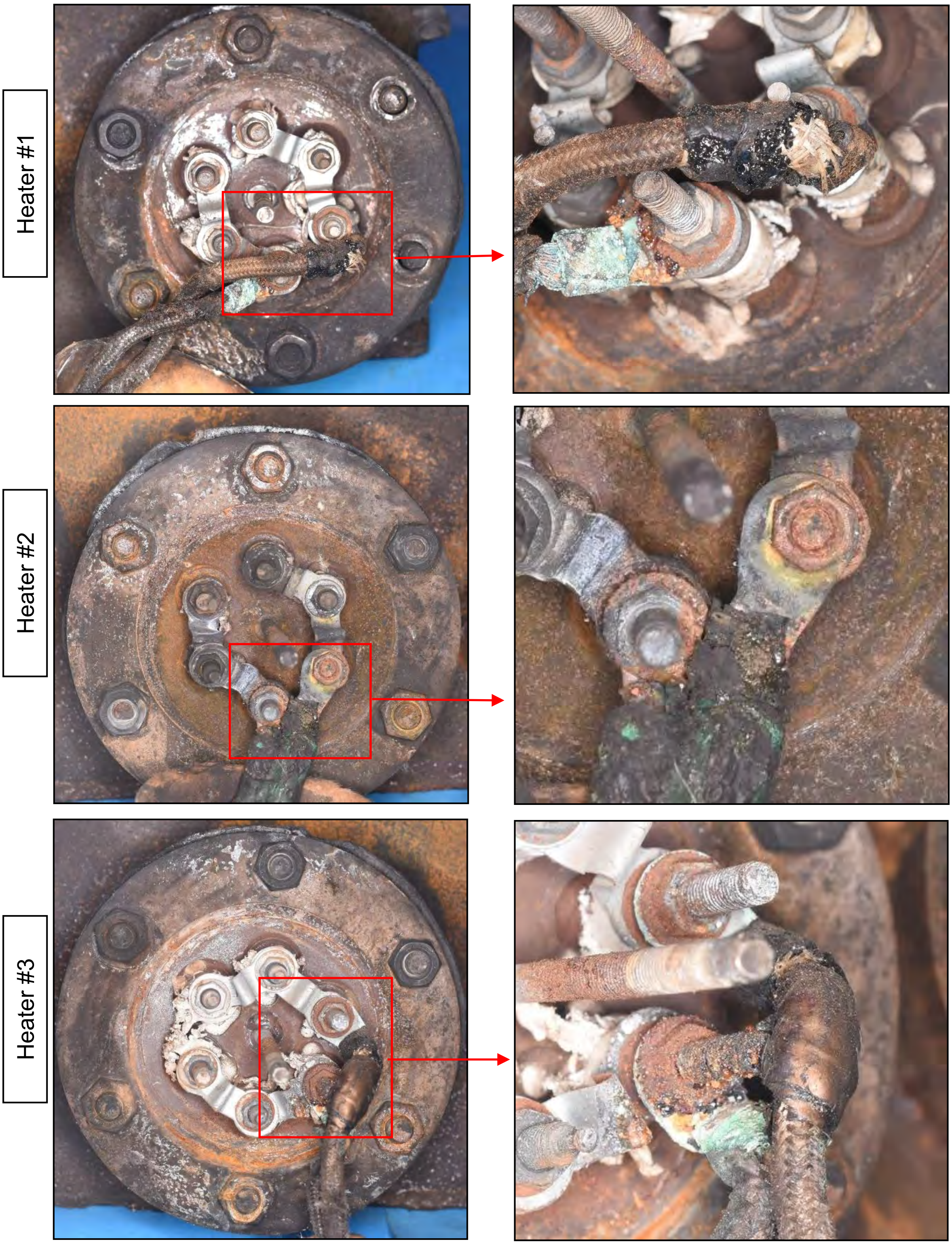

Figure 78: From top, heaters #1, #2 and #3, with close up view of their terminals.

Visual and Macroscopic Examination

Heater #2, terminals

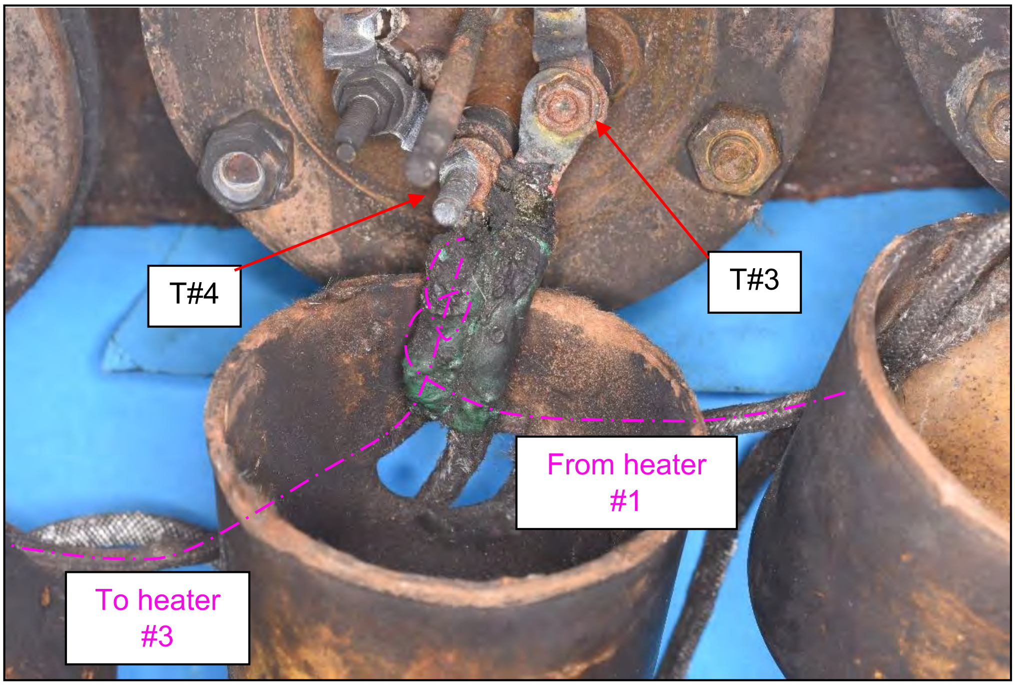

Figure 79: Green tapes were observed wrapped around the wires of both terminal #3 and terminal #4 of heater #2. The position of both wire lugs were close together.

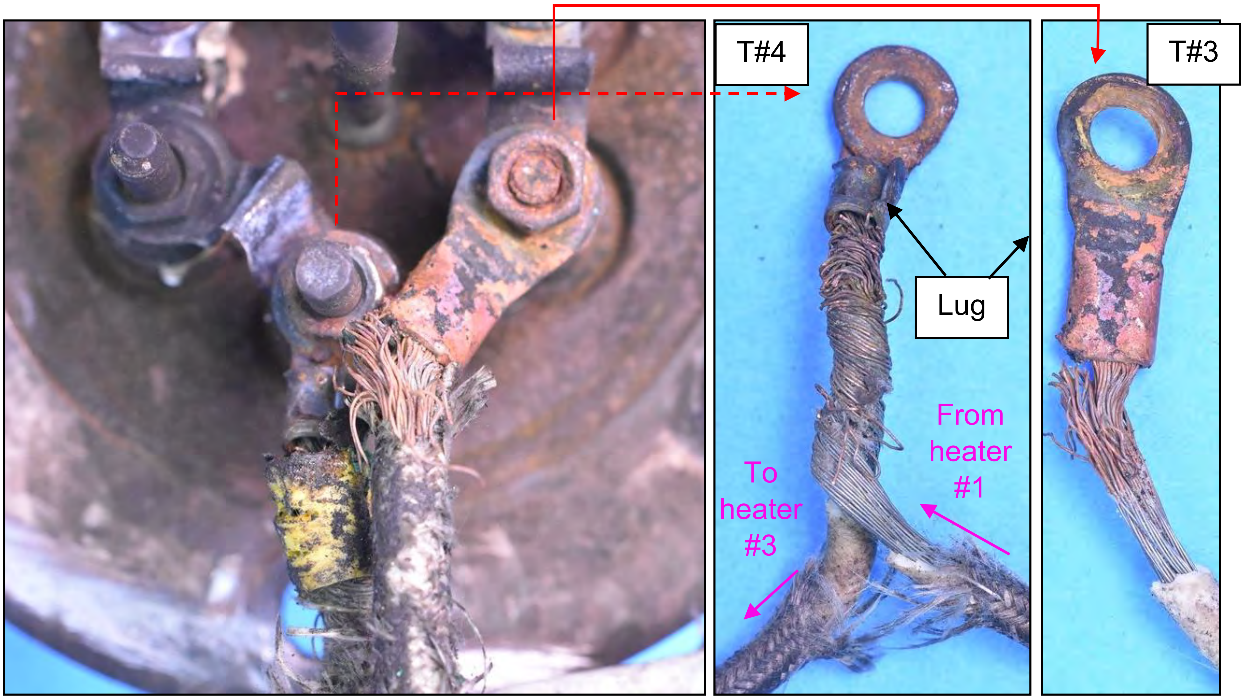

Figure 80: Beneath the green tape wrapped around the wires at terminal #4 was a yellow clip tab (left figure). The yellow clip tab and wire insulations were removed, revealing the wires shown in figures on the right. The wire from heater #1 were wound around the wire to heater #3 (see also Figure 82 to compare). Microscopic examination was conducted and presented in Figure 131.

Visual and Macroscopic Examination

Heaters #4 to #6

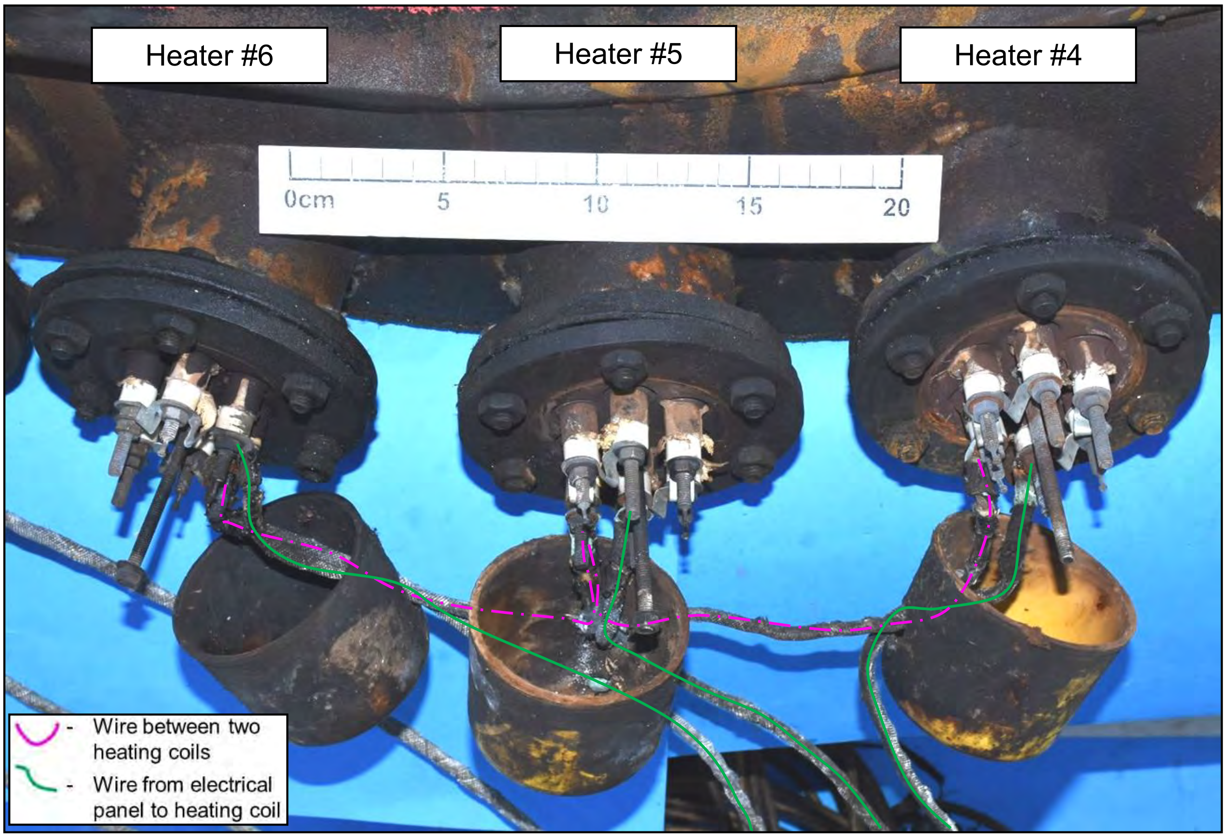

Figure 81: The as-received condition of the heaters (from right, heaters #4, #5 and #6). The flanges generally had blackish appearance. Some of the terminal covers (rounded yellow caps) were blackish on the internal surface as well.

Visual and Macroscopic Examination

Heaters #4 to #6

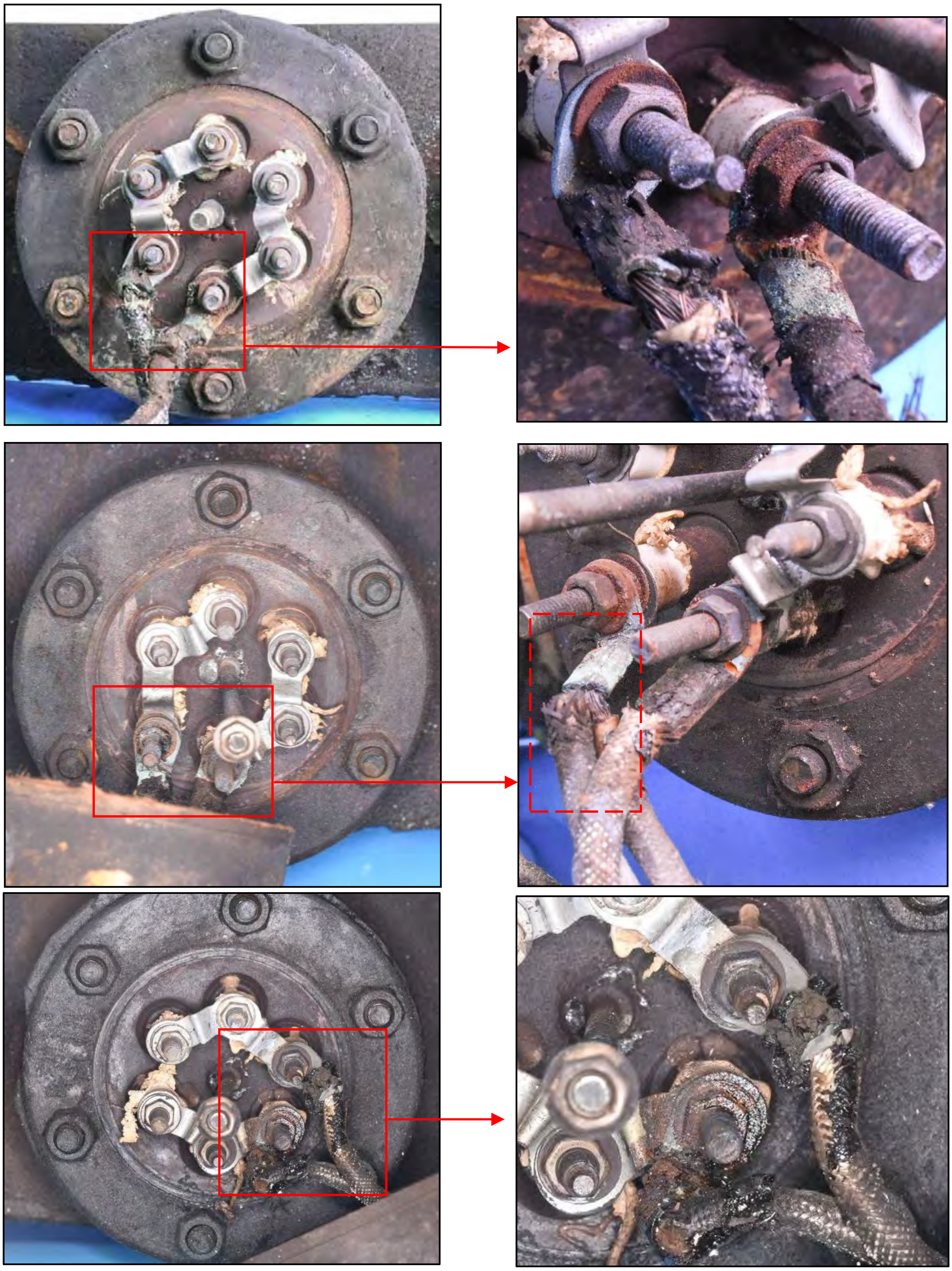

Heater #4

Heater #5

Heater #6

Figure 82: From top, heaters #4, #5 and #6, with close up view of their terminals. For heater #5, the wires from/to heaters #4 and #6 were clamp together by the lug (see red dotted line).

Visual and Macroscopic Examination

Heaters #7 to #9

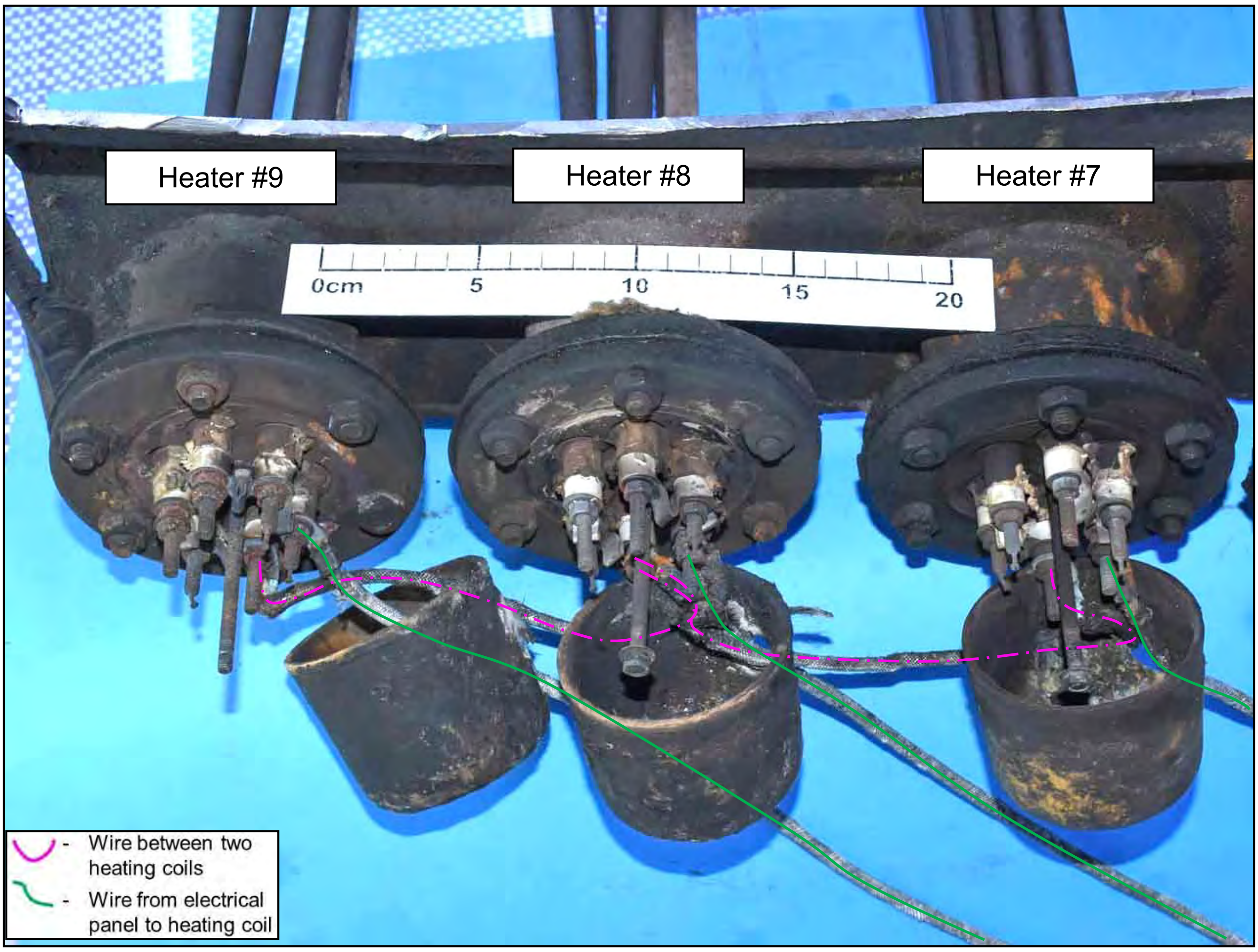

Figure 83: The as-received condition of the heaters (from right, heaters #7, #8 and #9). The flanges generally had blackish appearance. Some of the terminal covers (rounded yellow caps) were blackish on the internal surface as well.

Visual and Macroscopic Examination

Heaters #7 to #9

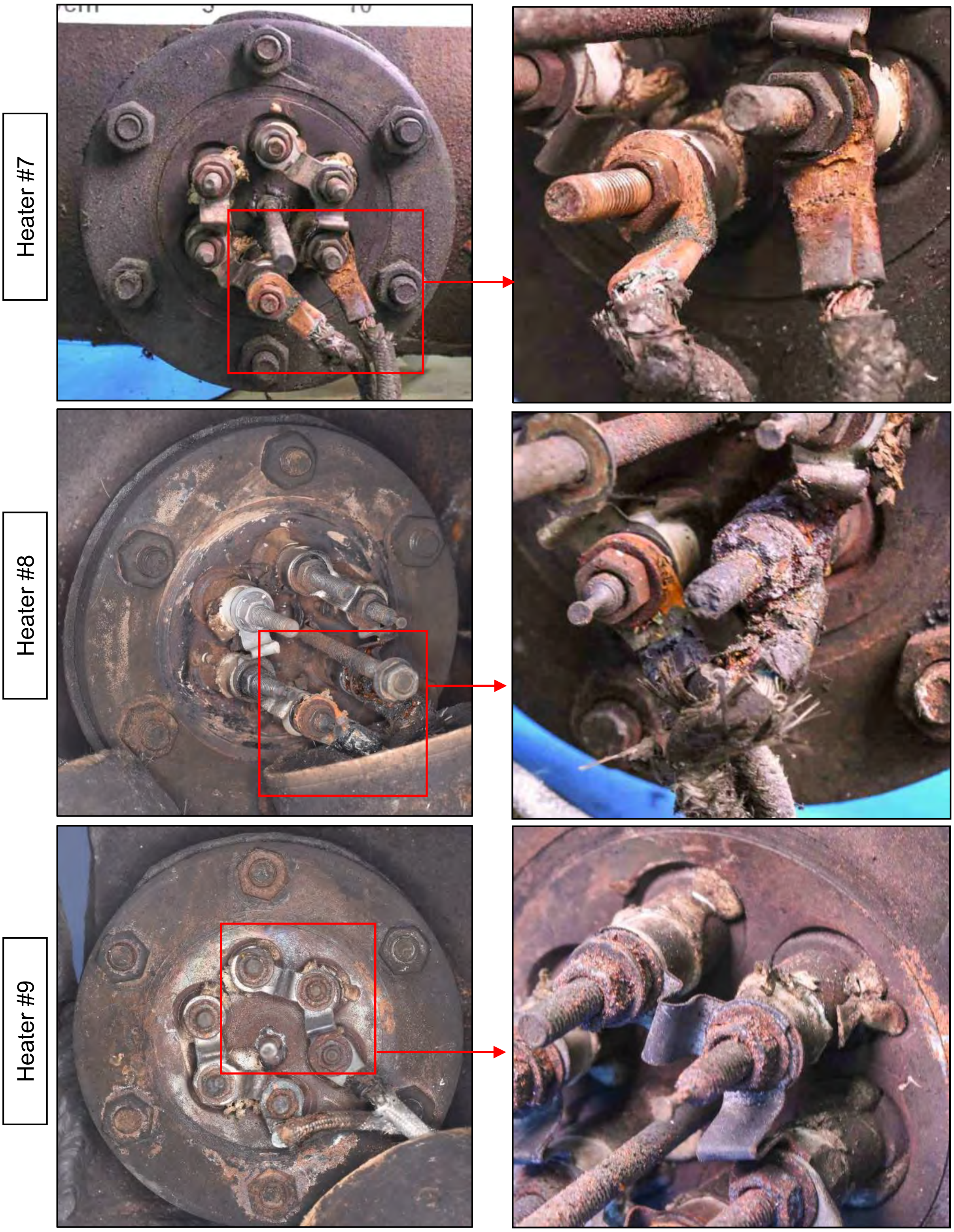

Figure 84: From top, heaters #7, #8 and #9, with close ups of their terminals.

Visual and Macroscopic Examination

Heters (Metal tubes)

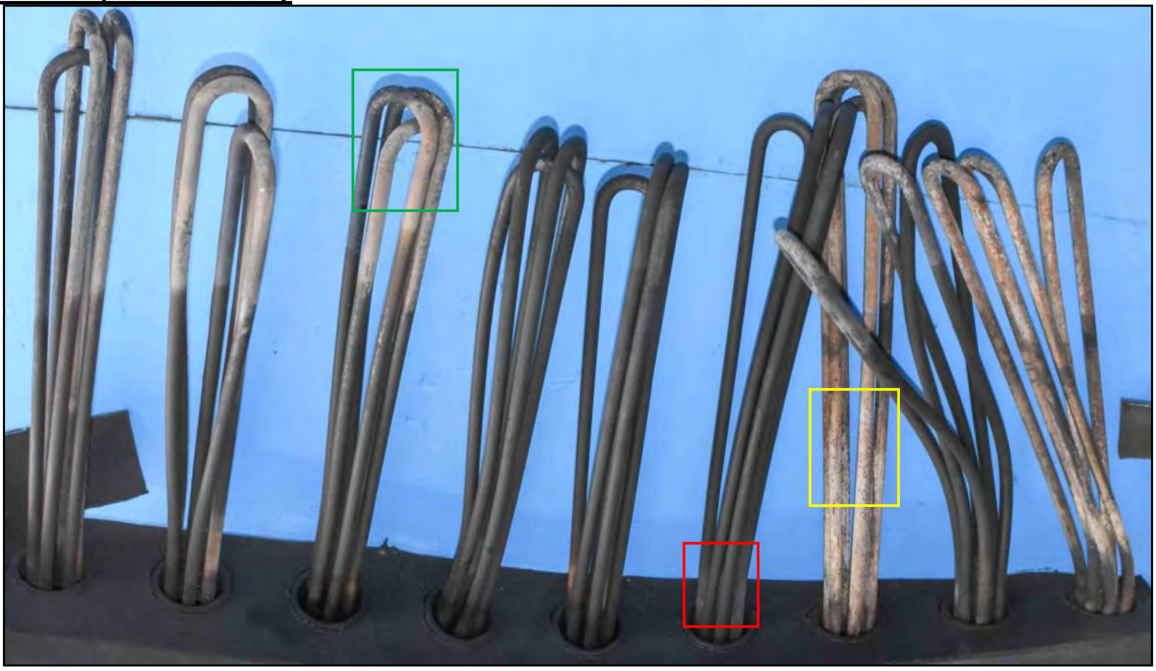

Figure 85: The heaters are sheathed-type heating elements (also known as Calrod™ heaters). The metal tubes of every heater sustained various degrees of deformation, which heaters #1 and #2 being most severe.

Figure 86: Signs of corrosion and peeling of coating were observed at various parts of the metal tubes.

Visual and Macroscopic Examination

Removal of heaters

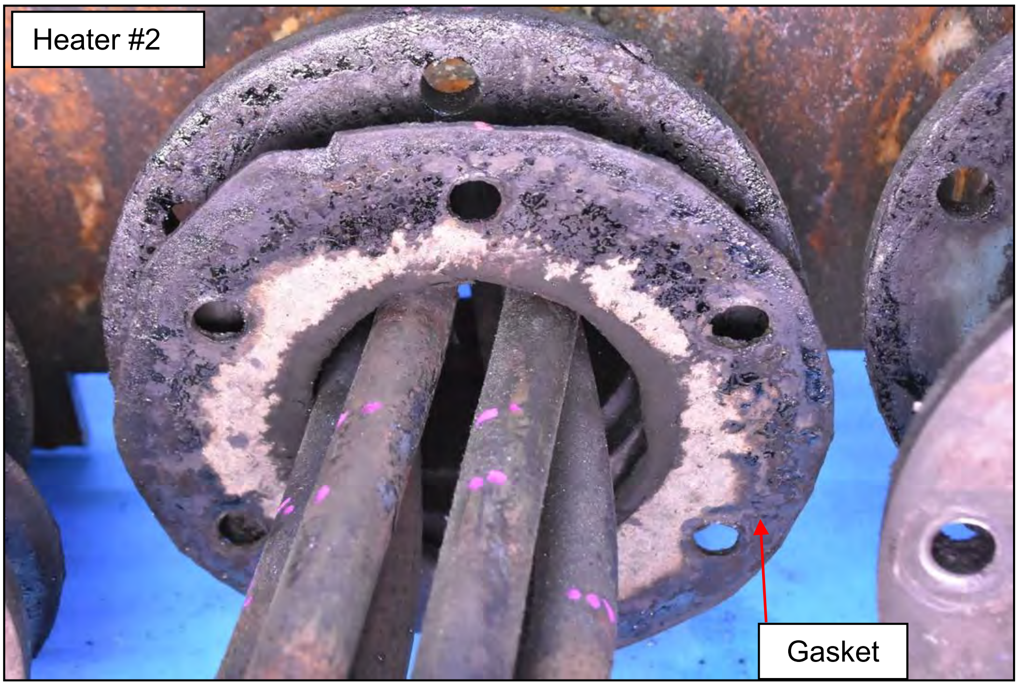

Figure 87: Due to the severe deformation, heaters #1, #2 and #3 cannot be removed without cutting the metal tubes. The gaskets were generally brittle with some parts still adhering to the flanges' surface.

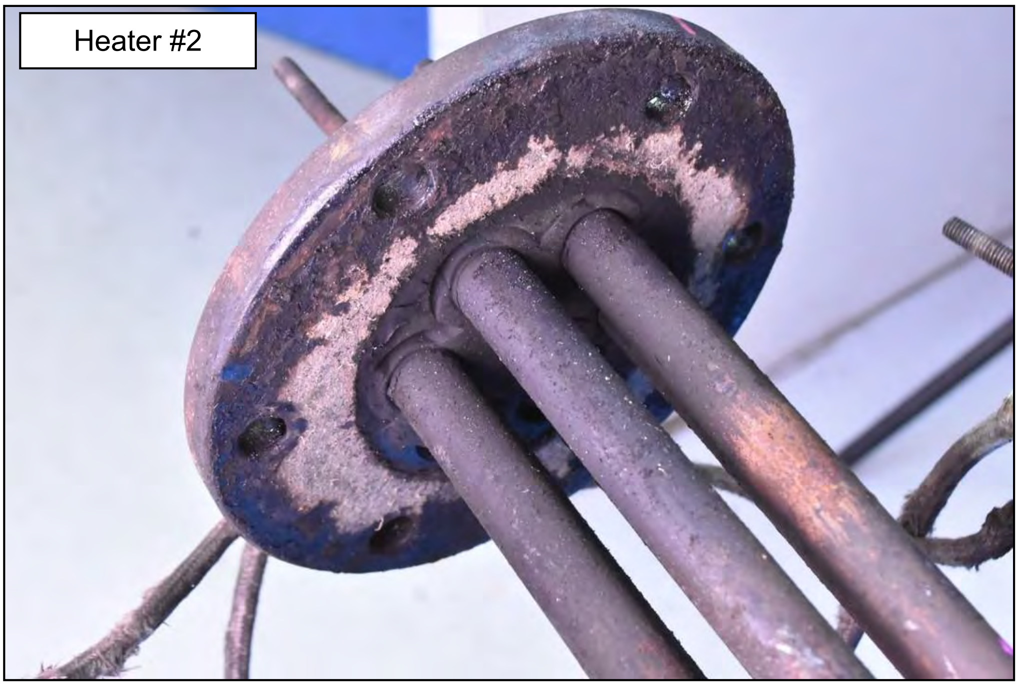

Figure 88: Heater flange condition from the side adhering to the gasket.

Visual and Macroscopic Examination

Flange

Figure 89: The rest of the heaters were removed, revealing generally similar flange condition. Oil residue were present inside.

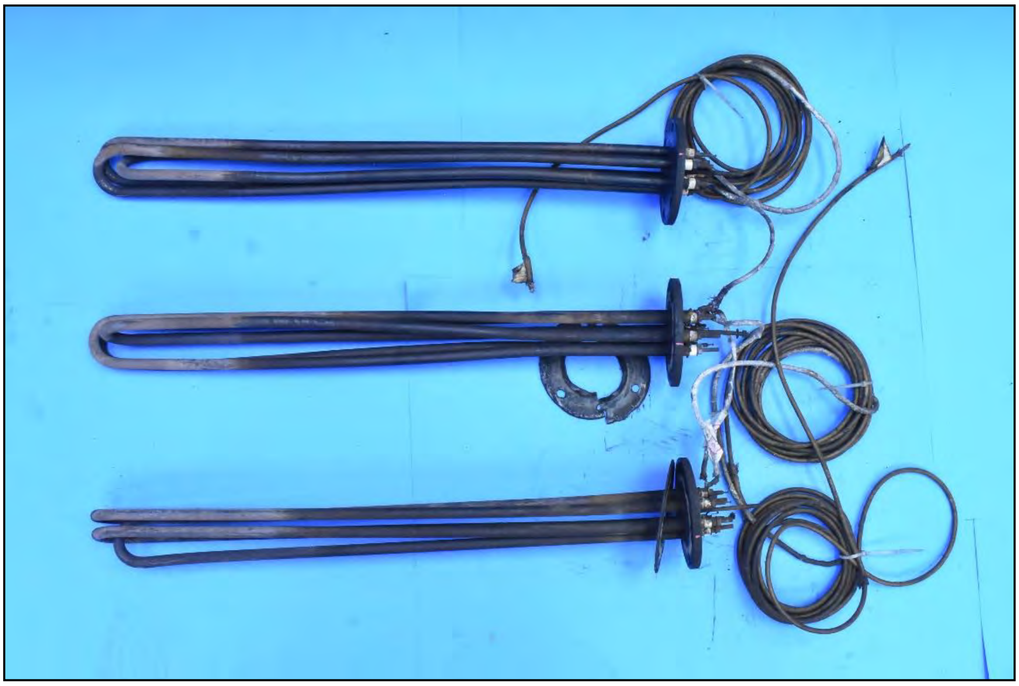

Figure 90: All the gaskets had degraded and were generally brittle to the point where they broke with slight pressure. Some broke during the removal of heaters.

Visual and Macroscopic Examination

Gaskets

Figure 91: General view of gasket for heater #2. Some parts were broken during the shore hardness testing.

Figure 92: For comparison, gasket for heater #9 which was located furthest from the main rupture zone and heater #2, was selected to undergo shore hardness testing. Similarly, parts of it were broken during the testing.

Visual and Macroscopic Examination

Heater #2

Figure 93: The LEW reported that heater #2 had unusual high resistance among the coils. With that reporting, the metal tubes were examined and the tube between terminals #3 and #6 were found to have a bulged area.

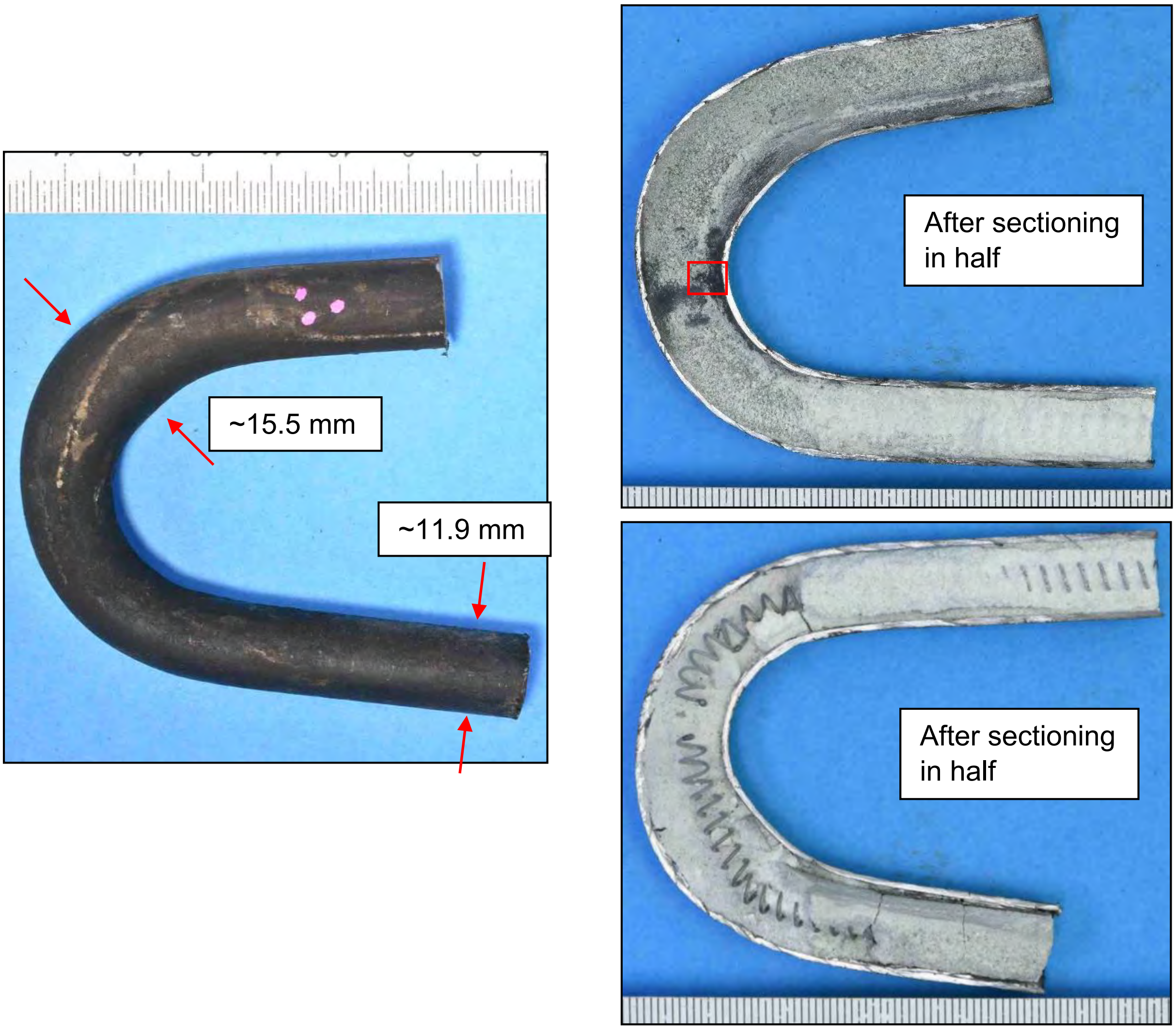

Figure 94: The normal outer diameter was approximately 11.9 mm while the bulged area had a maximum outer diameter of about 15.5 mm. The area was sectioned in half to reveal the internal condition. The resistance wire inside had separated and the surrounding insulation powder were very loose.

Visual and Macroscopic Examination

Heater #2

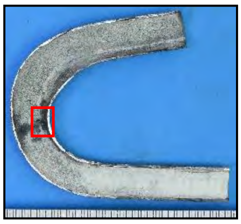

Figure 95: At the metal tube inner diameter wall corresponding to the location of the separated wire, a small melted bulb was observed adhering to the wall. .

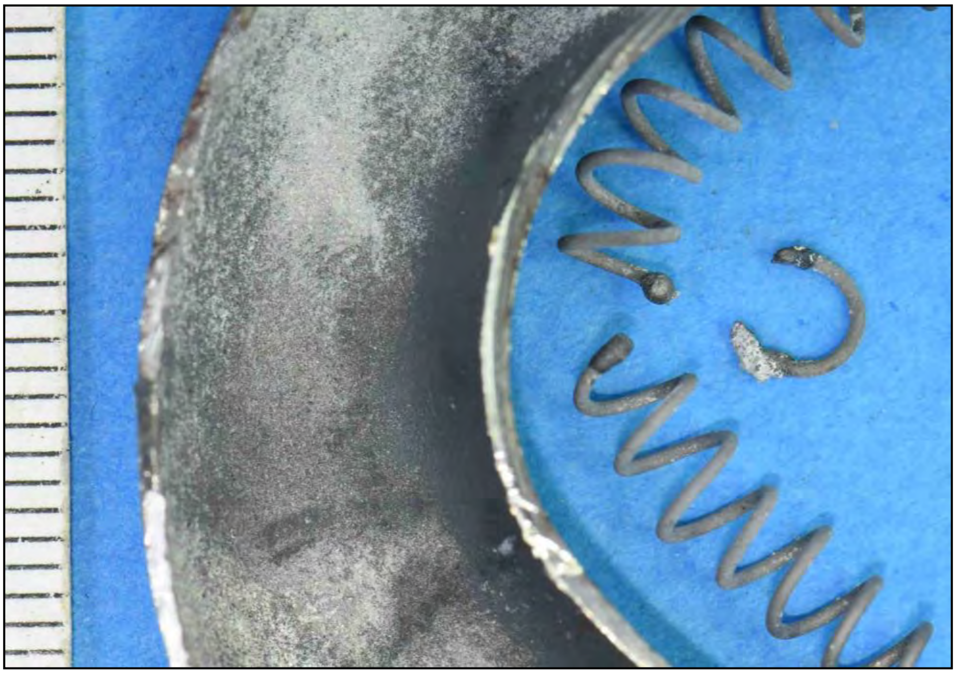

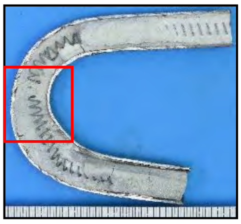

Figure 96: The tips of the wire had melted with some of the insulation powder fused onto the tip.

Visual and Macroscopic Examination

Access Port

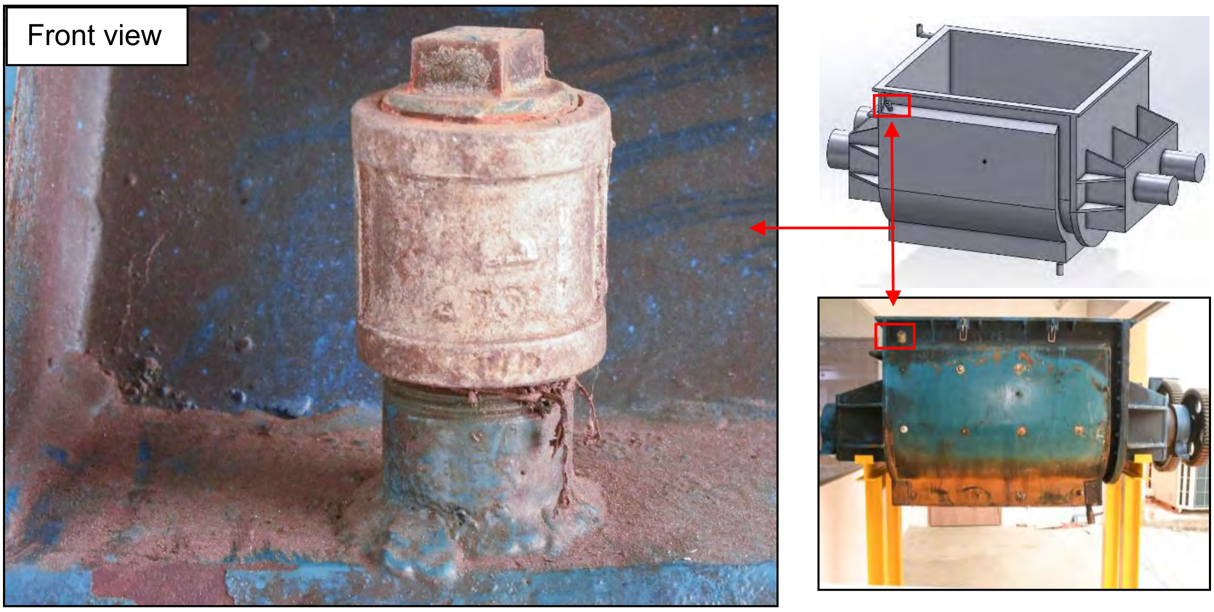

Figure 97: The access port had been plugged by a square head plug.

Vent Port

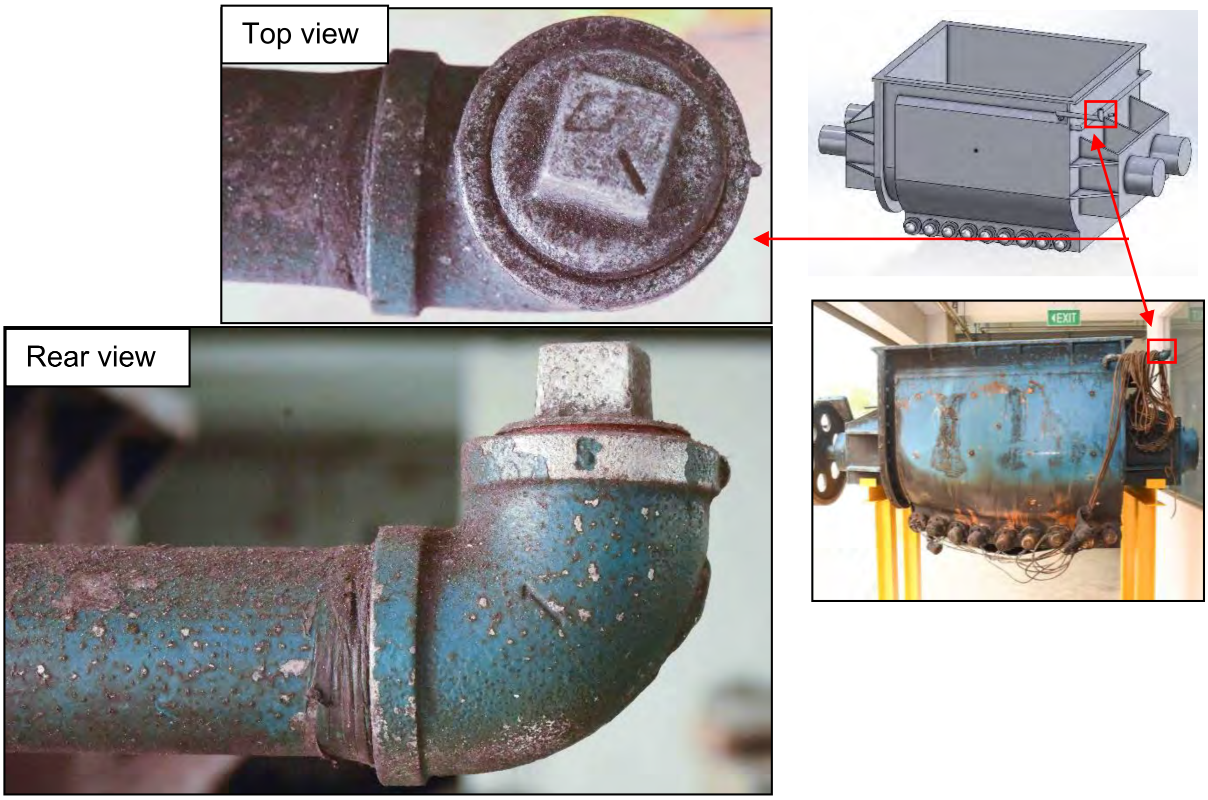

Figure 98: The vent port was also plugged by a square head plug.

Visual and Macroscopic Examination

Oil Funnel

Figure 99: The oil funnel was not in use and was found at the ground floor of the Factory during the retrieval of the Mixer Machine onsite.

Visual and Macroscopic Examination

Resistance temperature detector A (RTD A)

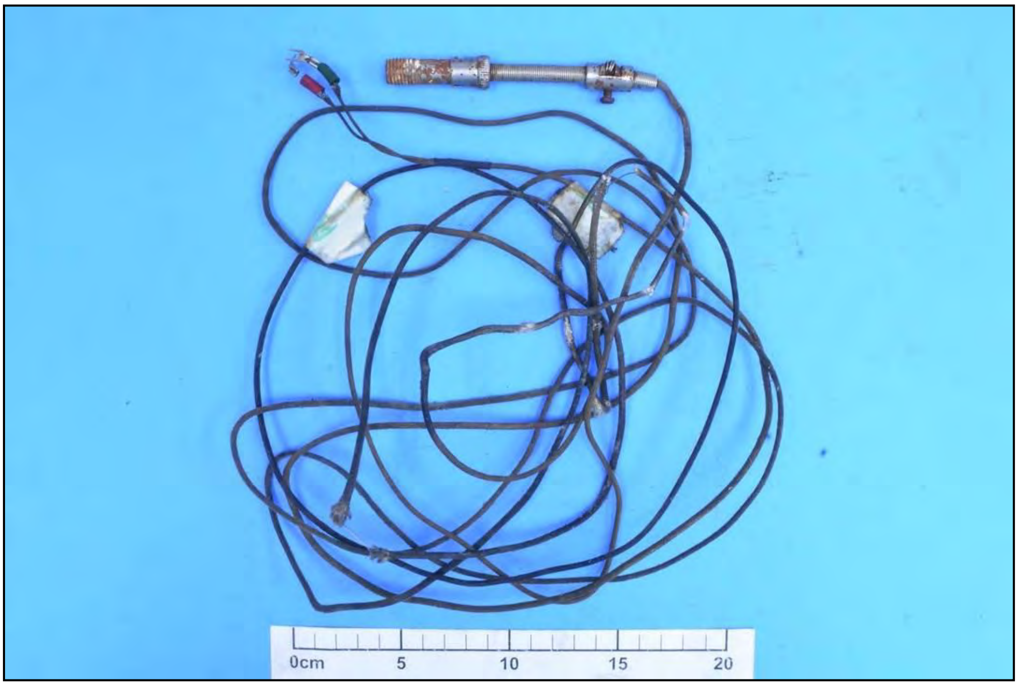

Figure 100: RTD A retrieved onsite.

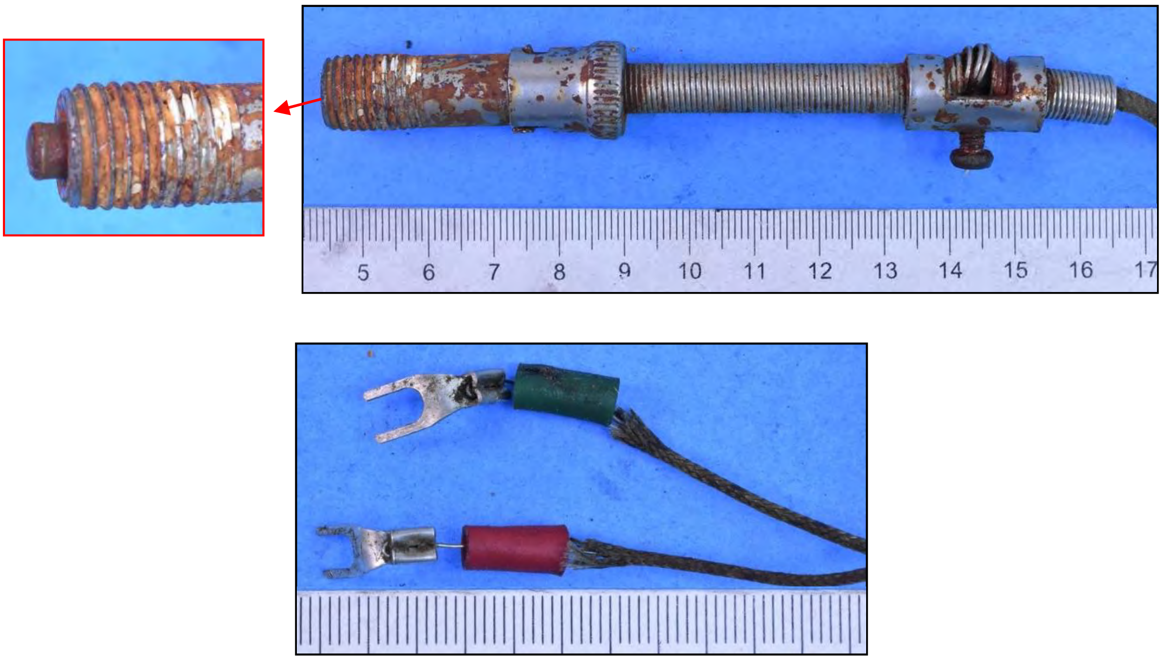

Figure 101: The RTD was still intact with the sensor. The wire connectors (red and green) were still intact, which was originally connected to the “Jacket temp” thermostat. See Figure 107.

Visual and Macroscopic Examination

RTD B

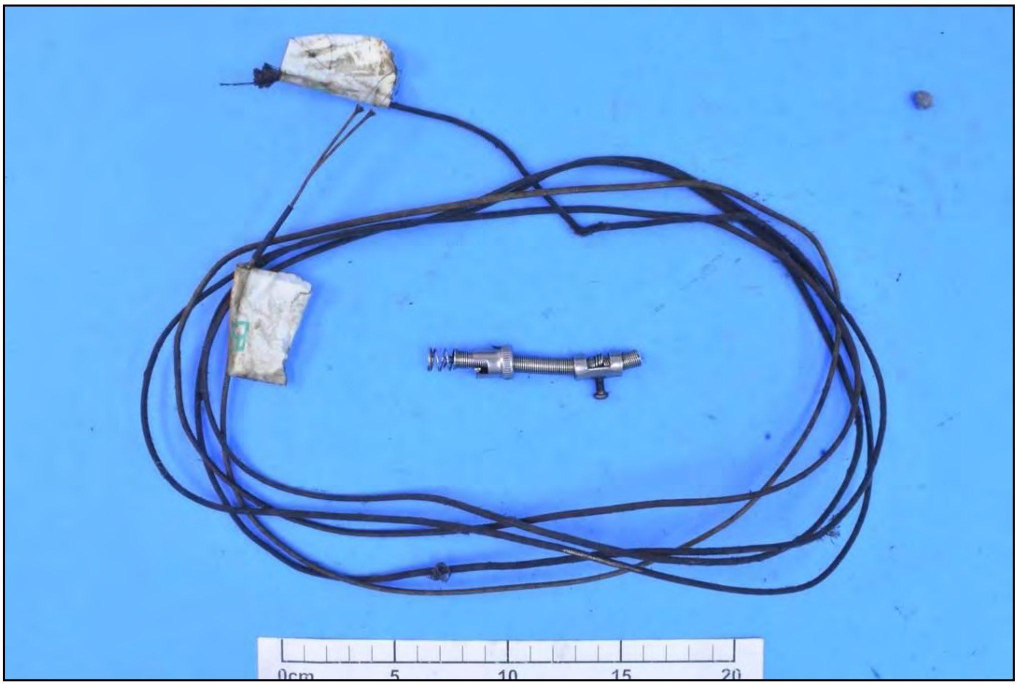

Figure 102: RTD B remnants retrieved onsite. Although this RTD was not attached to the electrical panel during the onsite inspection, the wires were originally connected to the "Material temp" thermostat as the connectors were still in place inside the panel. See Figure 107.

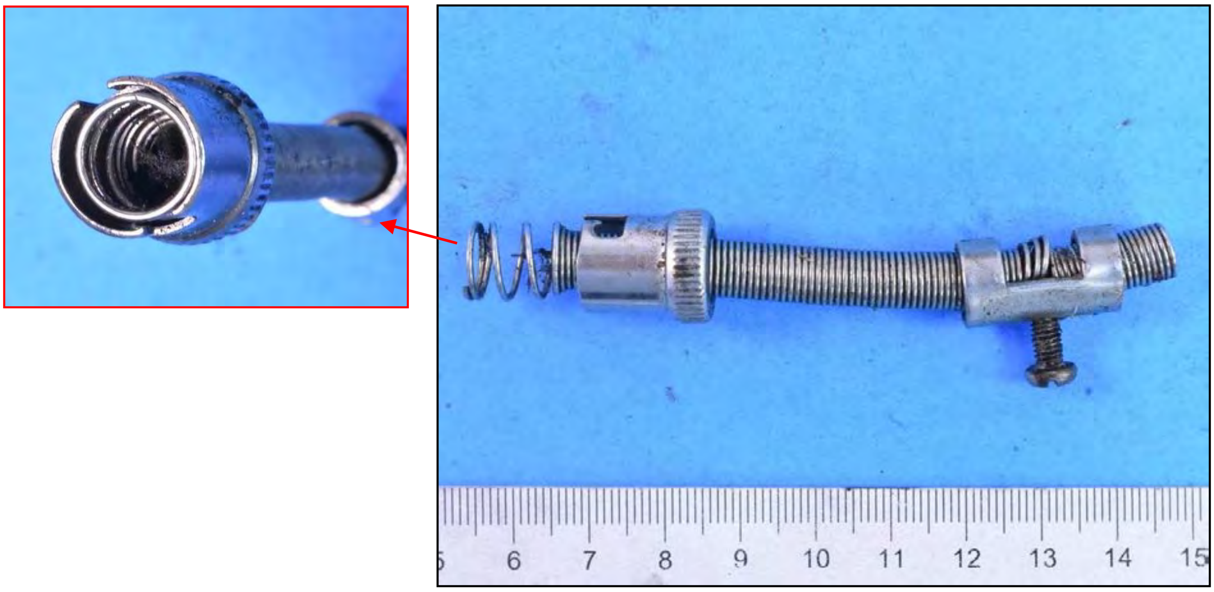

Figure 103: There was no sensor inside the holder.

Visual and Macroscopic Examination

Fixtures for RTD

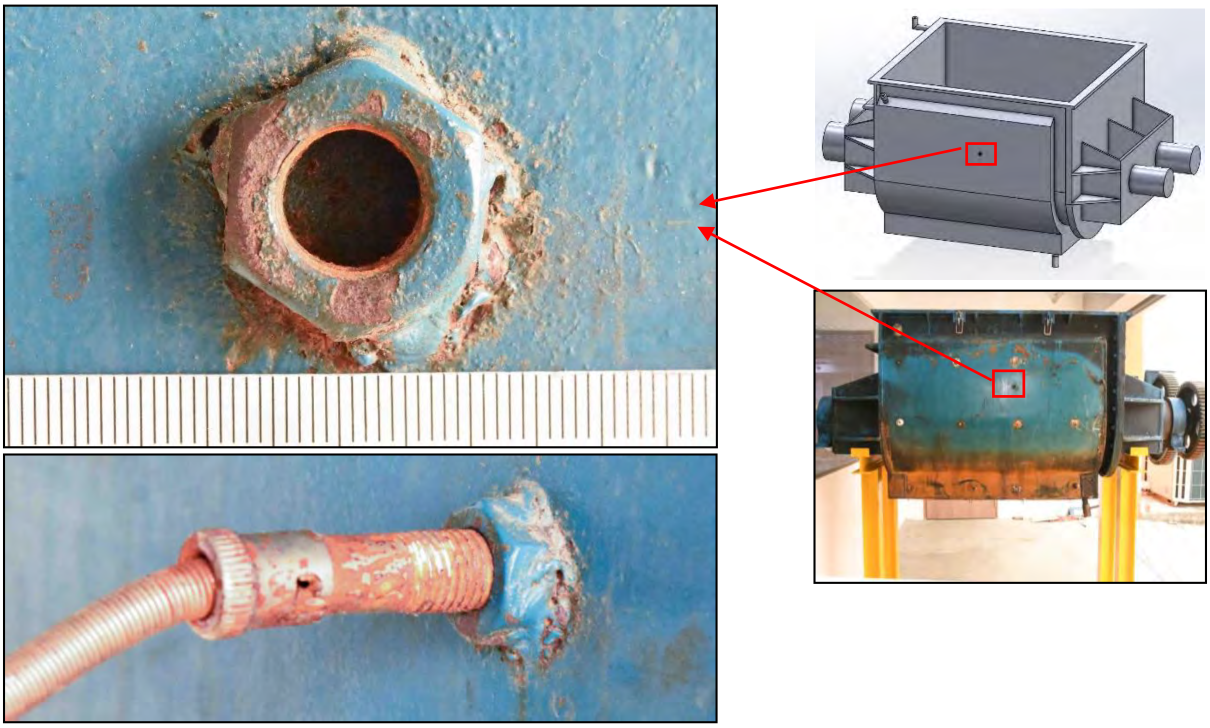

Figure 104: Close up view of the fixture intended for the RTD placement at the front side of the oil jacket. The fixture allows the sensor to reach the external surface of the oil jacket wall.

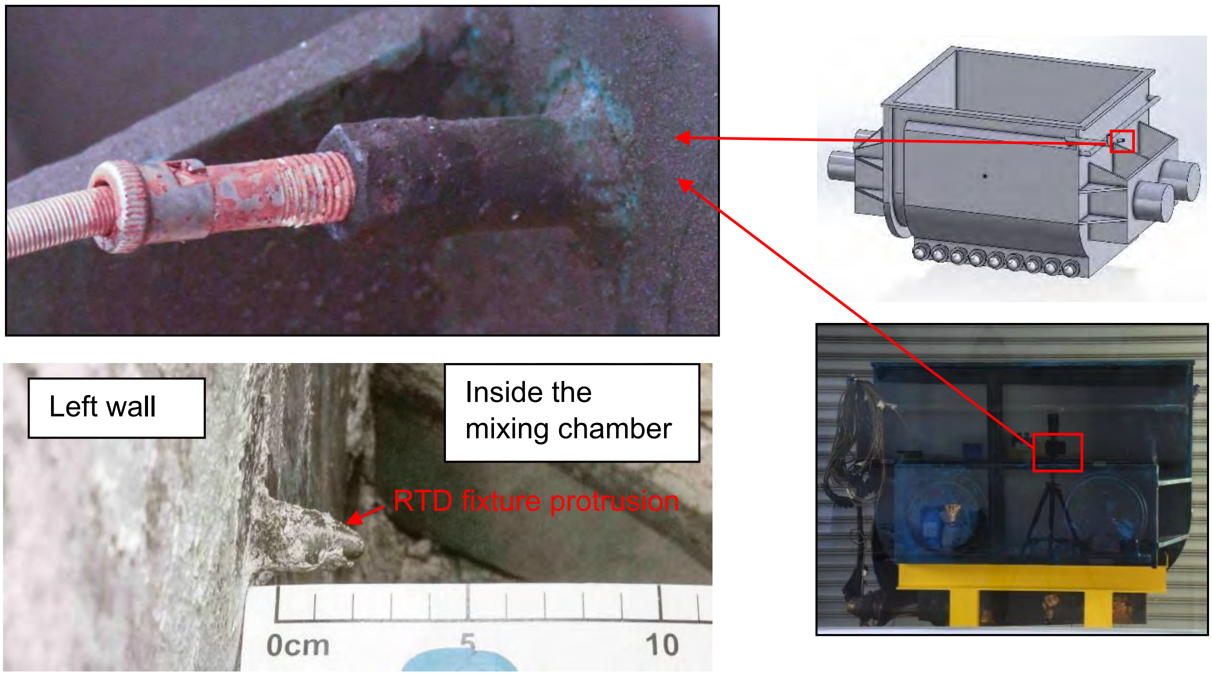

Figure 105: Close up view of the fixture intended for the RTD placement at the side of Mixer Machine nearest to the Platform stairs. This left wall is the wall containing the mixing material. The fixture slightly protruded into the wall thickness.

Visual and Macroscopic Examination

Fixtures for RTD

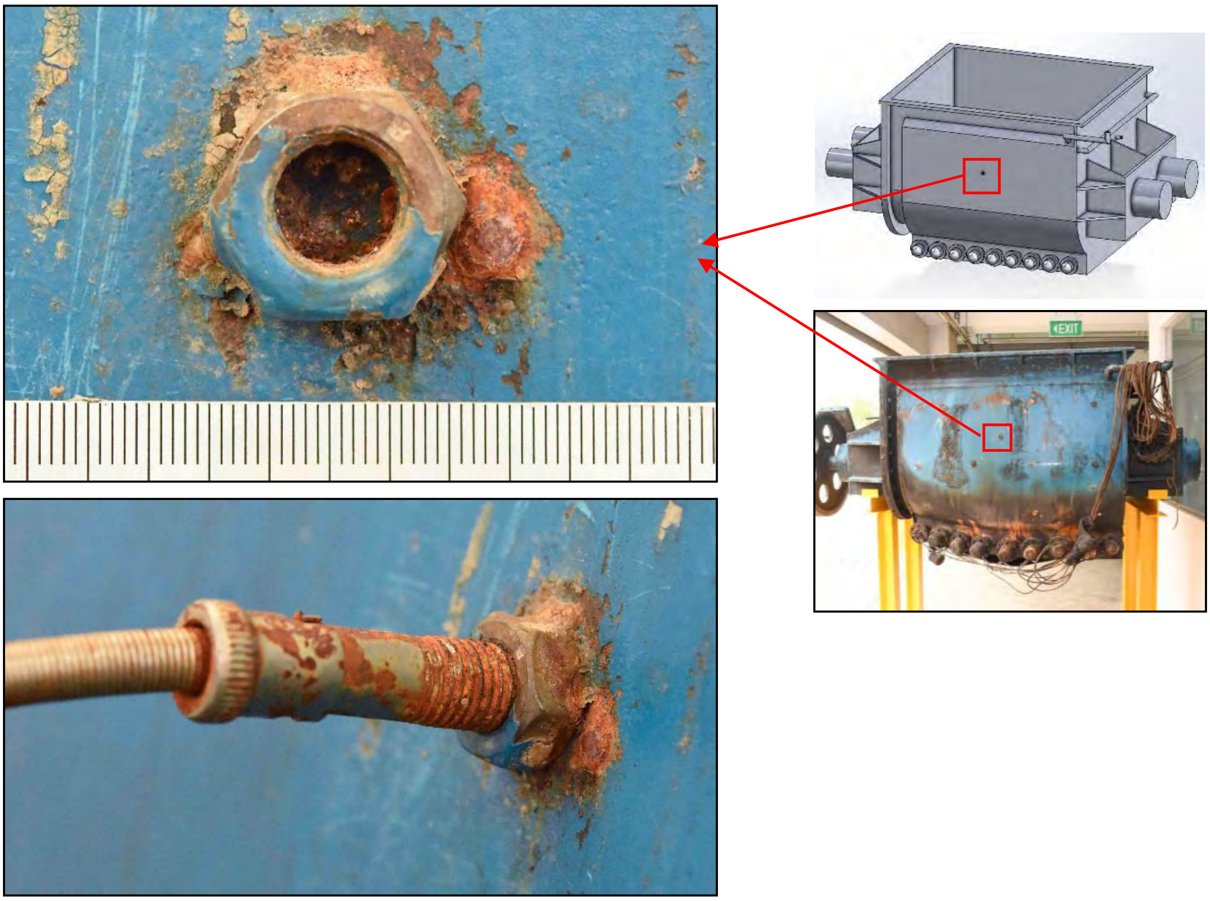

Figure 106: Close up view of the fixture intended for the RTD placement at the rear side of the oil jacket. The fixture allows the sensor to reach the external surface of the oil jacket wall.

Visual and Macroscopic Examination

Electrical Panel

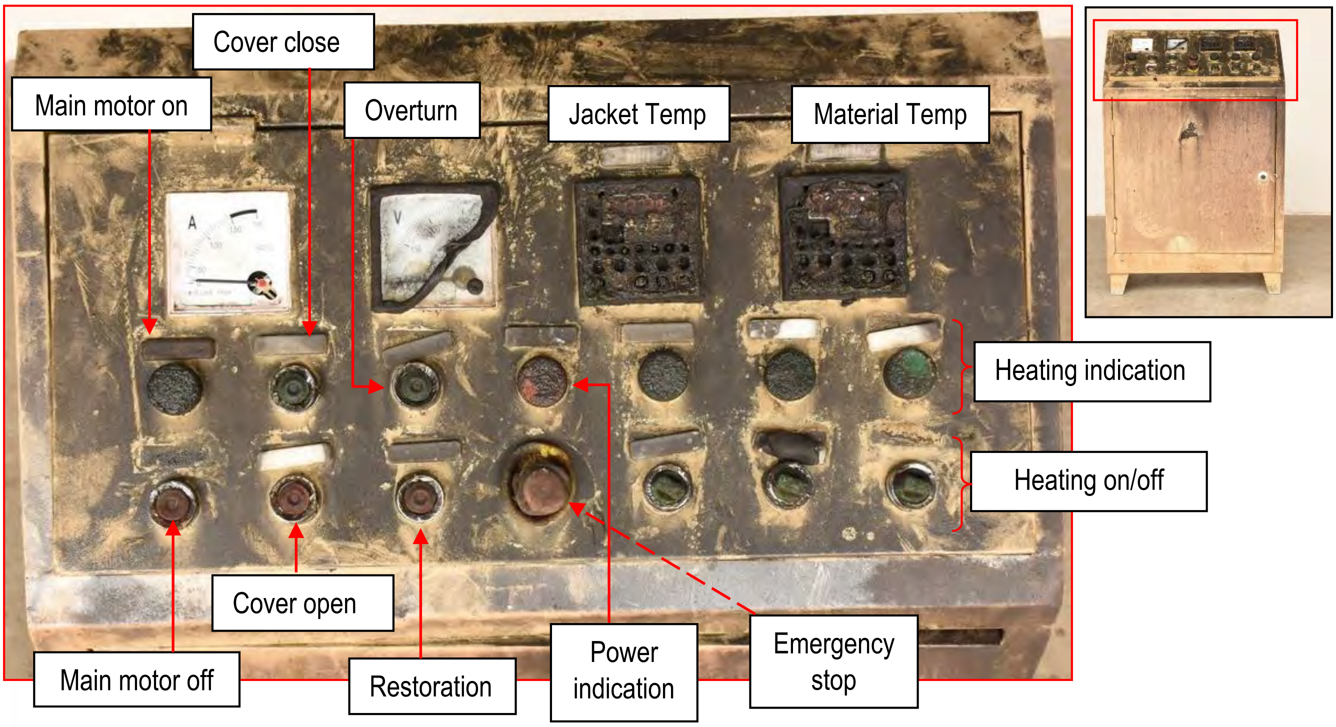

Figure 107: Electric panel – top area. The labels were made based on the reference photograph provided in *Annex 4*. The thermostats labelled “Jacket Temp” and “Material Temp” were used to indicate the temperature measured by RTDs A and B respectively. The thermostats and buttons sustained fire damages during the incident.

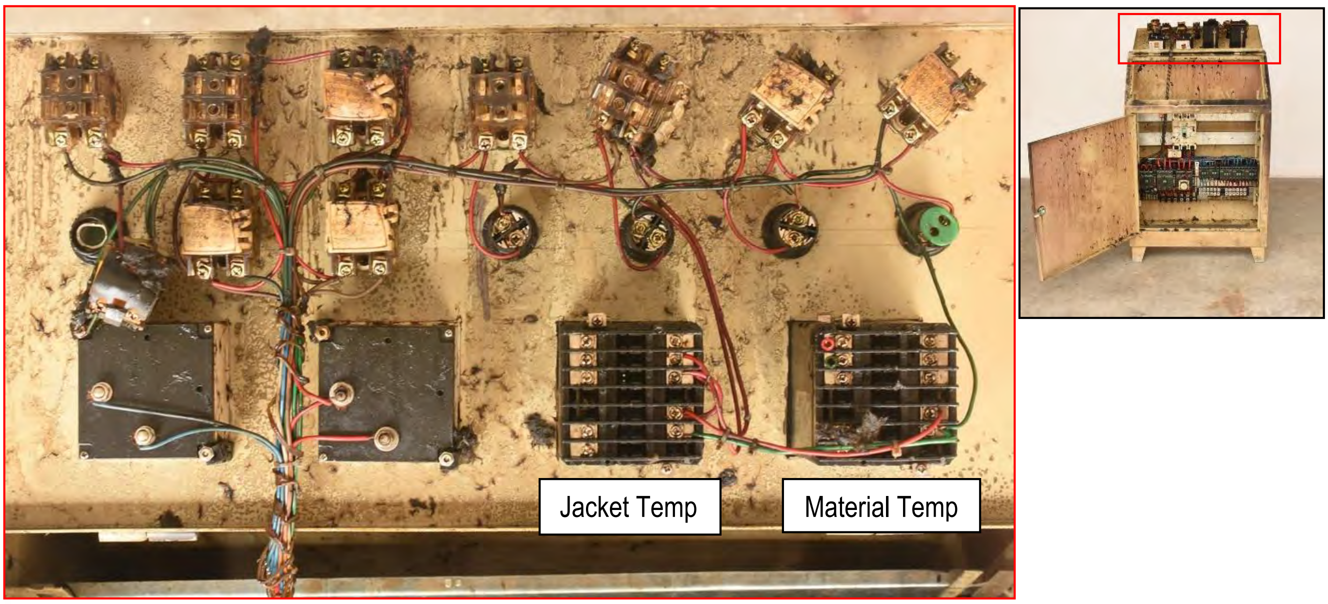

Figure 108: Inside of the electrical panel – top area.

Visual and Macroscopic Examination

Electrical Panel

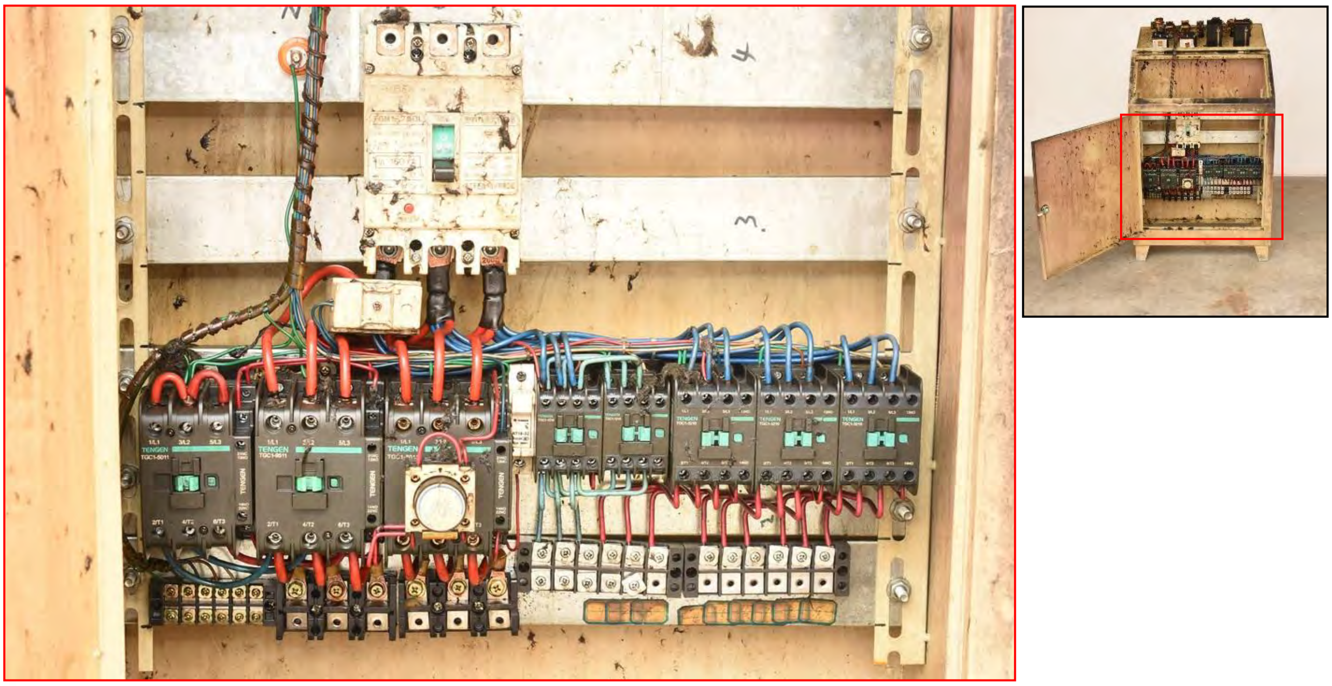

Figure 109: Electrical panel – bottom area.

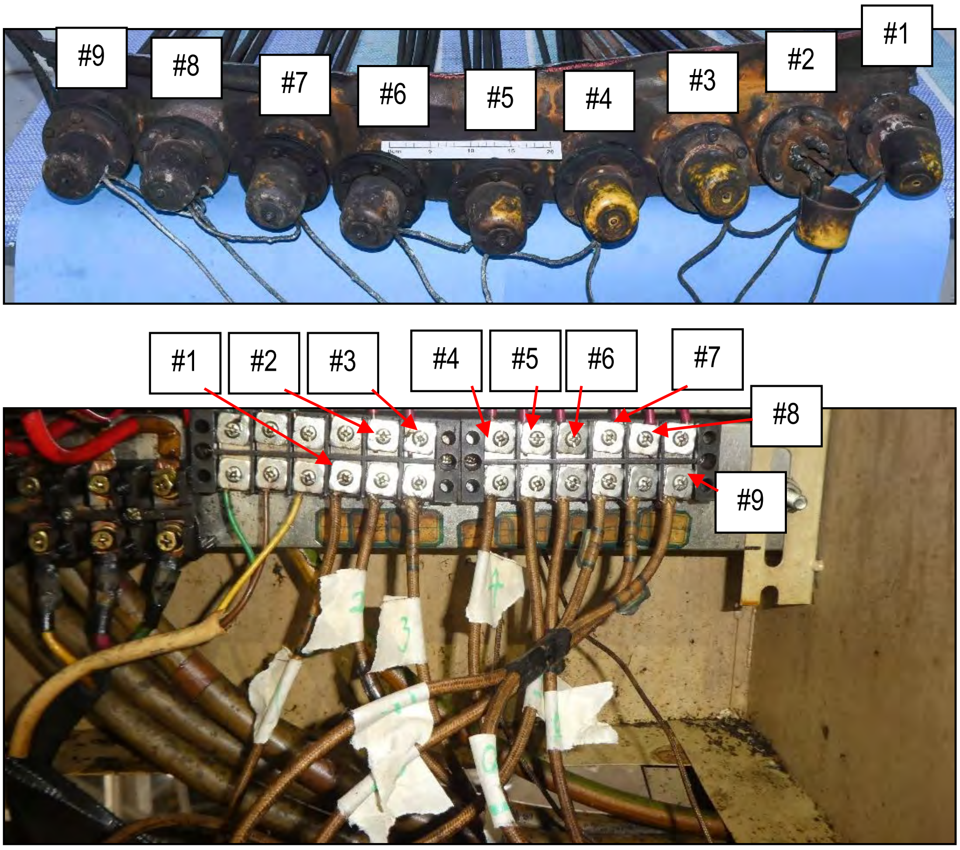

Figure 110: The wires inside the electrical panel were generally intact before the removal of the Mixer Machine to Matcor's laboratory.

Visual and Macroscopic Examination

Other heaters – unused/new

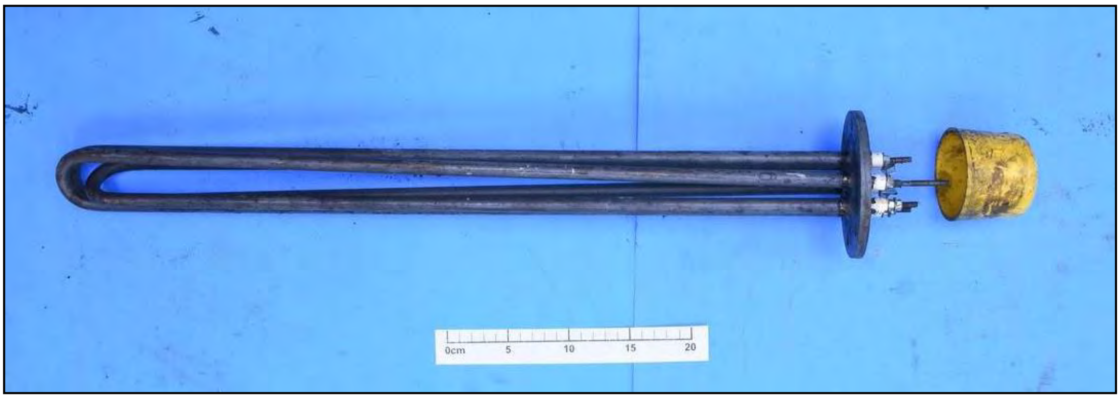

Figure 111: Heater found on the Platform beside the Mixer Machine. No significant damage was observed.

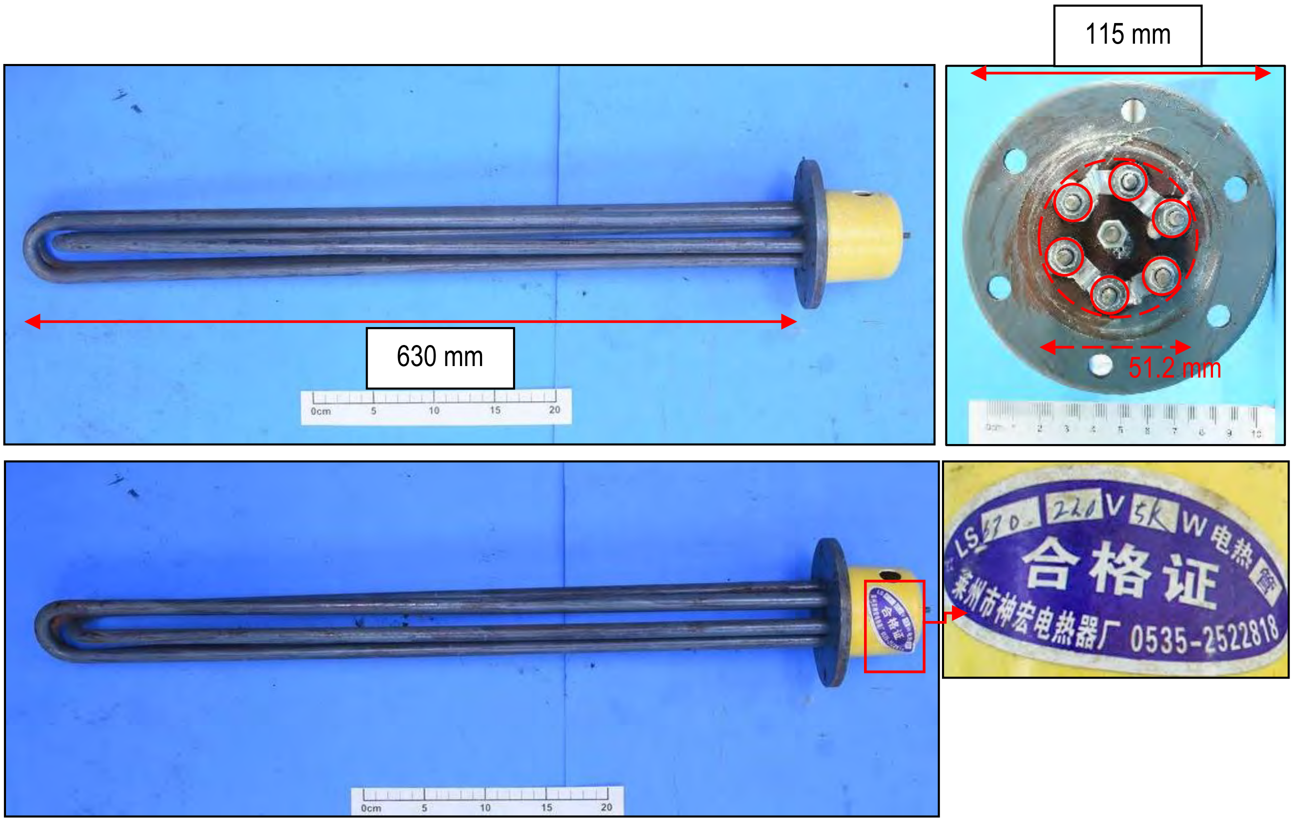

Figure 112: Two new heaters retrieved from storeroom on the second level of 32E Tuas Avenue 11 were used as reference. The measured length of the heater coils was about 630 mm, the outer perimeter (circular) of the coils was about 51.2 mm and the flange's outer diameter was about 115 mm. The label indicated that the heaters were designed with specifications of 220V and 5kW.

Visual and Macroscopic Examination

Used/Failed heaters

Figure 113: Used heater that were replaced after failure (received for analysis on 28th May 2021). This heater was reportedly replaced in August 2020 after it failed.

Figure 114: One of the coil had broken off from the heater. The metal tube had deformed and melted off around the breakage location as evidenced by the bulbous and droplet-like shape of the metal.

Visual and Macroscopic Examination

Used/failed heaters

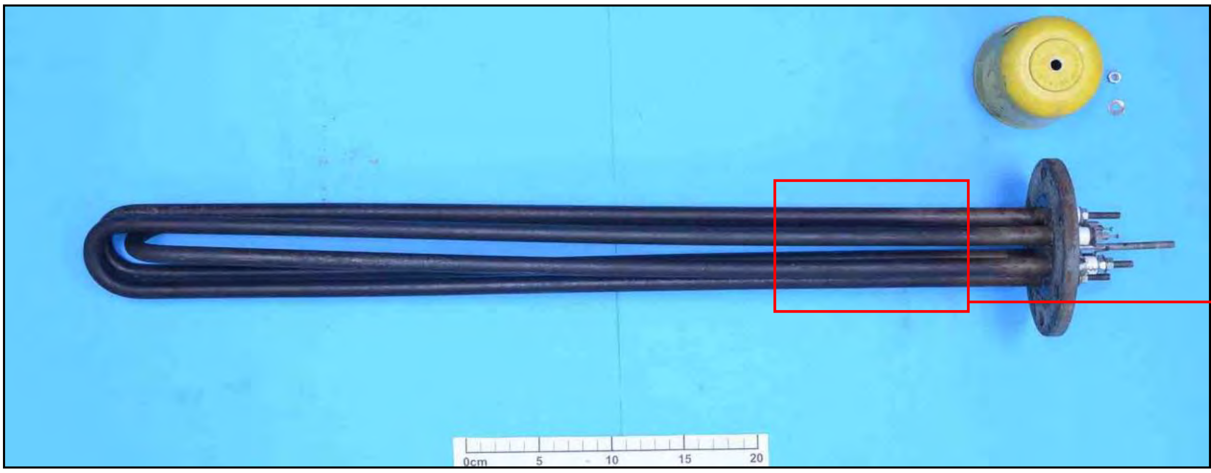

Figure 115: A heater that was used and replaced (received for analysis on 1st June 2021). Not much information was provided about this heater.

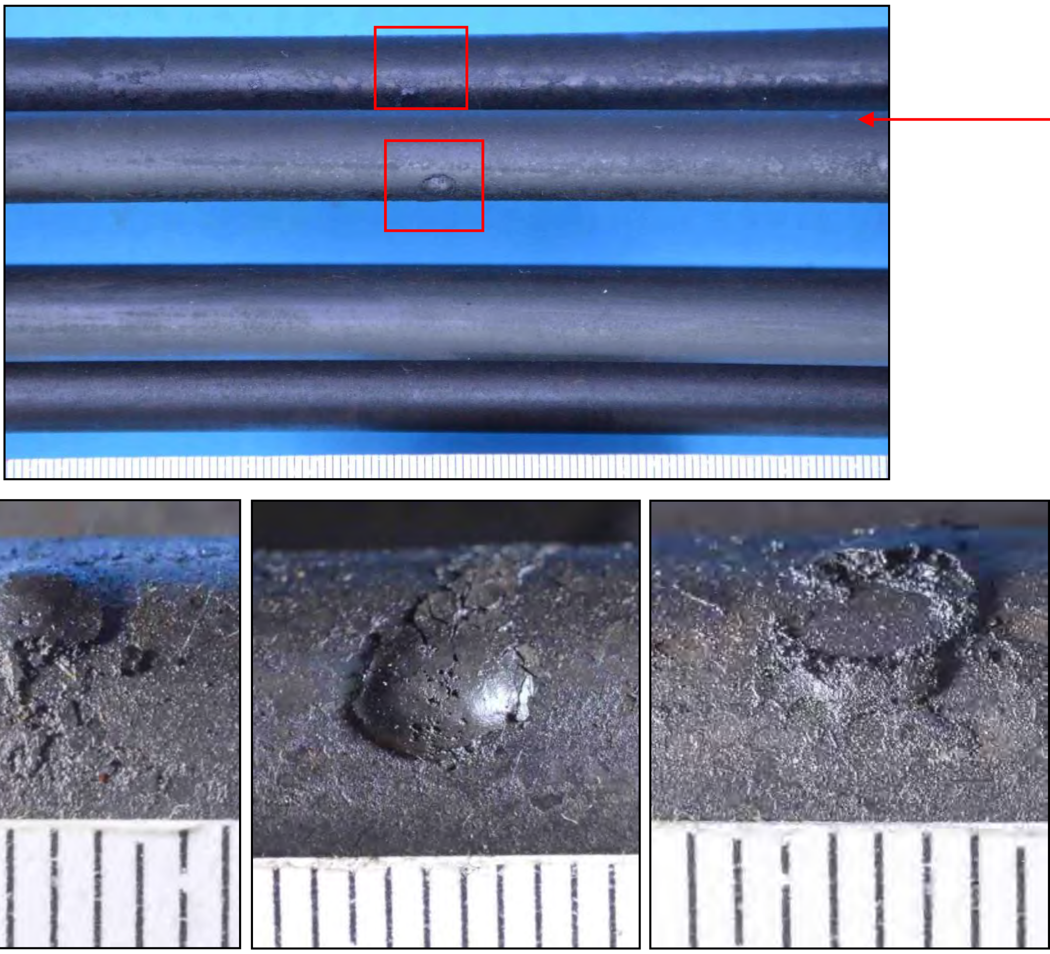

Figure 116: Several blisters of up to about 5 mm were observed on the metal tubes.

Appendix D:

Fractographic Examination using Digital Microscope and SEM

Fractographic Examination

Rear side, left edge weld

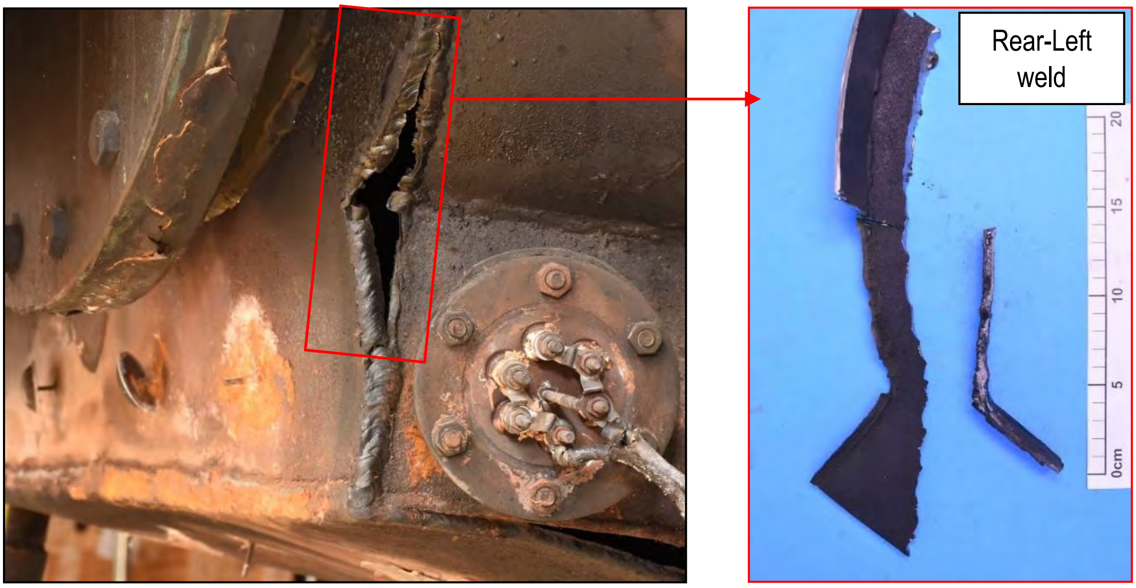

Figure 117: SEM examination was conducted on this part of the tank's rear-left weld. See Figure 119 to Figure 124.

Bottom face weld

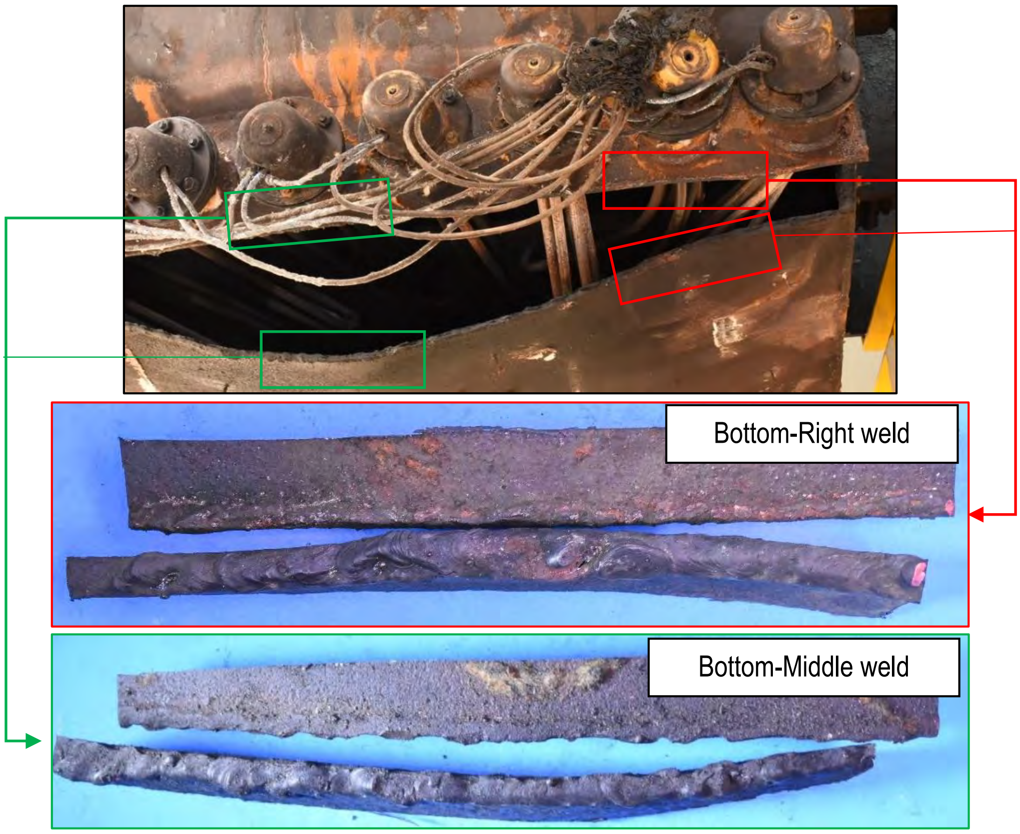

Figure 118: SEM examination was conducted on this part of the tank's bottom welds. See Figure 125 to Figure 130.

Fractographic Examination

Rear side, left edge weld

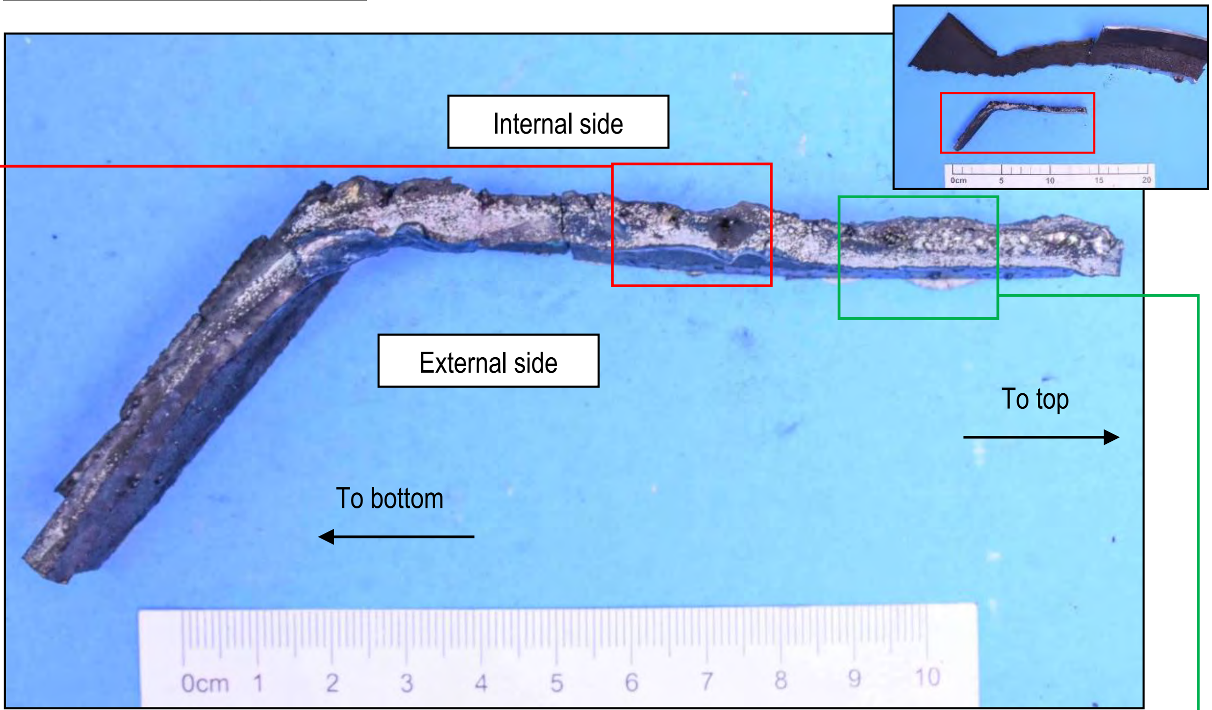

Figure 119: Fracture surface after cleaning in an ultrasonic bath of Alconox solution and subjected to SEM examination.

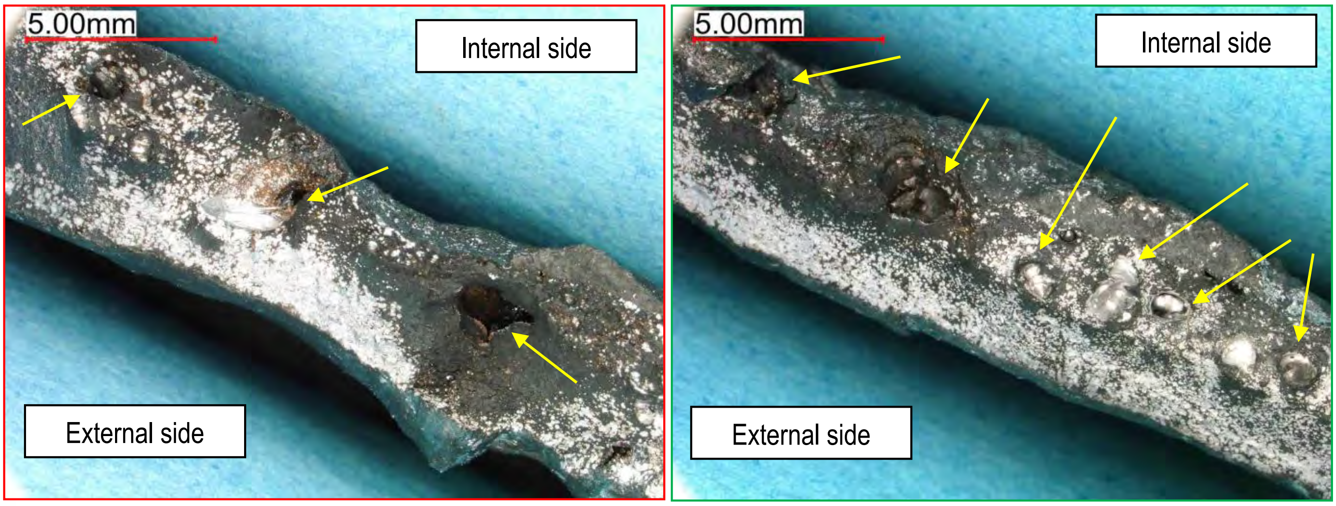

Figure 120: Macroscopic view of fracture surface. Weld porosities were observed throughout the fracture surface (which is the weld metal), predominantly at about the mid-depth from the external surface (indicated with yellow arrows).

Fractographic Examination

Rear side, left edge weld

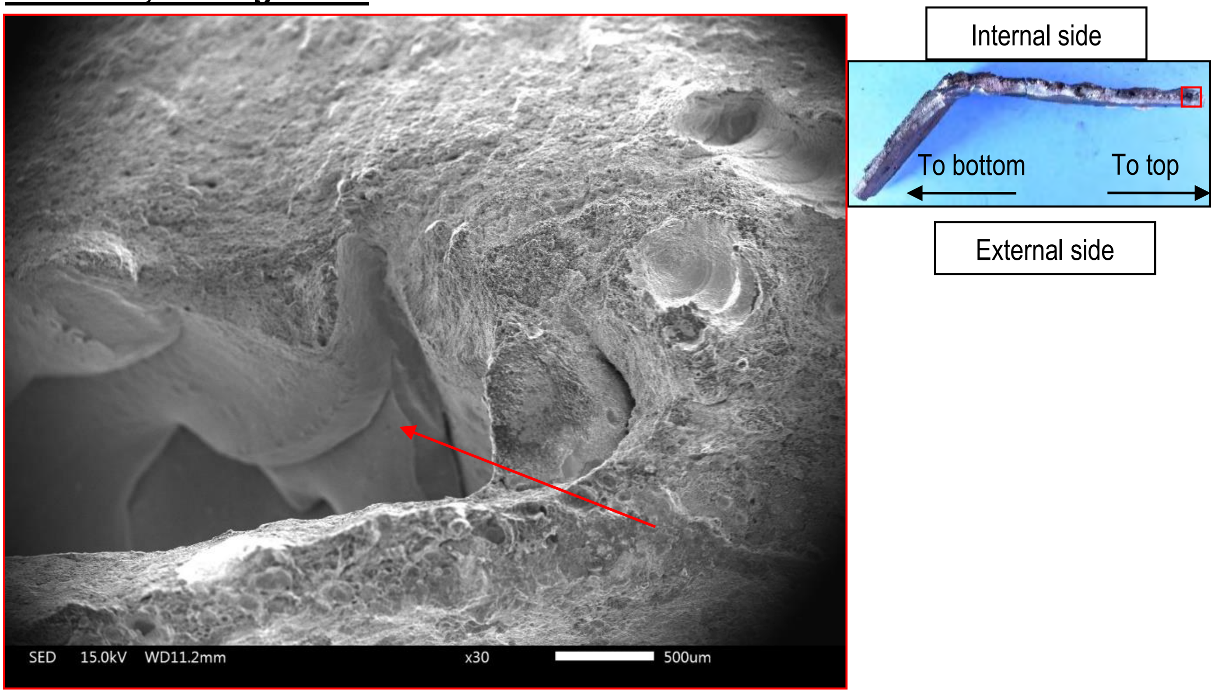

Figure 121: Voids were observed scattered on the fracture surface, consistent with weld porosities.

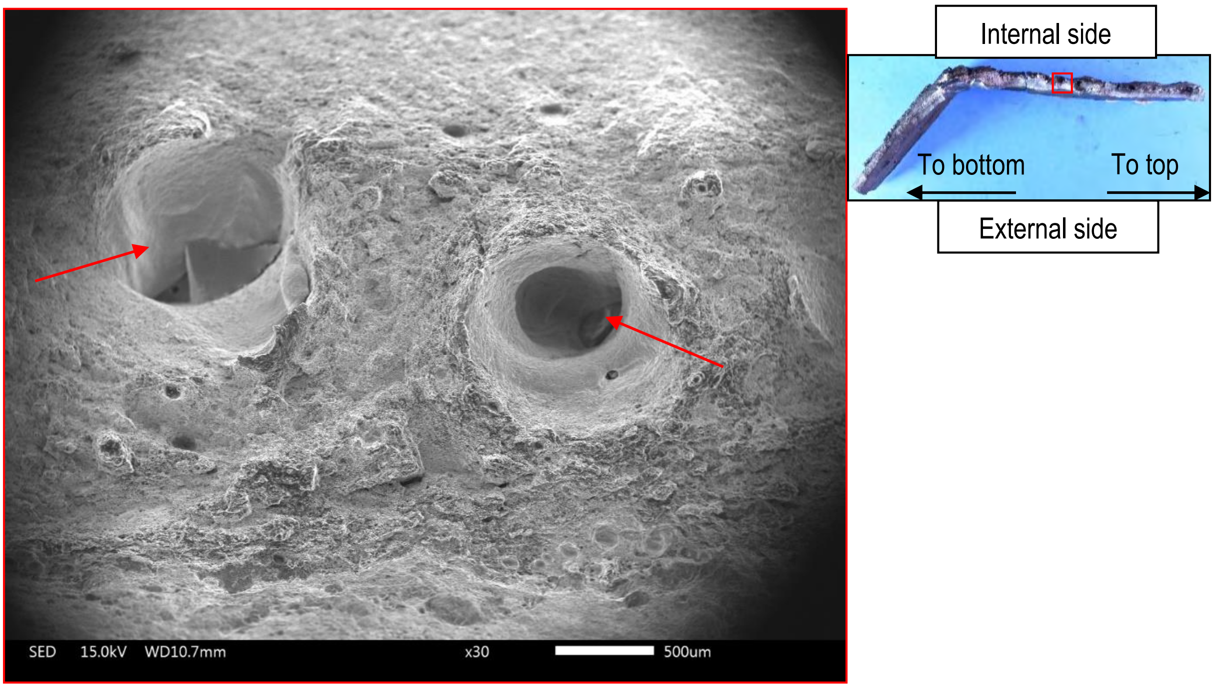

Figure 122: Voids were observed scattered on the fracture surface, consistent with weld porosities.

Fractographic Examination

Rear side, left edge weld

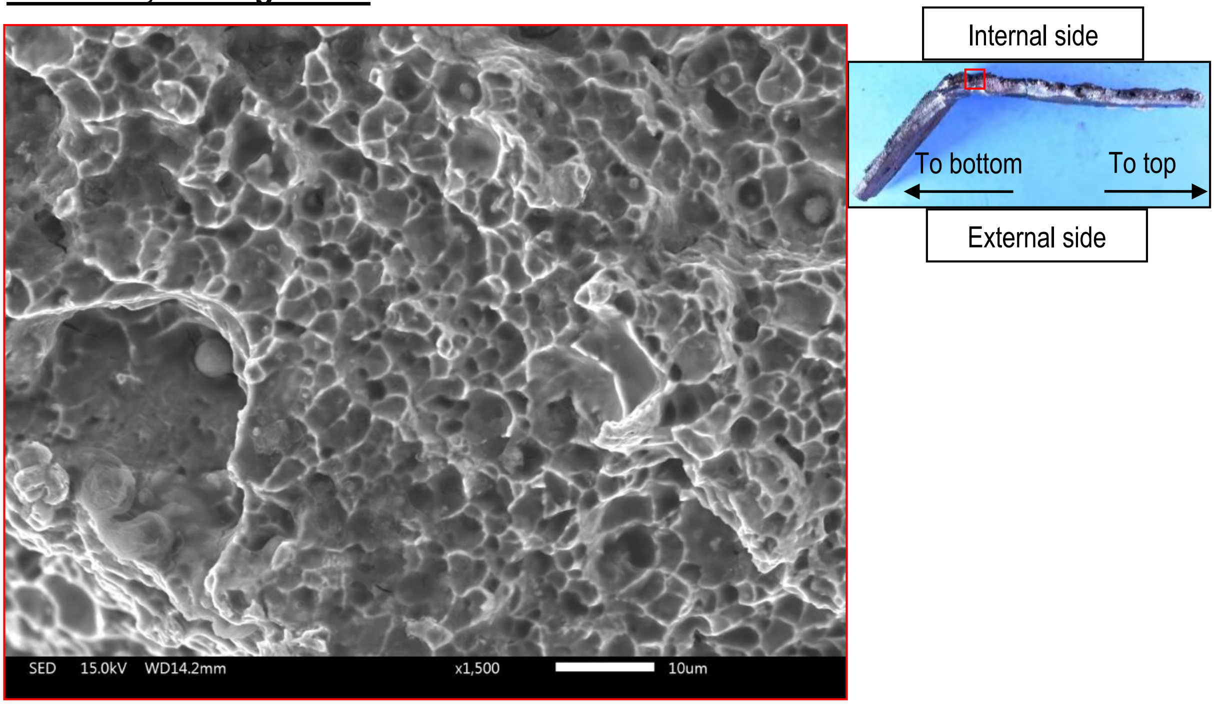

Figure 123: Relatively equiaxed dimples were generally observed throughout the fracture surface at regions adjacent to the internal side.

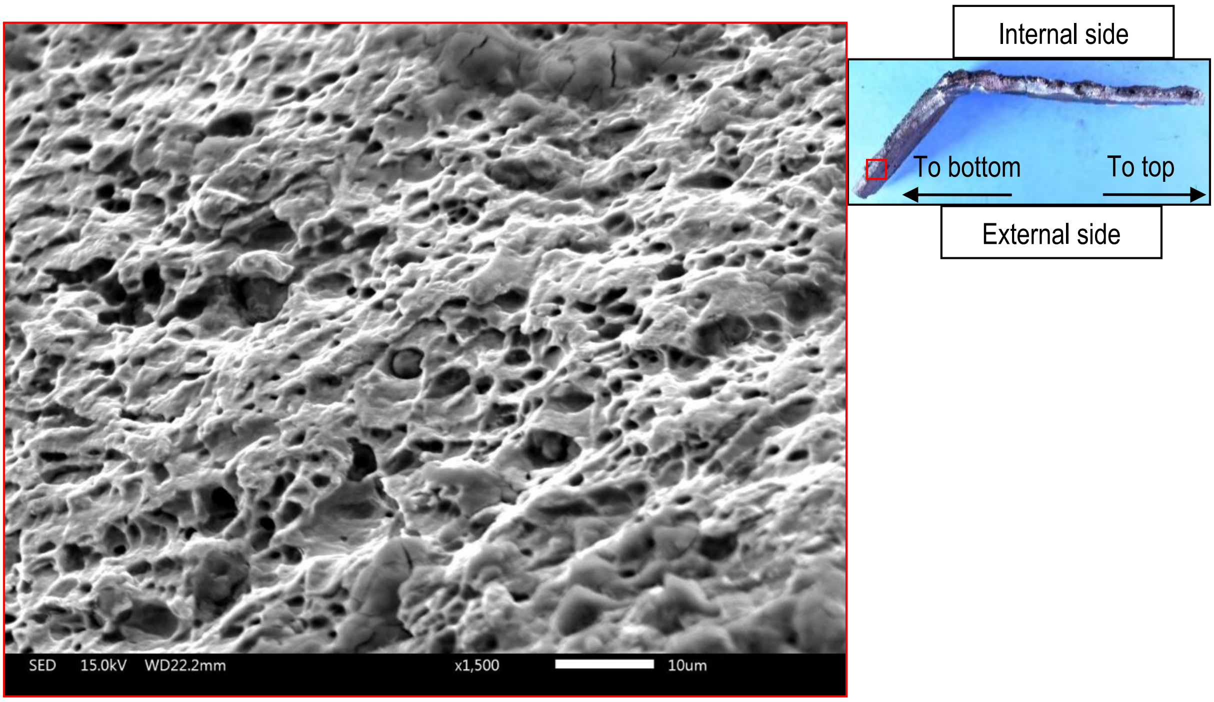

Figure 124: Elongated dimples were generally observed throughout the fracture surface at regions adjacent to the external side.

Fractographic Examination

Rear side, bottom right weld

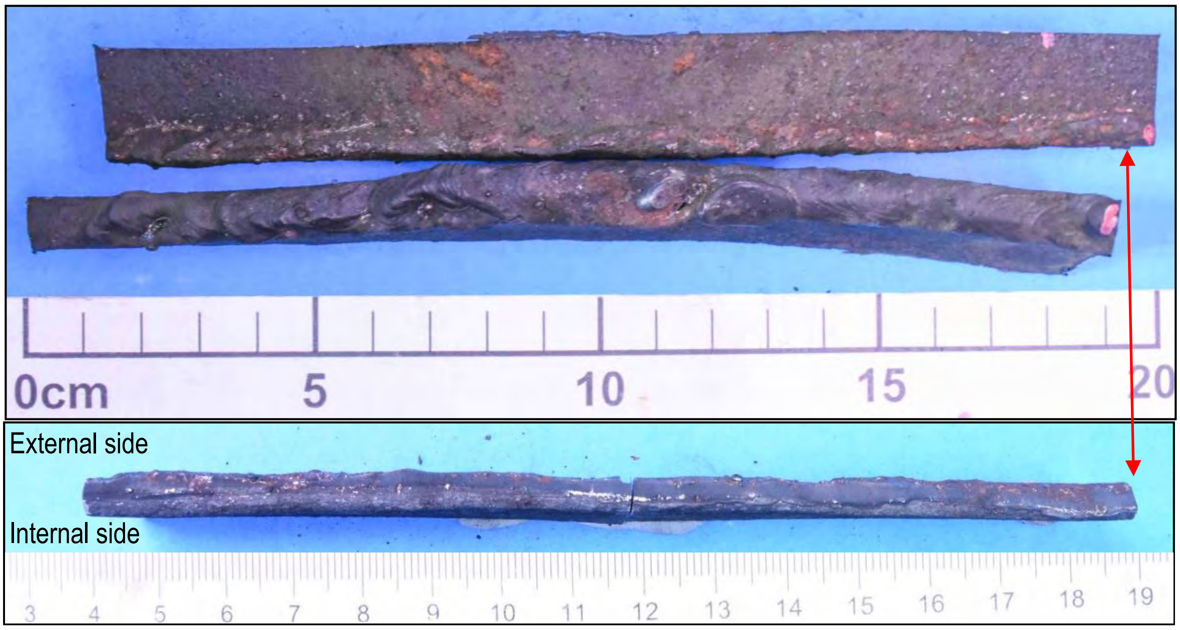

Figure 125: Rear side, bottom right weld. Fracture surface condition after cleaning in an ultrasonic bath of Alconox solution (bottom figure). See Figure 127 to Figure 128.

Rear side, bottom middle weld

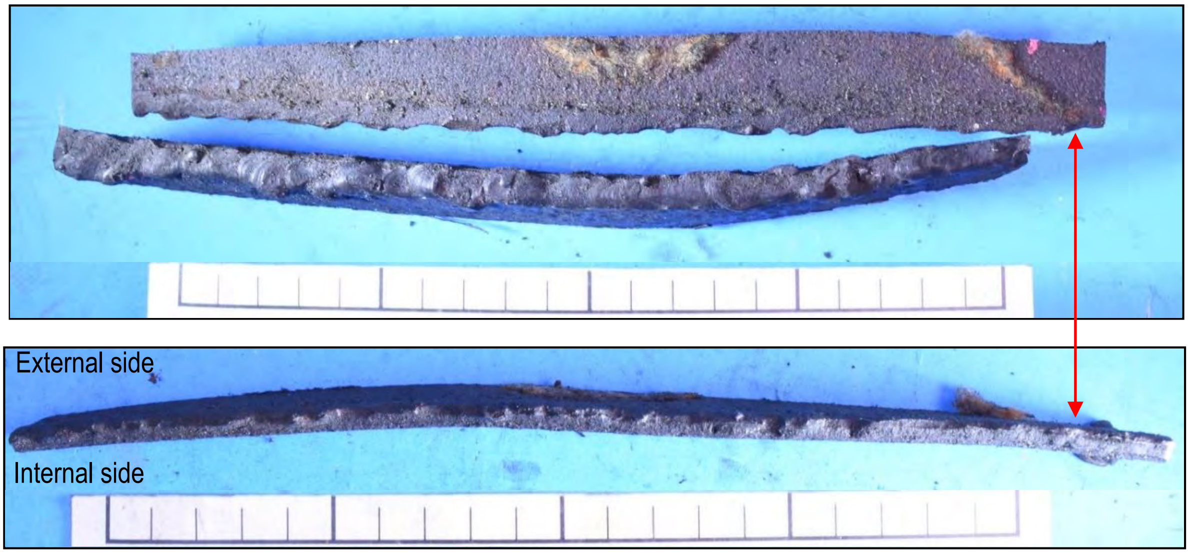

Figure 126: Rear side, bottom middle weld. Fracture surface condition after cleaning in an ultrasonic bath of Alconox solution (bottom figure). See Figure 129 to Figure 130.

Fractographic Examination

Rear side, bottom-right weld

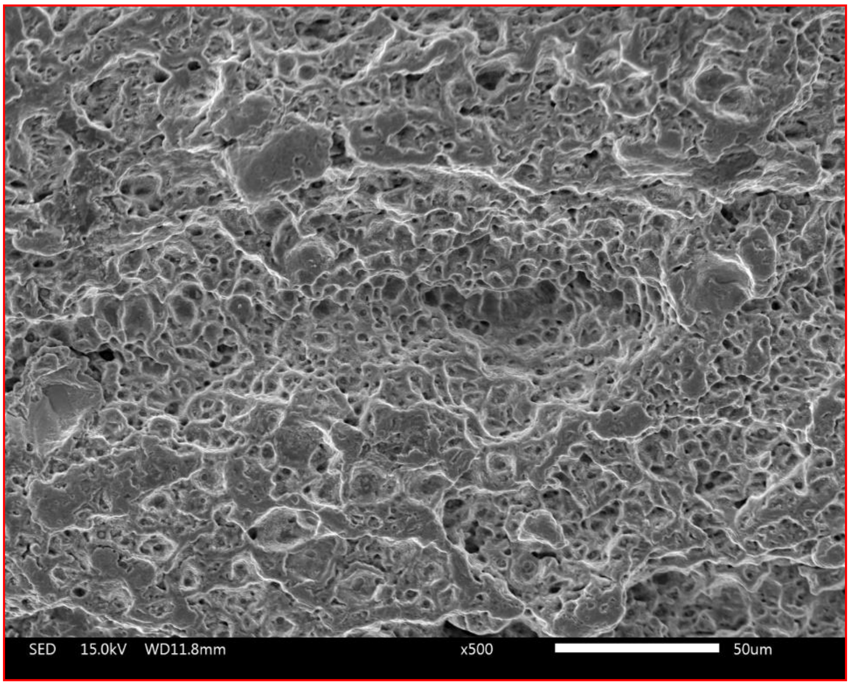

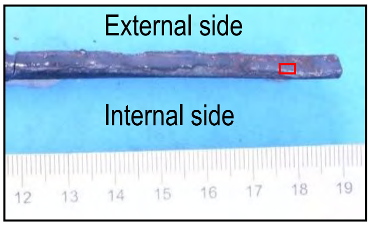

Figure 127: Equiaxed dimples were generally observed throughout the fracture surface at regions adjacent to the internal side.

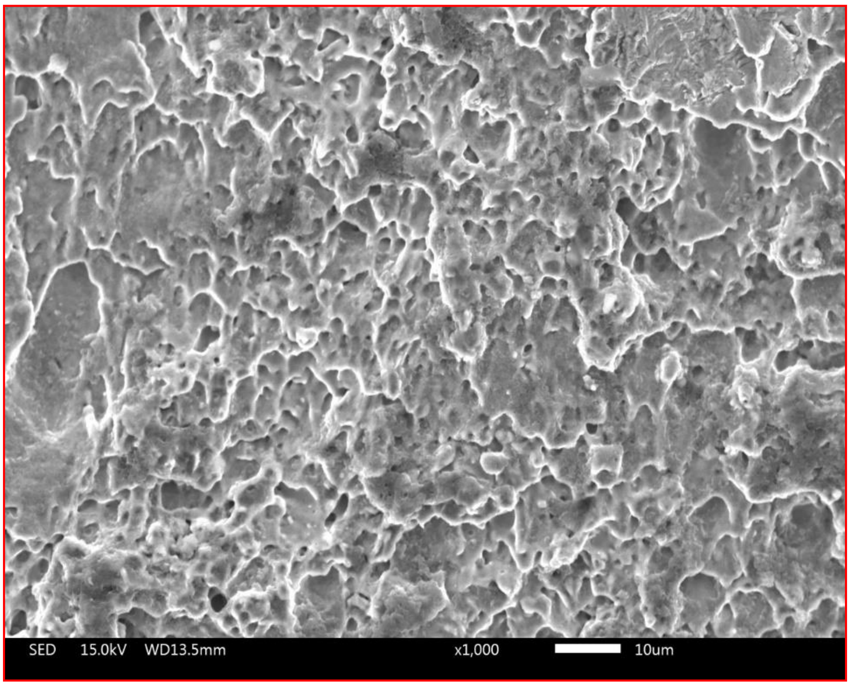

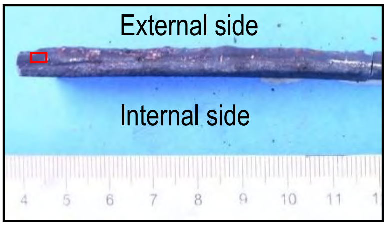

Figure 128: Elongated dimples were generally observed throughout the fracture surface at regions adjacent to the external side.

Fractographic Examination

Rear side, bottom-middle weld

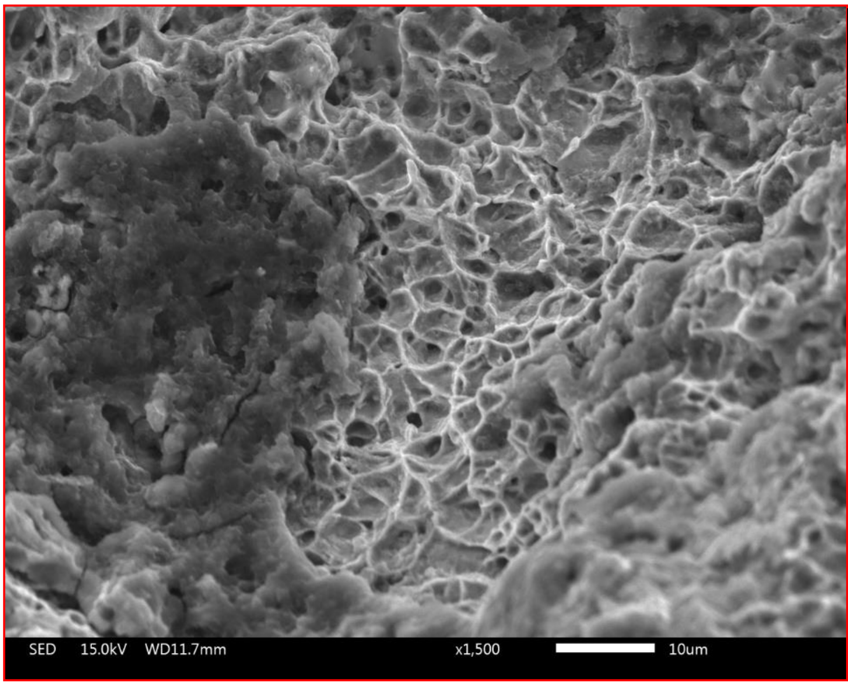

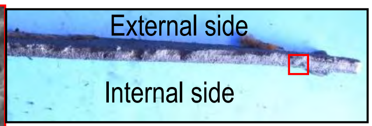

Figure 129: Equiaxed dimples were generally observed throughout the fracture surface at regions adjacent to the internal side.

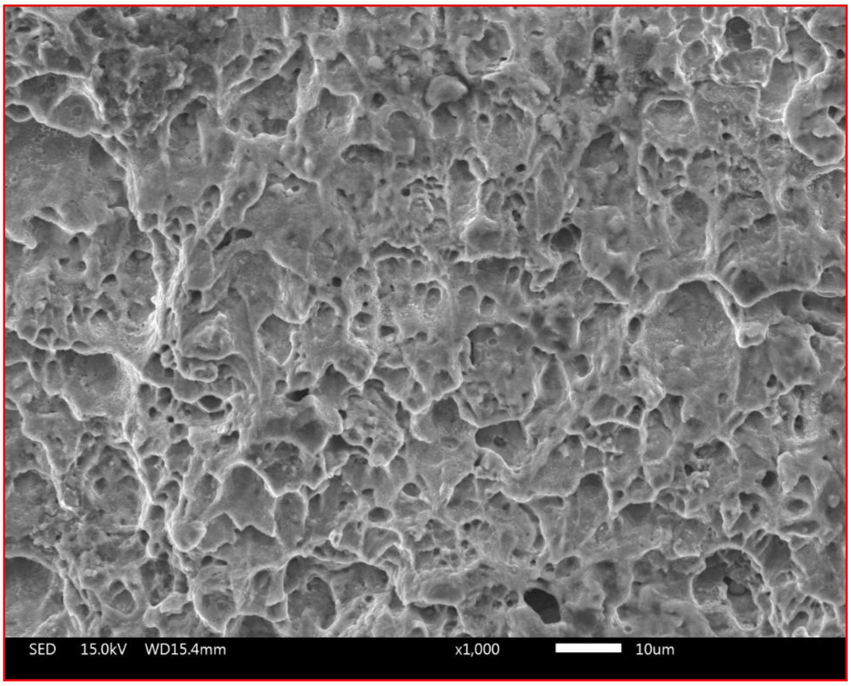

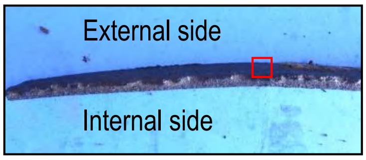

Figure 130: Elongated dimples were generally observed throughout the fracture surface at regions adjacent to the external side.

Microscopic Examination

Lugs from Heater #2

Lug from terminal 3

Figure 131: Wire and lug of heater #2, terminal 3.

Lug from terminal 4

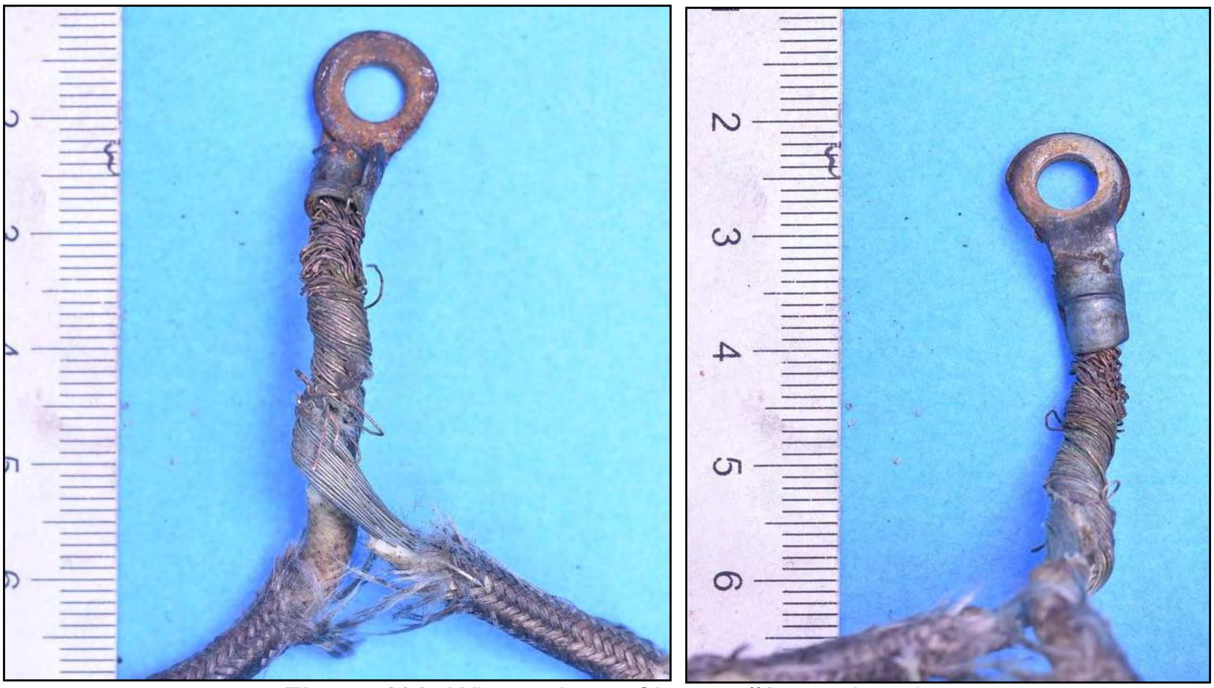

Figure 132: Wire and lug of heater #2, terminal 4.

Microscopic Examination

Lugs from Heater #2

Lug from terminal 3

Figure 133: Condition of lug before cleaning.

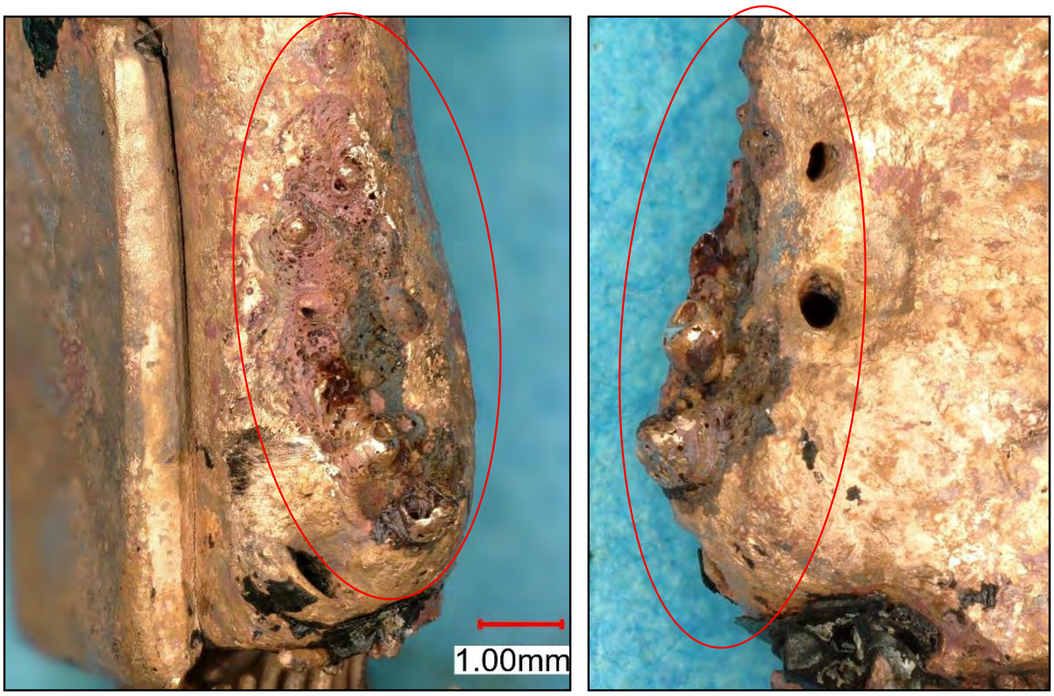

Figure 134: Condition of lug after cleaning in an ultrasonic bath of Alconox solution. Resolidification waves and high porosity, characteristics of arcing damage, were observed at the bottom edge of the lug.

Microscopic Examination

Lugs from Heater #2

Lug from terminal 3

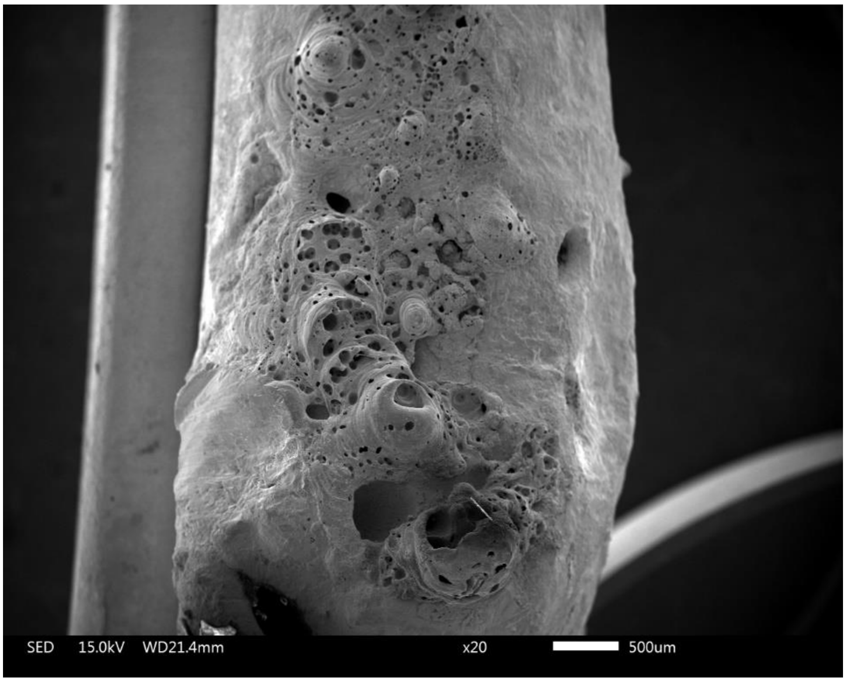

Figure 135: SEM confirms the arcing characteristic with large percentage of voids.

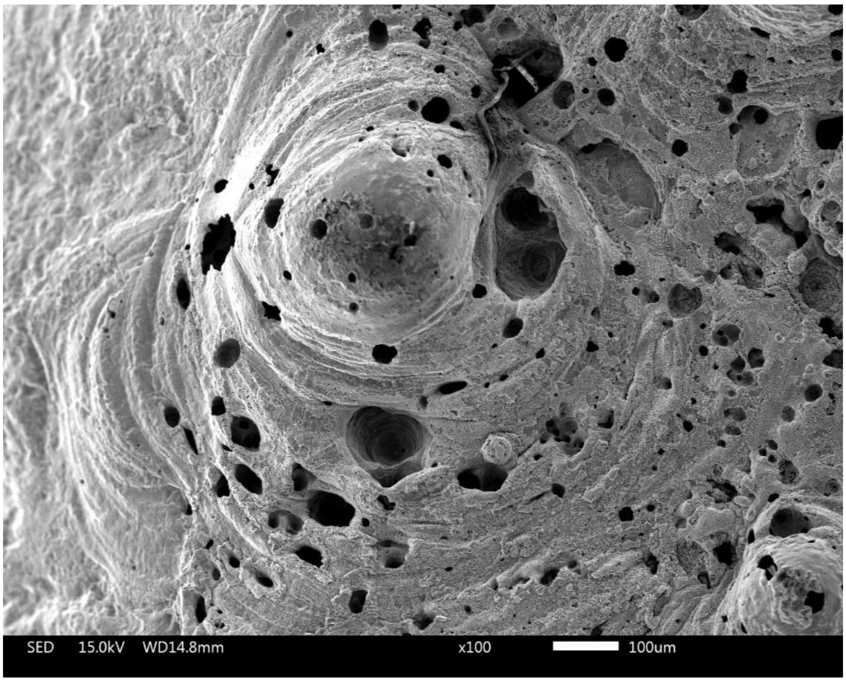

Figure 136: SEM confirms the arcing characteristic with large percentage of voids and concentric rings observed to be emanating from the centre of the arcing damage.

Internal Condition

Lugs from Heater #2

Lug from terminal 4

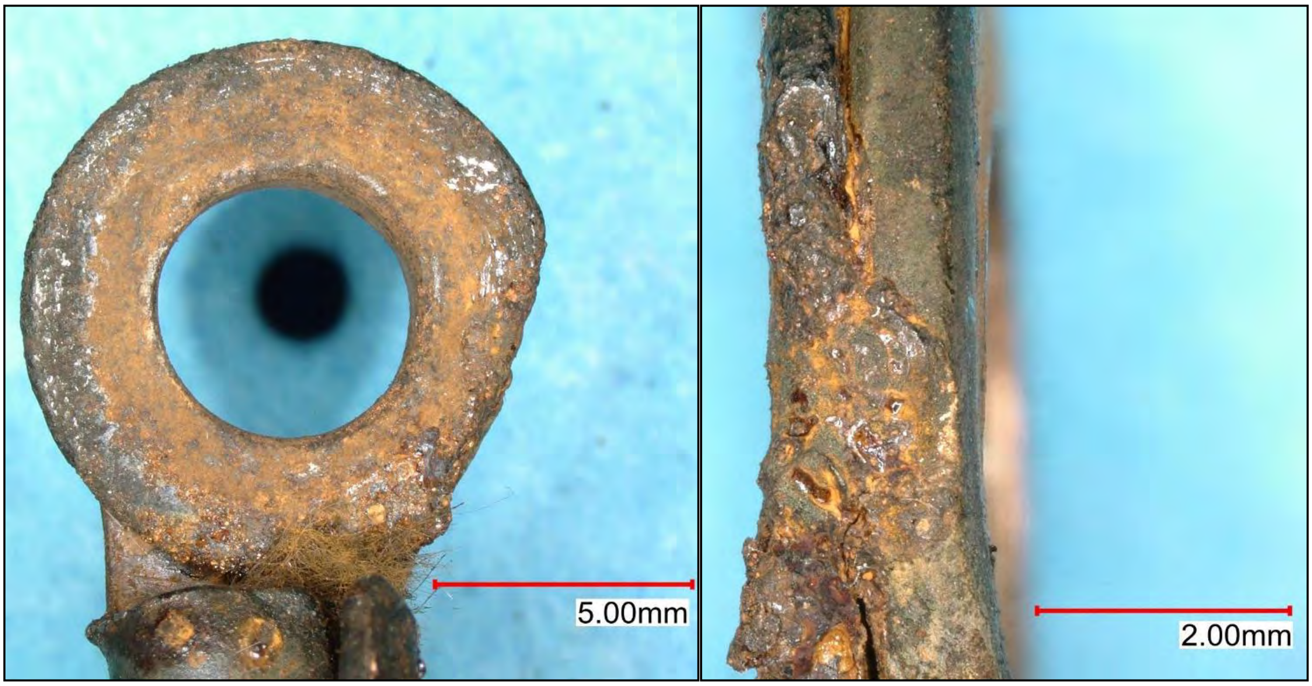

Figure 137: Condition before cleaning.

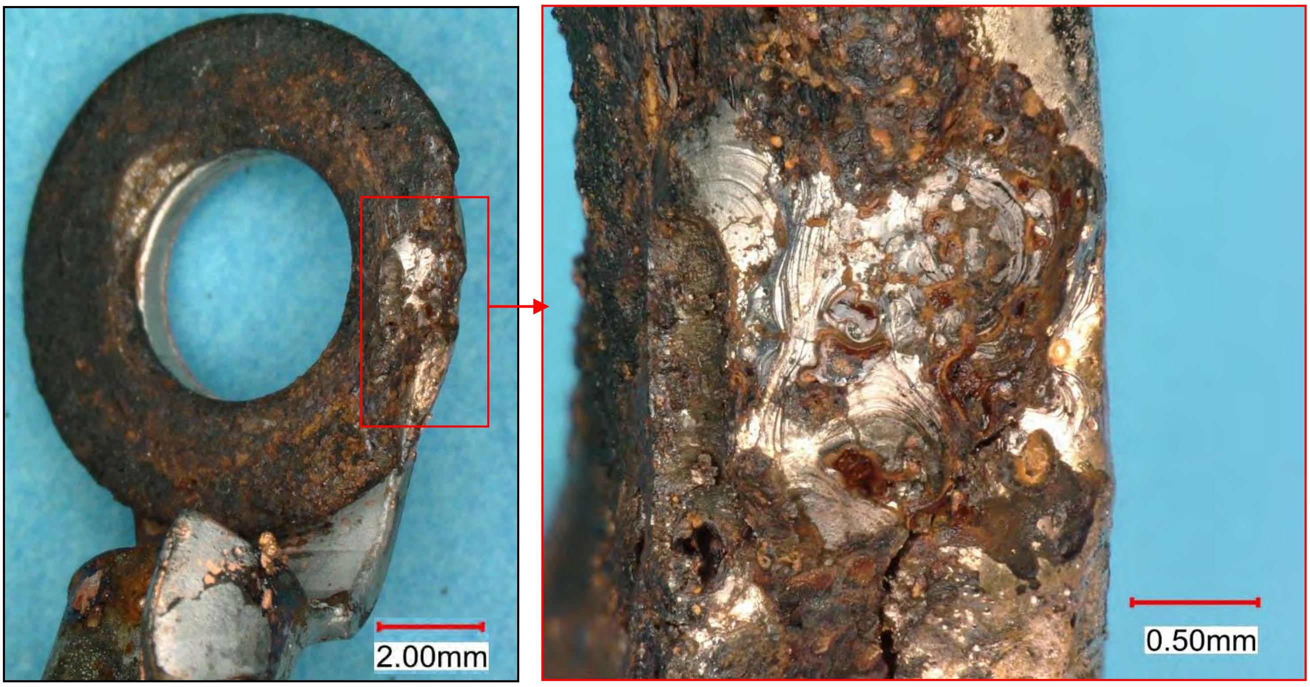

Figure 138: Condition of lug after cleaning in an ultrasonic bath of Alconox solution. Resolidification waves, a characteristic trait of arcing, observed at the lug and washer.

Internal Condition

Lugs from Heater #2

Lug from terminal 4

Figure 139: SEM confirms the arcing characteristic with concentric rings observed to be emanating from the centre of the arcing damage.

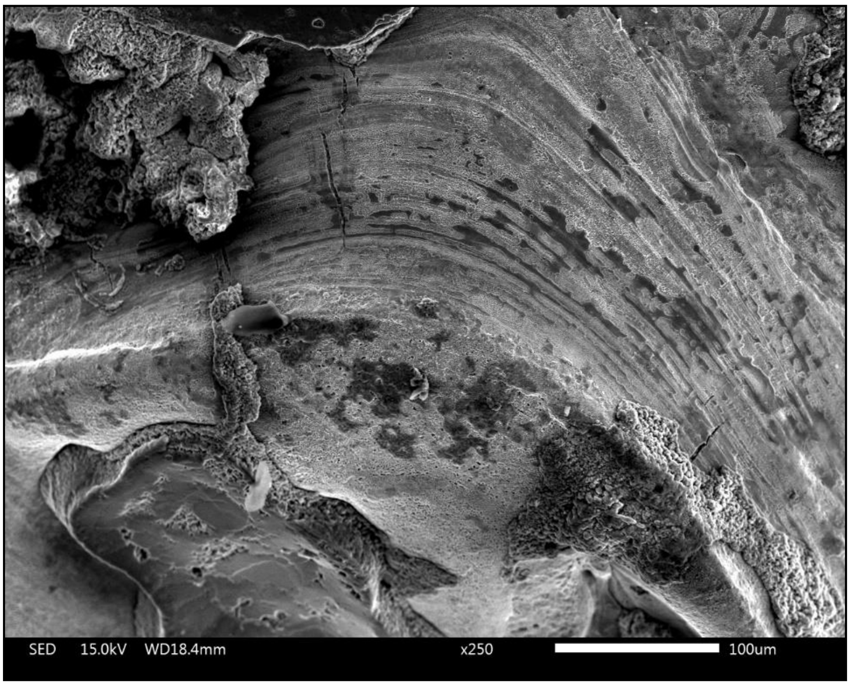

Figure 140: SEM confirms the arcing characteristic with concentric rings observed to be emanating from the centre of the arcing damage.

Appendix E:
Chemical and EDX Analysis

Chemical Analysis

Chemical analysis of oil jacket walls

Front left side wall (oil jacket)

Element	C	Mn	Si	Cr	Mo
Wt%	0.17	0.40	0.12	0.15	0.002

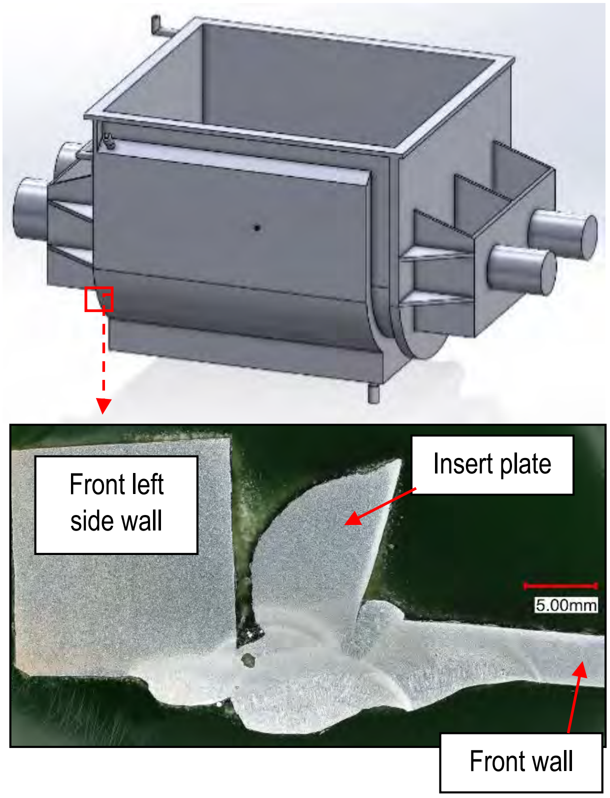

Insert plate

Element	C	Mn	Si	Cr	Mo
Wt%	0.18	0.404	0.14	0.16	<0.003

Front wall (oil jacket)

Element	C	Mn	Si	Cr	Mo
Wt%	0.15	0.39	0.15	0.013	<0.003

Rear wall (oil jacket)

Element	C	Mn	Si	Cr	Mo
Wt%	0.16	0.39	0.14	0.009	0.001

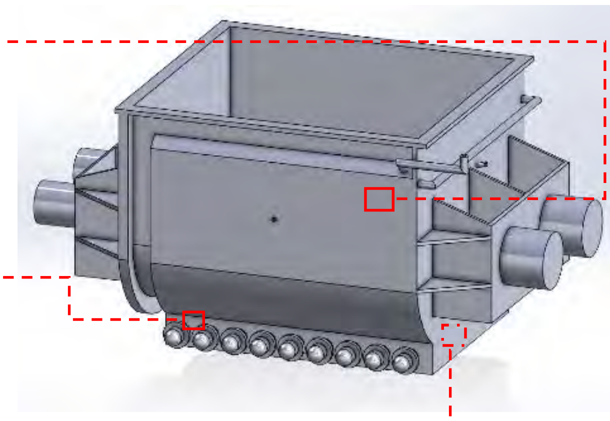

Rear wall, at vertical plane (oil jacket)

Element	C	Mn	Si	Cr	Mo
Wt%	0.17	0.37	0.13	0.013	0.001

Bottom face of oil jacket (beneath sketch view)

Element	C	Mn	Si	Cr	Mo
Wt%	0.17	0.39	0.14	0.009	0.001

Figure 141: Chemical analysis conducted on the various oil jacket walls revealed elements typical of low carbon steel material.

EDX Analysis

Fracture surface (of weld)

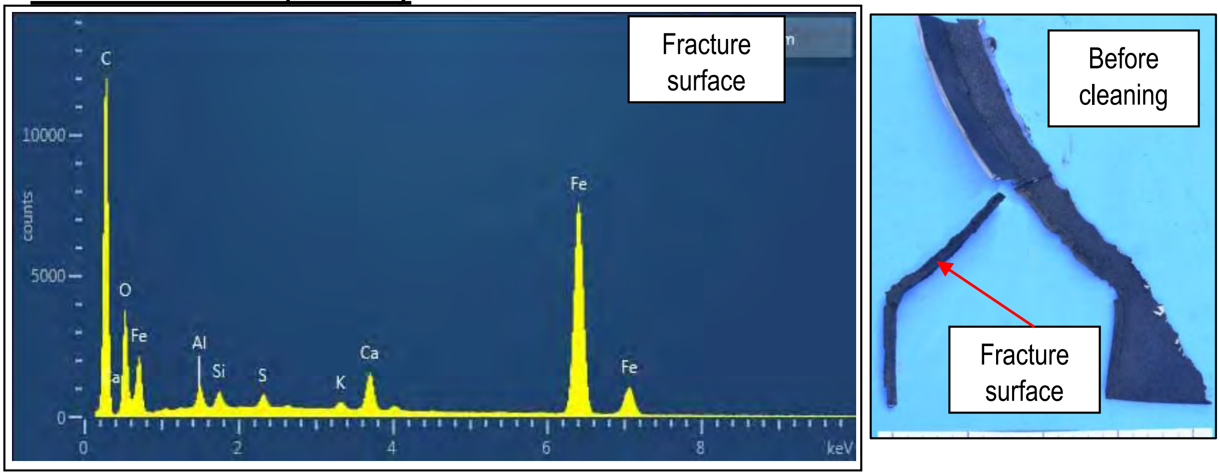

Figure 142: The major elements detected on the fracture surface were generally associated with the weld metal and constituents of the service medium.

Soot and debris from inside the oil jacket (see also Figure 40)

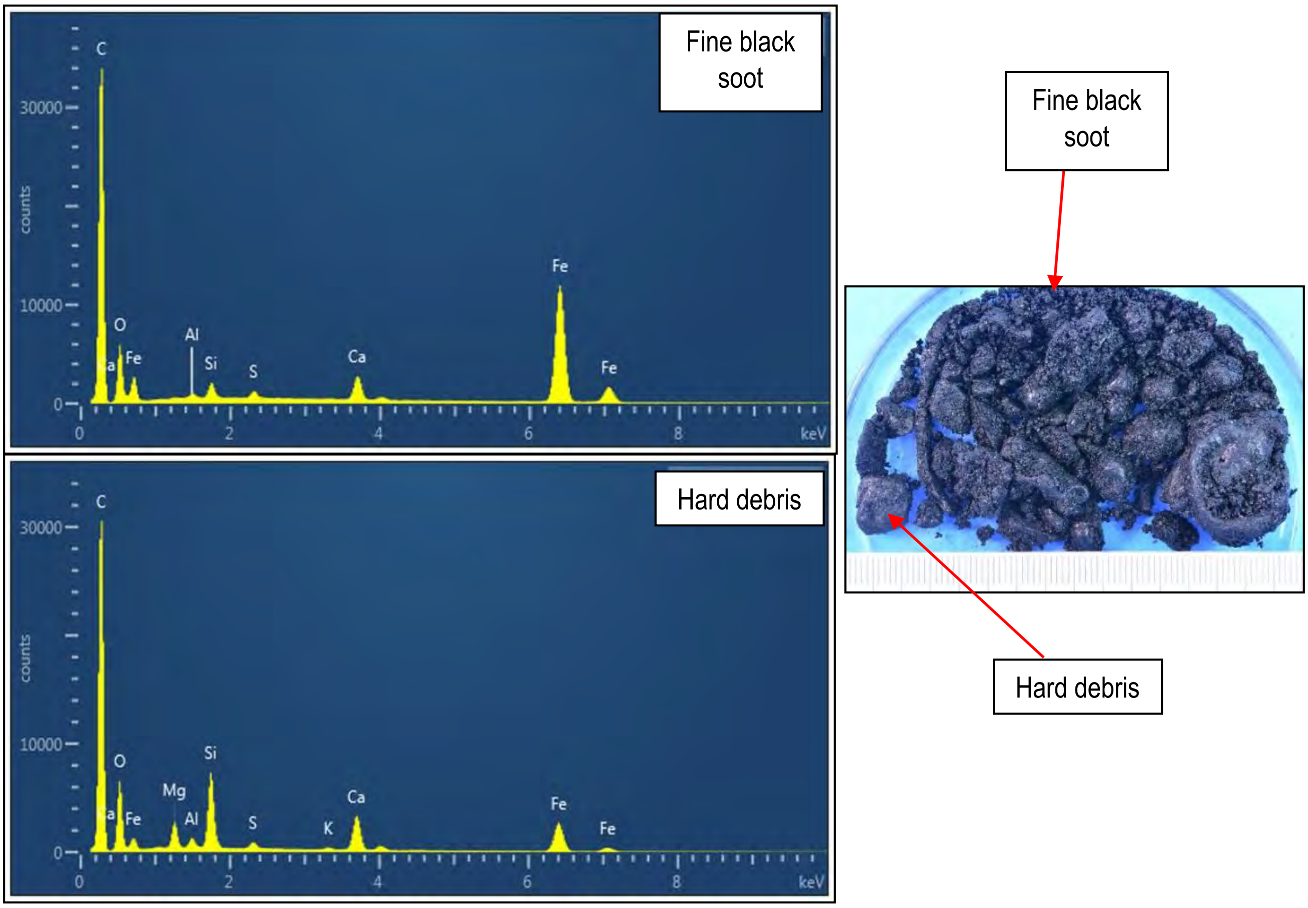

Figure 143: The major elements detected on the fine black soot were mainly associated with the thermic oil. The hard debris had high peaks of silicon and magnesium apart from elements associated with the service medium.

EDX Analysis

Heater materials

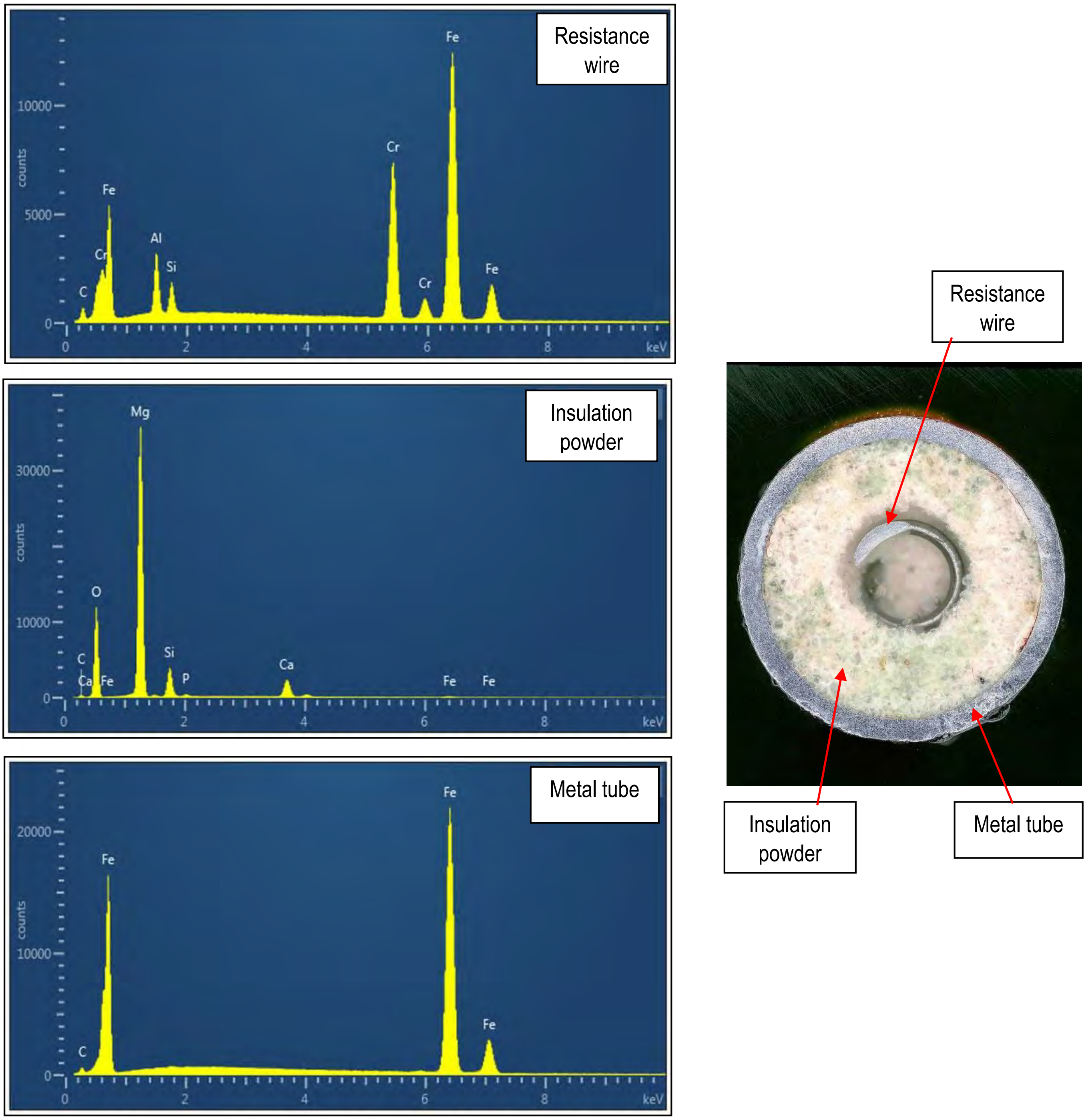

Figure 144: Based on the major elements detected, the resistance wire is most likely constructed using Kanthal or Fe–Cr–Al material. The insulation powder is mainly magnesium oxide. The metal tube is constructed using carbon steel. All the material are typical of heating element construction.

Appendix F:

Metallographic and Microscopic Examination

Metallographic Examination

Sections (Weld)

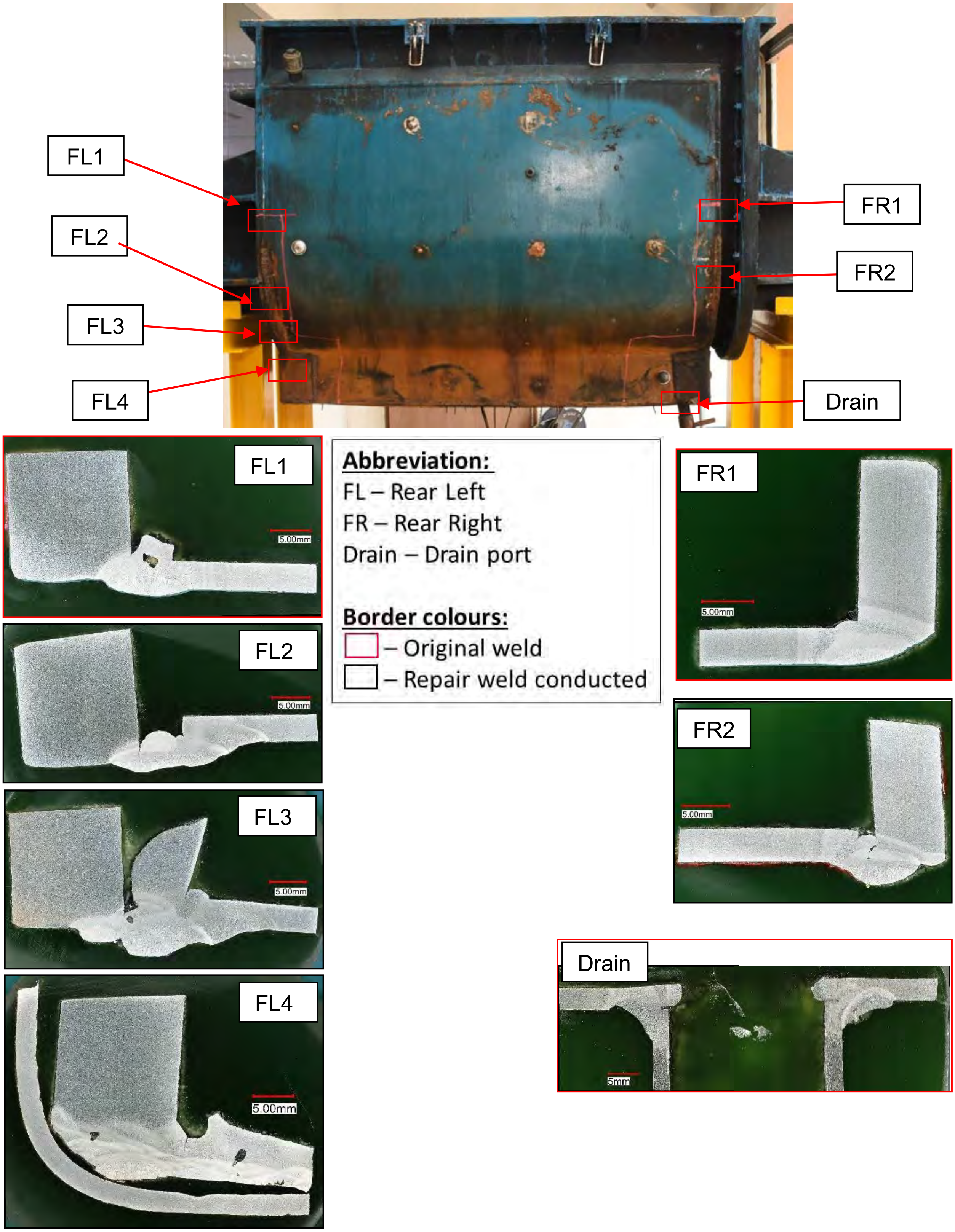

Figure 145: Samples for sectional metallographic examination.

Metallographic Examination

Sections (Weld)

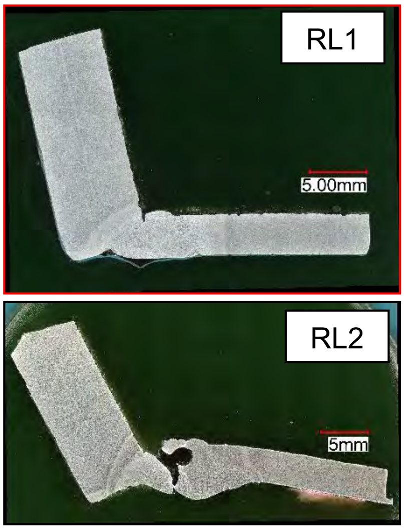

Abbreviation:
RL – Rear Left
RR – Rear Right
BM – Bottom Middle
BR – Bottom Right

Border colours:
– Original weld
– Repair weld conducted

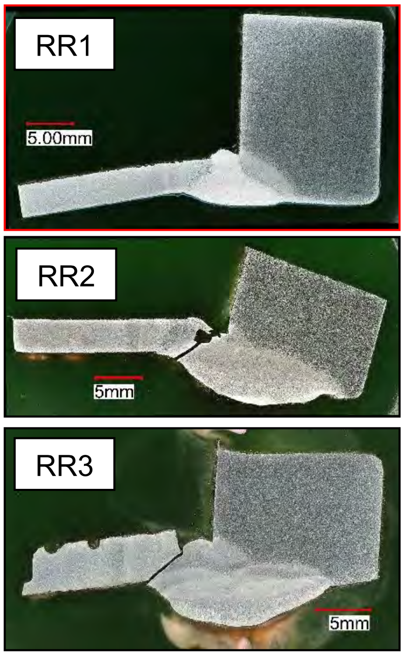

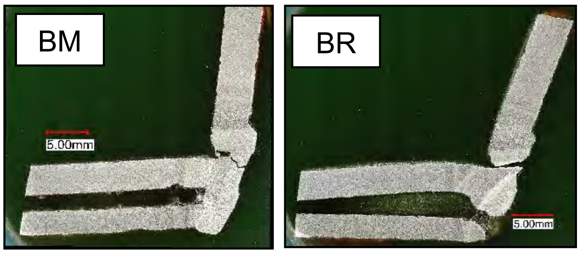

Figure 146: Samples for sectional metallographic examination.

Metallographic Examination

Front Left 1 (FL1)

Figure 147: Section metallographic examination was conducted across the original weld. Excessive root penetration was observed at this weld area. About 2 mm width void was observed in the middle of the weld root.

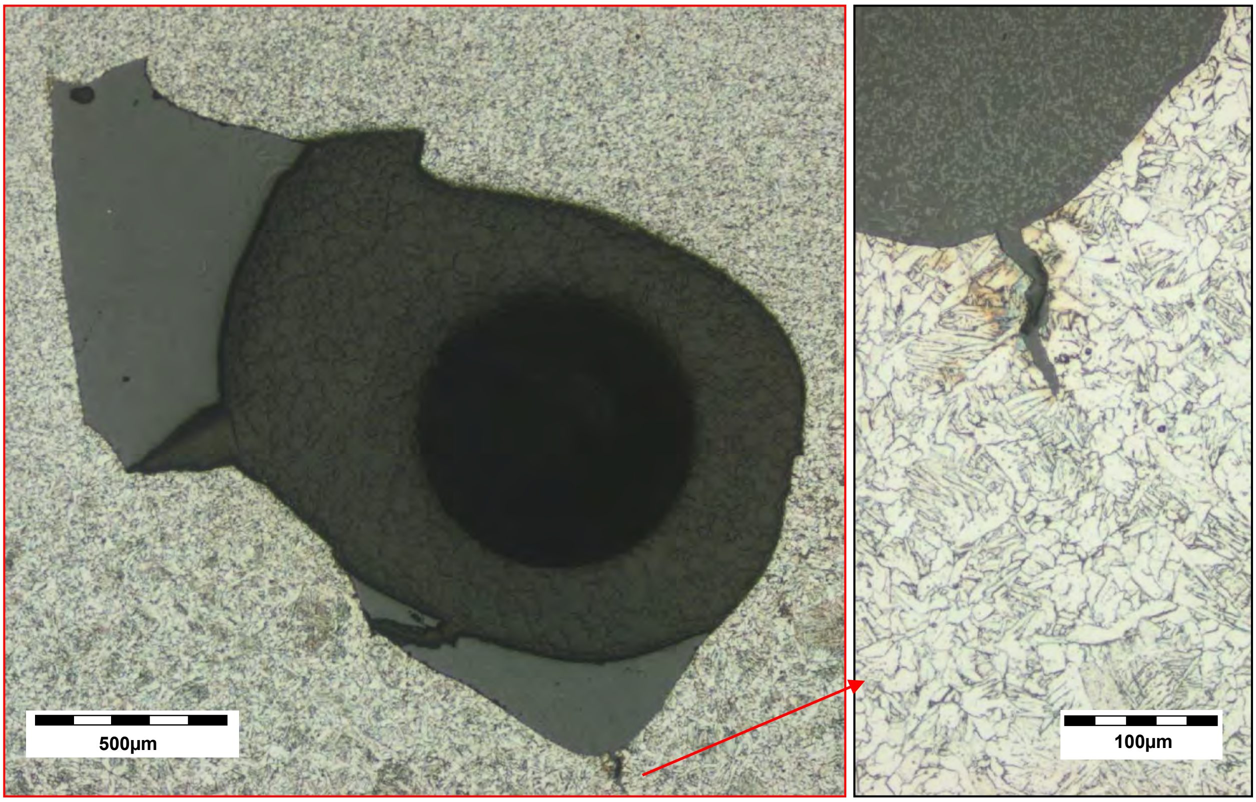

Figure 148: Micrograph of at 50x (left) and 200x (right) magnifications. A 115 µm incipient crack was at the edge of the void, propagating towards the weld face.

Metallographic Examination

Front Left 2 (FL2)

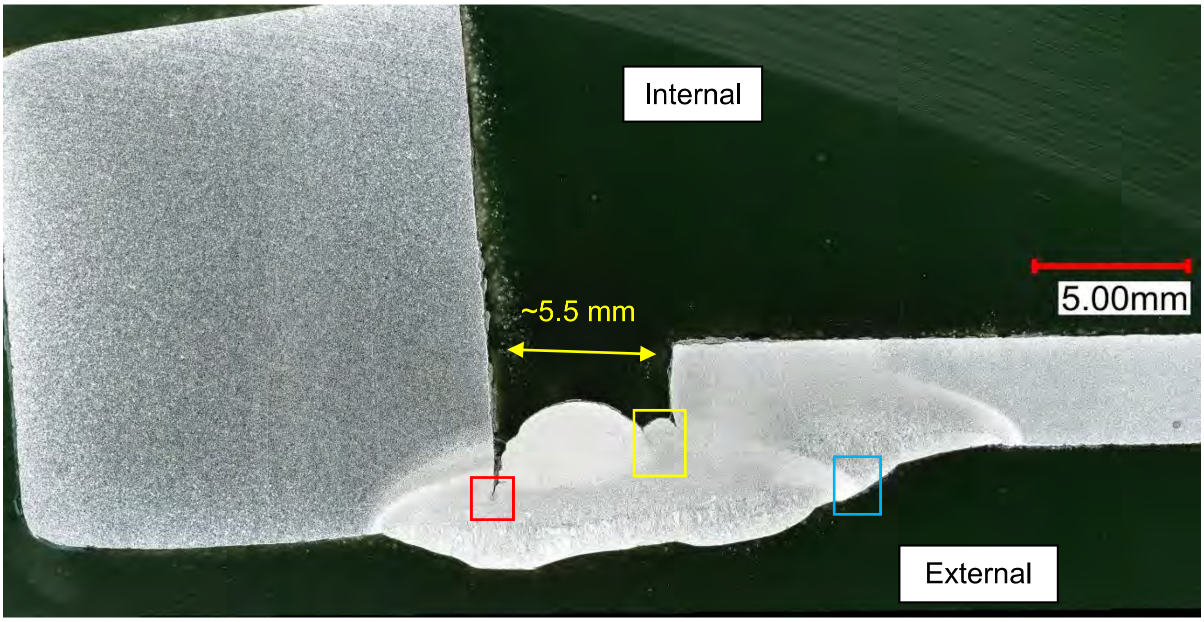

Figure 149: Sectional metallographic examination was conducted across the repair weld. Lack of root penetration was observed with a root opening of about 5.5 mm. Closer examination was made in the following colour bordered figures.

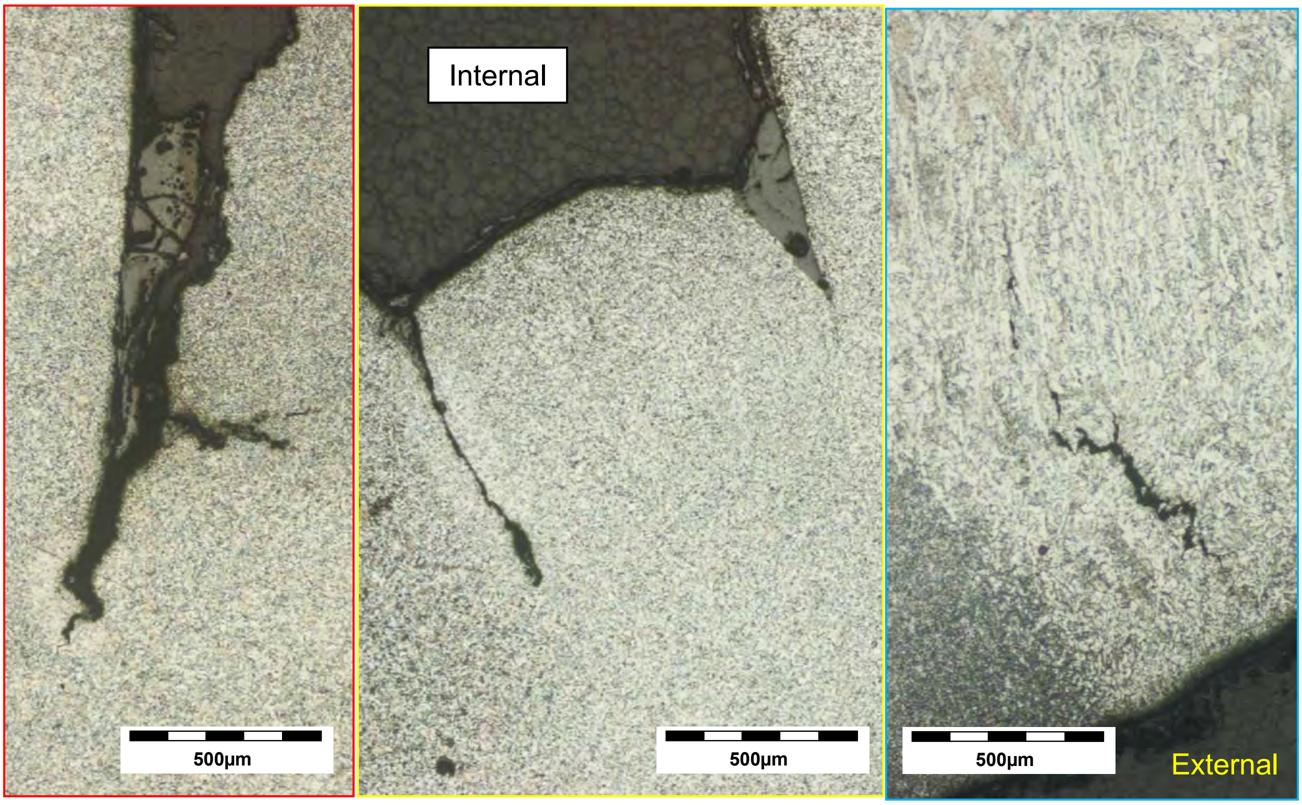

Figure 150: Micrographs at 50x magnification. Incipient cracks and discontinuities were observed at the weld root and near the weld face. The cracks were filled with oxide scales.

Metallographic Examination

Front Left 3 (FL3)

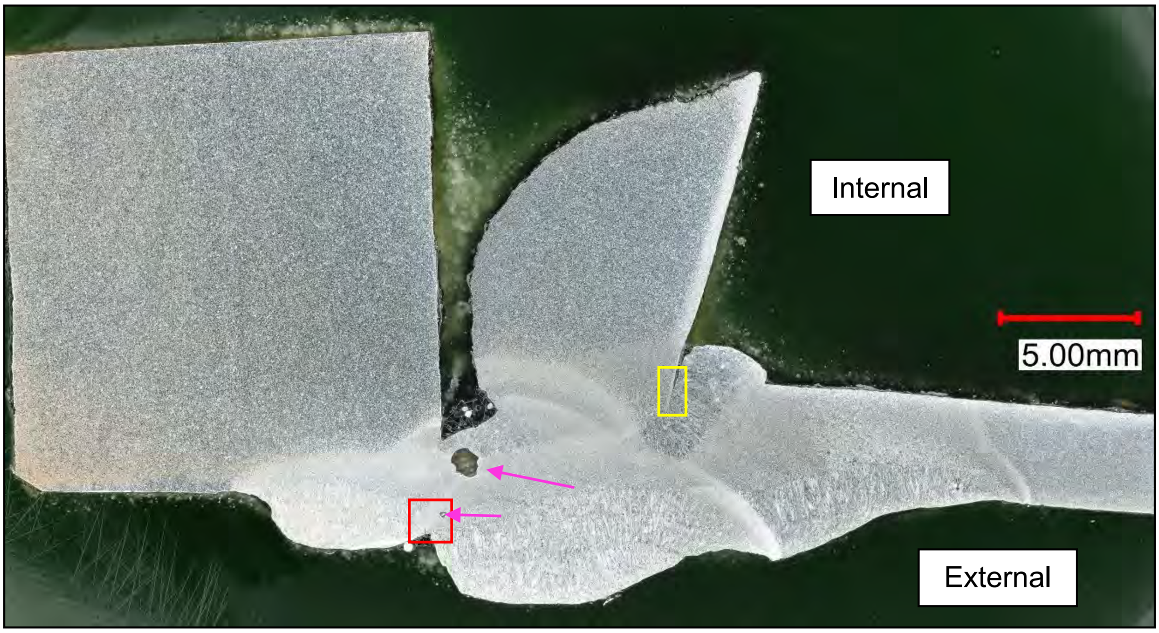

Figure 151: Sectional metallographic examination was conducted across the repair weld with a visible insert plate from the internal side (see Figure 47). Voids up to about 1.0 mm were observed (in pink).

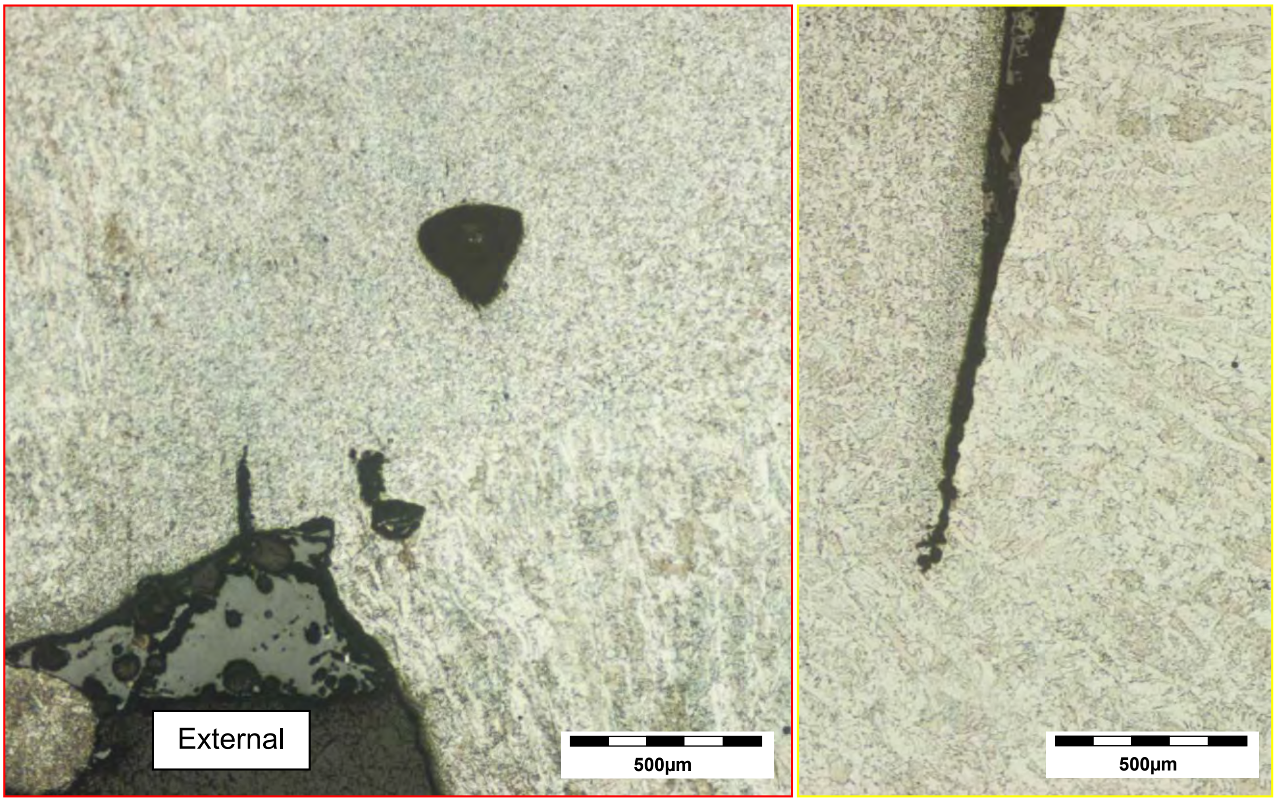

Figure 152: Micrographs at 50x magnification. Voids were observed within the weld metal (left). Oxide filled incipient crack was observed at the weld root (right).

Metallographic Examination

Front Left 3 (FL3)

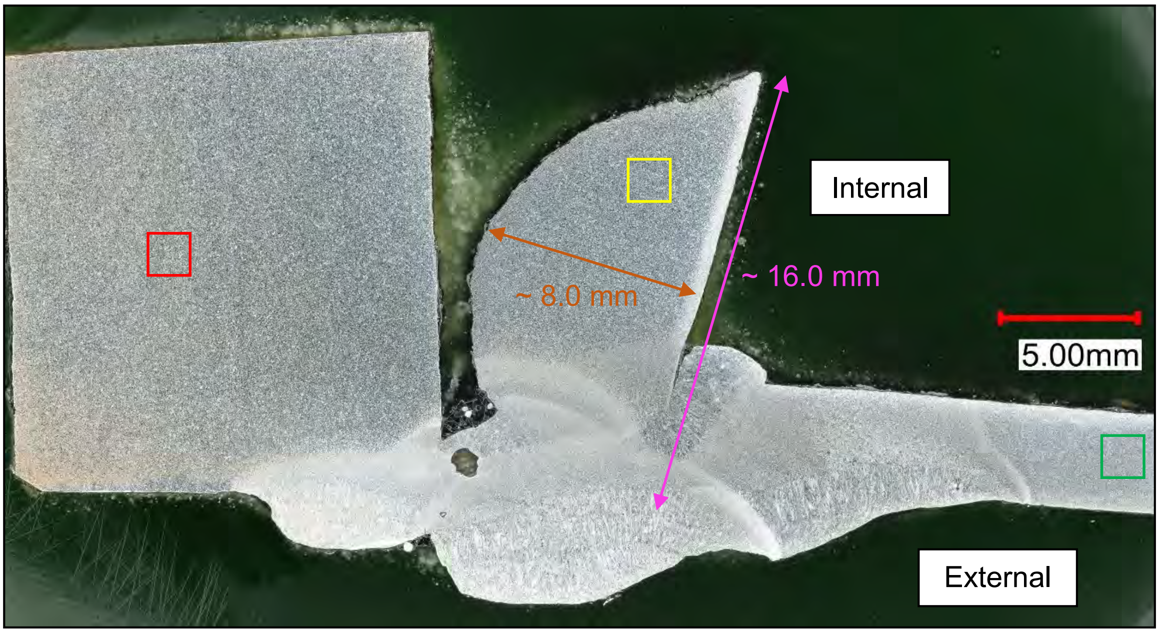

Figure 153: The insert plate is confirmed to be a separate metal piece welded between the front left side and front walls. The width and thickness of the insert plate were approximately 8.0 mm and 16.0 mm respectively (the length was measured earlier at about 120.0 mm).

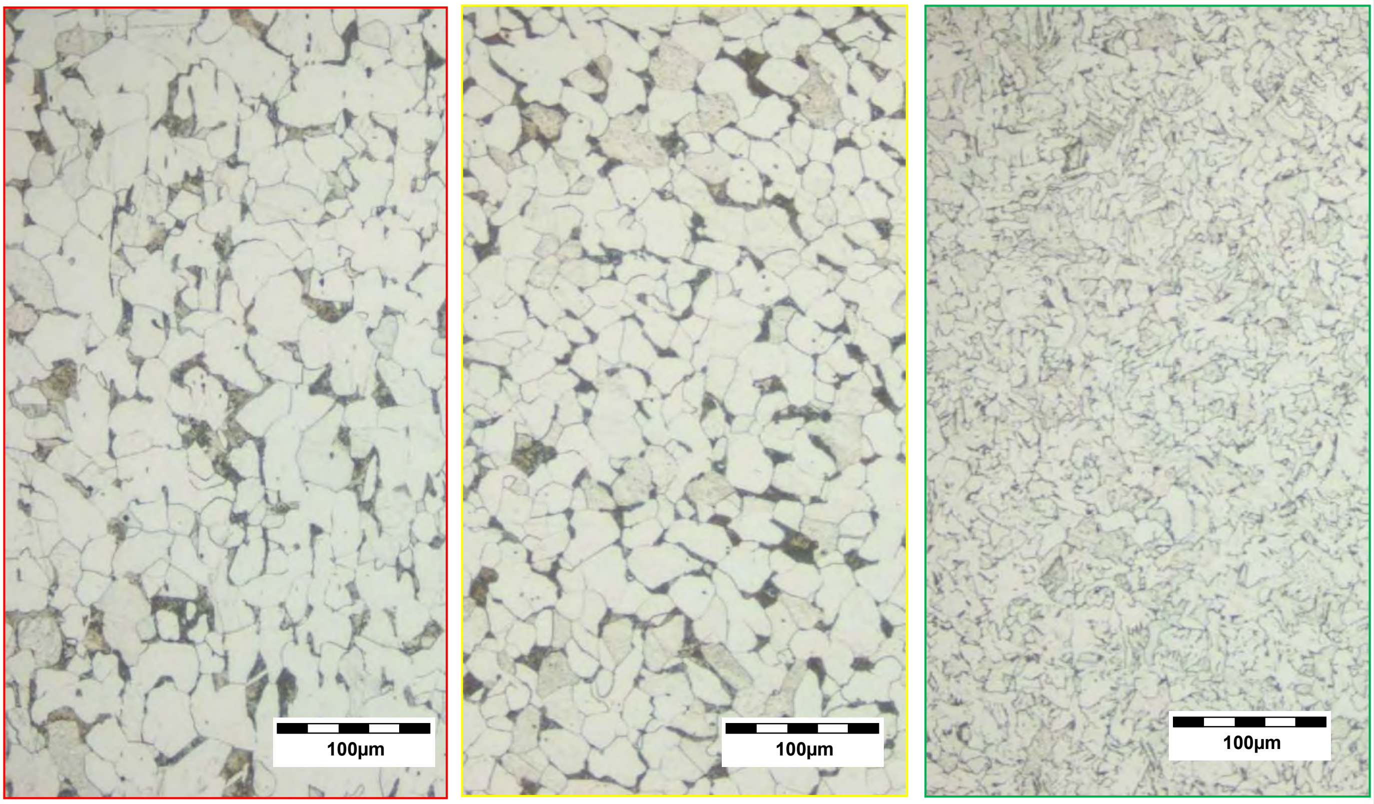

Figure 154: Micrographs at 200x magnification. The base metals of the oil jacket walls (left and right) and the added metal piece (middle) consisted of ferrite pearlite microstructure. Their microstructures differ such that the front left wall has flow lines from rolling process (manufacturing), the insert plate does not have flow lines and the front wall has finer grains.

Metallographic Examination

Front Left 4 (FL4)

Figure 155: Sectional metallographic examination was conducted across the repair weld and corner reinforcement plate. Lack of root penetration was observed with a root opening of about 3.5 mm wide. Voids of up to 2.5 mm wide were scattered in the weld metal (in pink).

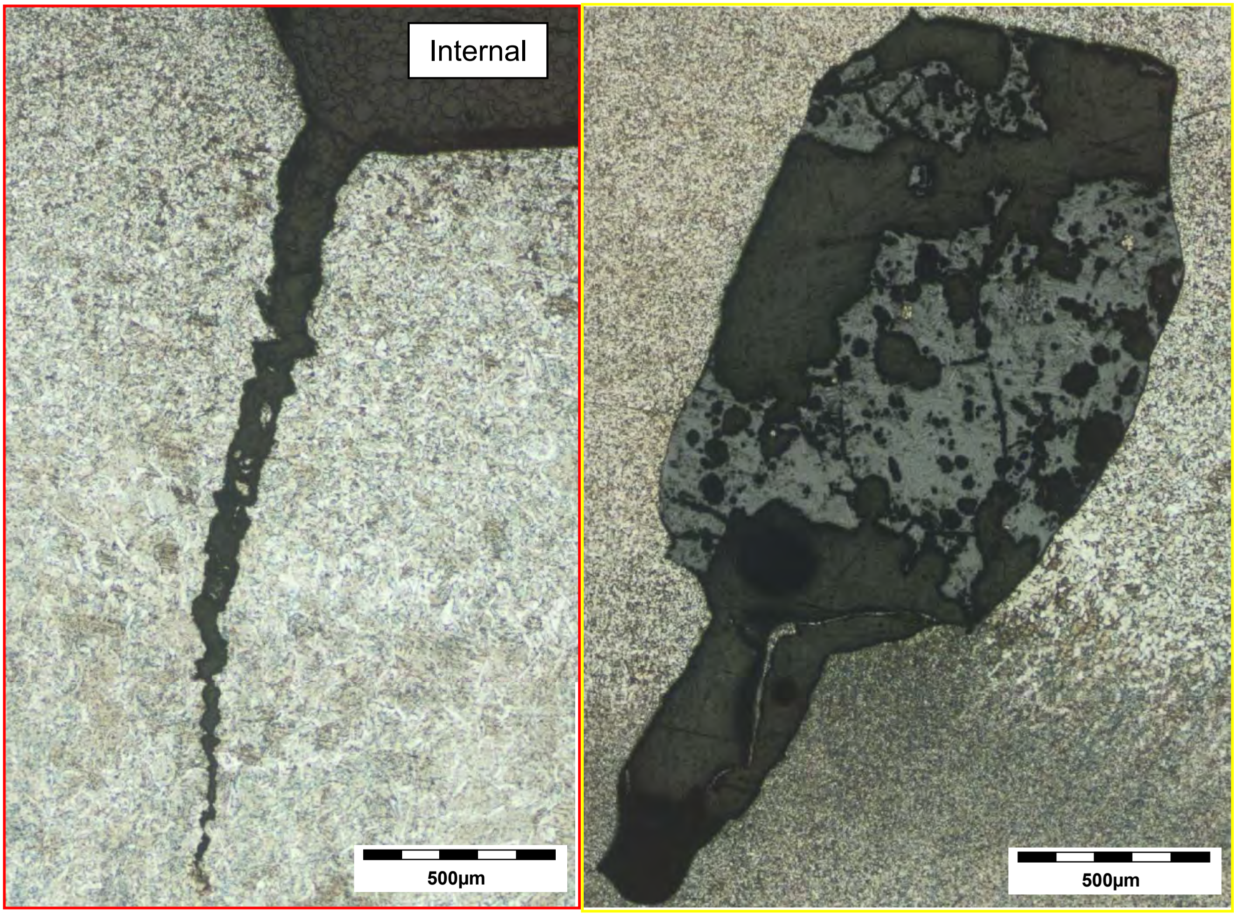

Figure 156: Micrographs at 50x magnification. Crack with a length of about 2.0 mm was observed to have initiated at the weld root and propagated towards the weld face.

Metallographic Examination

Front Right 1 (FR1)

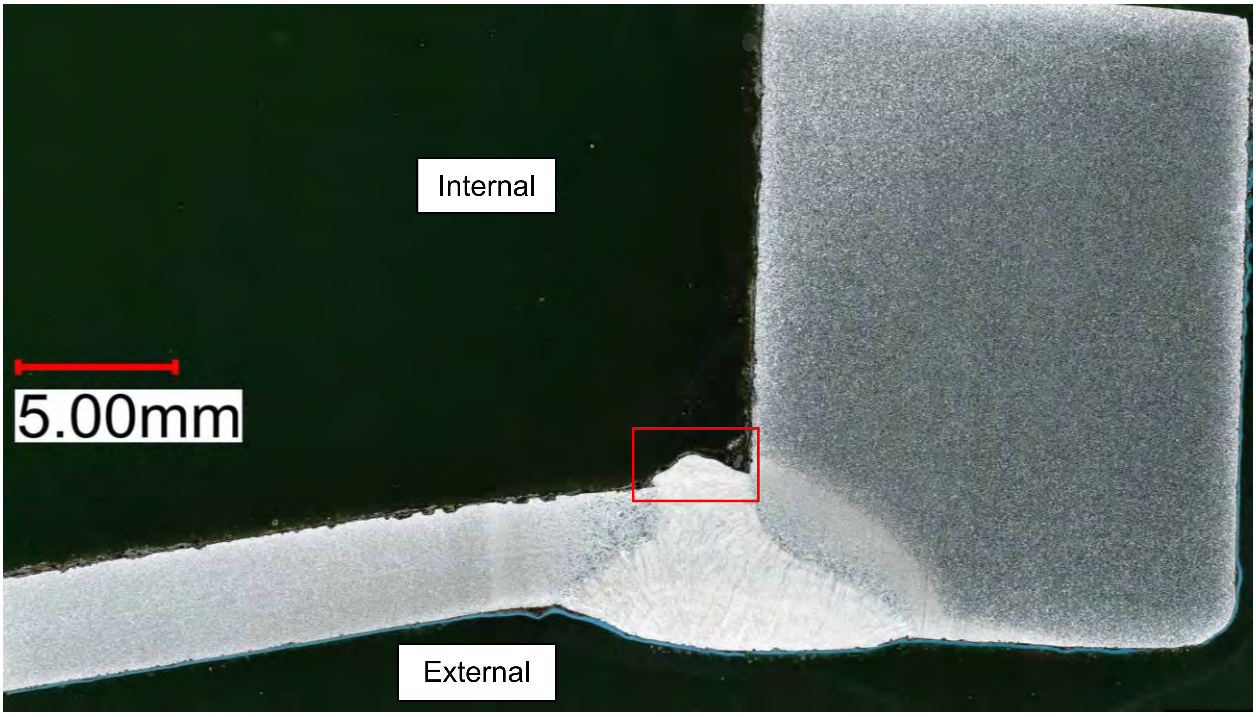

Figure 157: Sectional metallographic examination was conducted across an original weld. No discontinuity found at this weld joint.

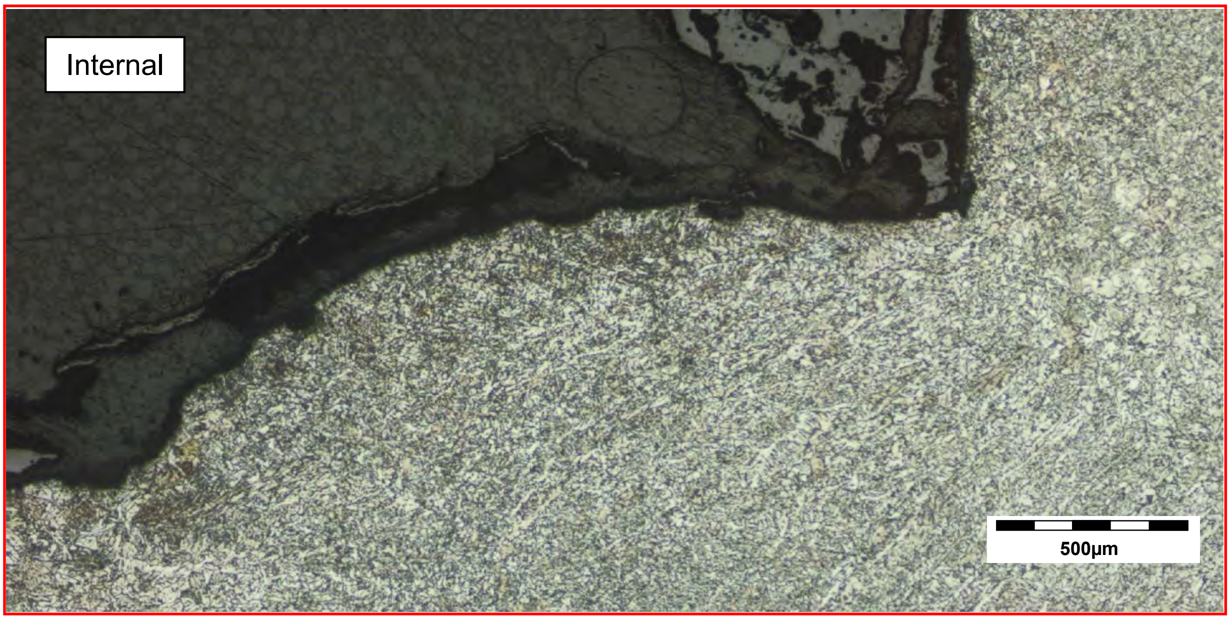

Figure 158: Micrograph at 50x magnification.

Metallographic Examination

Front Right 2 (FR2)

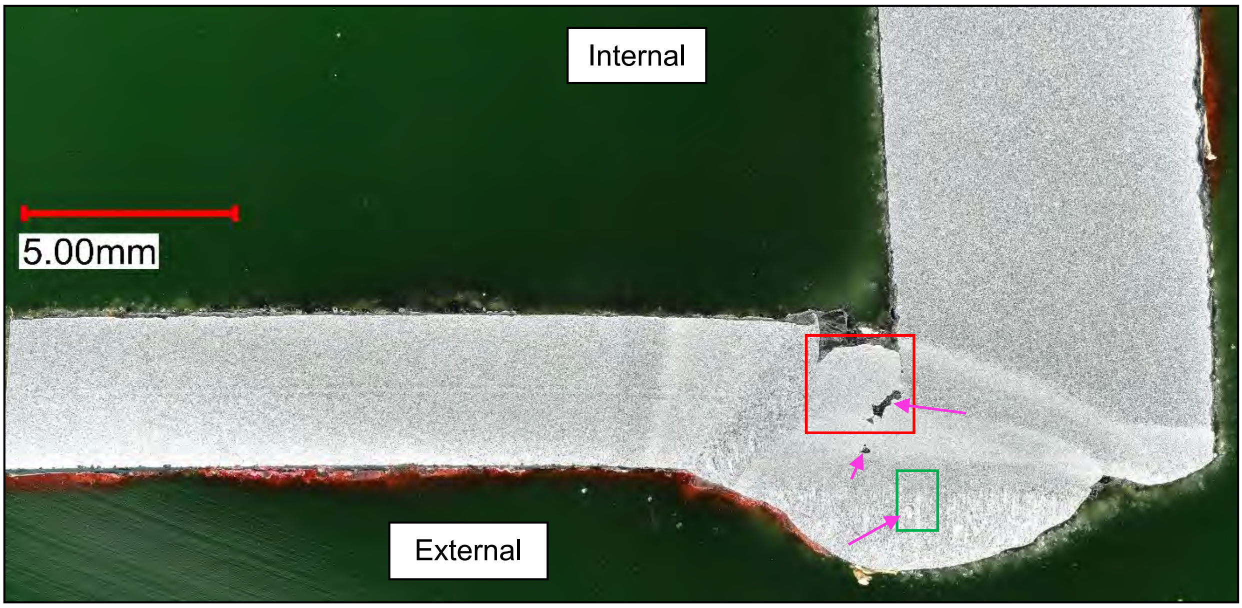

Figure 159: Sectional metallographic examination was conducted across the repair weld. Lack of root penetration was observed with a root opening of about 1.6 mm wide. Voids up to about 1.0 mm were observed in the weld metal.

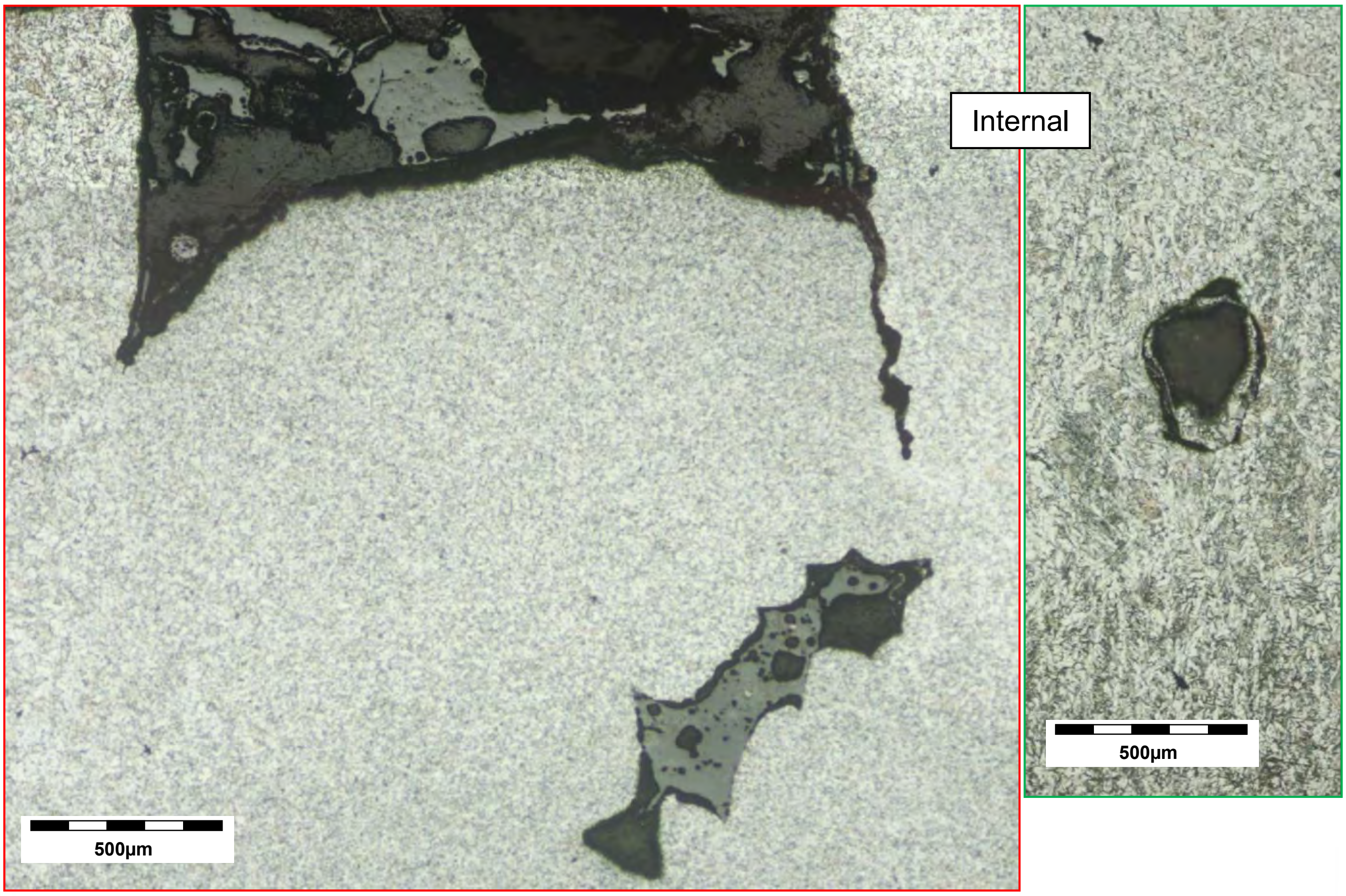

Figure 160: Micrographs at 50x magnification. Oxide filled incipient crack was observed at the weld root (left). Voids were scattered in the weld metal (right).

Metallographic Examination

Drain

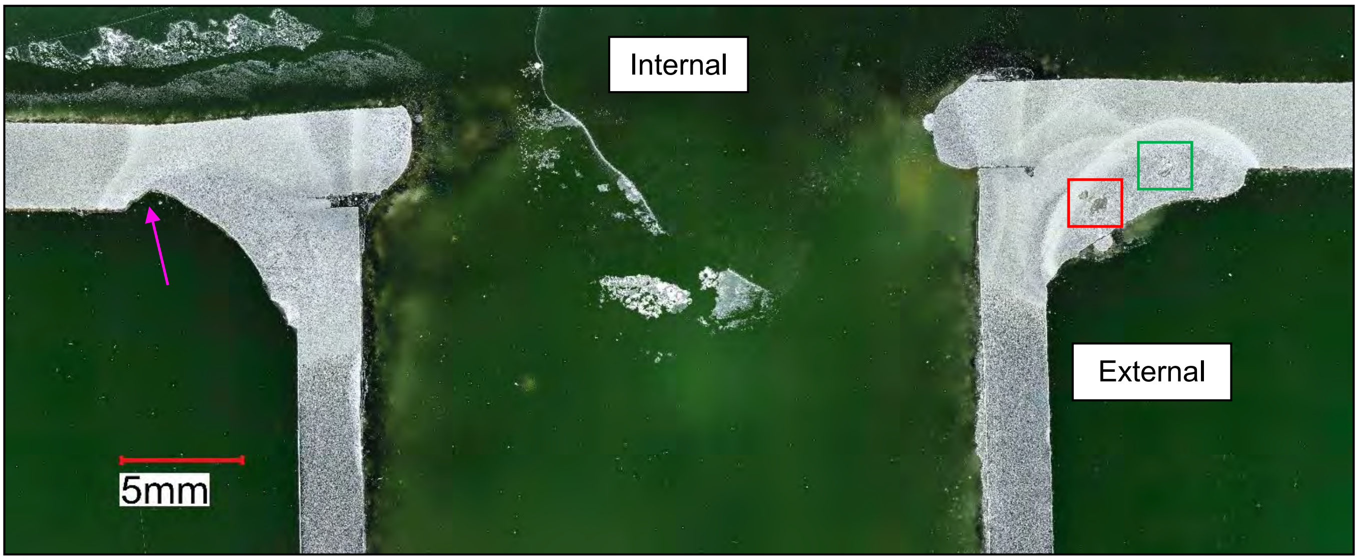

Figure 161: Sectional metallographic examination was conducted across the drain port. The weld had undercut at the weld toe (in pink arrow). Voids up to about 1.0 mm wide were observed scattered in the weld metal.

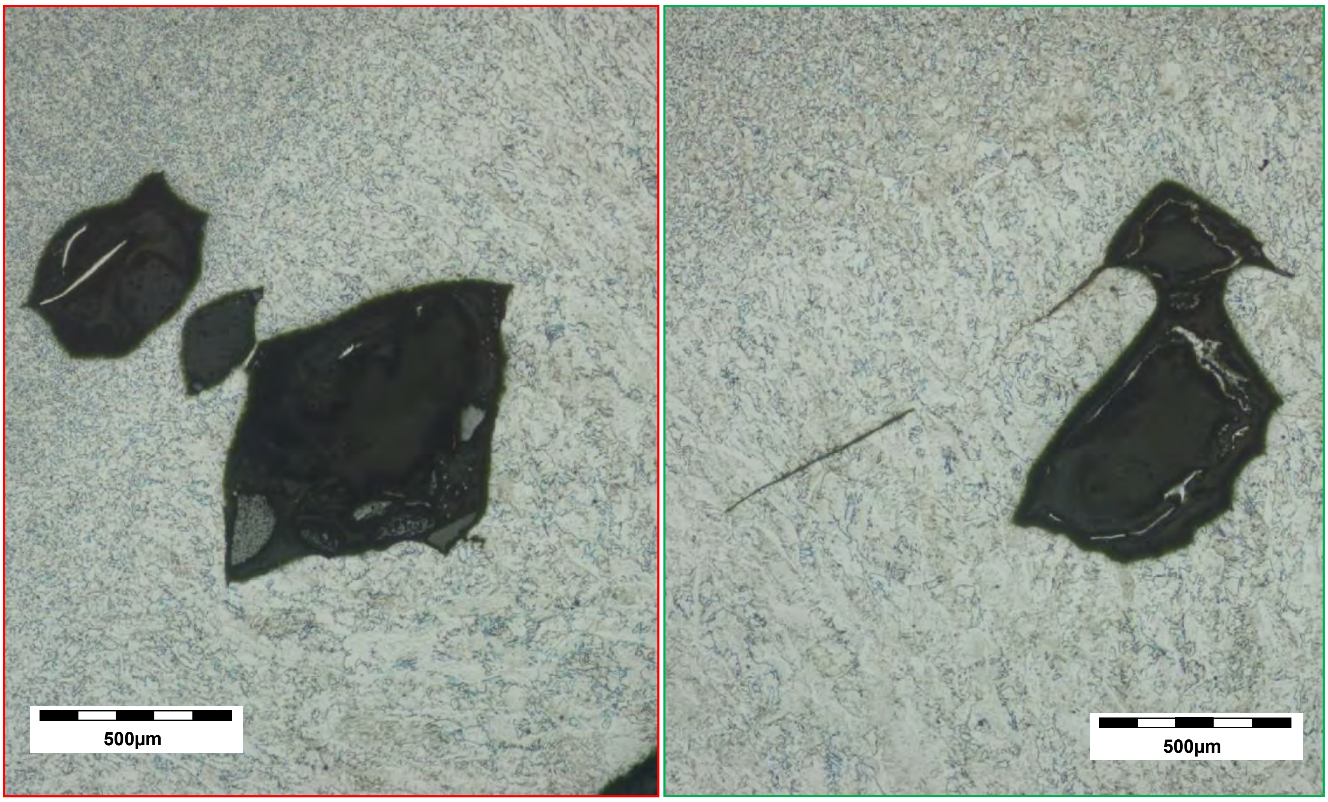

Figure 162: Micrographs at 50x magnification. Voids were scattered in the weld metal.

Metallographic Examination

Rear Left 1 (RL1)

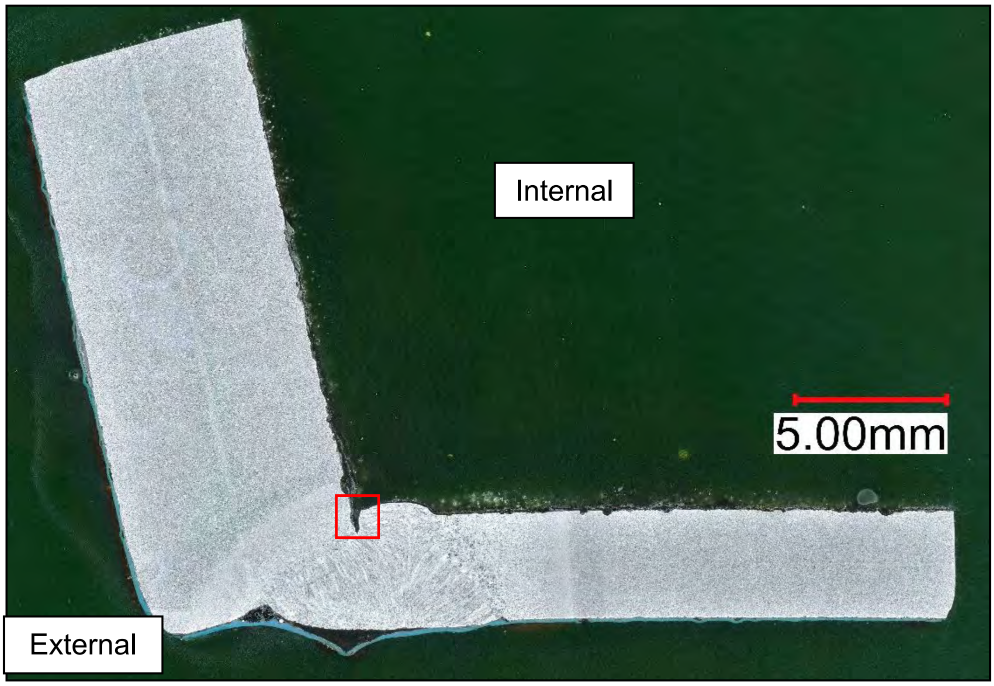

Figure 163: Sectional metallographic examination was conducted across the original weld. Incipient crack was observed at the weld root, propagated towards the weld face. Apart from that, no significant weld discontinuity was found.

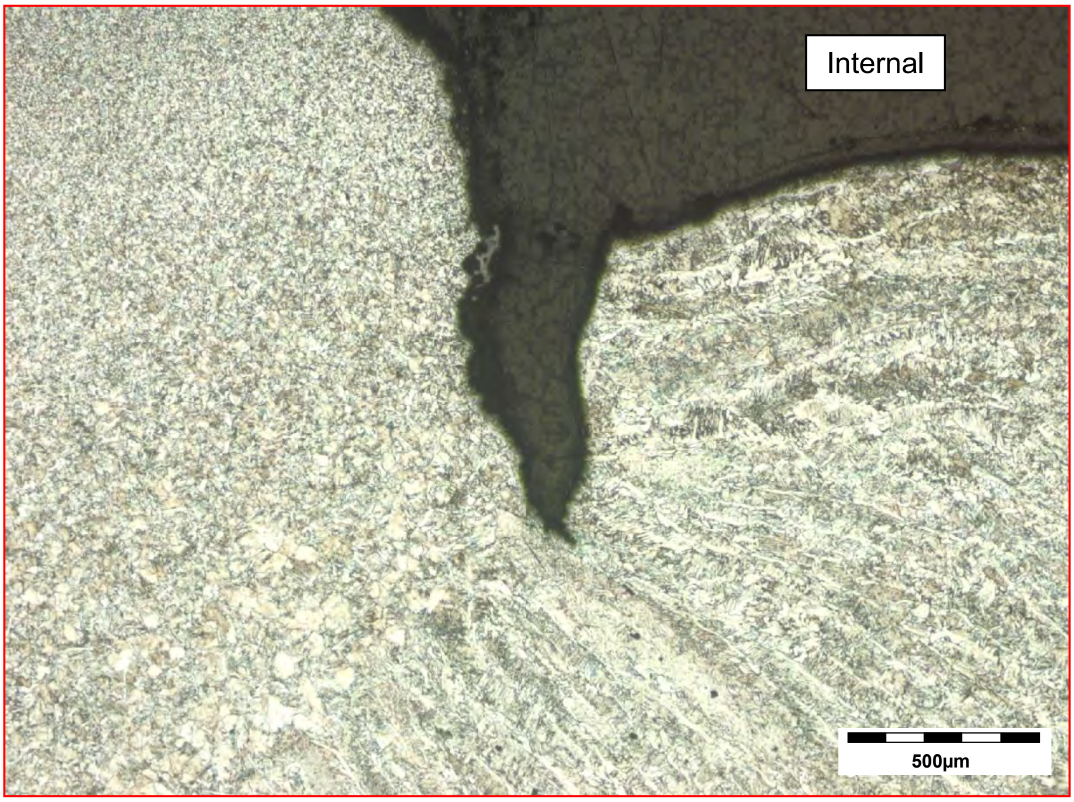

Figure 164: Micrographs at 50x magnification. Incipient crack (with some oxide scale) was observed at the weld root.

Metallographic Examination

Rear Left #2

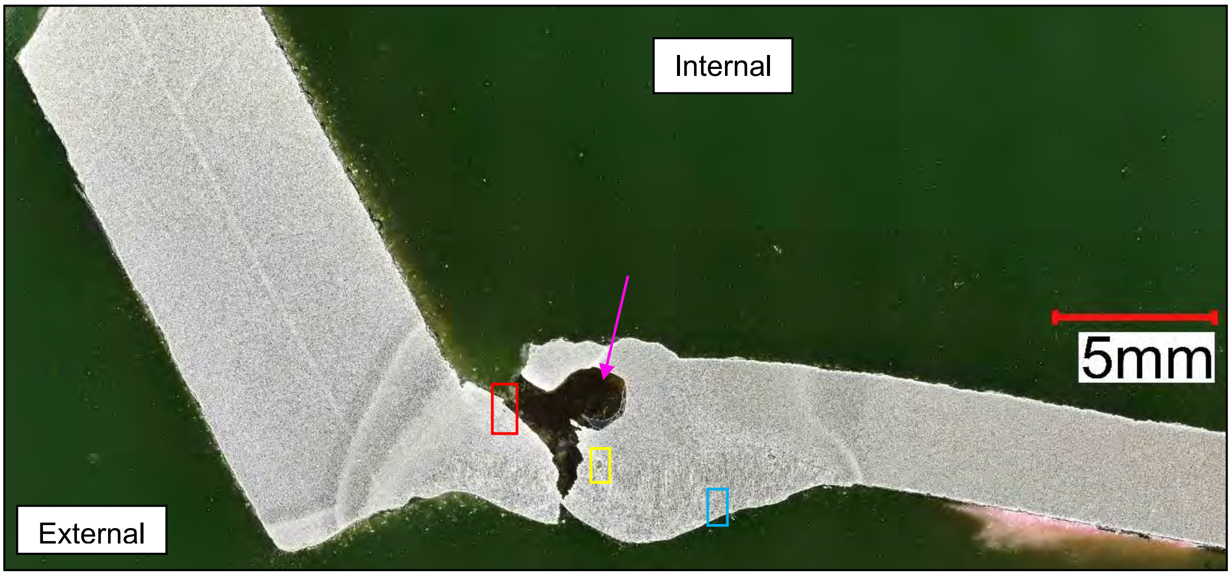

Figure 165: Sectional metallographic examination was conducted across the repair weld which had cracked through. Multiple voids were observed scattered in the weld metal with size up to about 1.7 mm wide.

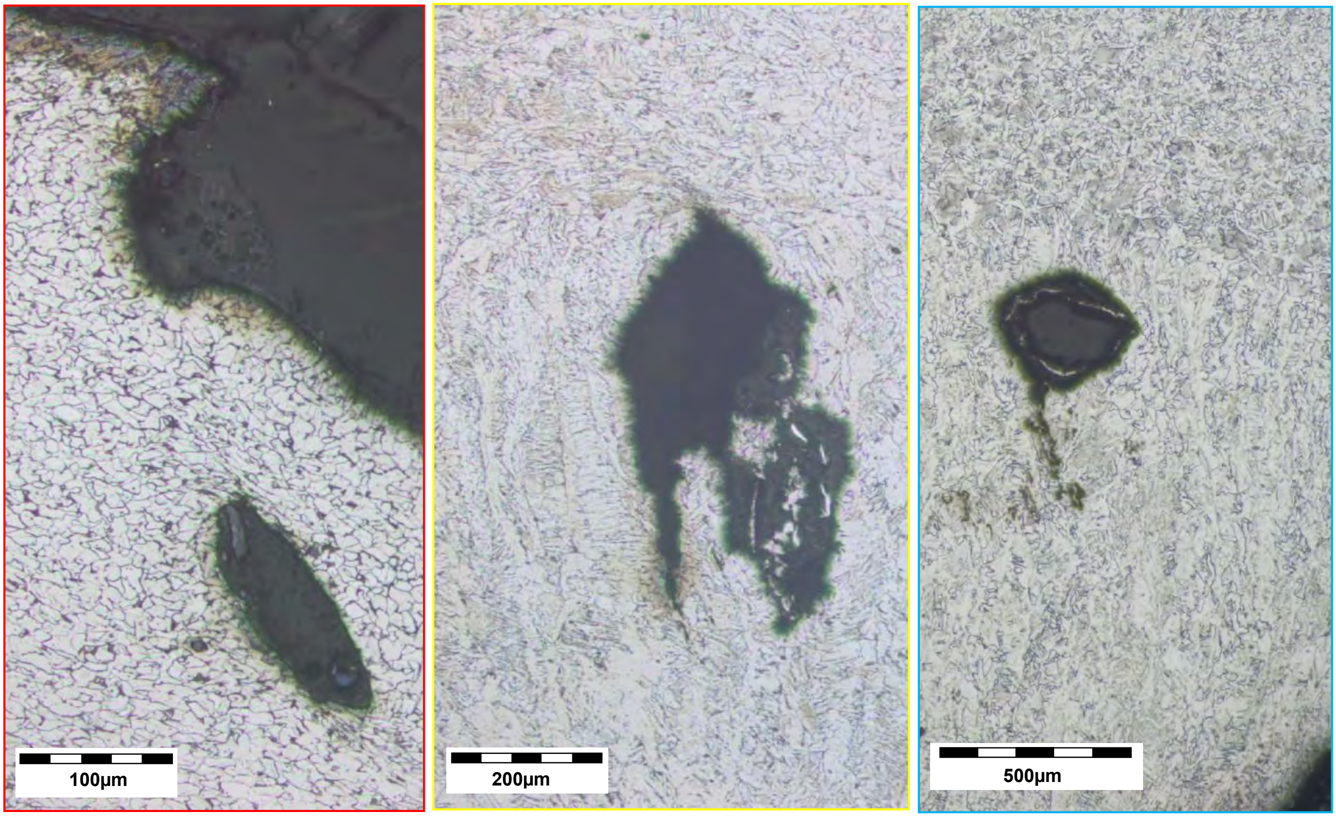

Figure 166: Micrographs at 200X (left), 100X (middle) and 50X (right) magnifications. Voids were scattered in the weld metal and along/across the crack path (left figure).

Metallographic Examination

Rear Right #1

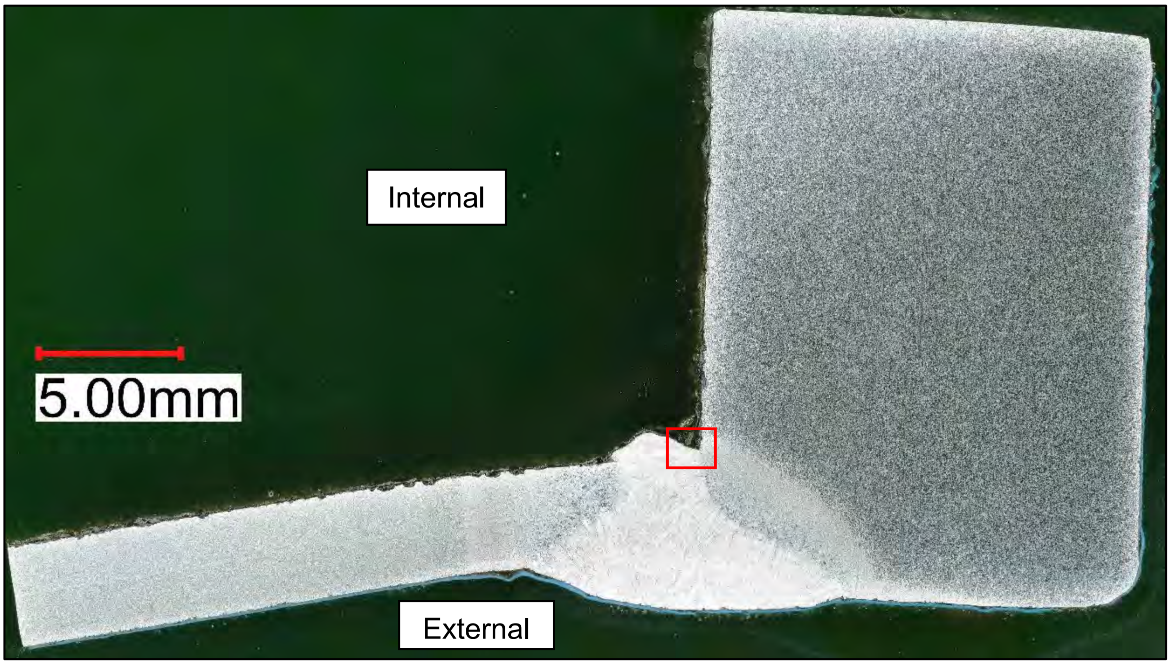

Figure 167: Sectional metallographic examination was conducted across the original weld. Apart from a small incipient crack initiated from the weld root, no weld discontinuity was found.

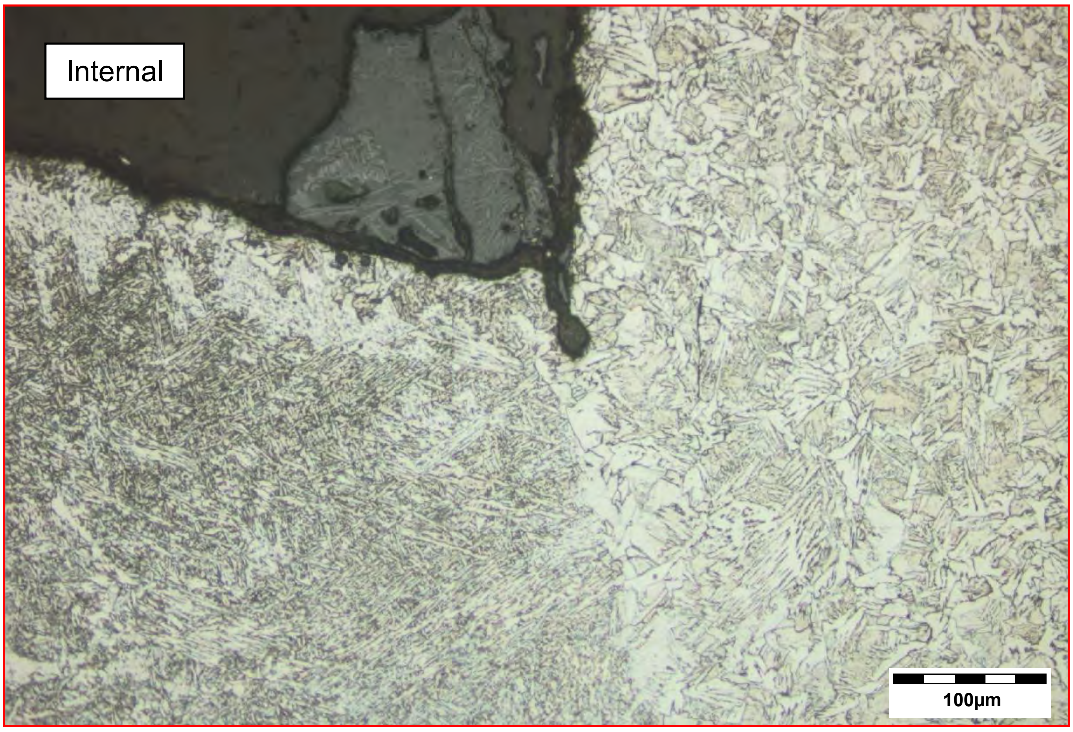

Figure 168: Micrograph at 200x magnification. A 60µm incipient crack (with some oxide scale) was observed at the weld root.

Metallographic Examination

Rear Right #2

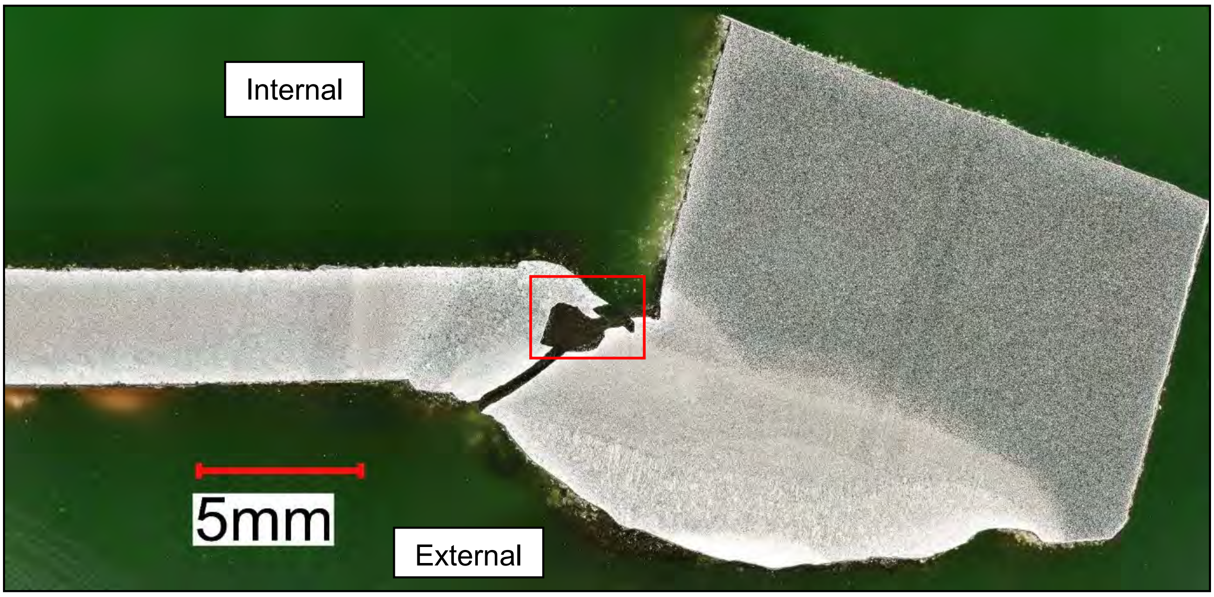

Figure 169: Sectional metallographic examination was conducted across the repair weld which had cracked through. Voids up to about 1.5 mm wide were in the weld metal (red box).

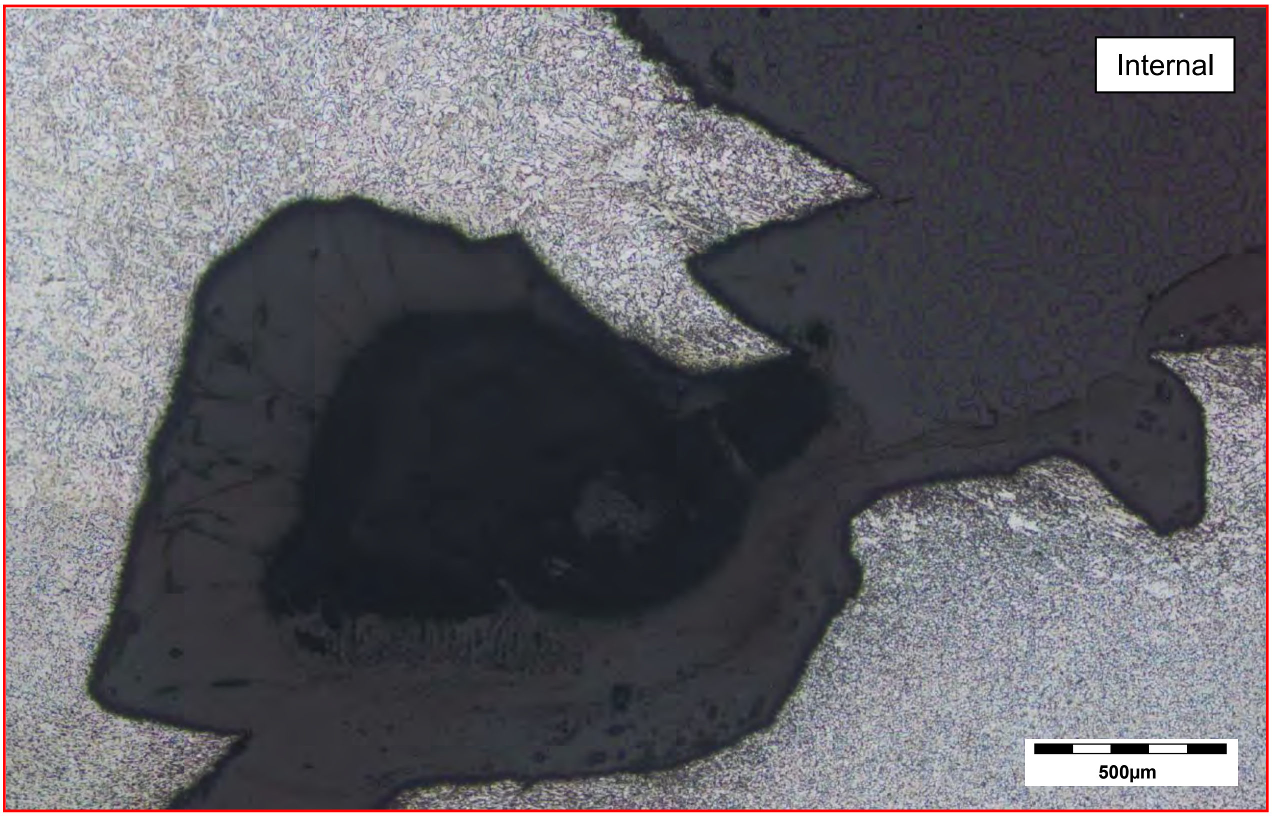

Figure 170: Micrographs at 50x magnification. The crack had propagated through the voids.

Metallographic Examination

Rear Right #3

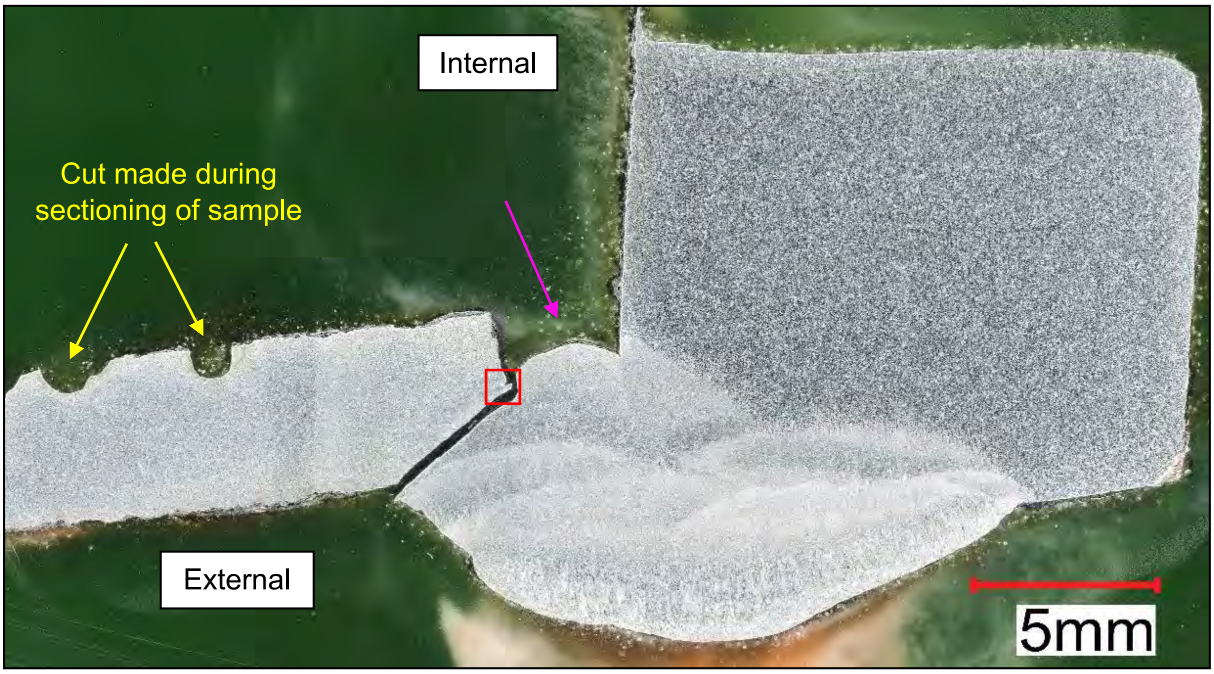

Figure 171: Sectional metallographic examination was conducted across the repair weld and through crack. The weld had lack of root penetration with root opening of about 3.0 mm wide (pink arrow).

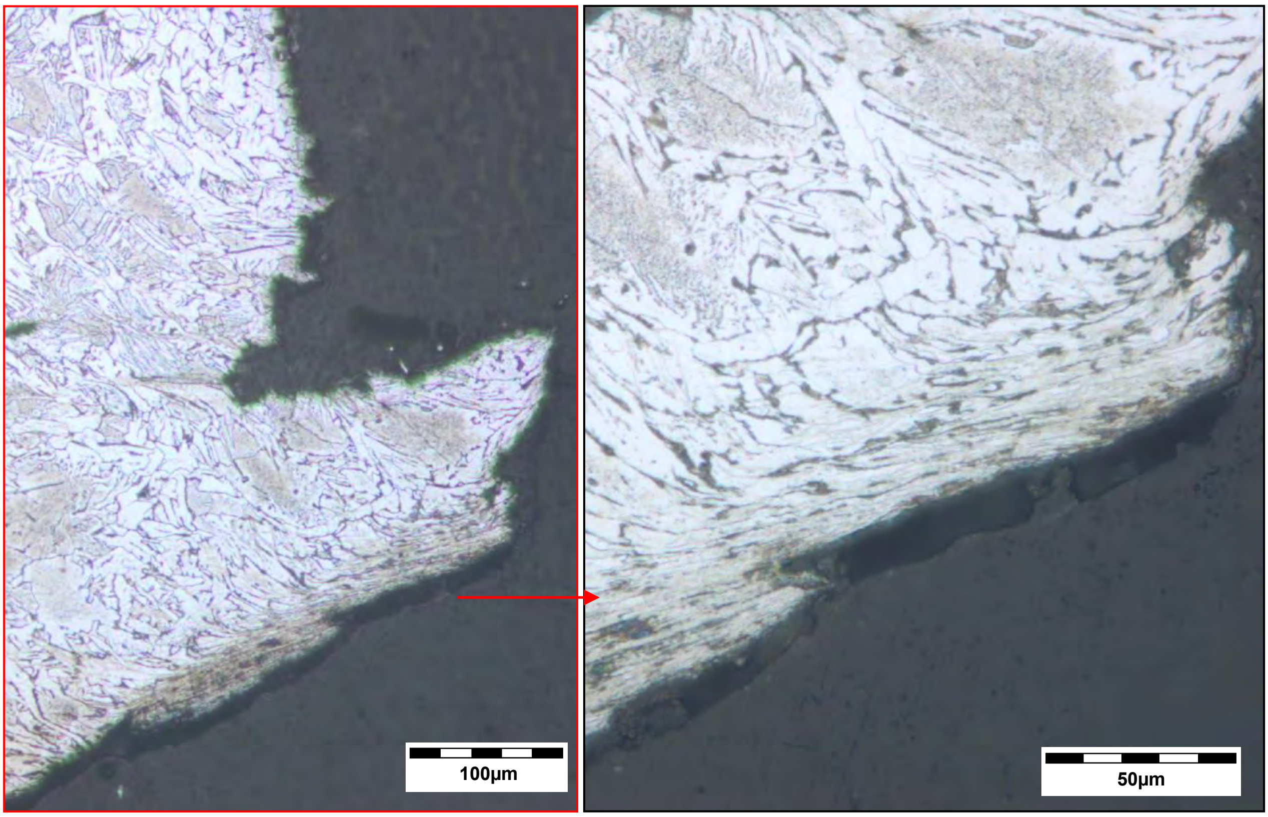

Figure 172: Micrographs at 200x (left) and 500X (right) magnifications. The structure along the crack edge had elongated grains, consistent with overload fracture.

Metallographic Examination

Bottom Middle

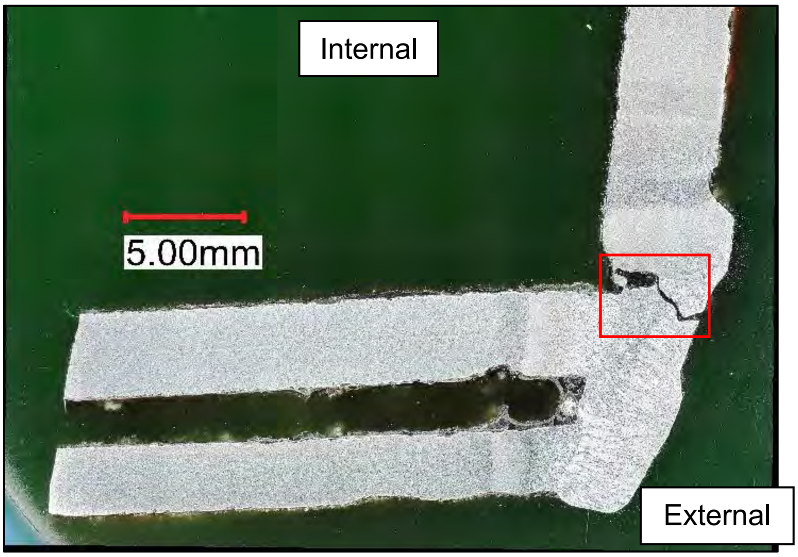

Figure 173: Sectional metallographic examination was conducted across the weld between bottom plate and reinforcement plate. A void of about 1.0 mm was observed (red box) along the through crack path.

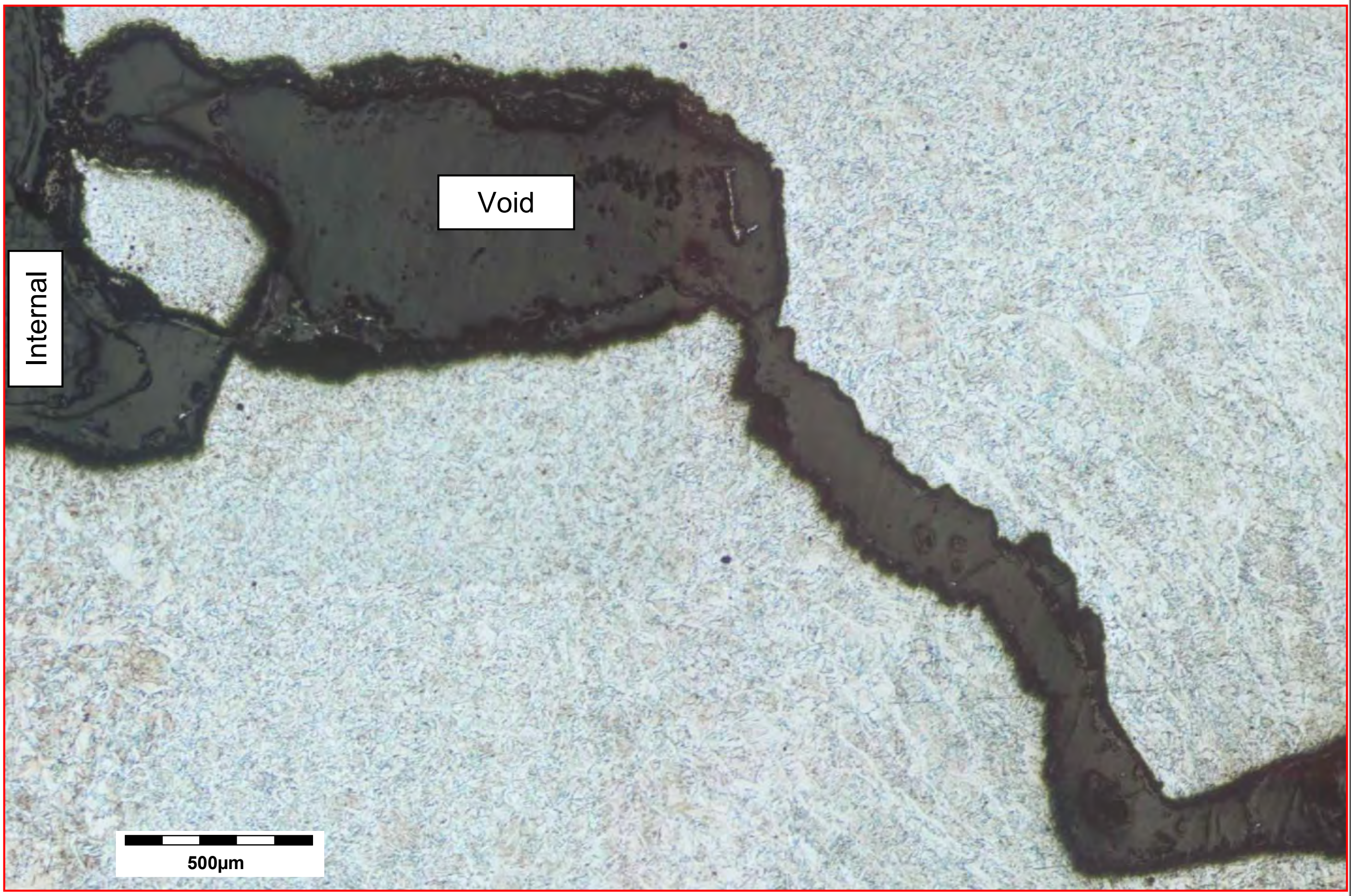

Figure 174: Micrographs at 50x magnification. The crack had propagated through a void before reaching the external side at the weld face.

Metallographic Examination

Bottom Right

Figure 175: Sectional metallographic examination was conducted across the weld between the bottom plate and reinforcement plate. A though-thickness void was observed at the weld joint of the reinforcement plate (pink arrow).

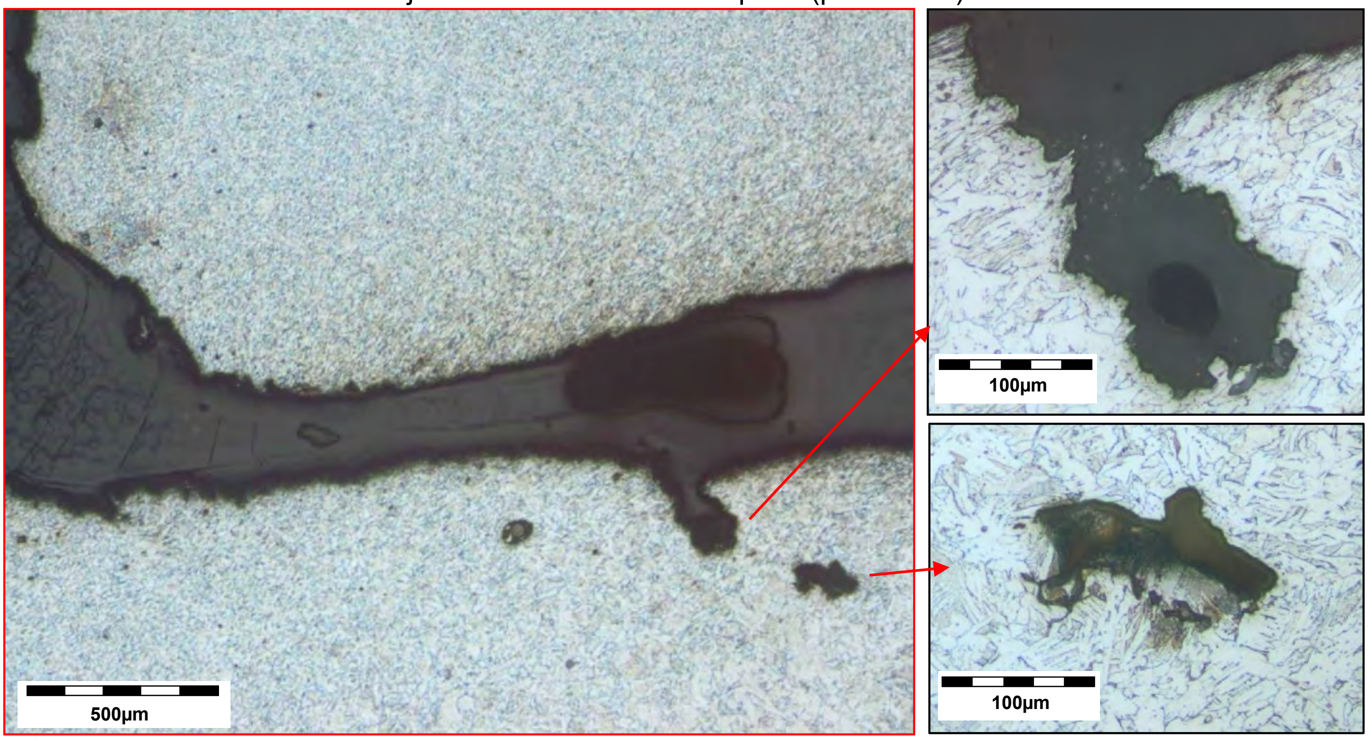

Figure 176: Micrographs at 50x (left) and 200X (right) magnifications. Closer examination along crack path at the weld joint between the oil jacket bottom plate and wall revealed voids of up to about 160 µm within the weld metal.

Microscopic Examination

Sections (Heater - Terminals)

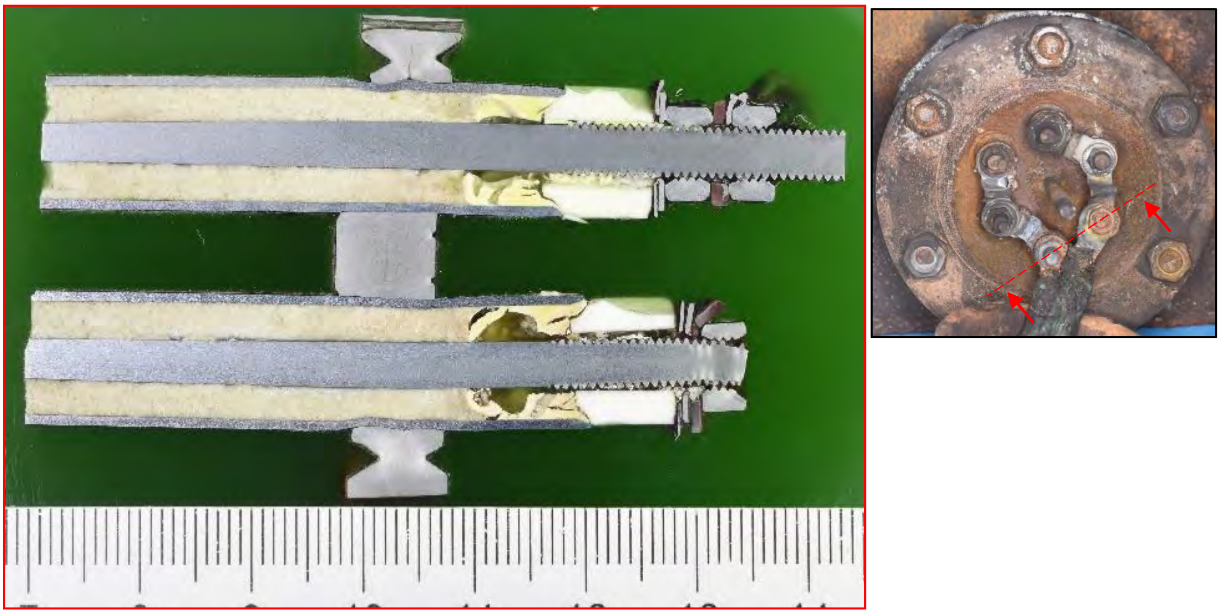

Figure 177: A section was made across the two lug-connected-terminals and flange of heater #2. The lug with arcing point was adjusted slightly to achieve the cross sectional view of it.

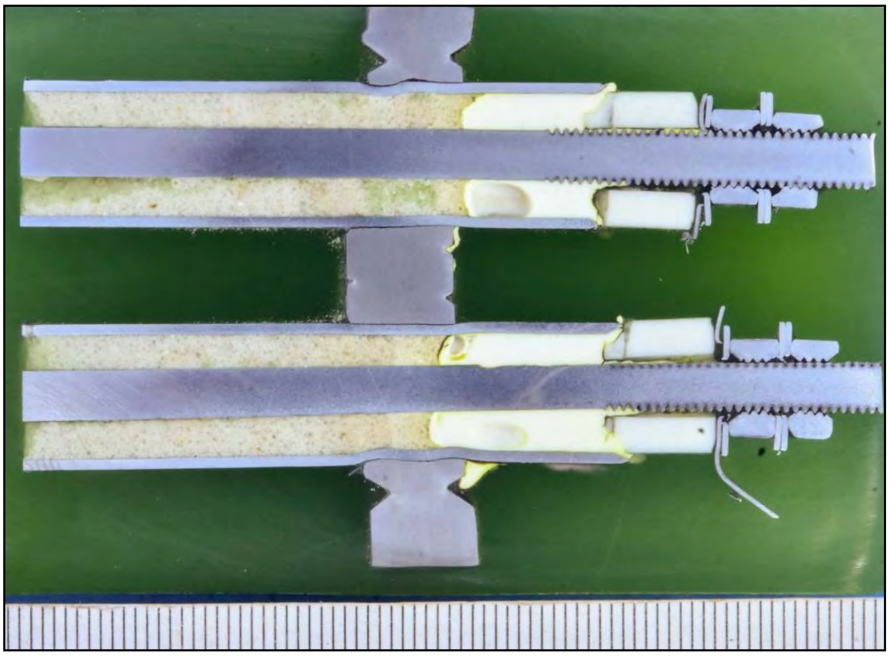

Figure 178: A section was made across two terminals and flange of a new heater as reference.

Metallographic Examination

Heater #2 (H2) - Terminals

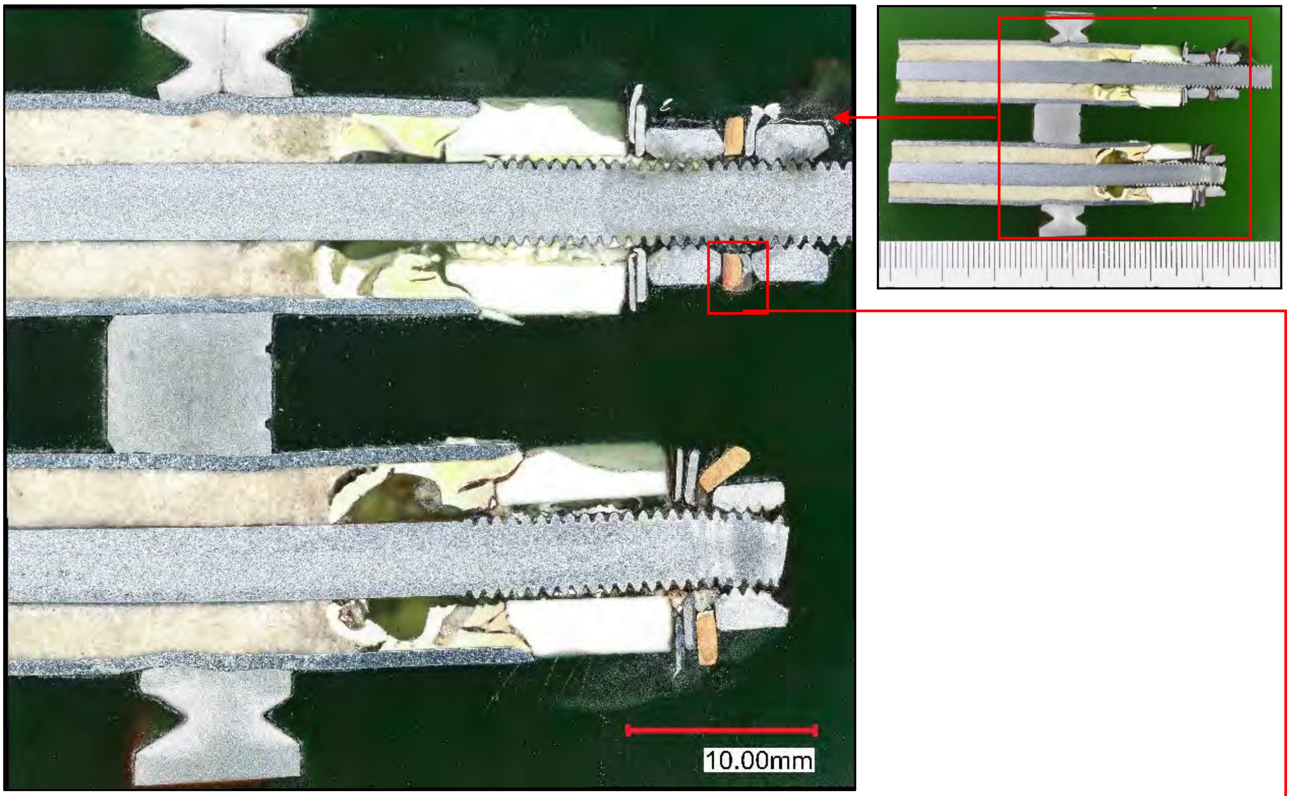

Figure 179: Sectional metallographic examination was conducted across the wired terminals (terminals #3 and #4). The arc damage is visible a the lug.

Figure 180: Close up view of the arcing location of the lug (see also Figure 138). The emanating pattern of melting and porosity (red arrows) confirm the arcing at this location.

Microscopic Examination

Sections (Heater – Metal tube)

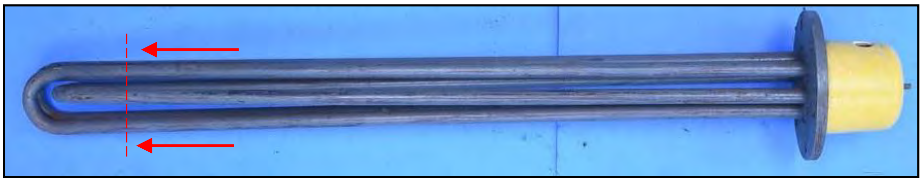

Figure 181: Heaters #2, #5 and #8 were sectioned 10 cm from the end of the heaters, across the metal tubes as shown in example above for metallographic examination. A new heater was sectioned the same way for comparison.

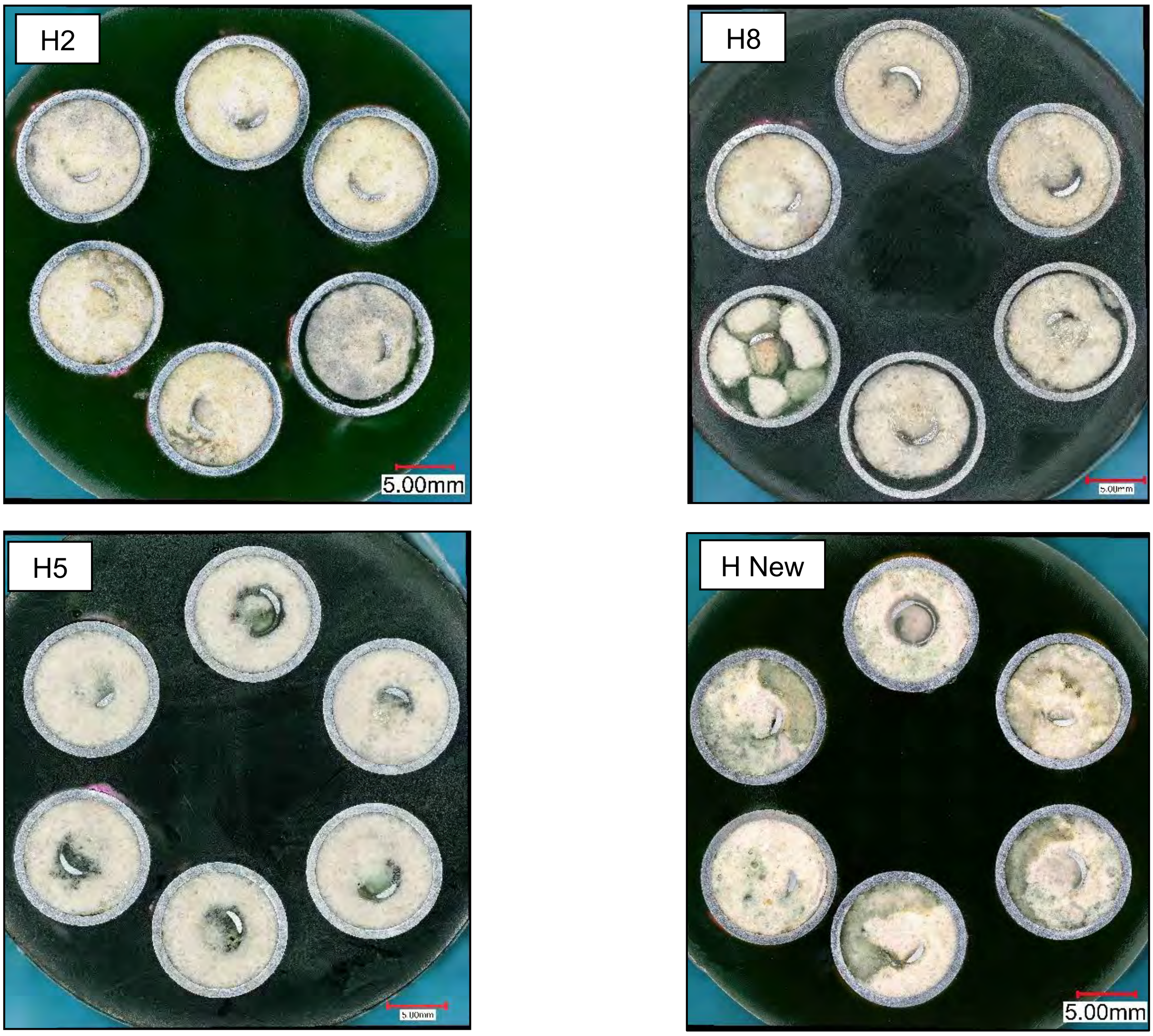

Figure 182: Cross sections for heater #2 (abbreviated as H2), heater #5 (abbreviated as H5), heater #8 (abbreviated as H8), new heater (abbreviated as H New).

Metallographic Examination

Heater #2 (H2) - Metal tubes

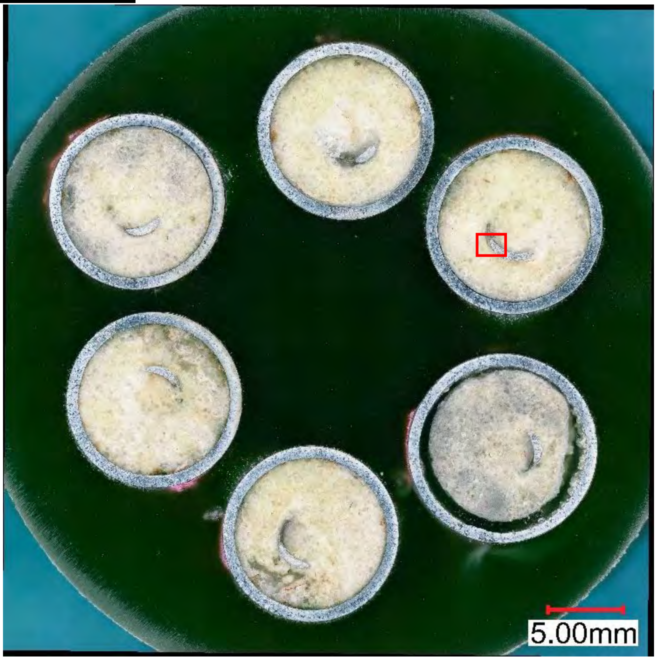

Figure 183: Sectional metallographic examination was conducted across metal tubes of heater #2.

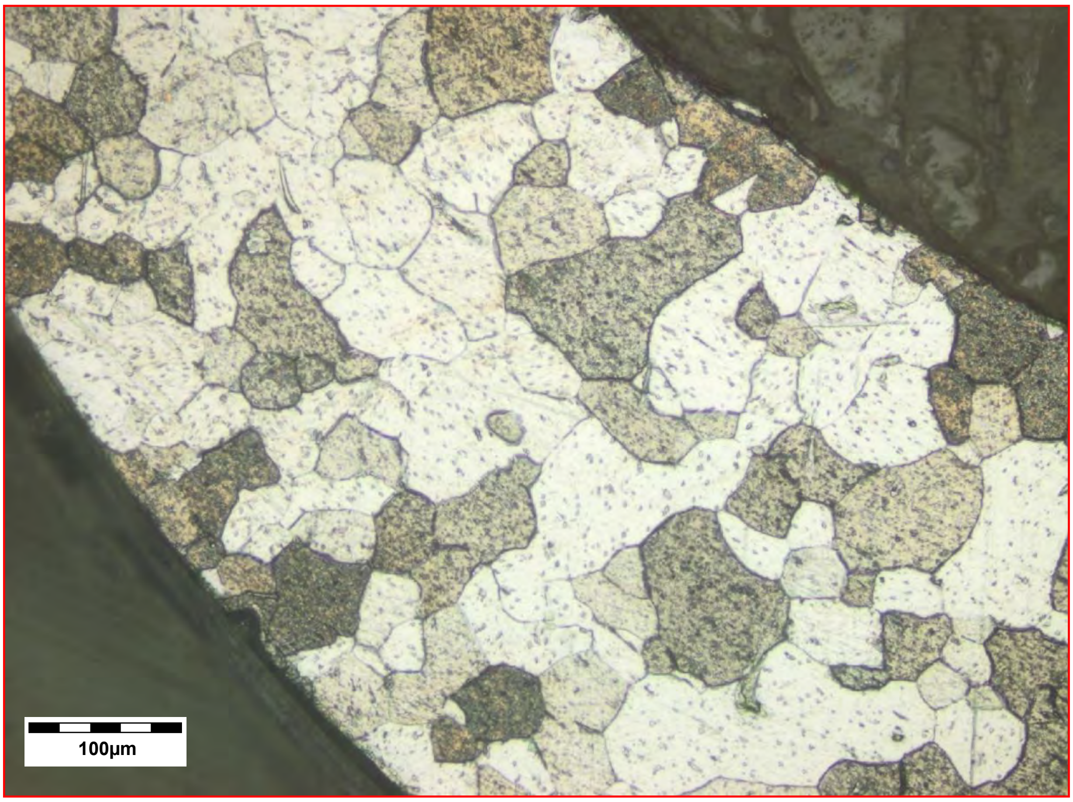

Figure 184: Micrograph of the resistance wire at 200X magnification. All the resistance wires within metal tubes were generally similar in microstructure had experienced grain growth (compared with H New, Figure 202).

Metallographic Examination

Heater #2 (H2) - Metal tubes

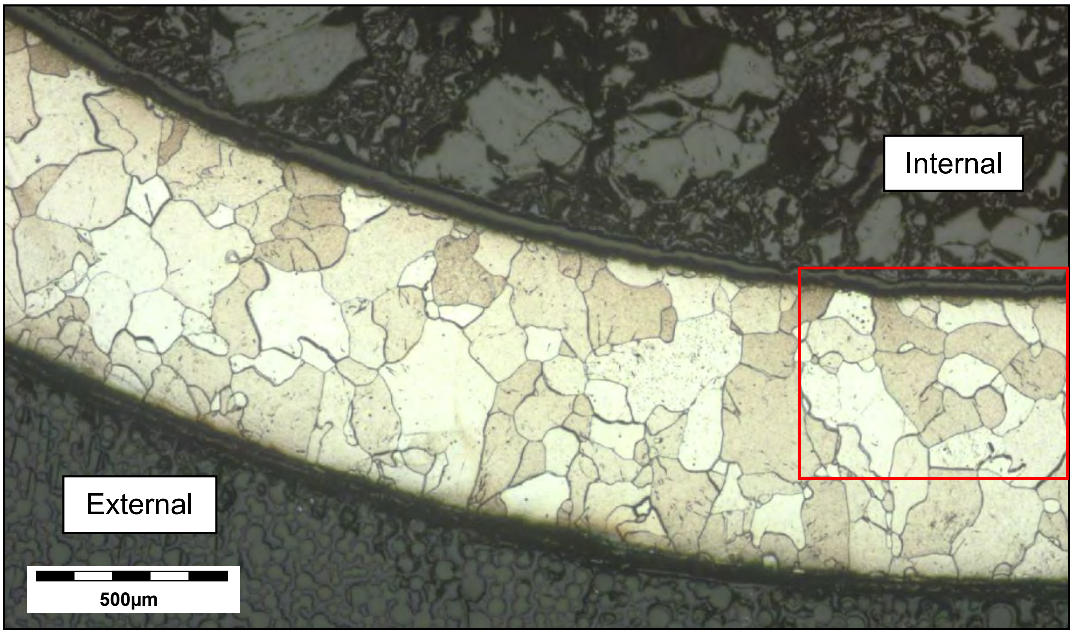

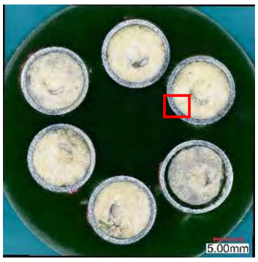

Figure 185: Micrograph of the metal tube at 50X magnification. All the metal tubes were generally similar in microstructure and had experienced grain growth (compared with H New, Figure 203).

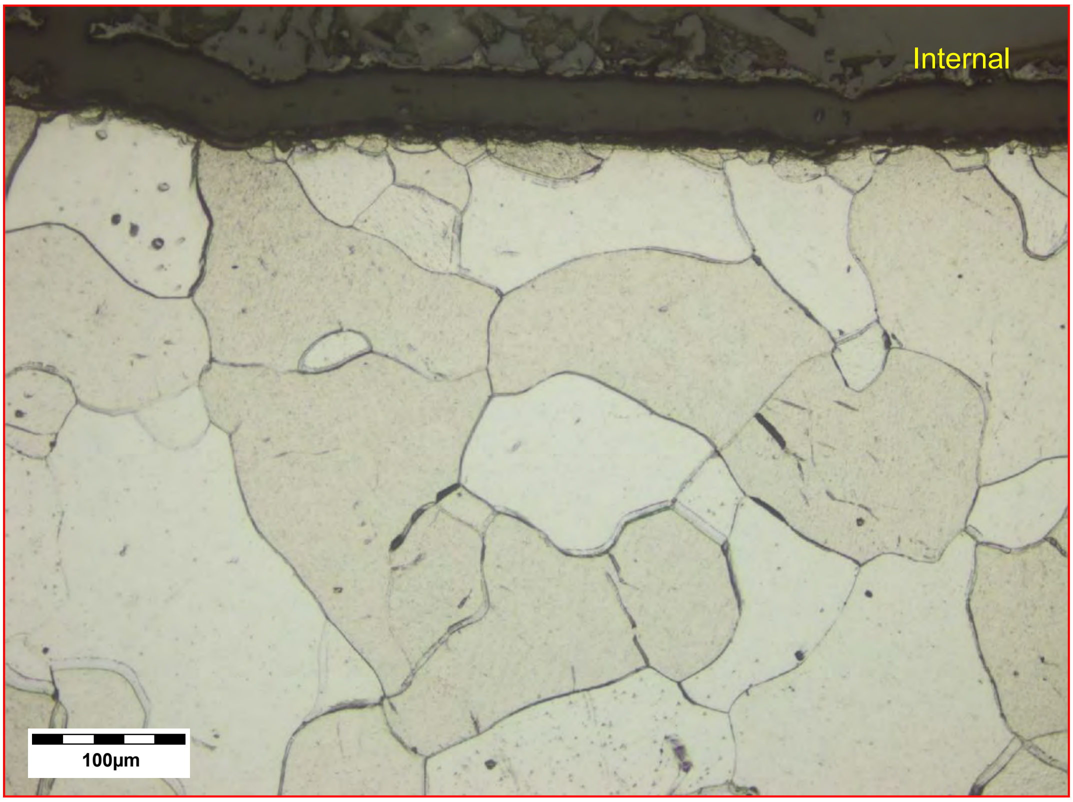

Figure 186: Micrograph of the metal tube at 200X magnification (compared with H New, Figure 204).

Metallographic Examination

Heater #2 (H2) - Metal tubes

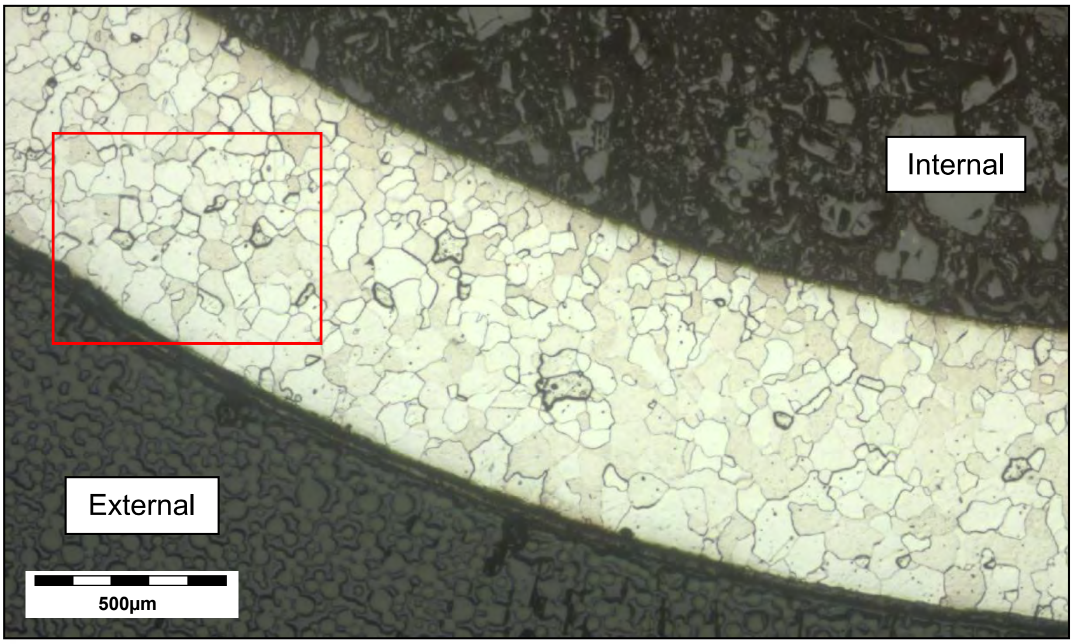

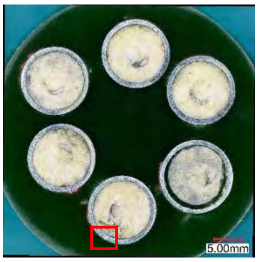

Figure 187: Micrograph of the metal tube at 50X magnification. All the metal tubes were generally similar in microstructure and had experienced grain growth (compared with H New, Figure 203).

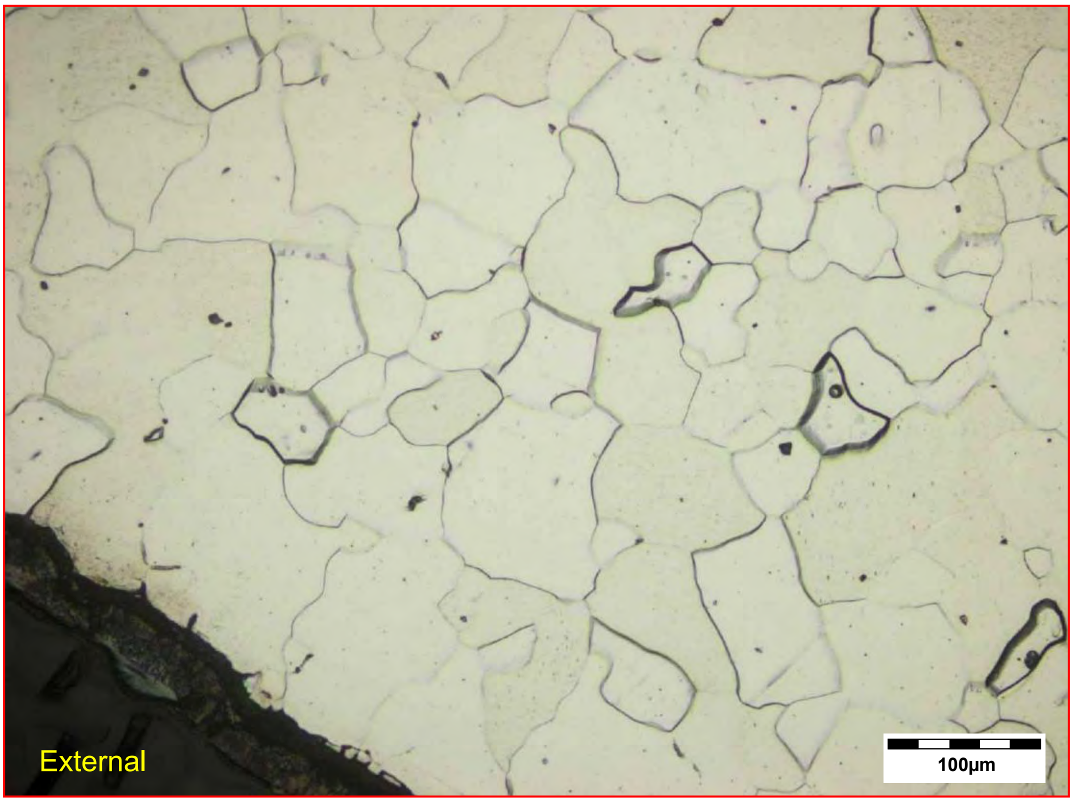

Figure 188: Micrograph of the metal tube at 200X magnification (compared with H New, Figure 204).

Metallographic Examination

Heater #5 (H5) - Metal tubes

Figure 189: Sectional metallographic examination was conducted across metal tubes of heater #5.

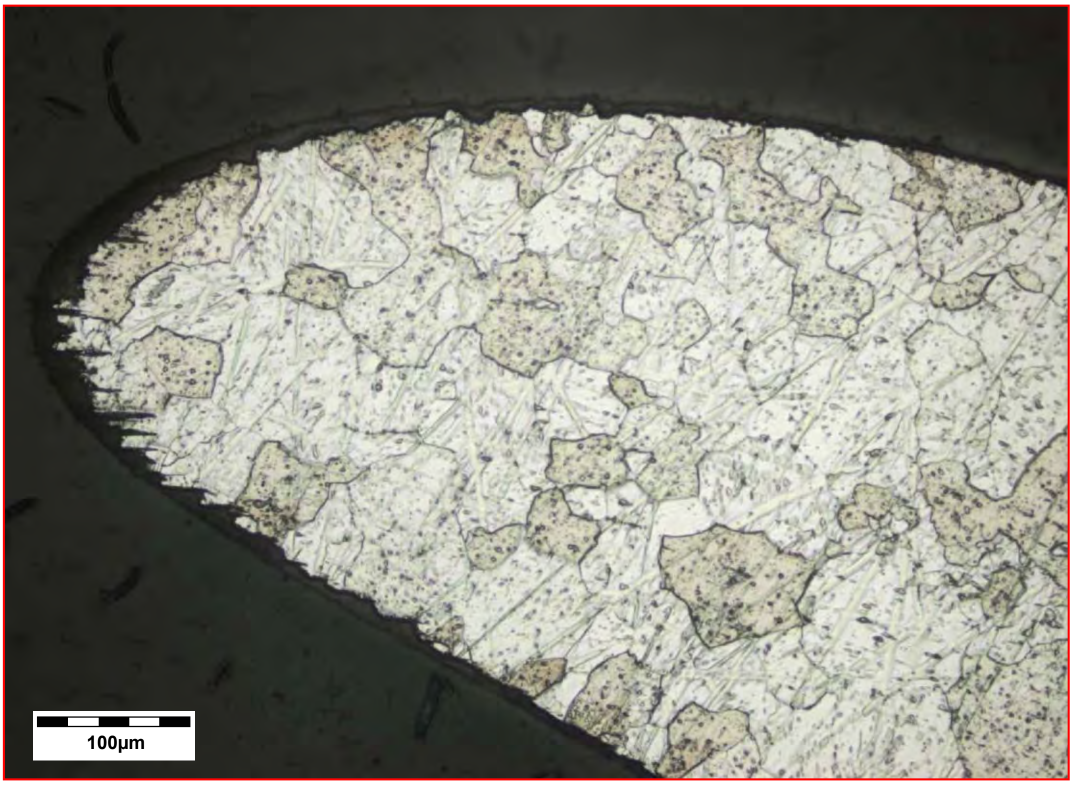

Figure 190: Micrograph of the resistance wire at 200X magnification. All the resistance wires within metal tubes were generally similar in microstructure had experienced grain growth (compared with H New, Figure 202).

Metallographic Examination

Heater #5 (H5) - Metal tubes

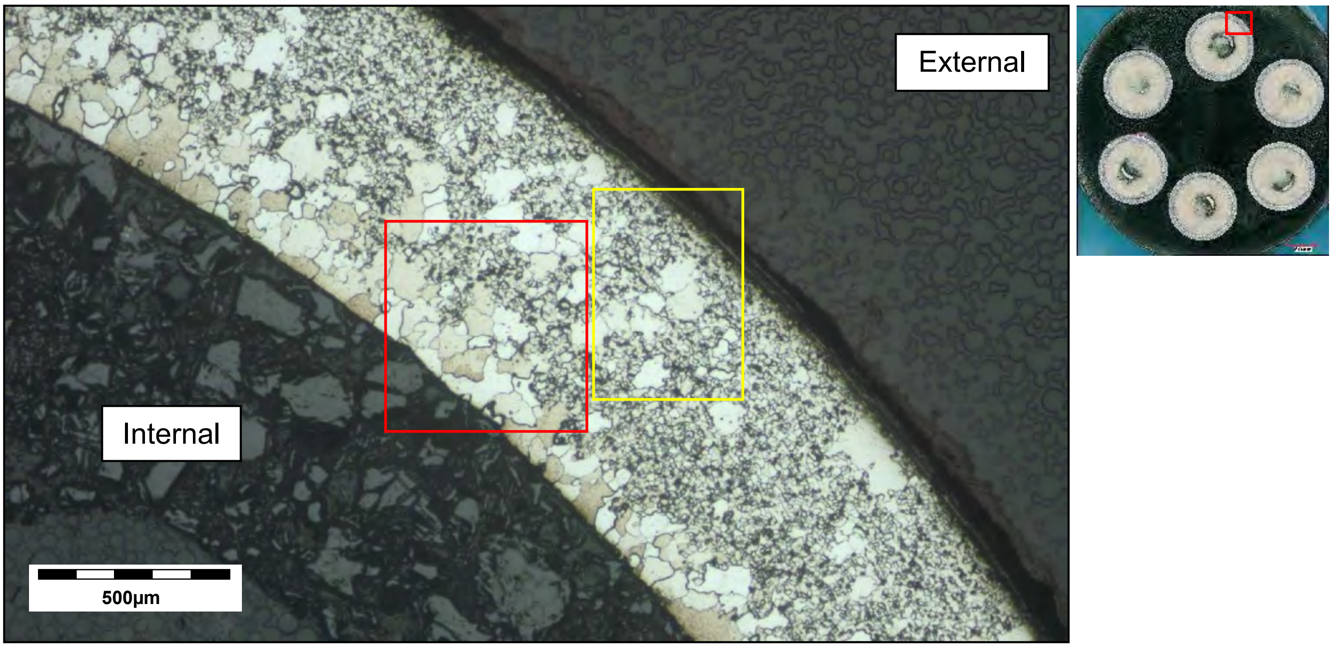

Figure 191: Micrograph of the metal tube at 50X magnification. All the metal tubes were generally similar in microstructure and had experienced grain growth starting from the internal surface up to about mid-wall thickness (compared with H New, Figure 203).

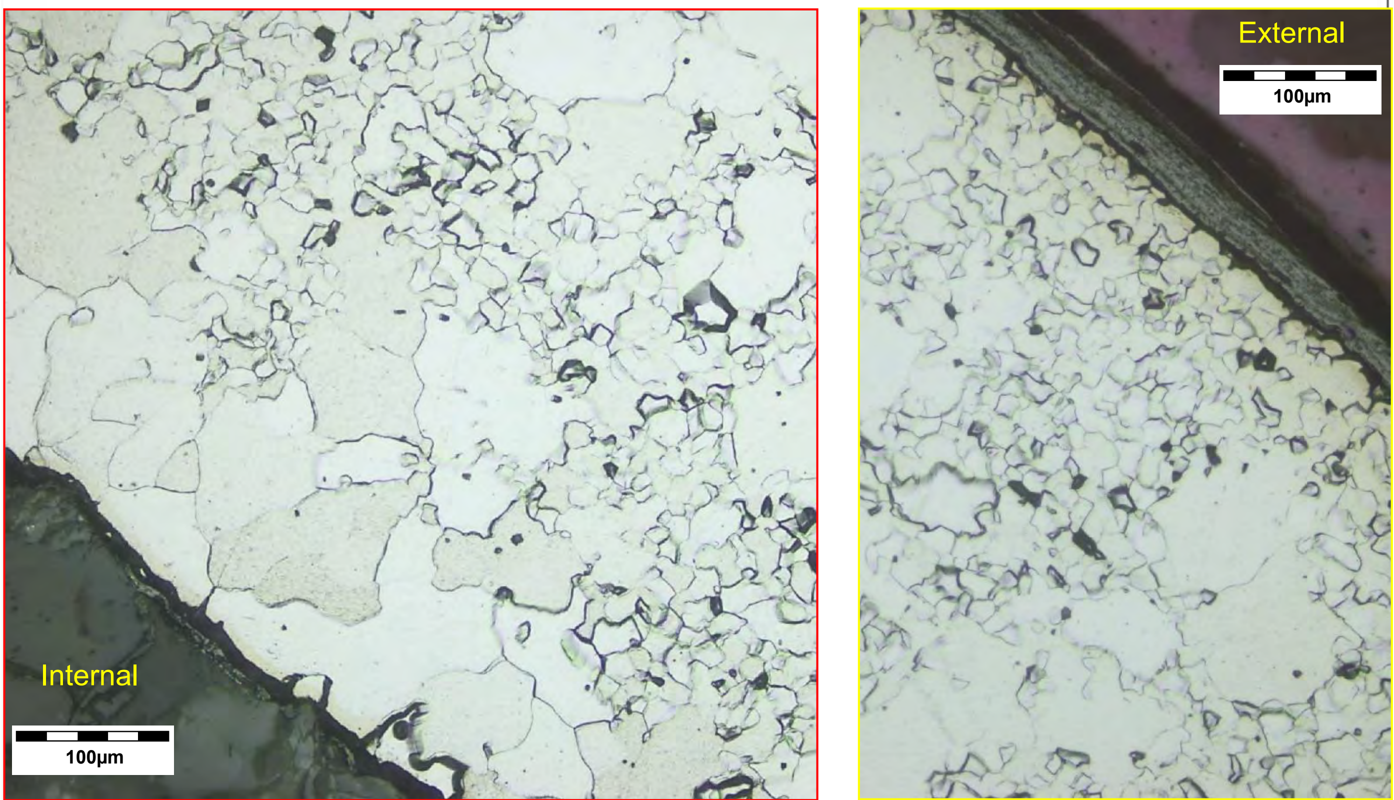

Figure 192: Micrographs of the metal tube at 200X magnification (compared with H New, Figure 204).

Metallographic Examination

Heater #5 (H5) - Metal tubes

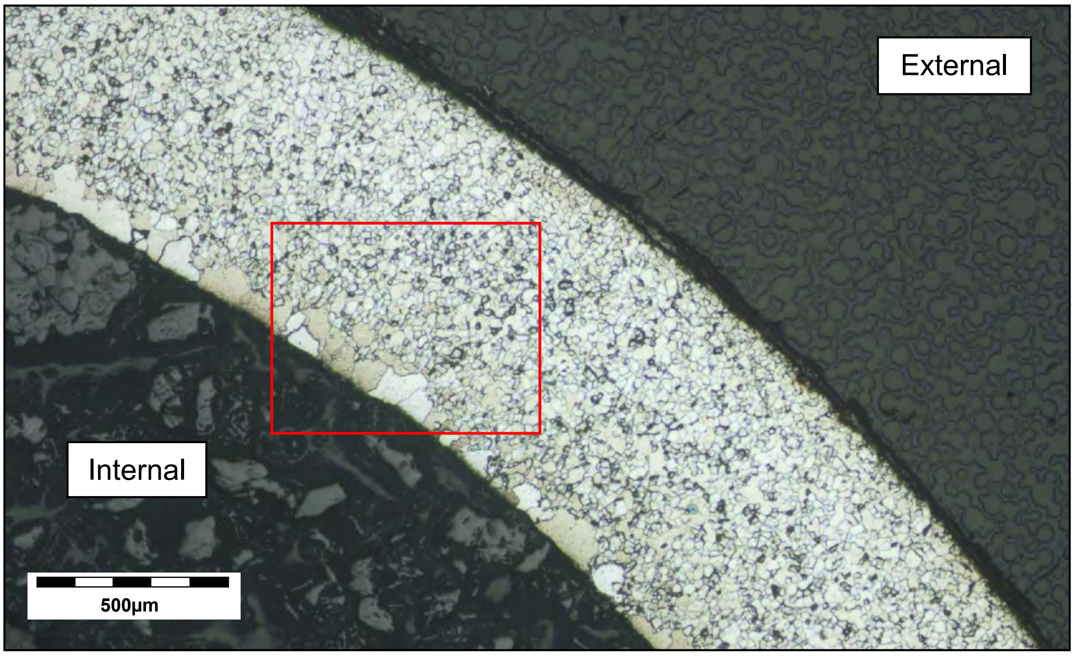

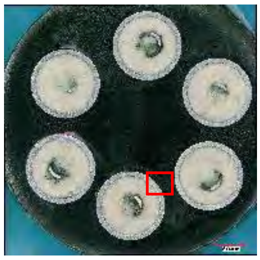

Figure 193: Micrograph of the metal tube at 50X magnification. All the metal tubes were generally similar in microstructure and had experienced grain growth starting from the internal surface (compared with H New, Figure 203).

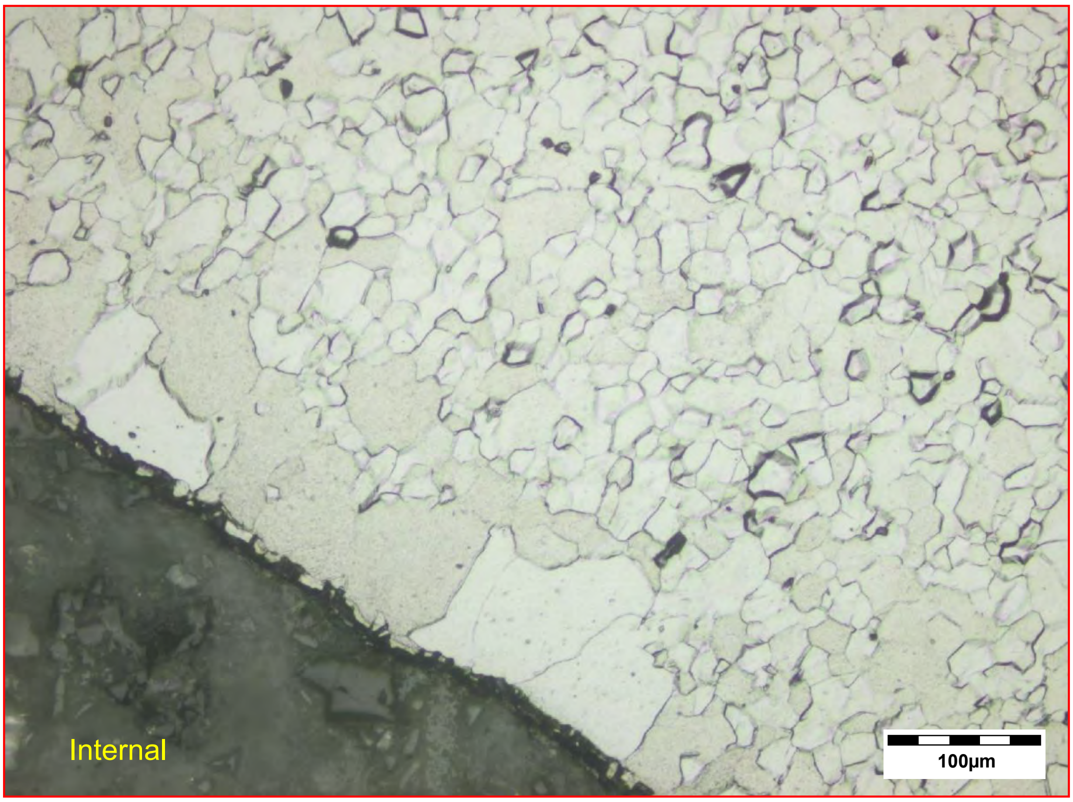

Figure 194: Micrograph of the metal tube at 200X magnification (compared with H New, Figure 204).

Metallographic Examination

Heater #8 (H8) - Metal tubes

Figure 195: Sectional metallographic examination was conducted across metal tubes of heater #8.

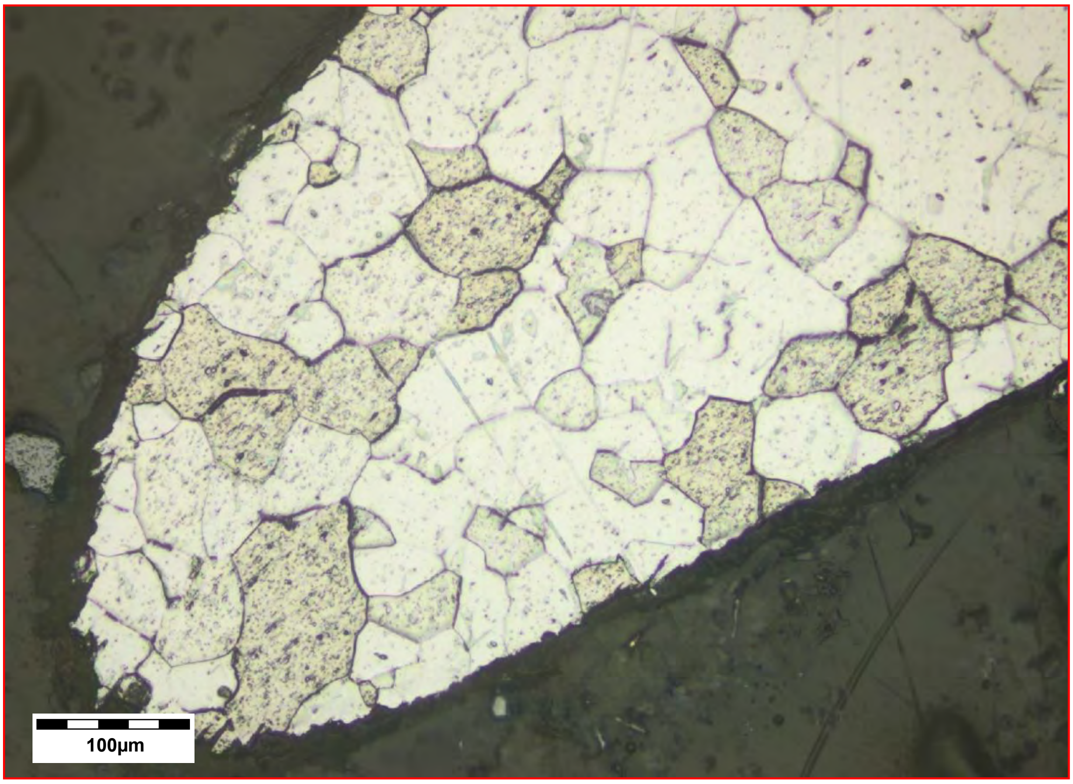

Figure 196: Micrograph of the resistance wire at 200X magnification. All the resistance wires within metal tubes were generally similar in microstructure had experienced grain growth (compared with H New, Figure 202).

Metallographic Examination

Heater #8 (H8) - Metal tubes

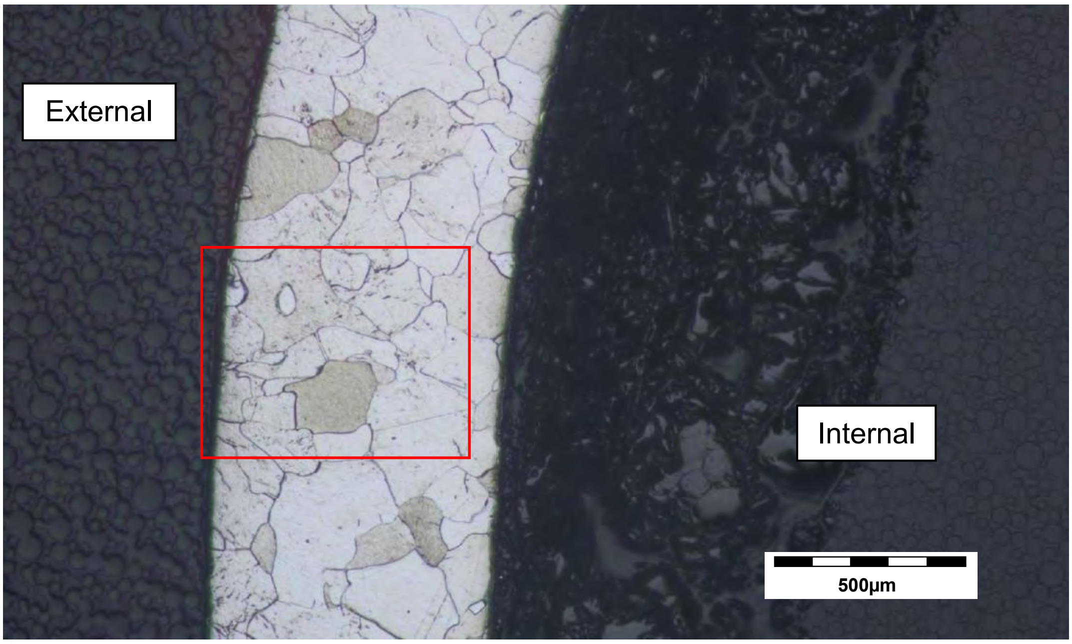

Figure 197: Micrograph of the metal tube at 50X magnification. All the metal tubes were generally similar in microstructure and had experienced grain growth (compared with H New, Figure 203).

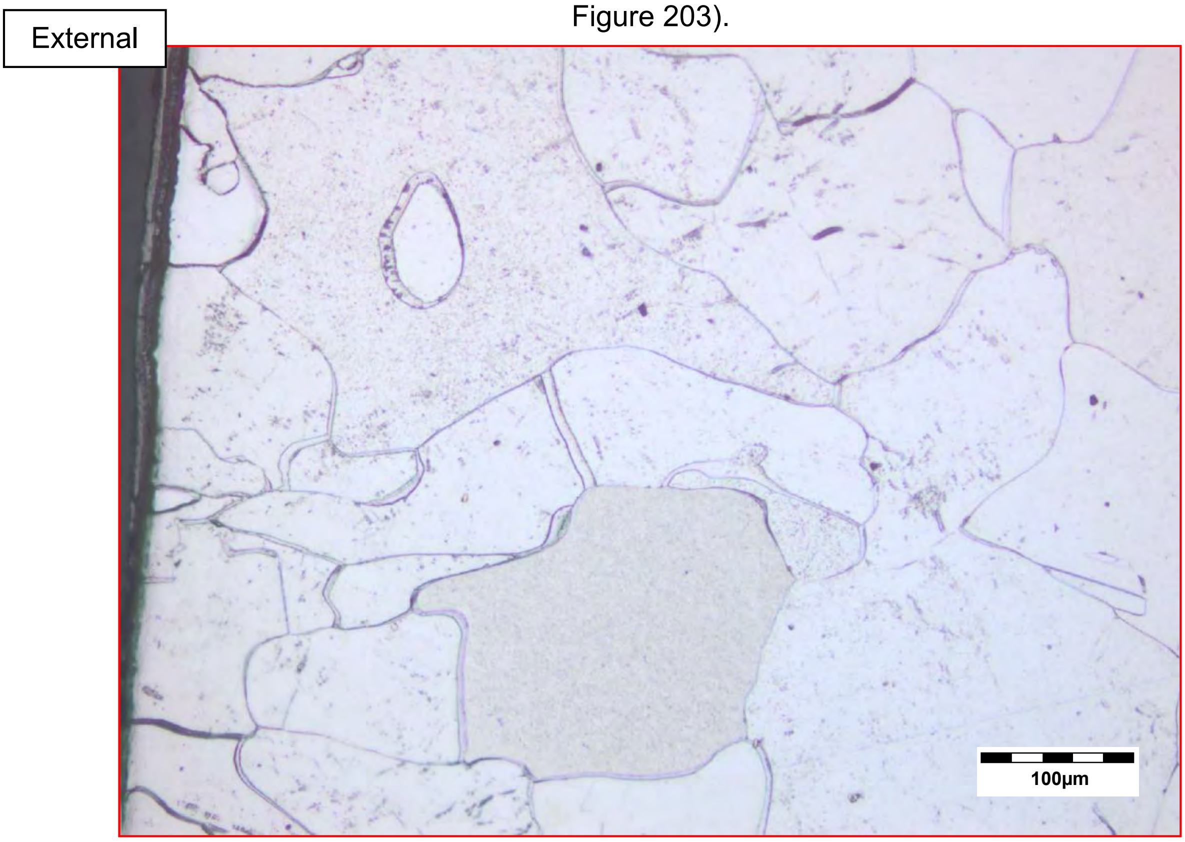

Figure 198: Micrograph of the metal tube at 200X magnification (compared with H New, Figure 204).

Metallographic Examination

Heater #8 (H8) - Metal tubes

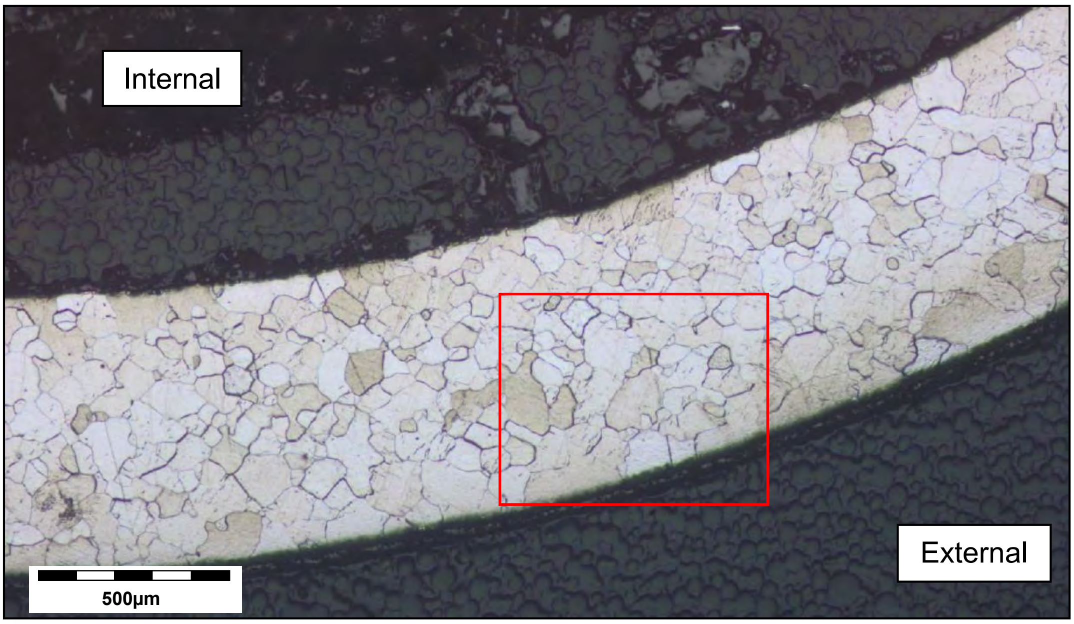

Figure 199: Micrograph of the metal tube at 50X magnification. All the metal tubes were generally similar in microstructure and had experienced grain growth (compared with H New, Figure 203).

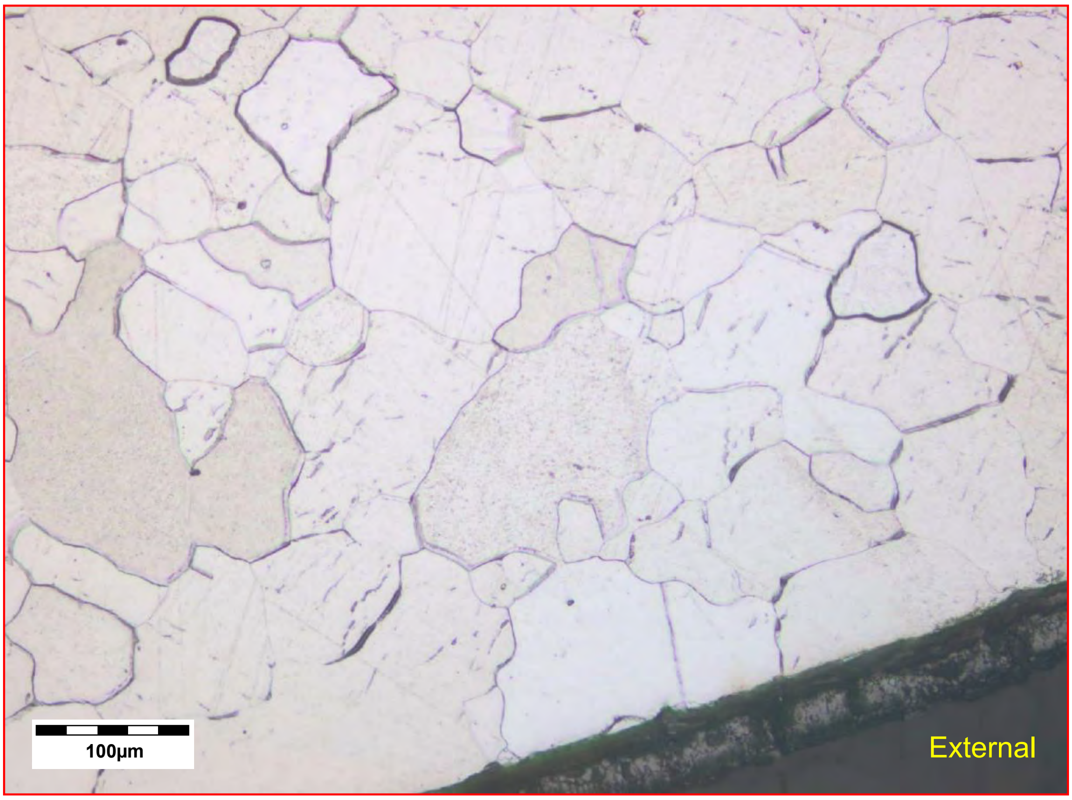

Figure 200: Micrograph of the metal tube at 200X magnification (compared with H New, Figure 204).

Metallographic Examination

New Heater (H New) - Metal tubes

Figure 201: Sectional metallographic examination was conducted across metal tubes of new heater.

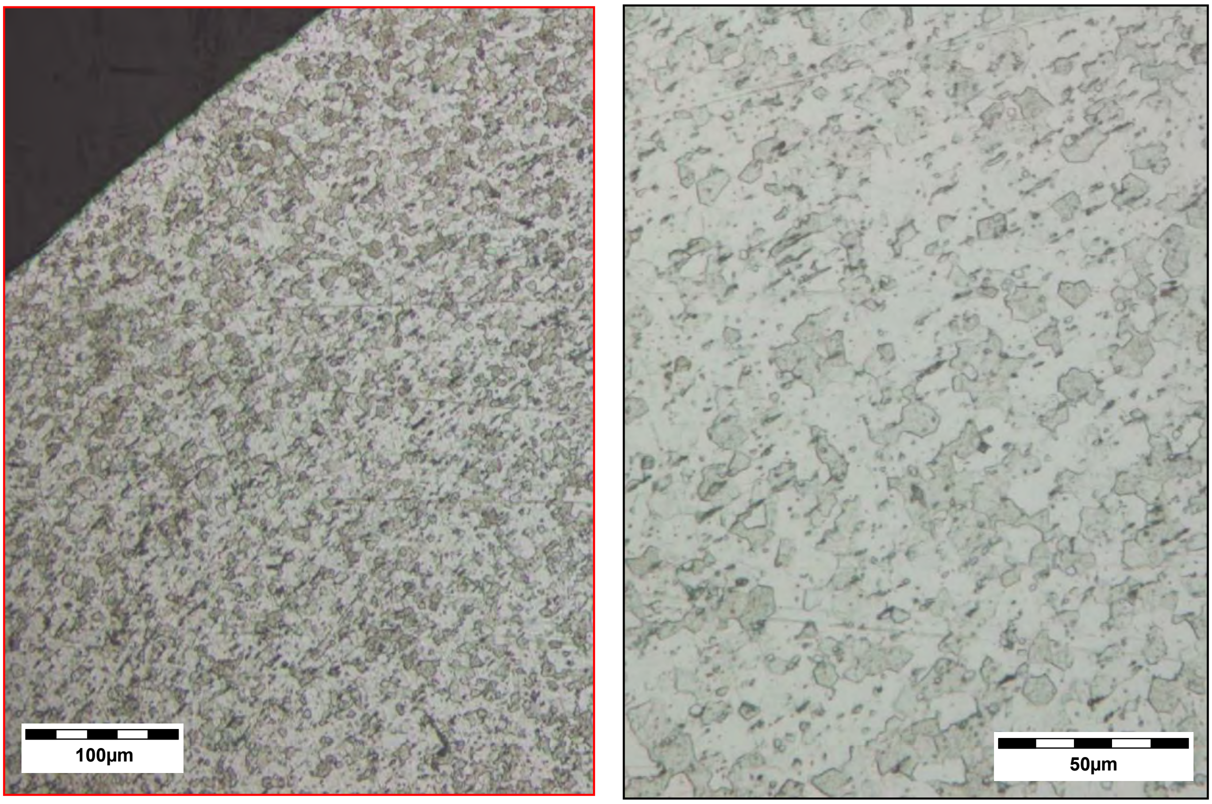

Figure 202: Micrographs of the resistance wire at 200X (left) and 500X (right) magnifications. All the resistance wires were generally similar in microstructure and grain size. The grain size is significantly smaller compared with the other examined heaters.

Metallographic Examination

New Heater (H New) - Metal tubes

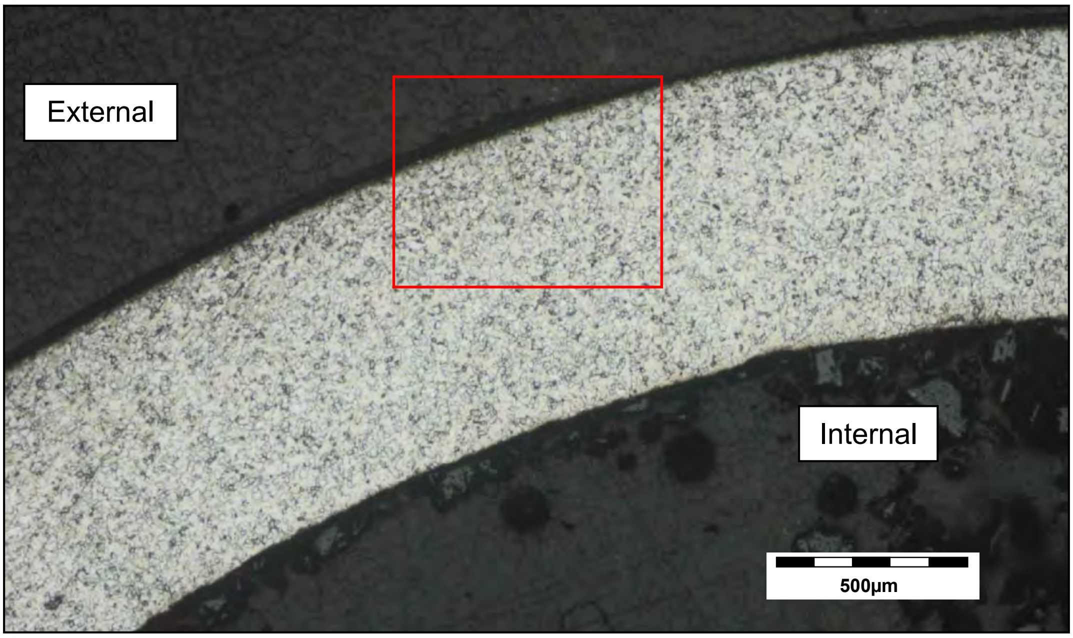

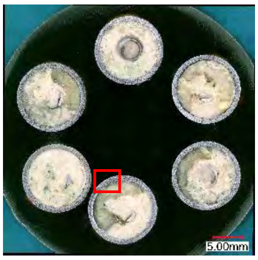

Figure 203: Micrograph of the metal tube at 50X magnification. All the metal tubes were generally similar in microstructure. The grain size is significantly smaller compared with the other examined heaters.

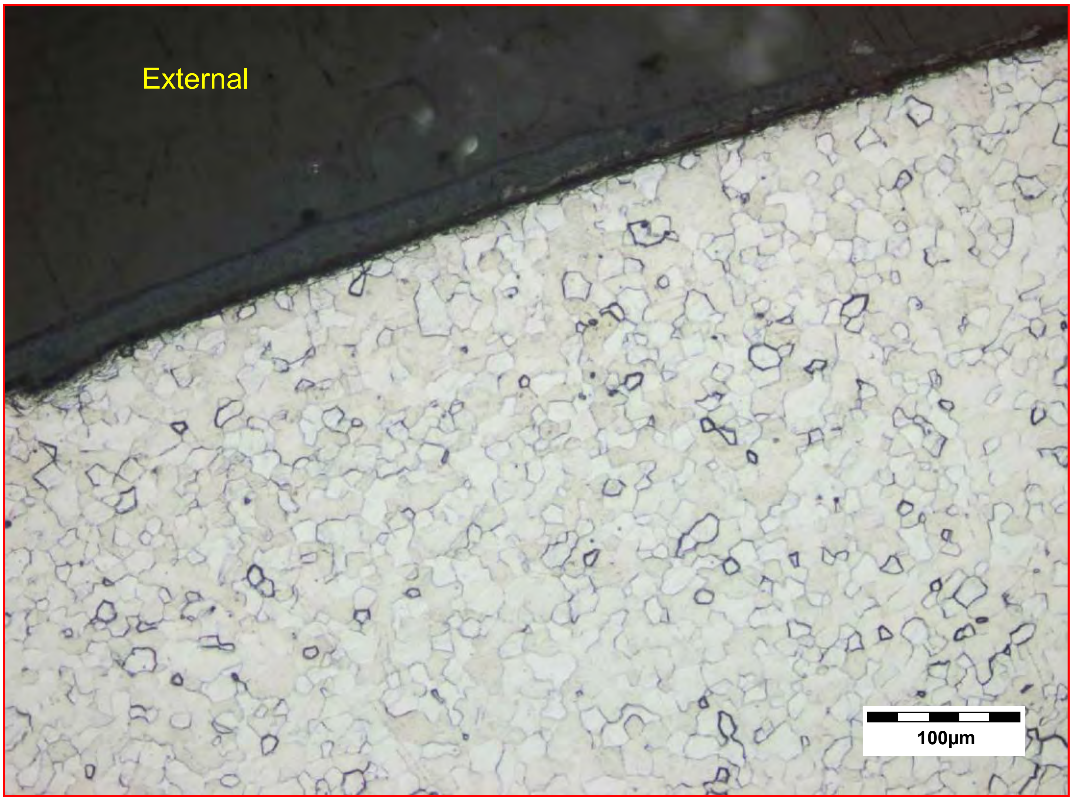

Figure 204: Micrograph of the metal tube at 200X magnification.

Microscopic Examination

Sections (Used Heater – Metal tube)

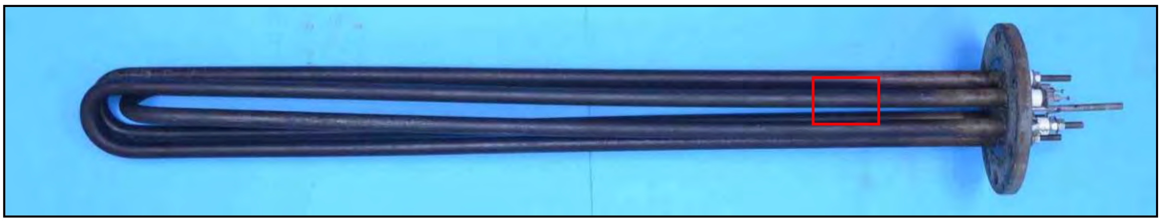

Figure 205: The used heater with blisters were sectioned across one of the blister.

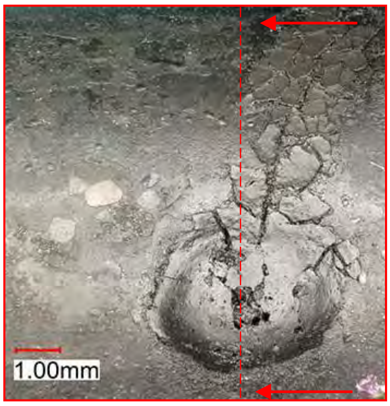

Figure 206: Cross section across the blister, metal tube and resistor wire of the used heater. The insulation powder inside the metal tube was removed for ease of metallographic examination.

Metallographic Examination

Used Heater (H Used) - Metal tubes

Figure 207: Sectional metallographic examination was conducted across a metal tube with blister of used heater.

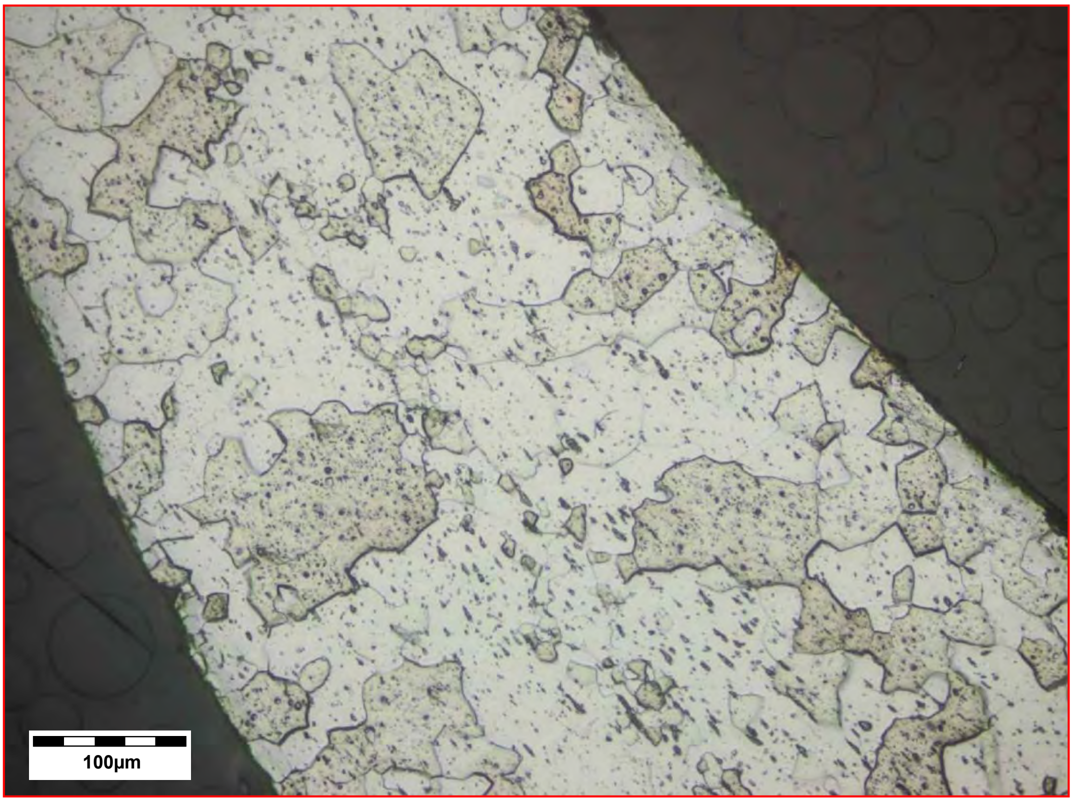

Figure 208: Micrograph of the resistance wire at 200X magnification. The resistance wire had experienced grain growth (compared with H New, Figure 202).

Metallographic Examination

Used Heater (H Used) - Metal tubes

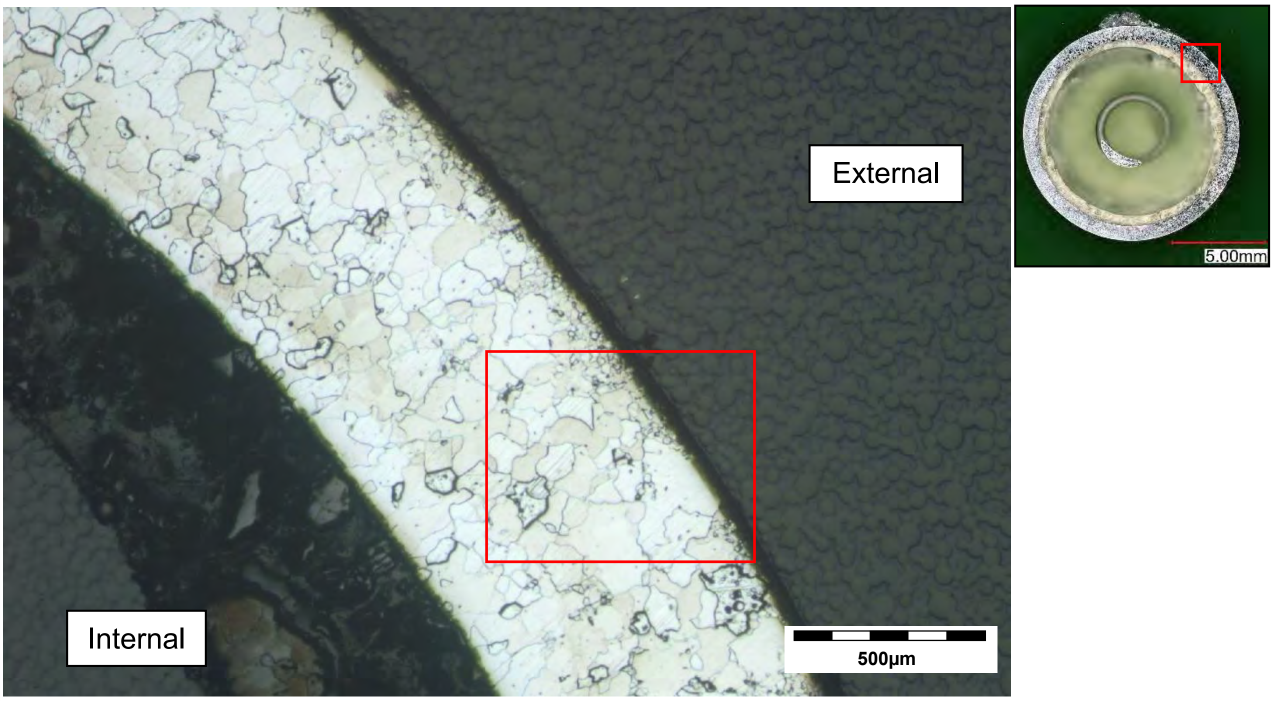

Figure 209: Micrograph of the metal tube at 50X magnification. All the metal tubes were generally similar in microstructure and had experienced grain growth (compared with H New, Figure 203).

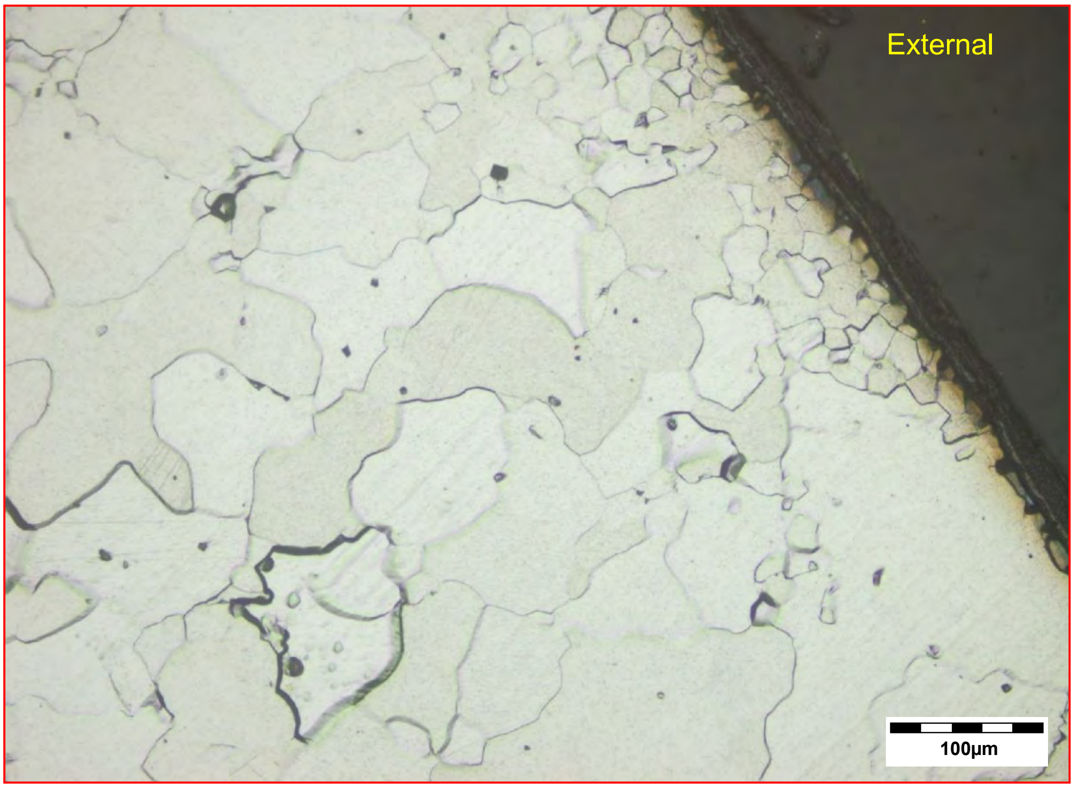

Figure 210: Micrograph of the metal tube at 200X magnification (compared with H New, Figure 204).

Appendix G:
3D Model and Volume Calculation

3D Model and Volume Calculation

40L oil level

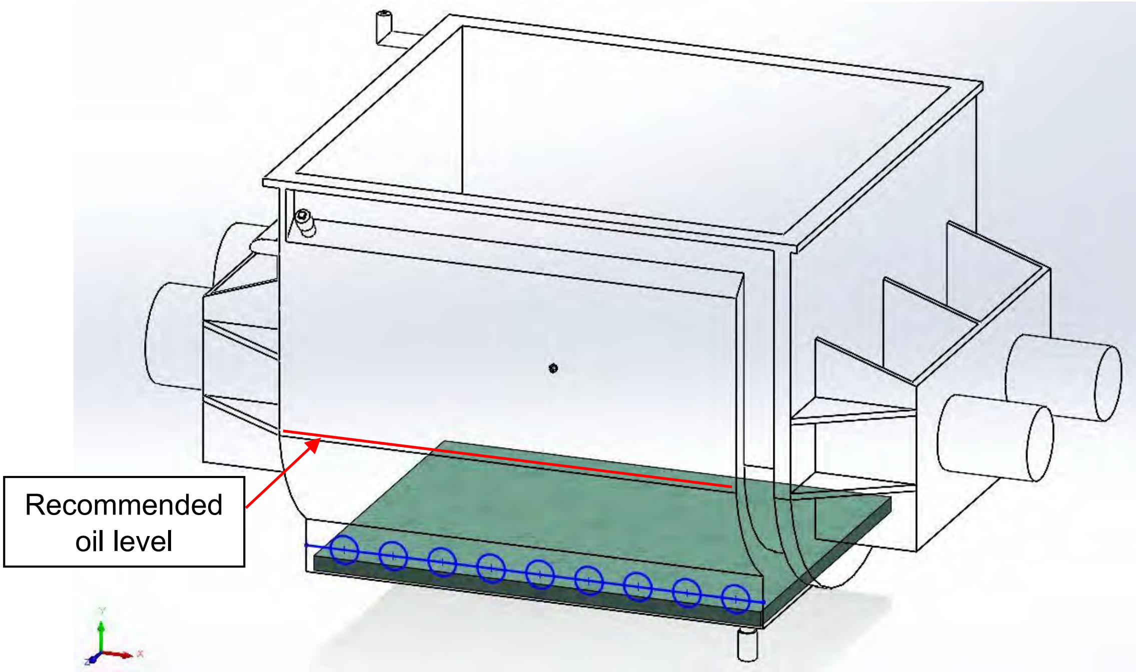

Figure 211: 3D model showing the oil fill level at 40L. The level is estimated to be below the heaters.

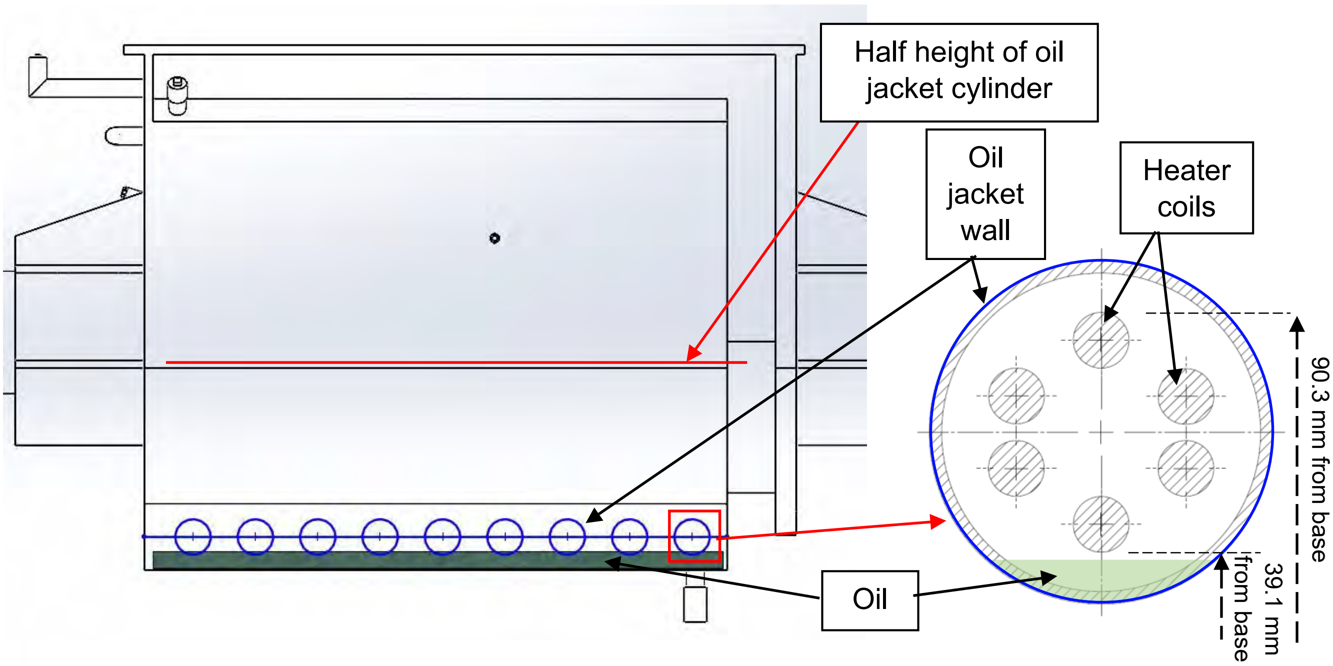

Figure 212: 3D model showing the oil fill level at 40L. The level is estimated to be 27 mm below the centreline of heaters.

3D Model and Volume Calculation

60L oil level

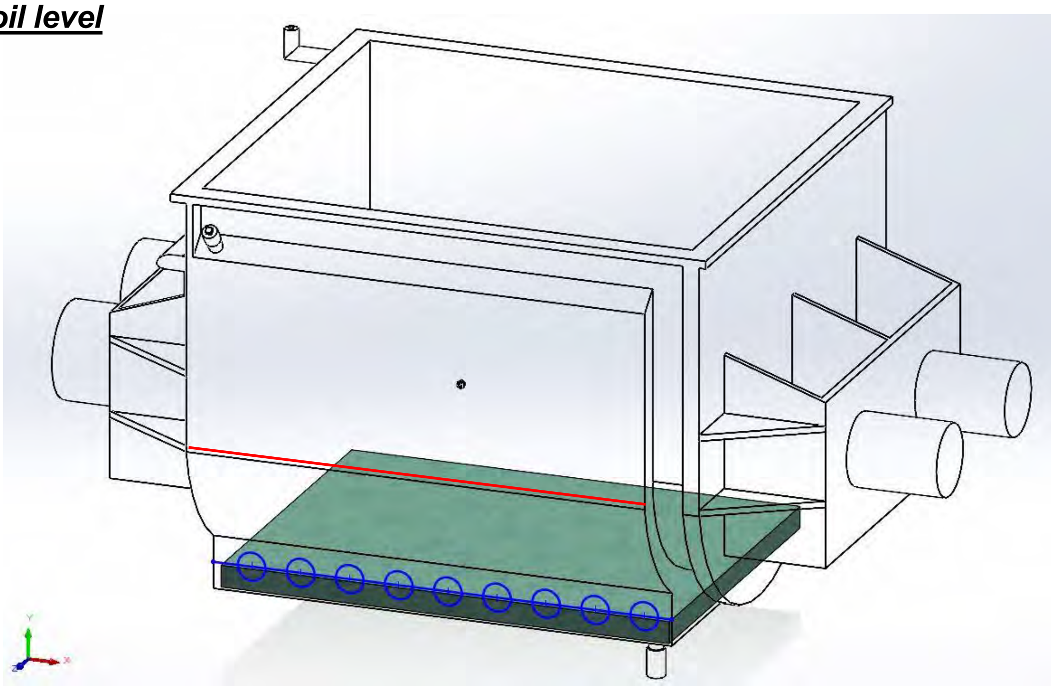

Figure 213: 3D model showing the oil fill level at 60L. The level is estimated to be slightly below the centreline of the heaters.

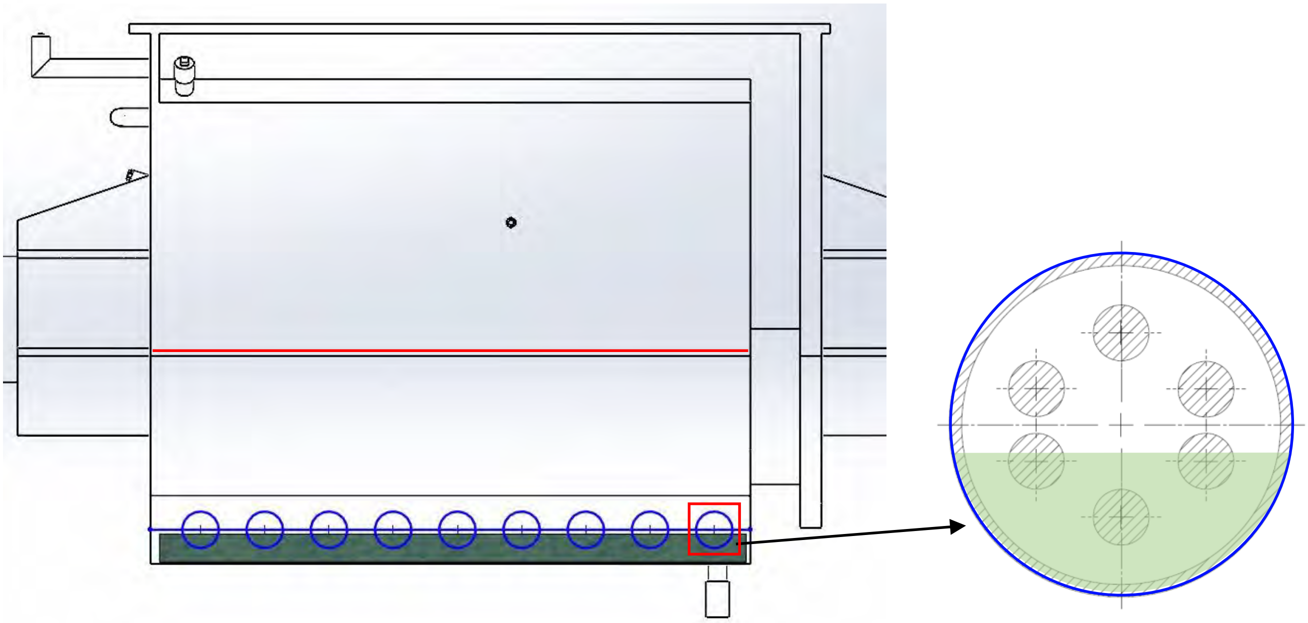

Figure 214: Model showing the oil fill level at 60L. The level is estimated to be 8 mm below the centreline of the heaters.

3D Model and Volume Calculation

80L oil level

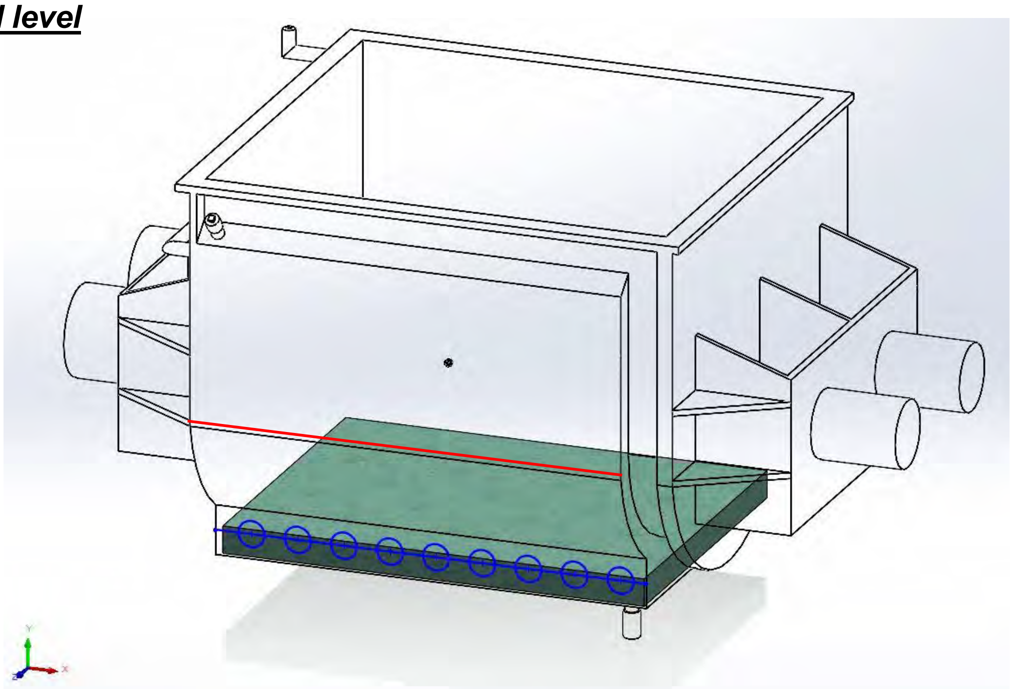

Figure 215: 3D model showing the oil fill level at 80L. The level is estimated to be slightly above the centreline of the heaters.

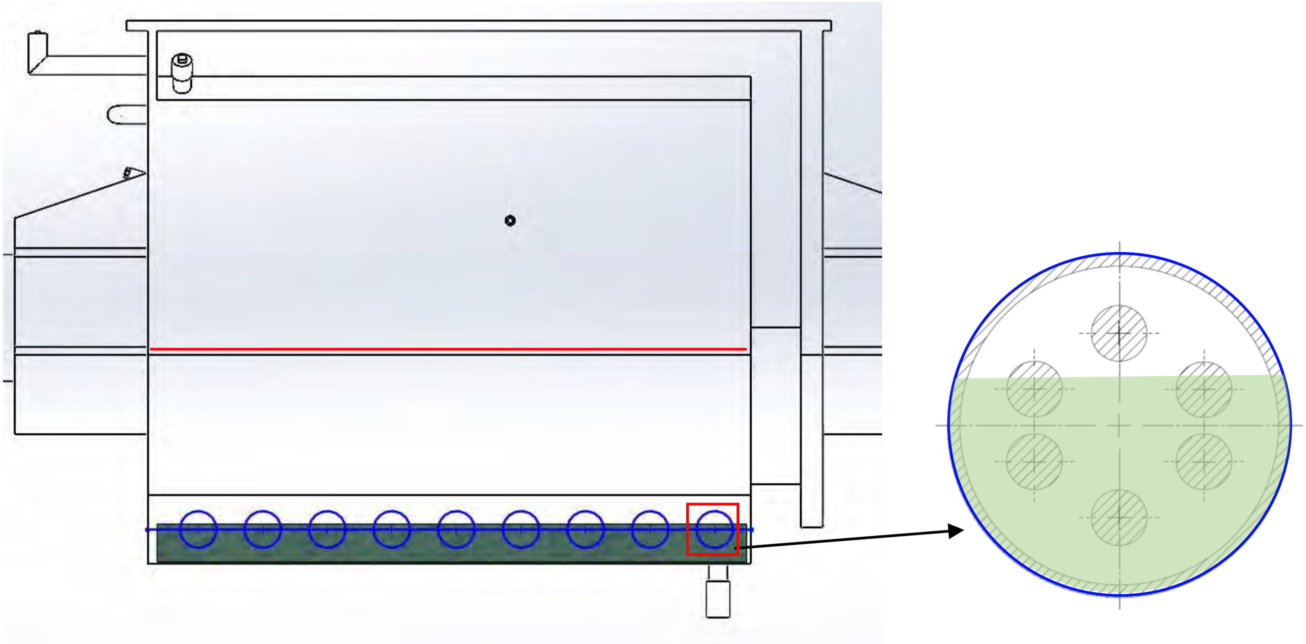

Figure 216: 3D model showing the oil fill level at 80L. The level is estimated to be 10 mm above the centreline of the heaters.

3D Model and Volume Calculation

100L oil level

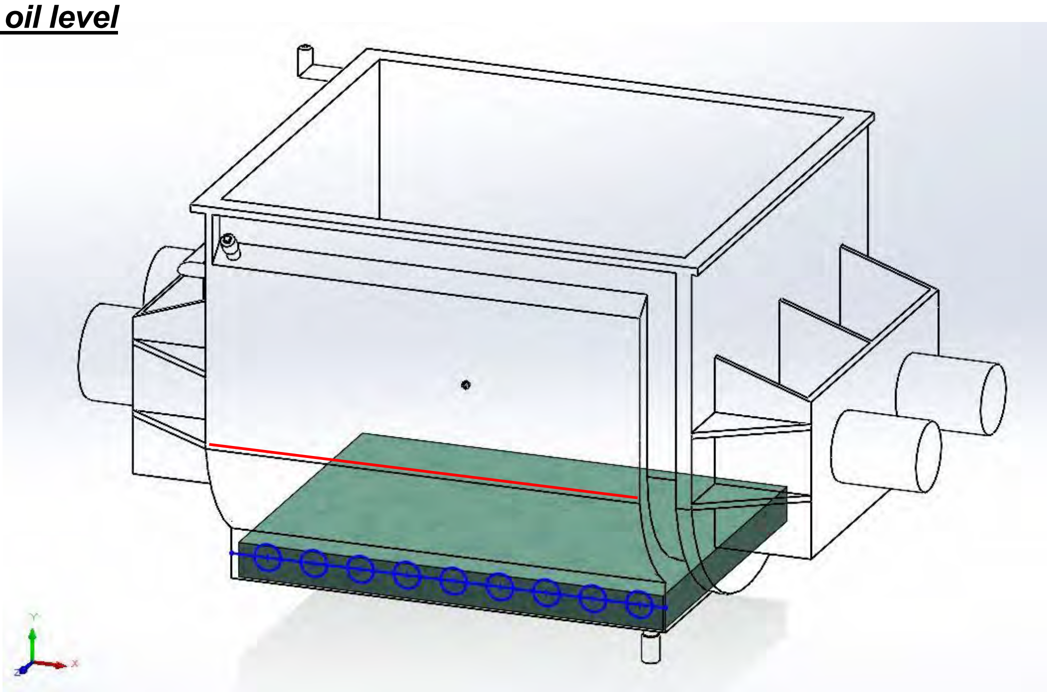

Figure 217: 3D model showing the oil fill level at 100L. The level is estimated to be slightly above the centreline of the heaters.

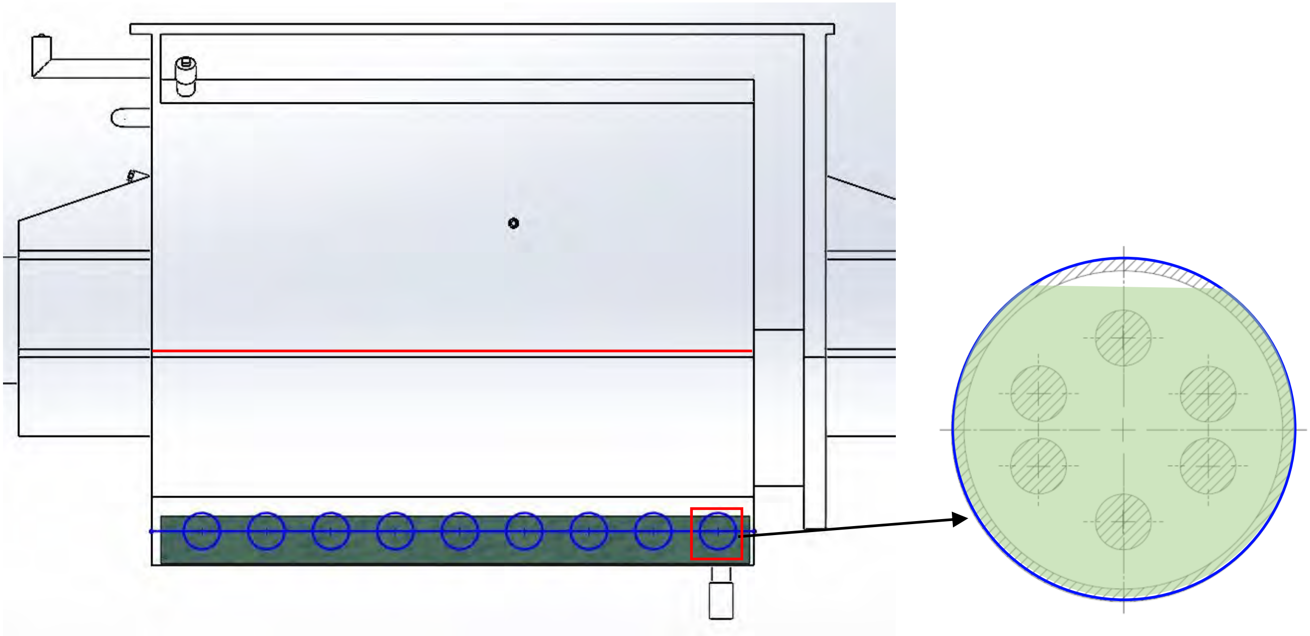

Figure 218: 3D model showing the oil fill level at 100L. The level is estimated to be 30 mm above the centreline of the heaters.

3D Model and Volume Calculation

120L oil level

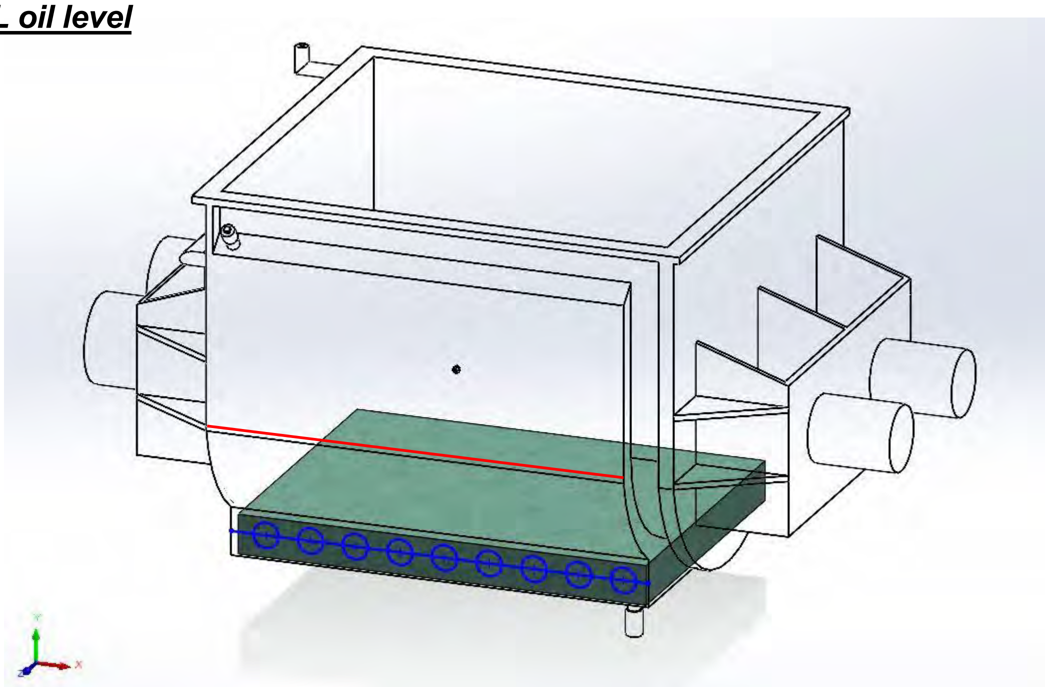

Figure 219: 3D model showing the oil fill level at 120L. The level is estimated to be slightly above the centreline of the heaters.

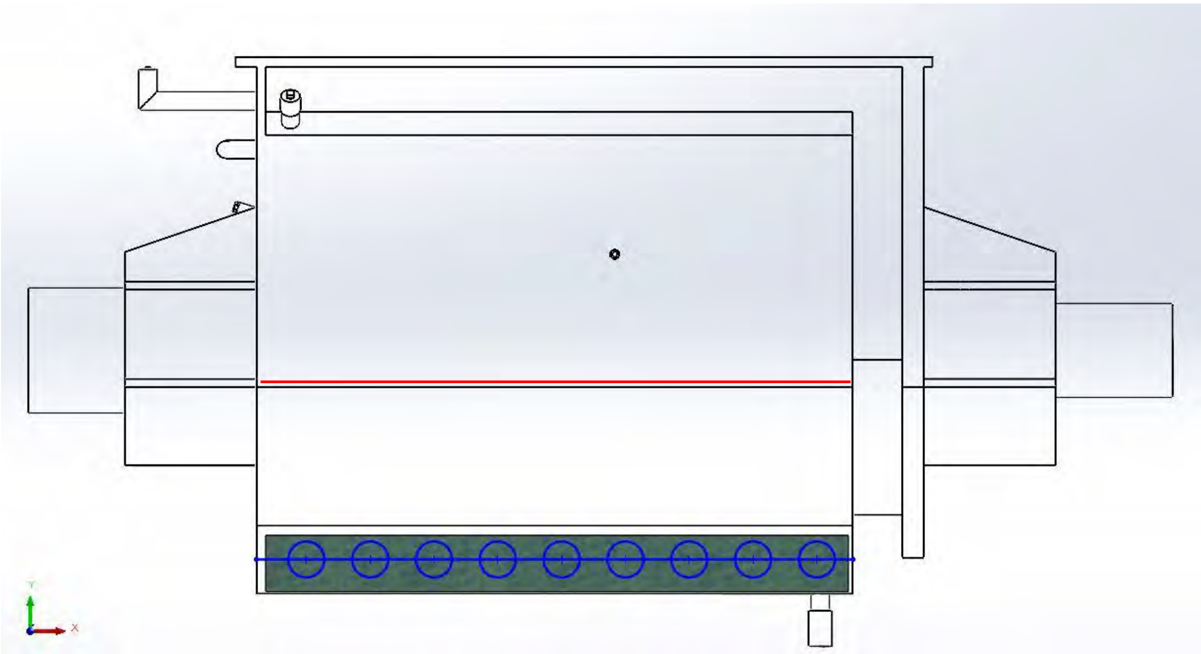

Figure 220: 3D model showing the oil fill level at 120L. The level is estimated to be fully covering the heaters.

3D Model and Volume Calculation

140L oil level

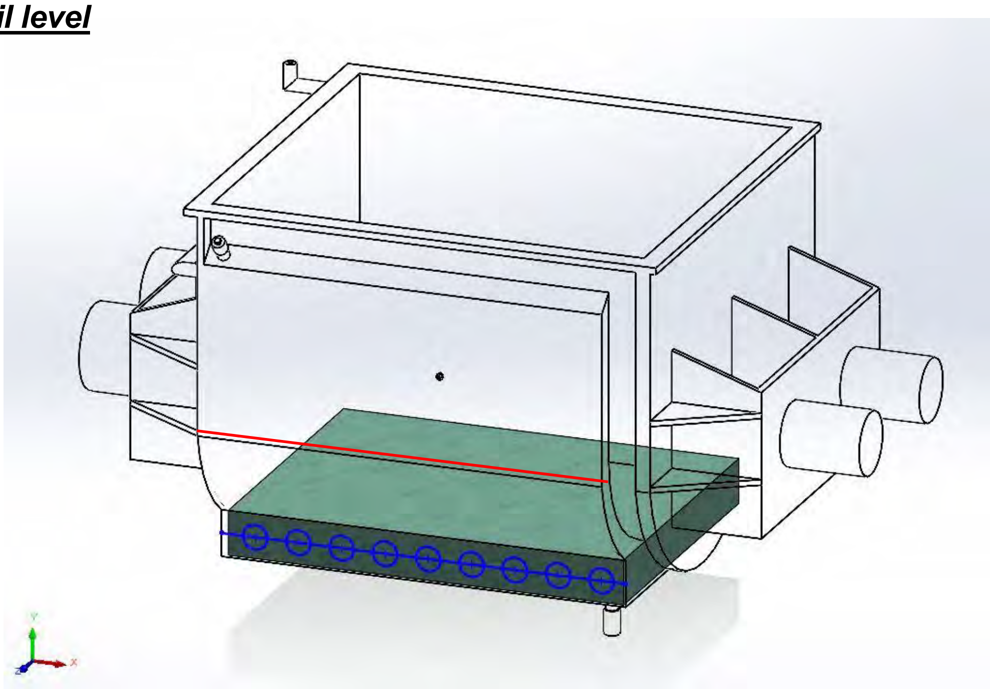

Figure 221: 3D model showing the oil fill level at 140L. The level is estimated to be slightly above the centreline of the heaters.

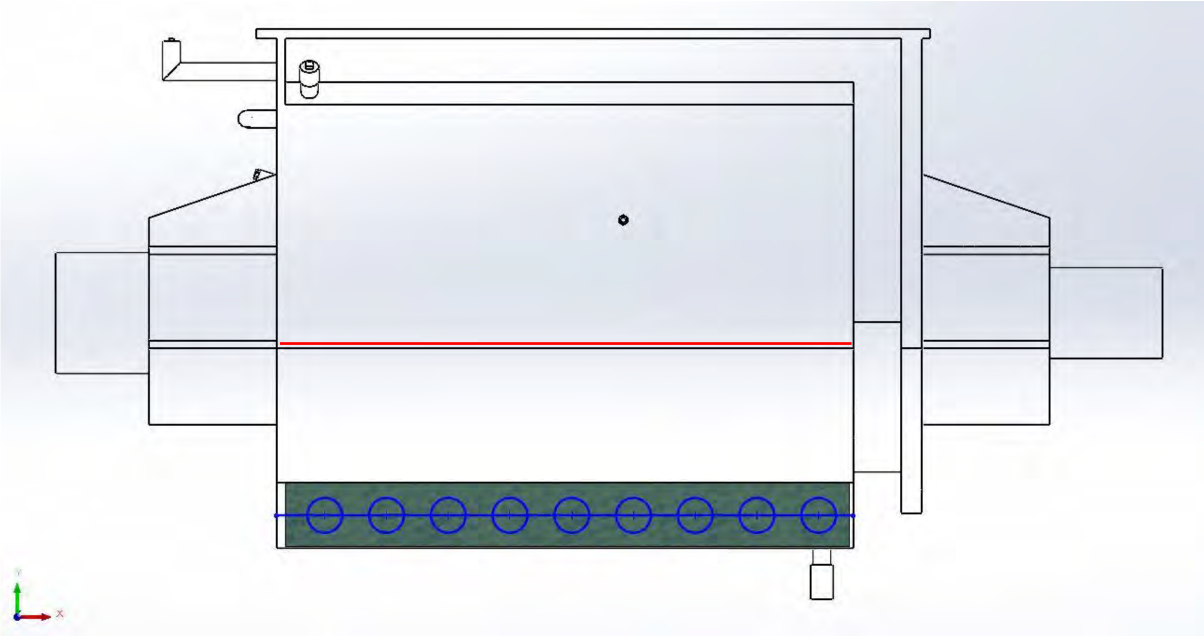

Figure 222: 3D model showing the oil fill level at 140L. The level is estimated to be fully covering the heaters.

3D Model and Volume Calculation

160L oil level

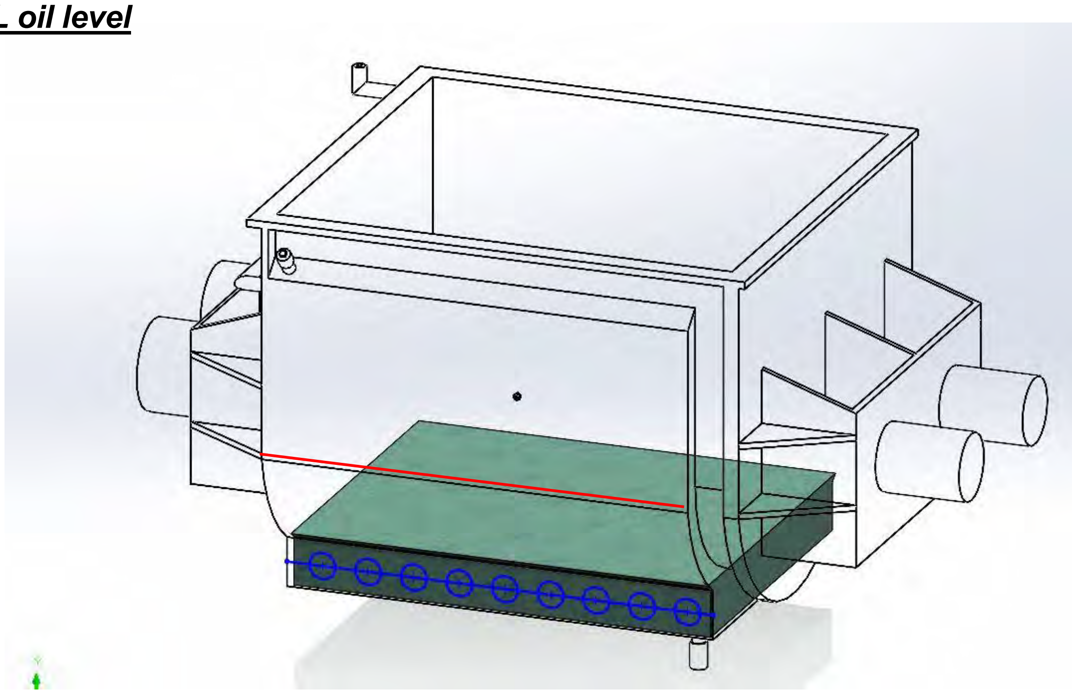

Figure 223: 3D model showing the oil fill level at 160L. The level is estimated to be slightly above the centreline of the heaters.

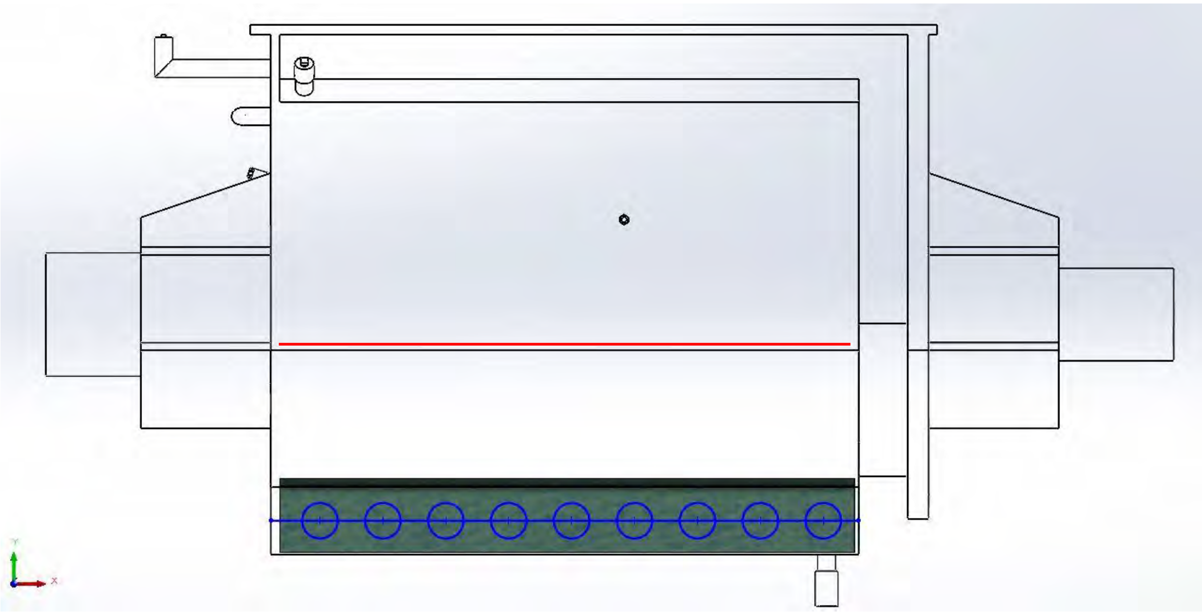

Figure 224: 3D model showing the oil fill level at 160L. The level is estimated to be fully covering the heaters.

3D Model and Volume Calculation

245L oil level

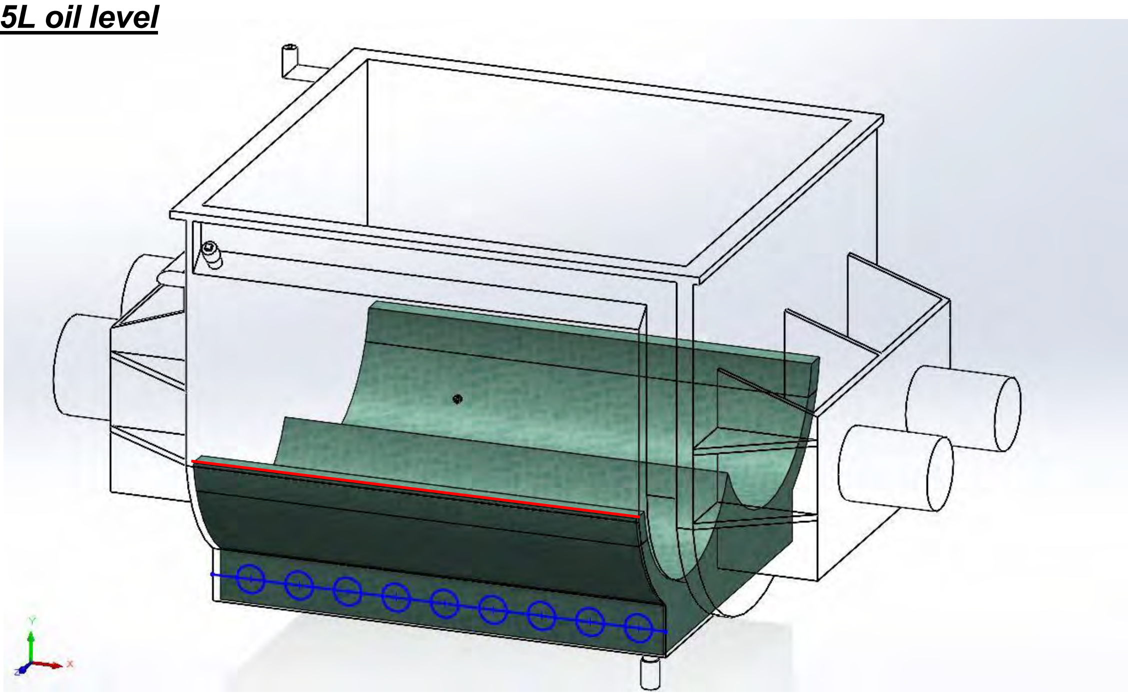

Figure 225: 3D model showing the oil fill level at 245L. This is the estimated volume needed to filled up to half the mixing cylinder height as per the User Guide.

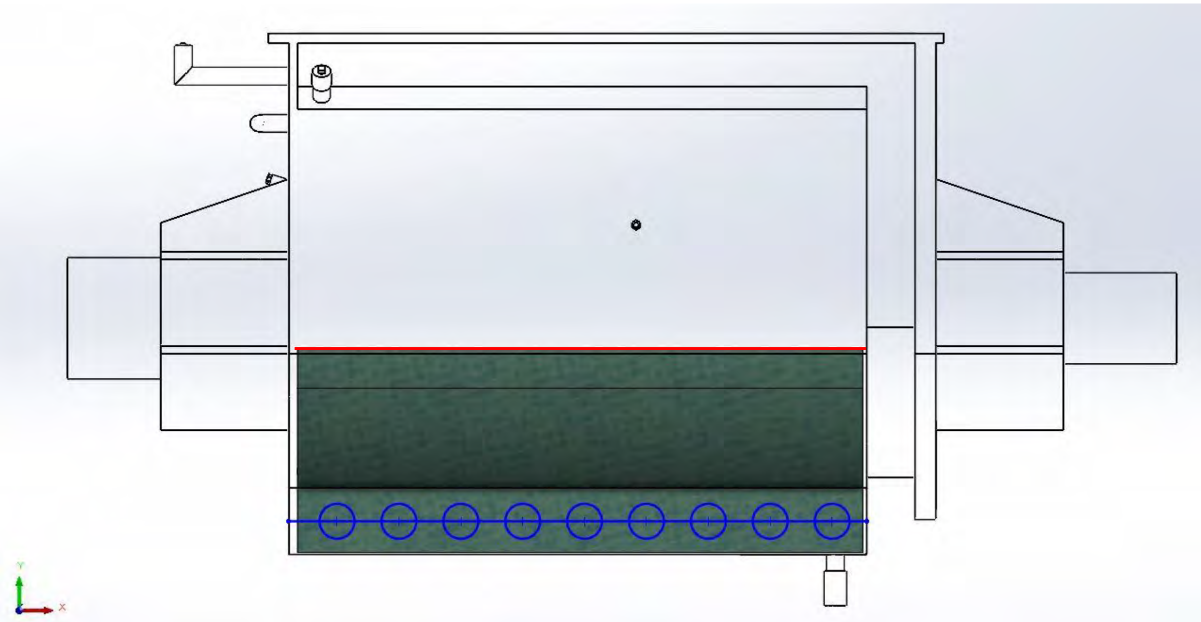

Figure 226: 3D model showing the oil fill level at 245L. This is the estimated volume needed to filled up to half the mixing cylinder height as per the User Guide.

3D Model and Volume Calculation

279L oil level

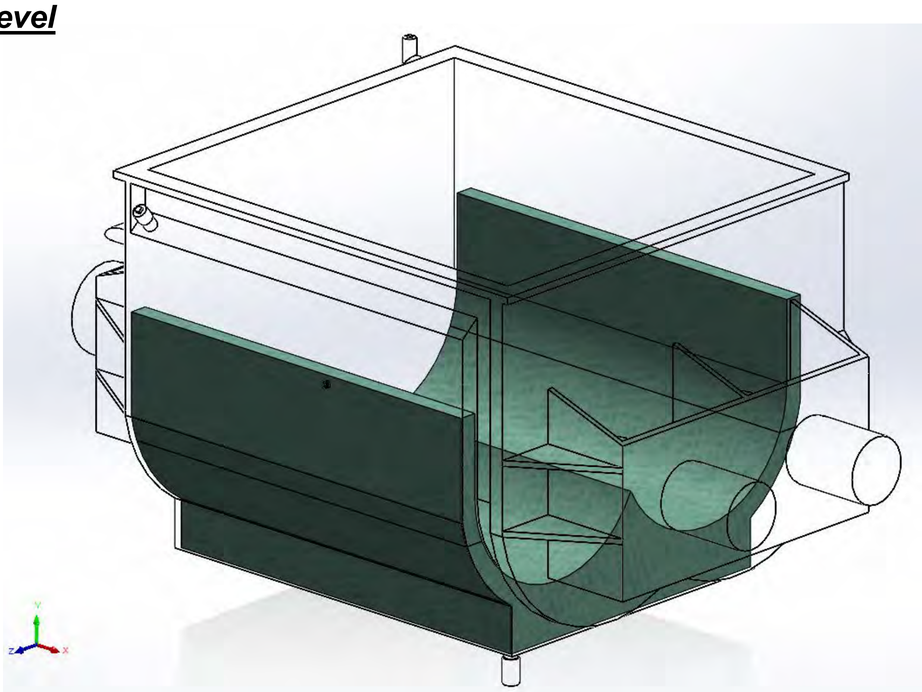

Figure 227: 3D model showing the oil fill level at 279L. This is the estimated volume needed to filled up to half the height of the oil jacket's RTD measure points.

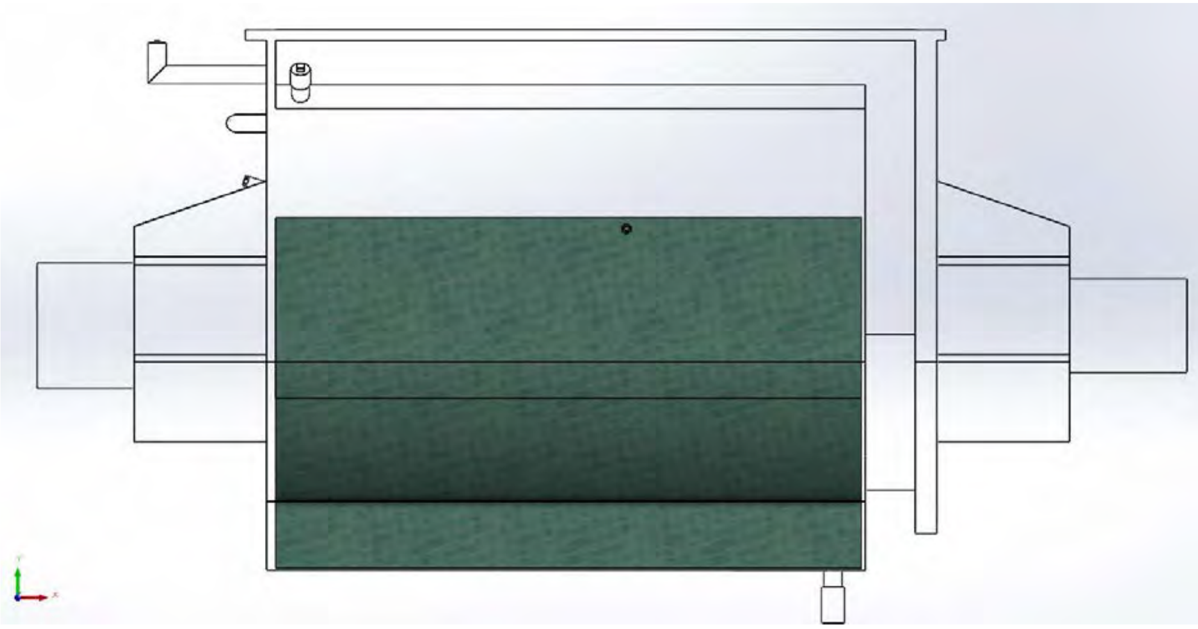

Figure 228: 3D model showing the oil fill level at 279L. This is the estimated volume needed to filled up to half the height of the oil jacket's RTD measure points.

Annex

1. NH Sigma Kneader USER'S GUIDE
2. Weld terminology (extracted from AWS A3.0:2001, Standard Welding Terms and Definitions, pg 78)
3. LEW Report
4. Photo of electrical panel, furnished by MOM
5. Oil jacket drawing with measured dimensions

Annex 1: User Guide pg1

NH Sigma Kneader

USER'S GUIDE

Laizhou Keda Chemical Machinery Co., Ltd.
Address: Xidingjia Village Shahe Town, Laizhou City, Shandong Province, China.
Tel: 0086-(0)535-2377668 Fax: 0086-(0)535-2377767 Website: www.kedahuaji.com

Annex 1: User Guide pg2

One. Product description

It is special used for mixing and kneading high-viscosity material. It has excellent effect for mixing, kneading, crushing and dispersing because of the intense shearing force which produced by two powerful rotary blades.

Kneader temperature adjustment can be done by using heat transfer oil circulation, electric heating, steam and water cooling. It can be made tank body jacket, wallboard jacket, stirrer passing cooling water, passing heat transfer oil and such structures for heating and cooling.

Two. Technical parameter

Discharge Way: hydraulic tilt, screw extruding, bottom valve.

Function: can be cooling or heating (electrical, cycle hot water/oil).

Type: normal type, pressure type, vacuum type.

Material: SS304, SS316 or carbon steel can be available.

Speed: controlled by inverter, or fixed

Blades & Chamber: can be fine polished

Three. Application

Widely used in high viscosity product

------Chemicals Industry:

Resins, Sealant, silicon rubber, glue/ adhesive, paint, Clay, Dye, BMC/CMC, pigment, plastics, batteries.

------Food Industry:

Bubble gum, dough, chewing gum, soft candy, cheese etc.

------Pharmaceutical:

Some medicines & medical materials.

Four. Technical specification

Model	Motor Power (KW)	Heating Way	Steam Pressure (Mpa)	Vacuum Degree (Mpa)	Pressure (Mpa)	Dimensions (M)	Weight (KG)
2L	1.1-2.2	Electrical/Cycle Steam/Hot Oil/Hot Water in Jacket	Usually 0.3(can add as requirement)	-0.09Mpa (Vacuum Type)	0.45 (Pressure Type)	1.1*0.4*0.5	150
5L	1.1-2.2					1.1*0.5*0.6	200
10L	1.1-2.2					1.2*0.5*0.6	300
50L	2.2-7.5					1.5*0.7*1.0	600
100L	4-11					1.6*0.7*1.3	1000
200L	5.5-15					2.0*1.2*1.5	1800
300L	5.5-22					2.3*1.2*1.8	2200
500L	11-22					2.6*1.2*1.8	3000
1000	15-37					2.8*1.2*1.8	4500

Annex 1: User Guide pg3

L							
1500 L	18.5-45					3.3*1.9*1.9	5500
2000 L	37-75					3.5*2.2*2.2	6800
3000 L	45-110					4.0*2.2*2.4	9500

Five. Structural characteristics and working principle

-The NH kneader is a horizontal double shaft parallel type, the stirring shaft is Σ type, the double paddles are horizontally arranged, rotate oppositely and have different speeds. When working, it is driven by the motor through the reducer to the active paddle, and the driven paddle is driven by the gear. So that the materials can be fully kneaded, blended, mixed, and sheared to accelerate physical and chemical reactions.

-Main feature:

1. Strong and powerful during mixing.
2. Large loading factor, and the charging is more at one time.
3. The diameter of the mixing blade is large and the spiral angle is excellent, the material has good axial flow during the kneading process.
4. Adopt chassis, easy to install and debug
5. Centralized electrical control, including the operation of the host, tilting cylinder and digital display temperature control, which is convenient for user operation and process control.

-Structure and working principle

The NH series kneader is mainly composed of the main body of the kneader, the transmission system, the tilting cylinder pouring system, the heating system, and the electrical control system.

The main body of the kneader is composed of a mixing cylinder, a mixing paddle, wall plates at both ends, a shaft seal, a bracket and a base. It is W-shaped, which is welded by two layers of steel plates. The inner layer is made of stainless steel. The bottom is composed of two semi-cylindrical columns. There is a horizontal dividing ridge in the middle. The jacket can be injected with cold and hot medium to carry out cold heat treatment on the material of the mixing tank.

The bottom of the electric heating mixing cylinder is provided with an electric heating tube. The jacket needs to be filled with heat conduction oil. The heat conduction oil is heated by the electric heating tube, and the heat conduction oil transfers the materials inside the mixing cylinder

After manually opening the cover, it is necessary to plug in the safety.

Six. Installation of the machine

1. Installation space

1) The height is 90cm, which is necessary for tilting the cover.
2) The minimum width space is reserved, 0.5m on the left and 0.8m behind the machine, which can be used for supporting pipelines and maintenance.
3) The operating space in front of the machine shall be set aside according to the specific requirements of customers.

Annex 1: User Guide pg4

2. Foundation requirements
1) Concrete floor thickness is more than 20cm.
2) Certificate cement base of specific level standard.
3. Installation and positioning

There are two positioning methods, one is welding, and the other is ground bolt.

1) For welding positioning, before and after the user purchases the machine, according to the foundation map provided by the supplier, six square irons can be directly welded when the foundation is poured.
2) Positioning of anchor bolt: The user reserves square holes for anchor bolts when pouring the foundation according to the foundation plan provided by the supplier. After the machine is purchased, it is moved to the foundation and the anchor bolts are fixed to the ground or pouring with cement.

Seven. Power

Power supply quality Voltage: 380V ± 10V
Frequency: 50Hz ± 5Hz

If regulated power supply can be used, the service life of motors and electrical components can be extended.

Eight. Electric heat source

Heating method: electric heating oil

1. Design of thermal jacket
1) Design temperature: 200 ℃
2) Operating temperature: 70-160 ℃
3) Working pressure: ≤0.2Mpa
2. This system uses heat conduction oil electric heating tube for heating, which has high requirements for the quality and material of heat conduction oil. It is recommended to use HD series high temperature heat conduction oil. Generally, the heat conduction oil should be preheated before being injected into the jacket of the mixing tank to facilitate the evaporation of the moisture of the oil. An oil vapor vent is provided at the highest point behind the machine, and the oil vapor vent is directly connected to the vent Pool. Care should be taken in the heating process, and avoid using hands to detect whether the pipes and the outside of the mixing tank are heated. It's easy to get burned.

Nine. Maintenance

A good device needs daily maintenance, the specific matters are as follows:

1. Transmission system:
1) The V-belt is a wearing part. The elasticity of the V-belt should be suitable. After the extension, the motor base can be adjusted.
2) Cylindrical gear reducer uses gear oil, the first maintenance is 500h.
3) The drive gear of the kneader should be filled with lubricating oil regularly.
4) Lubricant should be refilled regularly at the bearing end of the main shaft.
2. Hydraulic system

The hydraulic system should periodically replace the hydraulic oil, and pay attention to whether the oil quality is discolored. The hydraulic oil should be replaced once a year. The maintenance of the hydraulic cylinder should be checked for oil leakage and keep the piston rod clean.

Annex 1: User Guide pg5

3. Heating system

In the heat conduction oil heating system, it is strictly forbidden to dry the electric heating tube, and pay attention to check that the heat conduction oil in the jacket is added in time with the loss of heat conduction oil. A heating power of 800w, a total of three.

4. Shaft seal part

Daily inspection of the shaft seal should not be too loose, and should be adjusted to a slightly compressed state, but it should not be pressed too strongly. The shaft seal part should be maintained every six months, remove the seal seat, and clean the shaft diameter and seal chamber with silicone oil, replace the V-ring or PTFE packing, oblique incision should be taken.

5. Clean

After each work, the opening of the mixing tank should be cleaned and the cover closed.

Ten. Attached sheet of the equipment needs oil grade and quantity

Equipment name	Oil grade	Oil quantity
Reducer	45 # engine oil	Add it to see the oil by the window.
Vacuum pump	special oil for vacuum pump	It has been added before leaving the factory
Kneader jacket	HD320-350 #	When refueling, you need to open one side vent hole and add it to half the height of the cylinder.
Remarks: Observe the oil window and add various oils regularly		

Annex 2: Weld terminology (extracted from AWS A3.0:2001, Standard Welding Terms and Definitions, pg 78)

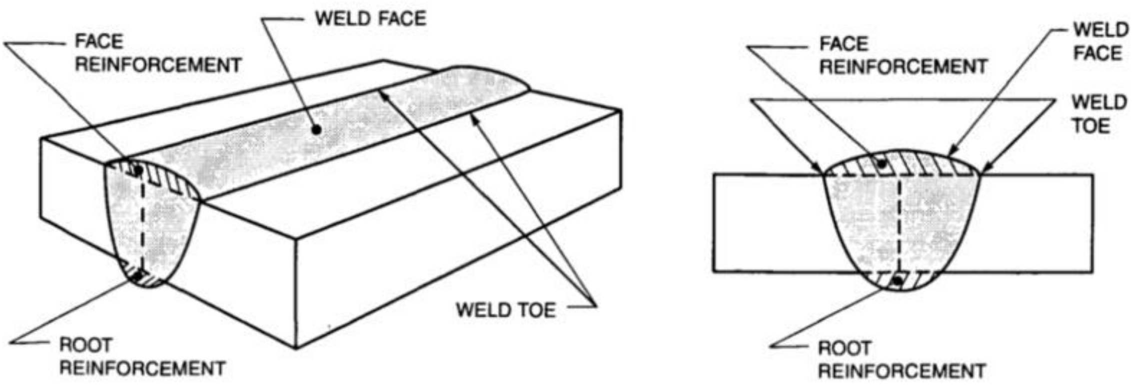

(A)

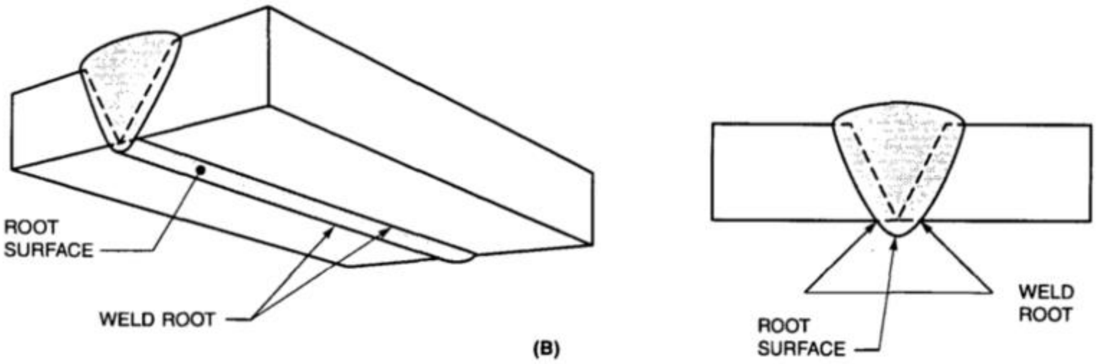

(B)

<u>Annex 3: LEW Report pg1</u>

YOGO ENGINEERING

71 Woodlands Ave 10 #08-18 Woodlands Ind Xchange Singapore 737743 Tel: 62009189, 97368842 (Reg No. 52912368A)
Email : yogoeng@gmail.com

ELECTRICAL REPORT ON LOCAL ELECTRIC PANEL

Retrieved From Fire And Explosion Incident
At 32E, Tuas Avenue 11

Date: 25th July 2021

Prepared by:

Yong Chun Hao
LEW 7
Yogo Engineering

EMA LICENSED WORKER
ELECTRICAL
YONG CHUN HAO
EMA NO: 7/071944
SINGAPORE

Vincent Char Poh Fang
Switchboard Manufacturer
One Electric Pte Ltd

Annex 3: LEW Report pg2

1 Termination from Local Control Panel to Heaters

1.1 Termination inside the local control panel

The as-received local control panel (LCP) was examined. An electrical schematic diagram was made based on the examination and presented in the Annex.

The termination of the heating coil wires

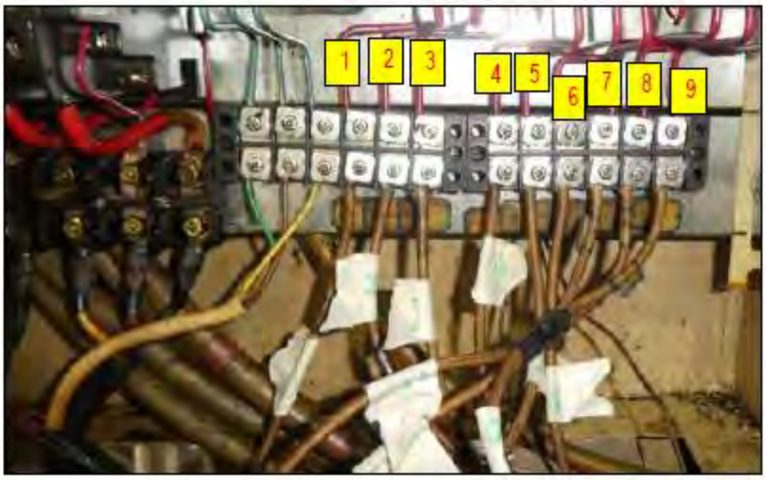

The above figure was furnished by Mr. Ashley Ng from Matcor, showing the termination of the heater wires in the LCP before removal on site. The wires terminated to the contactors are numbered (in yellow box) from left to right. The contactors correspond to the 3 switches at the top of the panel. Each switch controls the group of heaters linked to contactors 1 to 3, 4 to 6, and 7 to 9.

1.2 Connection to heating elements

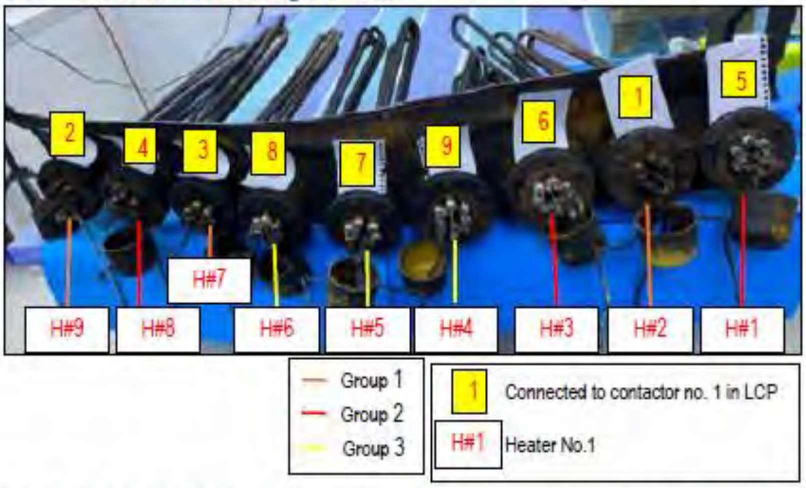

The figure above shows the 9 heaters and their corresponding wire termination in the LCP contactors.

Annex 3: LEW Report pg3

The termination for Group 1 & Group 2 heater switches to the heaters were incorrect. Such termination results in lower heating output if the switch for either group 1 or group 2 is turned off. This is depicted in the following sketch.

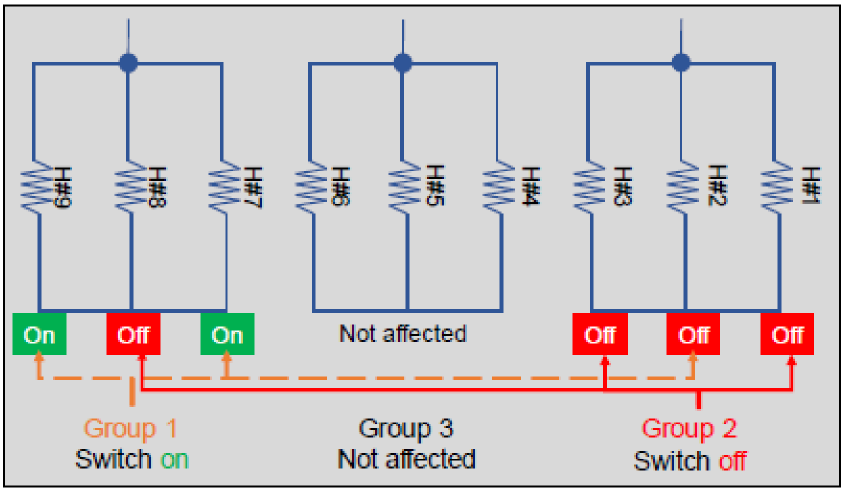

Operating state of heating coils when switch for Group 1 is turned on and switch for Group 2 is turned off.

When the switch for Group 1 heaters (consist of H#2, H#7 and H#9) is turned on and switch for Group 2 heaters (consist of H#1, H#3 and H#4) is turned off, only H#7 and H#9 will operate. This result in a 2/3 of heating output instead of the full 3 heaters capacity.

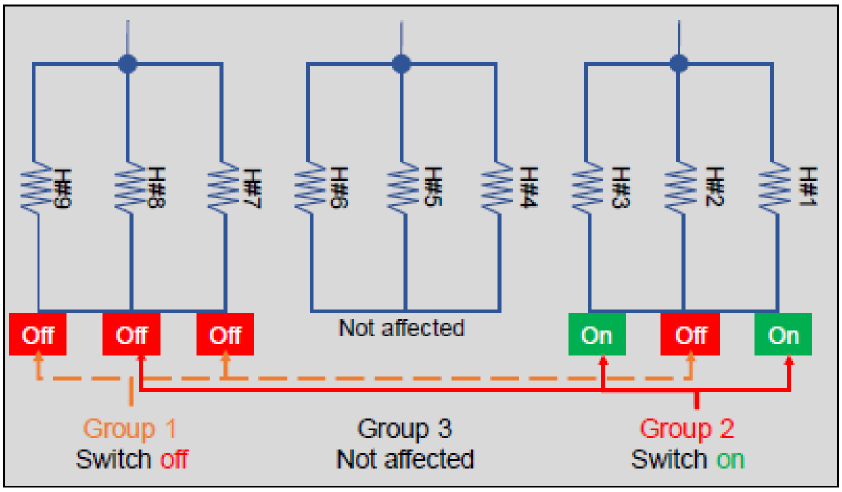

Operating state of heating coils when switch for Group 2 heaters is turned on and switch for Group 1 is turned off.

Annex 3: LEW Report pg4

When the switch for Group 2 heaters (consist of H#1, H#3 and H#4) is turned on and switch for Group 1 heaters (consist of H#2, H#7 and H#9) is turned off, only H#1 and H#3 will operate. This result to a 2/3 of heating output instead of the full 3 heaters capacity.

If the switches for all groups of heaters are turned on, all the heaters should operate at full capacity.

2 Components in Local Control Panel

An electrical circuit diagram was made based on the as-received LCP (see Annex).

There is no sign of malfunction and failure of the moulded case circuit breaker (MCCB), Fuse & Contactor.

- The 3 groups of heaters' contactors are interlocked with the "Jacket Temperature" thermostat. This means that all the heaters will stop heating when the "Jacket Temperature" thermostat detects a temperature (through RTD sensor) that exceed a pre-set temperature. The thermostat, serial number REXD-C7131*AN, has a detective temperature range of 0 - 400°C (see Annex for specification sheet of thermostat with model "REXD-C7131*AN").

Label with serial number and specification of the thermostat.

- RTD A resembled a 2-wire Pt100 sensor but cannot be confirmed due to lack of information or serial number.
- RTD A was tested by connecting the RTD terminals to a multimeter and heating the sensor with a lighter. The resistance increases with exposure to heat, confirming it is in working condition.

RTD A with working sensor on left.

- The only Overcurrent protection for the LCP is the incoming MCCB, there is no Thermal Overload protection device for the motors. The MCCB is at "OFF" state during examination.[1]
- There is no Earth leakage protection installed in the LCP.
- Emergency button was found depressed.

[1] It was later confirmed by SCDF as first responders that the MCCB was in "ON" state during their site investigation.

Annex 3: LEW Report pg5

3 Internal Resistance of Heaters

Test was conducted on the wire line to the earth of the heater (machine body) using a multimeter.

Circuit No :	IR value (Mega Ohm)			Remarks
	L1-E	L2-E	L3-E	
Heater No.1	0			Connected to contactor no.5 in control panel
Heater No.2		2.4		Connected to contactor no.1 in control panel
Heater No.3			2.4	Connected to contactor no.6 in control panel
Heater No.4	2.4			Connected to contactor no.9 in control panel
Heater No.5		0		Connected to contactor no.7 in control panel
Heater No.6			0	Connected to contactor no.8 in control panel
Heater No.7	2.4			Connected to contactor no.3 in control panel
Heater No.8		2.4		Connected to contactor no.4 in control panel
Heater No.9			2.4	Connected to contactor no.2 in control panel

Heaters 1, 5 and 6 were found shorted. The explosion may have caused the shorting of the heaters but the actual cause of the shorting is not certain.

4 Heating Resistance of Heaters

Test was conducted on the terminals to get the average heating resistance using a multimeter. The terminal bridges between coils of the heater were not removed hence the measured resistance values are the average of the coils of the heater.

Heater	Resistance
Heater No.1	26.6 Ohm
Heater No.2	207 Ohm
Heater No.3	13.7 Ohm
Heater No.4	10.3 Ohm
Heater No.5	9.1 Ohm
Heater No.6	14.0 Ohm
Heater No.7	17.0 Ohm
Heater No.8	10.0 Ohm
Heater No.9	11.4 Ohm

Heater No.2 had an abnormally high resistance value.

__Annex 3: LEW Report pg6__

Annex

Annex 3: LEW Report pg7

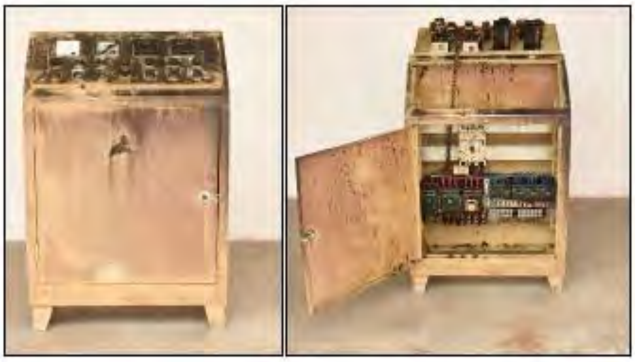

As-received condition of local control panel.

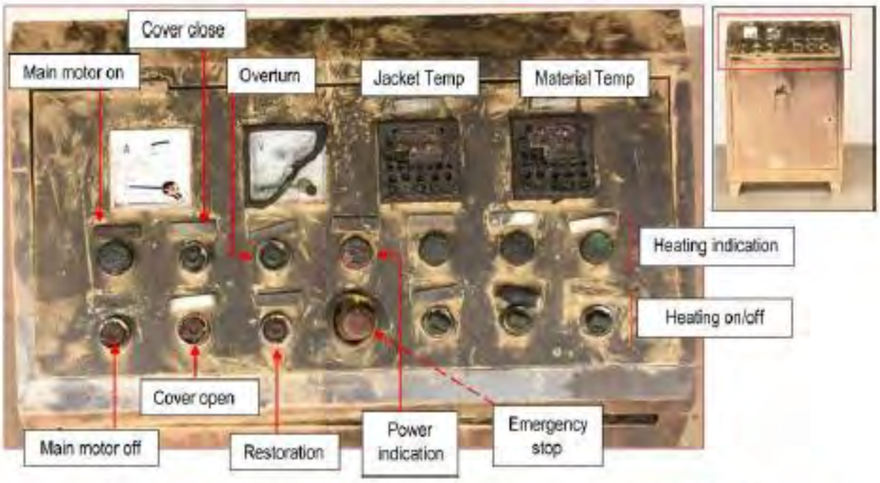

Components including buttons, switches and thermostats of LCP.

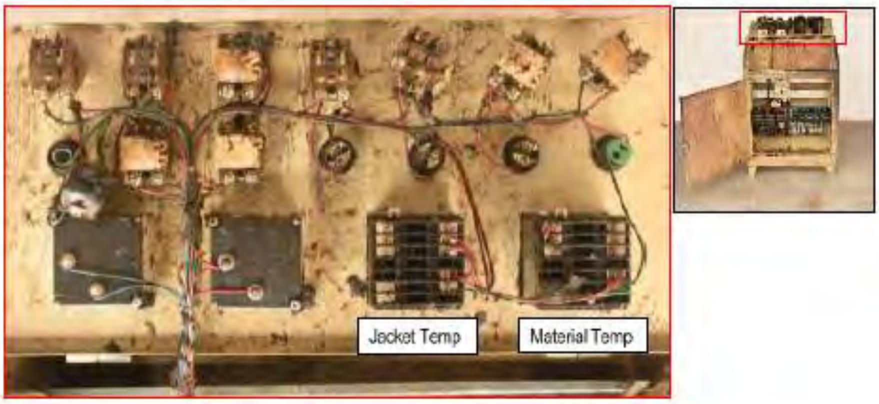

View of components from inside the LCP.

Annex 3: LEW Report pg8

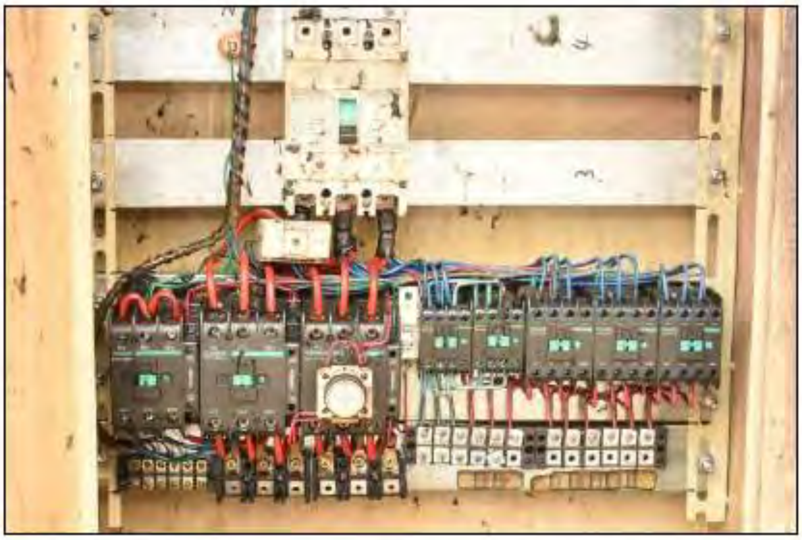

View of components from inside the LCP.

<u>Annex 3: LEW Report pg9</u>

Electric diagram of local control panel

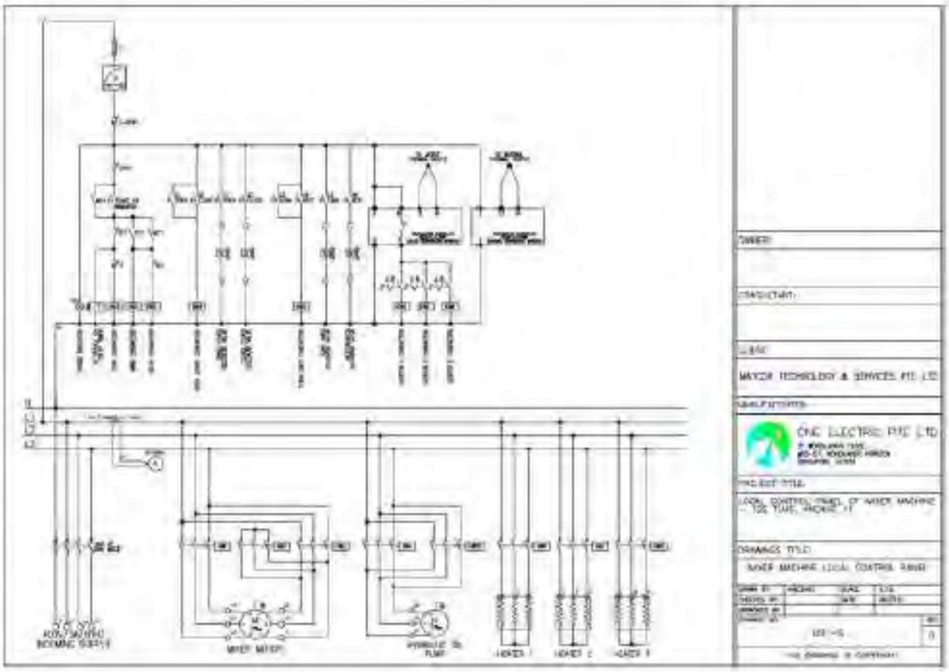

Annex 3: LEW Report pg10

Specification sheet for thermostat, serial number REXD-C7131*AN. (translation in blue box).
(Source: https://www.aliexpress.com/item/4000717329331.html?spm=2114.12057483.detail.3.7b9158b8qiV9I7)

主要技术指标

Main Technical Parameters

测量精度：±0.5%FS

冷端补偿误差：±2℃（0~50℃范围内可软件修正）

分辨力：14Bit

采样周期：0.5 Secretary

电源：AC200-AC220V 50Hz

Accuracy of measurements: ±0.5%FS

Production density compensation error: ±2°C (correction is possible with software for the temperature that ranges from 0°C to 50°C)

Resolution: 14 Bit

Sampling period: 0.5 Secretary

Power supply: AC200-AC220V 50Hz

控制方式采用工业及专家自整定 PID 技术，与传统 PID 控制相比具有控温迅速、

响应快、超调小、精度高等特点，控制方式

绝缘电阻：＞50MΩ（500VDC）

绝缘强度：1500VAC/1 分钟

功 耗：＜10VA

使用环境：0~50℃，30~85%RH 的无腐蚀性气体的场合

The professional self-tuning PID technology enables temperature control. Compared with the traditional PID control technology, it features a more responsive temperature control. It also boasts an ultra-small size and high precision.

Insulation resistance: > 50 MΩ (500VDC)

Other peak intensity: 1500VAC per minute

Power Consumption: <10VA

Operating environment: 0~50°C, 30~5%RH on occasions without corrosive gas

Annex 3: LEW Report pg11

Specification sheet for thermostat, serial number REXD-C7131*AN (translation in blue box).
(Source: https://www.aliexpress.com/item/4000717329331.html?spm=2114.12057483.detail.3.7b9158b8qiV9l7)

TAIZHOU 太洲工业调节仪/温度控制器

Taizhou Industrial Regulator/Temperature Controller

REXD 智能工业调节器/温度控制器
是一种高性能、高可靠性的智能型
工业调节仪，广泛应用于机械、化
工、陶瓷、轻工、冶金、石化、热
处理等行业的温度、流量、压力、
液位等的自动控制系统

REXD intelligent industrial regulator/temperature control is a high-performance, high-reliability intelligent industrial regulator, which is widely used in the temperature and flow of machinery, chemical industry, ceramics, light industry, metallurgy, petrochemical, heat treatment and other industries, Automatic control system of liquid level, etc.

模拟数字多重滤波
红绿双排数码管分色同时显示
测量值和设定值

Analog digital multiple filtering

Red and green double row digital color separation display at the same time

Measured maximum value and set value

传感器自由输入，所有参数
均由面板程序输入

The sensor is free to input, all parameters are input by the panel program

软件调零，整机无电位器
具有二级参数锁保护功能
自适应，自整定

Software zero adjustment, the whole machine has no potentiometer, has a secondary parameter lock protection function, self-adaptive, self-tuning

Annex 4: Photo of electrical panel, furnished by MOM

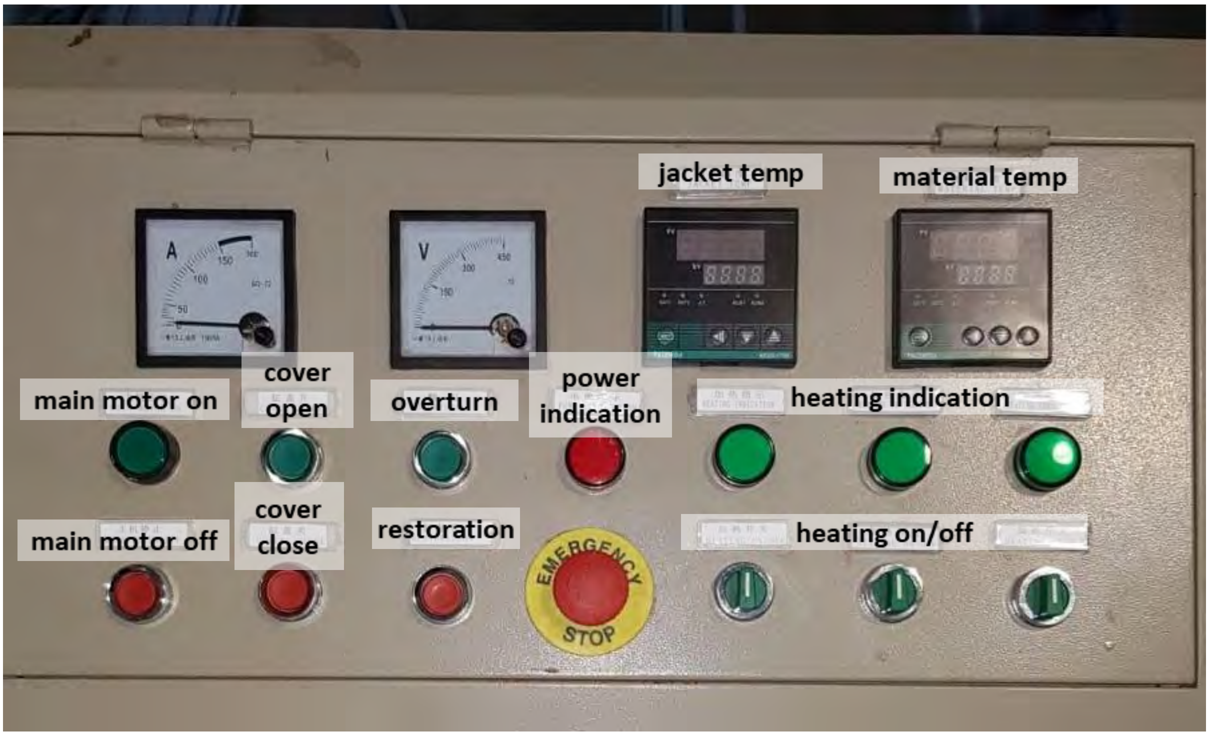

Annex 5: Oil jacket drawing with measured dimensions